

PATRICK POULIN

**CYCLE BIOGÉOCHIMIQUE DE L'AZOTE DANS
L'ESTUAIRE DU SAINT-LAURENT; RÔLE DES
MARAIS CÔTIERS**

Thèse présentée
à l'Université du Québec à Rimouski
dans le cadre du programme de doctorat en océanographie
pour l'obtention du grade de docteur ès sciences (Ph.D.Sc.)

INSTITUT DES SCIENCES DE LA MER À RIMOUSKI
UNIVERSITÉ DU QUÉBEC À RIMOUSKI
QUÉBEC

JUIN 2008

UNIVERSITÉ DU QUÉBEC À RIMOUSKI
Service de la bibliothèque

Avertissement

La diffusion de ce mémoire ou de cette thèse se fait dans le respect des droits de son auteur, qui a signé le formulaire « *Autorisation de reproduire et de diffuser un rapport, un mémoire ou une thèse* ». En signant ce formulaire, l'auteur concède à l'Université du Québec à Rimouski une licence non exclusive d'utilisation et de publication de la totalité ou d'une partie importante de son travail de recherche pour des fins pédagogiques et non commerciales. Plus précisément, l'auteur autorise l'Université du Québec à Rimouski à reproduire, diffuser, prêter, distribuer ou vendre des copies de son travail de recherche à des fins non commerciales sur quelque support que ce soit, y compris l'Internet. Cette licence et cette autorisation n'entraînent pas une renonciation de la part de l'auteur à ses droits moraux ni à ses droits de propriété intellectuelle. Sauf entente contraire, l'auteur conserve la liberté de diffuser et de commercialiser ou non ce travail dont il possède un exemplaire.

RÉSUMÉ

Les environnements marins côtiers sont affectés par des apports considérables d'azote organique et inorganique, tant de sources allochtone et autochtone qui ensemble, ont une forte incidence sur les biogéocycles s'articulant au sein de ces milieux. Afin de mieux comprendre les causes et conséquences de ces apports d'azote dans l'écosystème estuaire du Saint-Laurent, nous avons réalisé une étude ayant comme objectifs principaux : 1) d'identifier et de quantifier les principaux processus et les mécanismes saisonniers impliqués dans le cycle de l'azote à l'échelle de l'estuaire ainsi que dans les écosystèmes de type marais salant bordant son littoral, 2) de définir le rôle des marais côtiers (en tant que puits/source d'azote) sur la dynamique de l'azote en milieu estuaire et 3) de définir le potentiel de résilience du système estuaire face à l'activité anthropique. Afin d'atteindre efficacement ces objectifs généraux sans souffrir d'un cadre de travail trop vaste, la présente étude a été divisée en plusieurs objectifs spécifiques dont les faits saillants sont résumés ci-dessous.

Nous avons d'abord mis au point une technique de mesure de l'ammonium (NH_4^+) sur lecteur de microplaques offrant une limite de détection équivalente à 5 nM et une excellente reproductibilité analytique. Peu sensible aux charges dissoutes et particulières, cette technique nous permet de mesurer des échantillons aqueux de faible volume (< 10 mL) et de concentration variable (entre 10 et 0.05 μM), de façon rapide et efficace. De plus, cette approche fluorométrique nous permet d'évaluer avec précision certaines variables analytiques telles les blancs, l'effet matrice et la fluorescence intrinsèque des échantillons.

En second lieu, nous avons déterminé la variabilité spatiale des espèces de l'azote (et plus spécifiquement NH_4^+) présentes dans la colonne d'eau de l'estuaire au niveau de son axe principal au cours de chacune des saisons de l'année afin de documenter les différents processus impliqués. Les concentrations de NH_4^+ mesurées dans l'estuaire du Saint-Laurent présentent une importante variabilité spatiale et saisonnière; les plus fortes concentrations ayant été relevées en octobre 2005 (Av \pm SE; $2.02 \pm 0.69 \mu\text{M}$) dans l'estuaire supérieur ainsi qu'en mai 2003 ($0.84 \pm 0.20 \mu\text{M}$) dans la couche d'eau

intermédiaire froide de l'estuaire maritime. Deux types de processus ont été suggérés pour expliquer ce patron de distribution soit; les apports fluviaux et la production endogène. Notre étude a montré que la contribution allochtone est largement modulée par l'hydrologie du système ($980 \pm 434 \text{ T N mois}^{-1}$) alors que les processus de production pélagique sont essentiellement observés en période de forte productivité. D'après la composition chimique de la matière organique particulaire en suspension (SPM; Chl-*a*, rapport C/N, amino-acides hydrolysables) présente dans l'estuaire, nous pouvons affirmer que le NH_4^+ de source autochtone est issu de processus pélagiques couplés (c'est-à-dire broutage et excrétion zooplanctonique, dissolution et minéralisation microbienne) affectant la biomasse phytoplanctonique fraîche et sénescente.

En troisième lieu, à partir de données océanographiques obtenues dans l'estuaire maritime, nous avons élaboré une hypothèse, impliquant des processus d'assimilation et de respiration, pour expliquer les variations saisonnières simultanées d'oxygène dissous et d'azote inorganique dissous (DIN) au sein la colonne d'eau. En effet, une importante diminution des concentrations en DIN a été ponctuellement observée en juillet 2004 dans la masse d'eau hypoxique de l'estuaire maritime (passant de ~ 25 à $\sim 14 \mu\text{M}$). Alors que de fortes concentrations de Chl-*a* sont observées dans la masse d'eau superficielle, témoignant d'une forte activité autotrophe, le transfert de cette matière labile de source endogène vers la couche d'eau profonde a pu mener à un découplage des processus bactérien de nitrification/dénitrification au sein du compartiment hypoxique. Ce processus de dénitrification pélagique pourrait constituer un mécanisme de stabilisation des concentrations d'oxygène dissous prévenant le développement de conditions anoxiques dans la masse d'eau profonde riche en DIN.

En quatrième lieu, nous avons déterminé la variabilité spatiale et temporelle des communautés bactériennes hétérotrophes dans la colonne d'eau de l'estuaire du Saint-Laurent afin de comprendre l'influence du couvert de glace sur ces populations. Deux caractéristiques des populations bactériennes ont été prises en compte lors de cette étude, soit: les abondances totales et la structure des communautés (proportion de cellules contenant de fortes concentrations d'acide nucléique; %HNA). Alors que les populations

bactériennes présentent dans l'estuaire supérieur ne montre aucune variabilité significative (tant spatiale que temporelle), la distribution de bactérioplancton au sein de l'estuaire maritime présente un patron singulier; les abondances de cellules bactériennes décroissent avec la profondeur en période libre de glace et demeurent uniformément distribuées dans la colonne d'eau en période hivernale. Cette variabilité peut être expliquée à 81% par l'effet combiné de la température, de la salinité, de l'oxygène dissous, de la concentration SPM, en Chl-*a* et de la composition élémentaire de la SPM. Par ailleurs, la variabilité du %HNA peut être expliquée à 51% par l'effet combiné de la concentration en NH_4^+ , $\text{NO}_2^- + \text{NO}_3^-$, SPM et de la salinité. Ensemble, la variabilité des abondances totales et de la structure des populations indiquent que ces communautés sont sensibles à l'évolution des caractéristiques physicochimiques du milieu estuarien; l'abondance des cellules de type HNA demeurant essentiellement liée à la disponibilité des éléments nutritifs azotés.

En cinquième lieu, nous avons évalué les flux tidaux de nutriments inorganiques dissous (notamment $\text{NO}_2^- + \text{NO}_3^-$, NH_4^+) entre deux marais (un marais impacté et un marais témoin non impacté) de la région de Rimouski et la masse d'eau estuarienne. En utilisant un modèle hydrodynamique numérique (MIKE21-NHD) forcé par des marées prédéfinies, les flux saisonniers de nutriments ont été évalués afin de comprendre l'influence des rejets de source anthropique, l'importance relative de certains processus biochimiques (notamment l'assimilation et la minéralisation) et du couvert de glace sur le potentiel de rétention des marais. Les deux marais à l'étude se comportent généralement comme des sources de NH_4^+ (de 8.69 à 30.39 mg N $\text{j}^{-1} \text{m}^{-2}$) et des puits de $\text{NO}_2^- + \text{NO}_3^-$ (de 7.84 à 32.14 mg N $\text{j}^{-1} \text{m}^{-2}$) pour la masse d'eau estuarienne et ce, indépendamment de la saison ou du niveau de stress anthropique observé. Ces résultats suggèrent que les apports tidaux de $\text{NO}_2^- + \text{NO}_3^-$ sont réduit en NH_4^+ par l'activité bactérienne *via* la DNRA (dissimilatory nitrate reduction to ammonium). Puisque le NH_4^+ ainsi produit s'accumule sur la frange herbacé plus rapidement qu'il n'est consommé par les processus de nitrification/dénitrification et d'assimilation, un important flux de NH_4^+ vers l'estuaire est observé. Les flux tidaux étant peu affectés par la variabilité des apports de nutriments de source anthropique, nous croyons que ces écoulements (atteignant $1.93 \text{ m}^3 \text{ s}^{-1}$) ont généré davantage d'érosion que tout autre type d'altération écosystémique.

En sixième lieu, nous avons réalisé une série d'expériences en microcosme ayant pour but la détermination du potentiel dénitrifiant saisonnier des marais de l'estuaire maritime. Faisant appel à une technique d'enrichissement isotopique éprouvée, nous avons mesuré les vitesses de production de N₂ sous différentes conditions jugées représentatives du milieu à l'étude. Bien que les taux de dénitrification moyens mesurés varient de façon concomitante avec la température, passant de 9.6 µmol N₂ m⁻² h⁻¹ (2 °C) à 25.5 µmol N₂ m⁻² h⁻¹ (12 °C), aucune relation statistique n'a pu être démontrée. Répondant à plus de 80% de la demande en NO₃⁻, la nitrification a été identifiée comme la principale source d'azote pour la dénitrification. Puisque moins de 31% des NO₃⁻ consommés par le sédiment sont dénitrifiés, nous soupçonnons la présence d'un puits alternatif de NO₃⁻ dans les marais côtiers. La DNRA ainsi que certains mécanismes impliqués dans l'oxydation de la matière organique et des métaux comptent parmi les processus de consommation suspectés. L'ensemble des résultats obtenus témoigne de l'important potentiel épurateur des marais côtier sub-arctique.

En septième lieu, nous avons réalisé une étude visant à mieux comprendre les communautés microphytobenthiques (MPB) présentent dans deux marais de l'estuaire maritime affectés par des niveaux de stress anthropique forts différents. En nous penchant sur l'abondance et la diversité du MPB ainsi que sur les caractéristiques biogéochimiques du sédiment (abondance bactérienne totale, granulométrie, composition élémentaire, concentration de pigments, de polysaccharides). Une plus grande diversité de diatomées a été observée dans la zone supérieure du marais impacté avec une dominance des formes epipelic alors qu'aux autres sites, les formes épipsammic prédominent. Parmi les espèces epipelic les plus abondantes, nous avons noté la présence de *Diploneis interrupta*, *D. smithii*, *Gyrosigma fasciola*, *G. spenceri*, *Navicula cryptocephala*, *N. peregrina*, *N. radiosa* var. *tenella*, *N. salinarum*, *Nitzschia clausii* and *N. tryblionella*, alors que les espèces épipsammic sont principalement représentées par *Achnanthes delicatula*, *Navicula cryptocephala* and *Cocconeis disculus*. Nos analyses statistiques ont montré que l'abondance totale de diatomées est corrélée à la disponibilité des nutriments alors que l'abondance relative de cellule de type epipelic et episammic est corrélée à la taille des sédiments. Selon nos estimations, la biomasse associée MPB varierait de 11 à 71 g C m⁻²

dans le marais témoin non-impacté et de 24 à 486 g C m⁻² dans le marais impacté. L'ensemble de ces résultats montre que l'activité anthropique a un effet significatif sur la composition du MPB des marais côtiers.

L'ensemble des résultats obtenus dans cette étude nous a permis de réaliser un bilan annuel d'azote dans l'estuaire du Saint-Laurent. À partir de ce bilan, nous avons pu définir l'influence relative des principaux processus impliqués dans le cycle de l'azote à l'échelle de l'estuaire (eg. apports fluviaux : ~ 85 224 T N a⁻¹; advection verticale : ~ 240 000 T N a⁻¹) et présenter le rôle relativement modeste des marais côtiers (rétenzione de DIN : 96 - 660 T N a⁻¹ pour 90 km²). Conformément à ce bilan, nous pouvons affirmer que le potentiel de résilience de l'estuaire maritime demeure faible et qu'il demeure fort vulnérable aux problèmes engendrés par l'eutrophisation.

AVANT-PROPOS

Les travaux de cette thèse s'inscrivent dans le cadre général d'une vaste étude portant sur la pérennité des milieux côtiers des hautes latitudes dans une perspective de changements d'ordre géochimique, écologique et climatique, associés à l'intensification de l'activité anthropique. L'étude de ces milieux devenant urgente, le Dr. Émilien Pelletier de l'ISMER s'est vu décerner la Chaire de Recherche du Canada en Écotoxicologie Marine afin d'assurer un suivi temporel de l'état de santé relatif de ces milieux considérés comme forts vulnérables. La présente étude fournira une première série de données relatives à la dynamique biogéochimique des marais côtiers de l'estuaire du Saint-Laurent. L'un des principaux enjeux de cette étude est de documenter le cycle de l'azote au cours de chacune des saisons de l'année, plus particulièrement au cours de l'hiver, alors que les milieux à l'étude sont captifs des glaces.

REMERCIEMENTS

En premier lieu, j'aimerais vivement remercier, mon directeur de thèse, Monsieur Émilien Pelletier, pour le soutien et la confiance qu'il m'a accordé lors de mon travail de doctorant. C'est avec le plus grand enthousiasme que je le remercie de m'avoir si chaleureusement accueilli dans son équipe de recherche. Le laboratoire Pelletier fût et demeurera à mes yeux une véritable famille d'adoption. Merci Sylvie (Lévesque). Merci Ghislain (Canuel). Merci Richard (St-Louis).

J'aimerais également remercier Monsieur Jean-Claude Brêthes, professeur à l'université du Québec à Rimouski, qui m'a fait l'honneur d'exercer les fonctions de président du jury et de rapporteur de thèse.

Mes remerciements s'adressent ensuite aux membres du jury, Monsieur Urs Neumeier ainsi que Monsieur Christian Gagnon pour avoir eu l'amabilité et la patience de lire et de commenter le présent manuscrit.

Je désire exprimer ma plus profonde gratitude au professeur Karine Lemarchand, prof. Vladimir Koutitonski, prof. Urs Neumeier, prof. Phillippe Archambault, prof J-P Gagné, ainsi qu'au regretté professeur Gaston Desrosiers qui m'ont conseillé et guidé, chacun à leur façon, tout au long de mon projet. Votre collaboration et votre assistance furent appréciées au plus haut point.

J'exprime également mes remerciements à tout le personnel de l'UQAR, de l'ISMER et de RÉFORMAR dont l'aide et le soutien m'ont été précieux au cours de mon travail, et notamment M. Stéphan Simard, M. Michel Morisette, M. James Caveen, M. Sylvain Leblanc, M. Gilles Desmeules, M. Gervais Ouellette, M. André Richard ainsi que M. Michel Rousseau.

Je souhaite enfin inclure dans mes remerciements tous mes amis, les membres de ma famille, sans oublier ma fidèle partenaire de vie, Caroline, pour votre affection et votre appui ainsi que pour tous ces moments de joie qui auront fait de mon séjour à Rimouski une fantastique expérience.

TABLE DES MATIÈRES

RÉSUMÉ	i
AVANT-PROPOS	vi
REMERCIEMENTS.....	vii
TABLE DES MATIÈRES.....	viii
LISTE DES TABLEAUX	xii
LISTE DES FIGURES	xv
CHAPITRE I.....	1
INTRODUCTION	1
1.1 Introduction générale	1
1.2 Problématique environnementale	7
1.3 Objectifs généraux	9
1.4 Objectifs spécifiques	11
1.5 Sites à l'étude.....	13
1.5.1 Conditions climatiques	13
1.5.2 Description des marais à l'étude	14
1.5.3 Description du marais de Pointe-aux-Épinettes.....	16
1.5.4 Description du marais de Pointe-au-Père.....	16
1.6 Méthodologie	17
1.6.1 Procédure d'échantillonnage dans l'estuaire du Saint-Laurent	17
1.6.2 Procédure d'échantillonnage dans les marais côtiers	18
1.7 Référence	20
CHAPITRE II.....	26
DETERMINATION OF AMMONIUM USING A MICROPLATE-BASED FLUORESCENCE TECHNIQUE	26
2.1 Abstract.....	26
2.2 Introduction.....	27
2.3 Experimental	28
2.3.1 Reagents and solutions.....	28
2.3.2 Instrumentation	29
2.3.3 Sample collection and preservation	29
2.3.4 Sample preparation and incubation with working reagent	30
2.3.5 Microplate preparation.....	32
2.3.6 Calculation method (adapted from [7])	33
2.4 Results and discussion	34
2.4.1 Incubation period	34
2.4.2 Background fluorescence (RF_{BG})	35
2.4.3 Matrix effect (ME).....	35
2.4.4 Influence of salinity	36
2.4.5 Limit of detection and analytical reproducibility	37
2.4.6 Field examples	40

2.5 Conclusion	42
2.6 Acknowledgements	42
2.7 Reference	42
CHAPITRE III.....	44
TEMPORAL AND SPATIAL VARIABILITY OF AMMONIUM IN THE ST.	
LAWRENCE ESTUARY (QUÉBEC, CANADA): SIGNIFICANCE OF	
ALLOCHTHONOUS AND AUTOCHTHONOUS CONTRIBUTIONS.....	44
3.1 Abstract.....	44
3.2 Introduction.....	45
3.3 Materials and methods	47
3.3.1 Research area	47
3.3.2 Sampling strategy	48
3.3.3 Chemical analyses.....	50
3.3.4 Water column data analysis	52
3.4 Results.....	53
3.4.1 Temporal and spatial variability of water temperature, salinity and dissolved oxygen.....	53
3.4.2 Temporal and spatial variability of dissolved nutrients and SPM	55
3.4.3 Statistical analysis of nitrogen species variability	59
3.4.4 NH ₄ ⁺ transport through the USLE	61
3.4.5 Variability of nutrient stoichiometric ratios.....	63
3.5 Discussion	63
3.5.1 NH ₄ ⁺ transport through the USLE	63
3.5.2 Potential nitrogen limitation in the SLE	64
3.5.3 Endogenous NH ₄ ⁺ production in the SLE.....	65
3.5.4 Significance of PHAA pattern	67
3.6 Main findings and conclusion	69
3.7 Acknowledgements	69
3.8 References.....	70
CHAPITRE IV.....	75
EVIDENCE FOR NITRATE ASSIMILATION AND RESPIRATION IN HYPOXIC	
DEEP WATERS OF THE LOWER ST. LAWRENCE ESTUARY.....	75
4.1 Abstract.....	75
4.2 Introduction.....	76
4.3 Materials and Methods.....	77
4.3.1 Study area	77
4.3.2 Data collection and sampling.....	78
4.3.3 Chemical analyses.....	80
4.4 Results.....	80
4.5 Discussion	87
4.6 Conclusion	91
4.7 Acknowledgements	92
4.8 References.....	92
CHAPITRE V	96
BACTERIOPLANKTON DISTRIBUTION IN THE ST. LAWRENCE ESTUARY	
DURING ICE-FREE AND ICE-COVERED PERIODS: PROPORTION OF HIGH	
AND LOW NUCLEIC ACID CONTENT CELLS	96

5.1 Abstract.....	96
5.2 Introduction.....	97
5.3 Material and Methods	99
5.3.1 Study site.....	99
5.3.2 Sampling scheme	100
5.3.3 DIN, SPM and Chla analyses	101
5.3.4 Flow cytometry analyses for bacterial abundance and %HNA	102
5.3.5 Statistical analyses	103
5.4 Results	104
5.4.1 Physical variables	104
5.4.2 SPM, Chla and DIN distributions.....	104
5.4.3 Heterotrophic bacteria abundance and structure.....	107
5.4.4 Relationship between TB, %HNA and environmental variables	109
5.5 Discussion	110
5.6 Acknowledgement.....	115
5.7 References.....	115
CHAPITRE VI.....	120
SEASONAL NUTRIENT FLUXES VARIABILITY OF NORTHERN SALT MARSHES: EXAMPLES FROM THE LOWER ST. LAWRENCE ESTUARY.....	120
6.1 Abstract.....	120
6.2 Introduction.....	121
6.3 Site description	123
6.4 Material and Methods	127
6.4.1 Water sampling	127
6.4.2 Flow measurements, water and nutrients fluxes calculations.....	128
6.4.3 Ice cores collection and processing	131
6.4.4 Chemical Analysis	131
6.5 Results	131
6.5.1 Tributaries freshwater and dissolved inorganic nutrient inputs.....	131
6.5.2 Tides.....	134
6.5.3 Salt-marsh water-column characteristics	135
6.5.4 Seasonal nutrient tidal fluxes.....	139
6.5.5 Ice cores segments characteristics	142
6.6 Discussion	143
6.6.1 Validity of marshes nutrient fluxes calculations.....	143
6.6.2 Incidence of tributaries	144
6.6.3 Seasonal processes potentially implied in tidal nutrient fluxes	145
6.6.4 Role of sea ice	148
6.7 Conclusion	150
6.8 Acknowledgements	151
6.9 References.....	151
CHAPITRE VII	158
SEASONAL VARIABILITY OF DENITRIFICATION EFFICIENCY IN NORTHERN SALT MARSHES: AN EXAMPLE FROM THE ST. LAWRENCE ESTUARY	158
7.1 Abstract.....	158
7.2 Introduction.....	159

7.3 Materials and methods	160
7.3.1 Studied site.....	160
7.3.2 Sampling procedure	162
7.3.3 Laboratory incubations	162
7.3.4 Denitrification activity.....	163
7.3.5 Nitrogen species and dissolved oxygen fluxes	163
7.3.6 Analyses.....	164
7.3.7 Calculations	165
7.4 Results	167
7.5 Discussion	171
7.6 Acknowledgement.....	176
7.7 References.....	177
CHAPITRE VIII.....	182
MICROPHYTOBENTHOS COMMUNITIES FROM PRISTINE AND IMPACTED SALT MARSHES OF THE	182
ST. LAWRENCE ESTUARY (CANADA).....	182
8.1 Abstract.....	182
8.2 Introduction.....	183
8.3 Materials and methods	184
8.3.1 Study sites	184
8.3.2 Sampling and analyses.....	187
8.3.3 Statistical analyses	188
8.4 Results	188
8.4.1 Environmental variables	188
8.4.2 Microphytobenthos composition	190
8.5 Discussion	193
8.6 Acknowledgement.....	197
8.7 Literature cited	198
CHAPITRE IX.....	204
DISCUSSION GÉNÉRALE.....	204
9.1 Incidence des rejets d'azote de source anthropique sur l'estuaire du Saint-Laurent	204
9.2 Variabilité saisonnière des processus pélagiques impliqués dans le cycle de l'azote	208
9.3 Variabilité saisonnière des processus impliqués dans le cycle de l'azote au sein des marais côtiers de l'estuaire maritime	215
9.4 Incidence des marais côtiers dans la dynamique estuarienne du DIN.....	225
9.5 Potentiel de résilience de l'estuaire	228
9.6 Conclusion et perspective	230
9.7 References.....	235
ANNEXE 1.....	242
INVENTAIRE DES CONDITIONS PHYSICO-CHIMIQUES OBSERVÉES LORS DES CAMPAGNES D'ÉCHANTILLONNAGE DANS L'ESTUAIRE DU SAINT- LAURENT.....	242

LISTE DES TABLEAUX

Tableau II-1	Examples of ammonium determination ($n = 3$) in field samples with various physical and chemical properties.....	35
Tableau II-2	Determination of the practical limit of detection (LOD) of the method according to [16] and using five calibration curves obtained in five successive days.....	39
Tableau II-3	Comparison of analytical characteristics of ammonium determination procedures.....	40
Tableau III-1	Average values of the physical and chemical variables measured in SLE during each sampling period and calculated for USLE (0 m to bottom), LSLE-Surface (0 to 20 m), LSLE-Intermediate (20 to 150 m) and LSLE-Bottom (150 m to bottom). AV = Average, SE = Standard error, na = data not available.....	55
Tableau III-2	Average values of suspended particular matter characteristics measured in SLE during each expedition and calculated for USLE (0 m to bottom), LSLE-Surface (0 to 20 m), LSLE-Intermediate (20 to 150 m) and LSLE-Bottom +(150 m to bottom). AV = Average, \pm SE = Standard error.....	57
Tableau III-3	Average values of tyrosine molar ratio (Tyr/PHAA), PHAA concentration, PHAA-%N and DI measured in SLE during the July 2004, October 2005 and December 2005 expeditions. Values are calculated for USLE (0 m to bottom), LSLE-Surface (0 to 20 m), LSLE-Intermediate (20 to 150 m) and LSLE-Bottom (150 m to bottom). AV = Average, \pm SE = Standard Error and n = number of samples analysed.....	57
Tableau III-4	Result of two-way analyses of variance (ANOVAs) testing the effect among the regions of the Estuary (USLE – Surface and LSLE – Surface), and sampling periods (May 2003, July 2004, October 2005 and December 2005) and their interaction on ammonium (NH_4^+).....	60
Tableau III-5	Result of multiple stepwise (backward) regression models (stepwise procedure) to estimate the ammonium (NH_4^+) concentration in the Estuary and Gulf of St. Lawrence. Temperature (T , °C), \log_{10} salinity +1 (Sal, PSU), chlorophyll-a (Chl-a, $\mu\text{g l}^{-1}$), oxygen concentration (O_2 , mg l^{-1}), phosphate (PO_4^{3-} , μM), nitrite and nitrate ($\text{NO}_2^- + \text{NO}_3^-$, μM), silicate (Si(OH)_4 , μM), suspended particulate matter (SPM, $\mu\text{g l}^{-1}$), particulate organic nitrogen (PON, $\mu\text{g l}^{-1}$), particulate organic carbon (POC, $\mu\text{g l}^{-1}$) were the tested variables. ns: not significant. Partial R^2 is given below each regression coefficient (\pm SE), total R^2 , and mean squared errors (MSE) are also shown.....	60
Tableau III-6	Linear regression parameters defined for the mixing diagram of ammonium against salinity. Riverine and LSLE end members as well as nutrient fluxes were calculated from these regression lines. $P < 0.0001$ except for NH_4^+ in May 2003 ($P = 0.0002$) and July 2004 ($P = 0.1748$). Montly verage discharge at Quebec city (Station 1) calculated for each sampling period (http://www.osl.gc.ca/fr/donnees/debits/2000.html).....	61
Tableau III-7	Din fluxes through the USLE for each sampling period.	62

Tableau III-8	Stoichiometric analyses between Si, N and P in SLE superficial water mass (0 - 2 m) for each sampling period.	62
Tableau IV-1	Mean values of particulate organic carbon (POC, $\mu\text{g/l}$), C/N, chlorophyll-a (Chl-a $\mu\text{g/l}$), total dissolved inorganic nitrogen (DIN, μM), dissolved orthophosphate (P μM), dissolved oxygen (DO, μM), salinity and temperature ($^{\circ}\text{C}$) in bottom waters of lower St. Lawrence Estuary. Otherwise stated, numbers are average values of 2 samples collected between 250 and 330 m following station depth. ^a NA = data not available.....	84
Tableau IV-2	DO/DIN ratio, N* (nitrate deficit), dN (partial nitrification, $\mu\text{mol l}^{-1}$) and dN'' (denitrification, $\mu\text{mol l}^{-1}$) defined for the bottom waters of lower St. Lawrence Estuary using the average values of 2 samples collected between 250 and 330 m following station depth. ^a When Na > N > Nb, denitrification (dN'') is not contributing to the deficit. ^b Data not available.....	85
Tableau V-1	Comparison of environmental and biological variables in the USLE and in the LSLE during October and December 2005. The LSLE water column was analyzed as a three layer water mass, presenting a surface layer (0 to 20 m), and intermediate layer (20 to 150 m) and a bottom layer (>50 m). <DL: under the detection limit.....	105
Tableau V-2	Results of two-way analyses of variance (ANOVAs) testing the effect among the position in the Estuary (USLE Suf. and LSLE Suf.) and seasons (October 2005 and December 2005) and their interaction on bacterial abundance and % HNA. Transformations are mentioned when necessary to achieve the assumptions of the ANOVA. Note: LSLE = Lower St. Lawrence Estuary, USLE = Upper St. Lawrence Estuary.....	107
Tableau V-3	Results of two-way analyses of variance (ANOVAs) testing the effect among the water layers in the Lower St. Lawrence Estuary (0-20 m, 20-150 m and 150 m- bottom) and the seasons (October 2005, December 2005) and their interaction on bacterial abundance and % HNA. Transformation was not necessary to achieve the assumptions of the ANOVA. Note: Surf = Surface = 0 - 20m, Int = Intermediate = 20-150 m, Bot= Bottom = 150 m to the bottom.....	108
Tableau V-4	Spearman rank correlation coefficients between bacterial abundances (cell ml^{-1}) and %HNA ratios and environmental variables. The number of pair values in each data set is 88. Values** are significant at a level of $p < 0.01$ whereas values* are significant at a level of $p < 0.05$	109
Tableau VI-1	Outputs of hydrodynamic numerical model used for Outlet Flux calculation. Maximum tide heights observed at sites I and II (Max Tide Obs) and maximum tide heights computed by the model (Max Tide Model) for these sites are give according to the marsh surface (-0.5 m). The flooded marsh area (Flood Area) is the submerged area landward of the marshes cross section (dashed lines on Figure 2) at high tide. Max Tidal Flux stand for maximum tidal flux computed through the marshes cross section of Pointe-aux-Épinettes (PAE) and Pointe-au-Père (PAP) salt marshes.....	135

Tableau VI-2 Characteristics (average, AV, and standard deviation, SD) of ice core sections. Ice cores were collected the 4 February 2005 from one control pelagic site located offshore in the Saint-Lawrence estuary (SLE) as well as in the Pointe-aux-Épinette (PAE) and Pointe-au-Père (PAP) salt marshes.....	143
Tableau VII-1 Geochemical characteristics (mean values) of sediment samples collected in St. Lawrence Estuary salt marsh in 2005.....	168
Tableau VII-1 Mean values (AV) and standard deviations (SD) of sediment characteristics analyzed at stations PELM (Pointe-aux-Épinettes low marsh), PEHM (Pointe-aux-Épinettes high marsh), PPLM (Pointe-au-Père low marsh) and PPHM (Pointe-au-Père high marsh).	189
Tableau VIII-2 Mean values (AV) and standard deviations (SD) of microphytobenthic variables analyzed at stations PELM (Pointe-aux-Épinettes low marsh), PEHM (Pointe-aux-Épinettes high marsh), PPLM (Pointe-au-Père low marsh) and PPHM (Pointe-au-Père high marsh).	189
Tableau VIII-3 List of microphytobenthic species and their abundance (%) at stations PELM (Pointe-aux-Épinettes low marsh), PEHM (Pointe-aux-Épinettes high marsh), PPLM (Pointe-au-Père low marsh) and PPHM (Pointe-au-Père high marsh) in July 2005.	191
Tableau VIII-4 Results of multiple linear regression testing the effect of environmental variables on MPB density and abundance of epipelic and epipsammic forms at stations PELM (Pointe-aux-Épinettes low marsh), PEHM (Pointe-aux-Épinettes high marsh), PPLM (Pointe-au-Père low marsh) and PPHM (Pointe-au-Père high marsh).	192

LISTE DES FIGURES

Figure I-1	Le cycle de l'azote; les flèches noires représentent les processus de réduction et les flèches grises, les processus d'oxydation. (Adaptée de Madigan <i>et al.</i> , 2002).....	3
Figure I-2	Sites à l'étude; l'estuaire du Saint-Laurent (en haut), le marais de Pointe-aux-Épinettes (en bas à gauche) et le marais de Pointe-au-Père (en bas à droite).....	14
Figure I-3	Situation géographique des stations d'échantillonnage dans l'estuaire et le golfe du Saint-Laurent. USLE représente l'estuaire supérieur, LSLE l'estuaire maritime et GSL le golfe du Saint-Laurent.....	18
Figure I-4	Sites d'échantillonnage dans les marais côtiers de l'estuaire du Saint-Laurent. La bathymétrie est exprimée en mètre.	20
Figure II-1	Time course of the reaction of OPA with ammonium at room temperature (22 °C). Field samples were collected in a small river and a saltmarsh in the provincial park of Bic close to Rimouski. Samples were incubated in 25 mL borosilicate test tubes. Aliquots were transferred into microplate following given time intervals for fluorescence reading.	31
Figure II-2	Time course of the ammonium/OPA reaction at room temperature (22 °C). Incubation carried directly in polystyrene microplates was compared with incubation in glass tubes followed by reading in microplates. Natural freshwater samples were collected from Rimouski River.....	31
Figure II-3	A typical 48-well microplate scheme showing standards in triplicate on the left side, reagents background blanks (BF in 5 wells) and sample background blanks (BG) in the middle. Samples and samples with surrogate to determine matrix effect (ME) are located on the right side of the plate. The reading of the whole plate takes 30 seconds.....	33
Figure II-4	Influence of salinity on the fluorescence signal obtained for ammonium (1.00 µM) in five successive determinations over the entire range of salinity (0-35). Deviation is calculated against the response obtained for the same ammonium concentration in deionised freshwater used as reference.....	37
Figure II-5	Standard curves obtained following a 4h-incubation at 22°C. A) low, B) medium, C) high ammonium concentrations. Measurements were repeated in triplicate over three consecutive days.	38
Figure II-6	Ammonium concentration determined during a complete tidal cycle in the Pointe-au-Père saltmarsh. Symbols stand for ammonium (●); temperature (□); salinity (Δ) and suspended particular matter (◊).....	41
Figure III-1	Sampling area. Numbers in black circle correspond to the sampling station labels. The dotted line represents the virtual geographical separation between the Upper (USLE) and Lower (LSLE) St. Lawrence Estuary. GLS = Gulf of St. Lawrence.....	50
Figure III-2	Vertical profile of ammonium along the main axis of St. Lawrence Estuary between Québec Bridge (station 1) and Anticosti Island (station	

12) for the four cruises. Black circles correspond to sampling depth.	
Note that the scales of the 2 different axes are different.	59
Figure III-3 Mean (\pm SE) of surface (0 - 20 m) ammonium concentration obtained for each sampling period in both St. Lawrence Estuary regions. Different letters indicate a significant difference between regions at a given sampling period ($\alpha = 0.05$).....	60
Figure III-4 Mixing diagram of ammonium concentration against salinity in the USLE. (\circ = May 2003, \square = July 2004, \diamond = October 2005 and Δ = December 2005).....	62
Figure IV-1 Sampling area in Lower St. Lawrence Estuary. Letters in black circle correspond to the sampling stations.....	79
Figure IV-2 Dissolved oxygen profiles of the four stations sampled in different seasons. Lines state for in situ CTD profiles whereas forms indicate the depth at which Winkler titrations were performed (\diamond = July 2004, \circ = October 2005, \square = December 2005 and \circledcirc = February 2006).....	81
Figure IV-3 Nitrate + nitrite profiles of the four stations sampled in different seasons. Forms indicate analysed samples.....	81
Figure IV-4 Suspended particulate organic matter C/N ratio profiles of the four stations sampled in different seasons. Forms indicate analysed samples....	82
Figure V-1 Sampling area and location of the sampling stations. The dotted line represents the geographical separation between the Upper (USLE) and Lower (LSLE) St. Lawrence Estuary.	99
Figure V-2 Longitudinal profiles of total bacteria (TB) abundance and %HNA with depth along the sampling area during (A) October 2005 and (B) December 2005. Sampling depths are indicated by black dots. The produced 2D figures present a compressed vertical scale magnitude $\times 1450$ compared to the horizontal scale.	106
Figure V-3 Distribution of HNA and LNA cells at station 9 in the surface (SL), intermediate (IL) and deep (DL) layers of LSLE in (A) October and (B) December 2005. Bacteria were detected in a plot of green fluorescence recorded at 530 ± 30 nm (FL1) versus side angle light scatter (SSC) and were presented on logarithmic scales on the cytograms. Fluorescent beads were added as an internal standard to normalize cell fluorescence emission and light scatter values of each sample.	110
Figure VI-1 The Lower St. Lawrence estuary (G1) nested grid set-up used to compute tidal volume fluxes at the seaward boundaries of each Pointe-aux-Épinettes (PAE; G4) and Pointe-au-Père (PAP; G5) marshes, with intermediate grids G2 and G3. On grid G1, contour interval is 50 m.	124
Figure VI-2 The G4 and G5 grids enclosing the Pointe-aux-Épinettes (PAE) and Pointe-au-Père (PAP) marshes. A, B, C, D, E, F and G represent sampled tributaries, I and II represent marshes outlet sampling sites and the dashed lines represent the virtual limit between marshes and estuary used for flux calculations. Bathymetries are in meter and the zero contour is the mean sea level. Stations I and II are both 0.5 m below the map zero. The lower marsh is located between -0.5 and + 1.0 m and upper marsh is landward of the 1.0 m contour line. Bathymetry of the	

	study areas comes from high resolution field survey while bathymetry from deeper area is taken from marine chart.....	126
Figure VI-3	Typical example of tide cycle (tide height above marsh surface at site II) with associate temporal patterns of modeled tide level (top) and flow (bottom). Dashed line stand for field observation and solid line for numerical simulation. The asymmetry of observed tide curve is induced by wind effects, barometric pressure changes, marsh roughness (small scale irregularities) and sediment porosity.	130
Figure VI-4	Mean monthly streams discharge vs mean monthly stream nutrient concentrations showed for Pointe-aux-Épinettes marsh (PAE) and Pointe-au-Père marsh (PAP) on a log/log scale.....	133
Figure VI-5	Affluent nutrient fluxes from Pointe-aux-Épinettes (PAE) and Pointe-au-Père (PAP) marshes (monthly average \pm standard deviation from weekly measurements taken from 17 June 2003 to 18 June 2004). From December to March, there is no data in PAE since streams are turned to ice. Nutrients fluxes are presented in a log scale.....	134
Figure VI-6	Diurnal variations of tide height above marsh surface, Chl- a average concentration, temperature and salinity monitored at station I (Pointe-aux-Épinettes, PAE) and II (Pointe-au-Père, PAP) during the four seasonal surveys.....	136
Figure VI-7	Diurnal variations of ammonium (NH_4^+), phosphate (PO_4^{3-}), nitrite + nitrate ($\text{NO}_2^- + \text{NO}_3^-$) and silicate (Si(OH)_4) average concentrations monitored at station I (Pointe-aux-Épinettes, PAE) and II (Pointe-au-Père, PAP) during the four seasonal surveys.....	138
Figure VI-8	Runoff nutrient concentrations from Pointe-aux-Épinettes (PAE) and Pointe-au-Père (PAP) marshes registered at low tide at station I and II (monthly average \pm standard deviation from weekly measurements taken from 17 June 2003 to 18 June 2004). Filled symbols indicate nutrient concentrations registered during seasonal survey.....	139
Figure VI-9	Estimated marsh nutrients fluxes for Pointe-aux-Épinettes (PAE) and Pointe-au-Père (PAP) marshes. Average \pm standard deviation values are given for the four seasonal surveys. Error bars represent variability in nutrient concentration between the triplicate nutrient samples.	141
Figure VI-10	Estimated marsh nutrients fluxes in the lower St. Lawrence Estuary marshes. Average \pm standard deviation values are given for the four seasonal surveys.....	142
Figure VII-1	Map of Pointe-au-Père salt marsh located along the St-Lawrence Estuary south shore in Rimouski. The white area represents the infra-littoral zone, dark grey area the inter-tidal zone and light grey area the supra-littoral zone. The black square represents the 10-m ² sampling area.	161
Figure VII-2	Contribution of denitrification rates produced within the sediment cores by nitrification (Dn in grey) and denitrification rates coming from overlying water (Dw in black) to total denitrification (Dt) as a function of incubation temperatures. Values represent mean \pm SD (n = 8).....	169
Figure VII-3	Dissolved oxygen uptake rates as a function of incubation temperatures. Values represent mean \pm SD (n = 4).....	169

Figure VII-4	Nitrate consumption rates (in grey) and ammonium production rates (black) as a function of incubation temperatures. Values represent mean \pm SD ($n = 4$)	170
Figure VII-5	Typical HPLC chromatogram of THAA extracted from Pointe-au-Père salt marsh sediment sampled in August 2005. main identified amino acids are aspartic acid (Asp), glutamic acid (Glu), serine (Ser), threonine (Thr) and alanine (Ala).	171
Figure VIII-1	Map of the St. Lawrence Estuary showing the location of the Pointe-aux-Épinettes (PE) and the Pointe-au-Père (PP) salt marshes along with sampling stations.....	186
Figure IX-1	Concentration d'azote organique dissous (DON) mesurées à la station 8 (Rimouski). Les triangles représentent les données de 1970 Brindle et d'Amour, (1977) obtenues mensuellement entre août 1973 et octobre 1974. Les cercles noirs représentent les données obtenues lors des campagnes mai 2003 et juillet 2004.	206
Figure IX-2	Concentration d'azote inorganique dissous (DIN) mesurées à la station 8 (Rimouski). Les triangles représentent les données de 1970 Brindle et d'Amour, (1977) obtenues mensuellement entre août 1973 et octobre 1974. Les cercles noirs représentent les données obtenues lors des campagnes mai 2003 et juillet 2004.	206
Figure IX-3	Ratios stochiométriques des éléments nutritifs mesurés à la station 8 (Rimouski) dans la masse d'eau de surface (2 m). Les triangles représentent les données de 1970 selon Brindle et d'Amour, (1977) obtenues mensuellement entre août 1973 et octobre 1974. Les cercles noirs représentent les données obtenues lors des campagnes mai 2003 et juillet 2004.	208
Figure IX-4	Composition isotopique du carbone organique particulaire (exprimée en ‰ par rapport à PDB) dans l'estuaire du Saint-Laurent au cours de la campagne mai 2003.	210
Figure IX-5	Composition isotopique de l'azote particulaire total (exprimée en ‰ par rapport à air) dans l'estuaire du Saint-Laurent au cours de la campagne mai 2003.	211
Figure IX-6	Bilan saisonnier d'azote inorganique dissous (DIN) pour le marais de Pointe-aux-Épinette (PAE; présenté en kg N 90j ⁻¹). Les flux négatifs indiquent une perte en azote pour le système alors que les flux positifs indiquent un gain. Les flux inscrits in gras sont issus de mesures directes alors que ceux inscrits en italiques sont estimés. fix = fixation; dénit. = dénitrification; préc. = apports atmosphériques solides et liquides; marées = échanges tidaux; trib. = apports continentaux; assim. = assimilation et minér. = minéralisation.....	218
Figure IX-7	Bilan saisonnier d'azote inorganique dissous (DIN) pour le marais de Pointe-au-Père (PAP; présenté en kg N 90j ⁻¹). Les flux négatifs indiquent une perte en azote pour le système alors que les flux positifs indiquent un gain. Les flux inscrits in gras sont issus de mesures directes alors que ceux inscrits en italiques sont estimés. fix = fixation; dénit. = dénitrification; préc. = apports atmosphériques solides et liquides;	

	marées = échanges tidaux; trib. = apports continentaux; assim. = assimilation et minér. = minéralisation.....	219
Figure IX-8	Bilan saisonnier de NO ₂ - + NO ₃ - (bleu) et NH ₄ ⁺ (rouge) pour le marais de Pointe-aux-Épinette (PAE; présenté en kg N 90j ⁻¹). Les flux négatifs indiquent une perte en azote pour le système alors que les flux positifs indiquent un gain. fix = fixation; dénit. = dénitrification; préc. = apports atmosphériques solides et liquides; marées = échanges tidaux; trib. = apports continentaux; assim. = assimilation, ammo. = ammonification; DNRA = réduction dissimilatrice des nitrate en ammonium et nitr. = nitrification.....	222
Figure IX-9	Bilan saisonnier de NO ₂ - + NO ₃ - (bleu) et NH ₄ ⁺ (rouge) pour le marais de Pointe-au-Père (PAP; présenté en kg N 90j ⁻¹). Les flux négatifs indiquent une perte en azote pour le système alors que les flux positifs indiquent un gain. fix = fixation; dénit. = dénitrification; préc. = apports atmosphériques solides et liquides; marées = échanges tidaux; trib. = apports continentaux; assim. = assimilation, ammo. = ammonification; DNRA = réduction dissimilatrice des nitrate en ammonium et nitr. = nitrification.....	223
Figure IX-10	Bilan annuel d'azote inorganique dissous (DIN) dans l'estuaire du Saint-Laurent (présenté en T N a ⁻¹) (moyenne ± équart type).	227
Figure A-1	Mai 2003	243
Figure A-2	Juillet 2004.....	244
Figure A-3	Octobre 2005.....	245
Figure A-4	Décembre 2005	246

CHAPITRE I

Introduction

1.1 Introduction générale

L'azote est l'un des éléments clé de la synthèse de la matière organique à partir de la matière minérale. Élément constitutif principal des protéines et des gènes, sa disponibilité contrôle le fonctionnement de nombreux écosystèmes marins (Vitousek *et al.*, 1997; Herbert, 1999). En régulant la productivité des communautés phytoplanctoniques, l'azote joue un rôle prépondérant sur les premiers maillons de la chaîne trophique de nombreux environnements marins côtiers où il agit à titre d'élément biolimitant (Carpenter et Capone, 1983). Au sein de tels milieux, l'azote assimilé par les organismes autotrophes (majoritairement sous forme d'ammonium NH_4^+ et de nitrate NO_3^-) provient essentiellement d'apports allochtones d'origine continentale ainsi que d'apports autochtones issus de la minéralisation de la matière organique (MO) par les communautés microbiennes (Blackburn et Sorensen, 1988). Indépendamment de son origine, la MO contient une part de macromolécules azotées telles que des protéines, des acides nucléiques, des peptides ainsi que des composés de faible poids moléculaire tels les acides aminés ou l'urée. En milieu marin, ces composés organiques sont affectés par de multiples réactions d'oxydo-réduction catalysées par des communautés microbiennes spécialisées conduisant à la formation de produits intermédiaires susceptibles d'être utilisés à leur tour comme nutriment par d'autres communautés (Herbert et Nedwell, 1990).

Alors que dans les environnements océaniques, le recyclage de la MO s'opère directement dans la colonne d'eau (généralement sous la thermocline) supportant une production dite régénérée (Mann et Lazier, 1991), la dynamique des environnements côtiers peu profonds est fortement couplée à celle du compartiment benthique (Davidson-Arnott *et al.*, 2002). Ainsi, la régénération des nutriments azotés au sein du compartiment sédimentaire (principalement contrôlé par la quantité et la qualité des sédiments fraîchement déposés, par la diffusion à l'interface eau/sédiment ainsi que par la

bioturbation (Mermilliod-Blondin *et al.*, 2004) constitue une importante source d'espèces azotées pour la production primaire. Lorsque les microfaunes hétérotrophes sont exposées à des flux sédimentaires de faible intensité, ces derniers parviennent à dégrader la fraction labile de la MO déposée avant qu'elle ne soit enfouie par les macro-organismes benthiques. Sous de telles conditions, la minéralisation de la MO s'effectue principalement au niveau des sédiments de surface (0-2 cm) *via* la respiration aérobie. Par ailleurs, en milieu côtier peu profond, le flux de matière organique est fréquemment supérieur aux potentialités de dégradation aérobie. L'oxygène dissous présent dans les eaux porales est ainsi rapidement consommé par l'activité microbienne hétérotrophe dans la colonne sédimentaire. En absence d'oxygène, les accepteurs d'électrons tels les nitrates (NO_3^-), le manganèse (Mn^{4+}), le fer (Fe^{3+}), les sulfates (SO_4^{2-}) et les ions bicarbonates (HCO_3^-) peuvent être utilisés de façon successive comme agents oxydants par des communautés bactériennes anaérobies. Ainsi, dans les environnements sédimentaires anoxiques, la minéralisation de la MO est effectuée par l'action conjuguée de communautés bactériennes qui possèdent des activités métaboliques complémentaires. L'utilisation successive de ces oxydants par les communautés bactériennes induit des conditions physico-chimiques distinctes au sein de chacun des horizons sédimentaires qui à leur tour, vont soutenir des processus bactériens spécifiques. Ainsi, le cycle de l'azote dans les environnements marins côtiers répond à une dynamique complexe, contrôlée à la fois par des facteurs physico-chimiques et des processus biologiques.

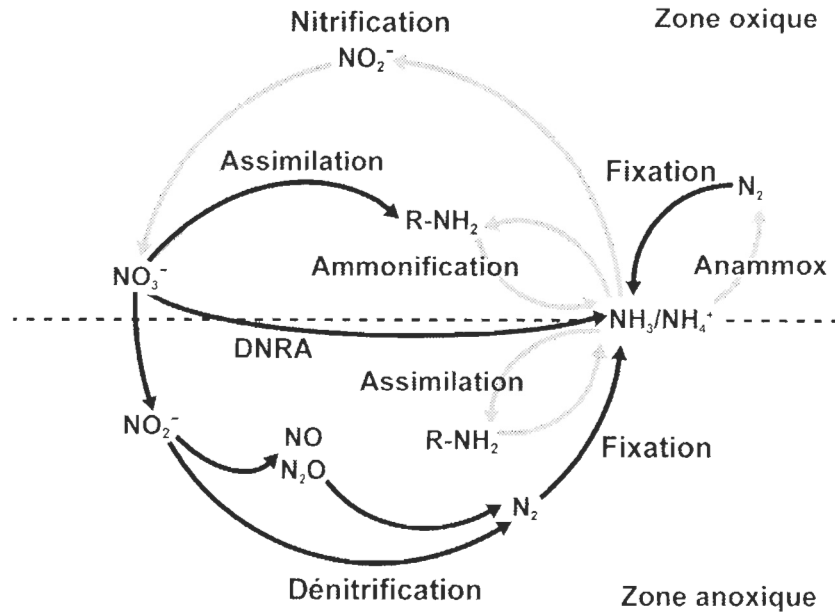


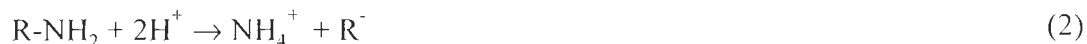
Figure I-1 Le cycle de l'azote; les flèches noires représentent les processus de réduction et les flèches grises, les processus d'oxydation. (Adaptée de Madigan *et al.*, 2002).

Le cycle de l'azote, présenté de façon schématique à la figure I-1, décrit la succession de modifications subies par les différentes espèces de l'azote (azote organique, NH_3 , NH_4^+ , N_2 , N_2O , NO , NO_2^- , NO_3^-) dans un environnement sédimentaire côtier type, présentant une couche de surface oxique et un horizon basal anoxique. Indépendamment des apports advectifs, qui constituent la principale source d'azote pour les organismes évoluant en milieux côtiers, la fixation biologique est un processus possédant une grande portée écologique, et ce plus spécialement en milieu oligotrophe, car elle permet un transfert direct de l'azote atmosphérique vers le biotope. Bien que 79% de l'atmosphère terrestre soit composée d'azote moléculaire libre (N_2), cet important réservoir ne constitue une source nutritionnelle que pour un nombre restreint d'organismes capables d'opérer une réduction de cet azote, retrouvé dans ce réservoir sous sa forme la plus stable (c'est-à-dire $\text{N} \equiv \text{N}$). Ces organismes dits diazotrophes, appartiennent au groupe des procaryotes et possèdent un enzyme particulier; la nitrogénase. La nitrogénase, présente notamment chez certains genres de cyanobactéries incluant, les *Chromatiaceae*, les *Chlorobiadeae*, les *Chloroflexaceae* et les *Rhodospirillaceae*, catalyse la réaction suivante :



Cette réaction inhibée par la présence d'oxygène est effectuée tant par des bactéries autotrophes, hétérotrophes photosynthétiques que par des bactéries non photosynthétiques. Par ailleurs, le coût énergétique de la fixation de l'azote étant élevé (16 ATP par N₂) il apparaît clair que les bactéries diazotrophes autotrophes aient un avantage sélectif comparé aux organismes hétérotrophes. Dans les environnements marins côtiers, le processus de fixation est reconnu pour avoir une importante incidence sur la disponibilité de l'azote au sein des communautés microbiennes (Whitney *et al.*, 1975). De plus, les bactéries fixatrices associées aux rhizomes et racines des communautés de macrophytes (par exemple : *Spartina alterniflora*, *Zostera marina*), présentes dans les environnements intertidaux, sont reconnues pour stimuler la croissance des végétaux hôtes (Patriquin et Knowles, 1972; Capone et Taylor, 1980; Blackburn *et al.*, 1994). Par ailleurs, la faible distribution des communautés bactériennes possédant cette capacité et l'importante disponibilité de nutriments azotés (notamment NH₄⁺) restreignent l'influence de ce processus sur le bilan global d'azote des milieux côtiers (Carpenter *et al.*, 1978).

Tel que précédemment mentionné, l'un des aspects cruciaux du cycle de l'azote en milieu côtier concerne la minéralisation microbienne de la MO labile fraîchement déposée. Dépendamment de sa source et de sa structure moléculaire, la MO subit soit; une simple réaction de déamination ou encore une série de réactions métaboliques complexes impliquant des hydrolyses enzymatiques qui contribuent à fractionner les macromolécules azotées (par exemple: protéines, acides aminés, acides nucléiques, polypeptides) en monomères solubles (ammonium). Ce processus, nommé ammonification peut-être exprimé de façon schématique comme suit :



L'ammonification est un processus largement répandu en milieu marin côtier, effectué par une vaste gamme de micro-organismes possédant des enzymes protéinases et peptidases. Parmi ces organismes, mentionnons les membres des genres, *Bacillus*, *Clostridium*, *Proteus*, *Pseudomonas*, *Serratia* et *Vibrio* (Alexander, 1977). Dans les environnements

côtiers peu profonds, affectés par des flux de MO importants, il a été démontré que l'ammonification pouvait soutenir jusqu'à 80% de la production primaire de ces milieux (Jensen *et al.*, 1990). Par ailleurs, l'ensemble de l'ammonium ainsi produit n'est pas entièrement disponible pour les organismes autotrophes occupant ces zones de transition. Dépendamment des conditions physico-chimiques qui prévalent au sein de la colonne sédimentaire, l'ammonium peut être adsorbé sur la fraction argileuse (Mackin et Aller, 1984), subir une réaction d'oxydation (supportée par les nitrites) en milieu anoxique pour être transformé en azote moléculaire (anammox) (Dalsgaard *et al.*, 2003) ou être oxydé en nitrites et nitrates, en milieu oxique, par des bactéries chimiotrophes dite nitrifiantes (Nishio *et al.*, 1983).

Constituant un pont entre les espèces réduites et oxydées, la nitrification est un processus clé du cycle de l'azote jouant un rôle prédominant dans la majorité des écosystèmes. Agissant comme un puits d'ammonium et comme une importante source de nitrates pour les processus de réduction bactérienne des nitrates (dénitrification et ammonification des nitrates), la nitrification procure également une source d'azote importante pour la production primaire dite régénérée. De plus, le couplage de ce processus aérobie et des processus anaérobiques, comme la dénitrification, joue un rôle écologique significatif dans les environnements marins côtiers puisqu'il permet le réacheminement de l'azote fixé vers le réservoir atmosphérique sous forme d'oxyde d'azote et d'azote moléculaire (Blackburn et Sorensen, 1988). La nitrification (l'oxydation bactérienne de l'ammonium en nitrate en milieu aérobie strict) s'effectue en deux étapes. La première étape, catalysée par des bactéries dites nitrosantes (dont les genres les mieux connus sont *Nitrosonas*, *Nitrosococcus*, *Nitrosospira*, *Nitrosolobus* et *Nitrosovibrio*), conduit à la production de nitrites à partir de l'ammonium, alors que la seconde étape, effectuée par les bactéries dites nitratantes (*Nitrobacter*, *Nitrosococcus*, *Nitrospina* et *Nitrospira*) permet l'oxydation des nitrites en nitrates (Bock *et al.*, 1992).



Dans les milieux naturels, la nitrification est reconnue pour être régulée par de nombreux facteurs environnementaux tels la température, le pH, la salinité, la concentration en ammonium et en oxygène dissous ainsi que par la présence de racines de macrophytes et de terriers de la macrofaune épibenthique (Herbert, 1999).

Alors que la nitrification implique l'oxydation séquentielle des espèces réduites de l'azote par des bactéries aérobies, la dénitrification est un processus réductif par lequel des bactéries chimiotrophes utilisent les nitrates comme accepteur d'électrons lors de la respiration (Blackburn et Sorensen, 1988). La production d'espèces azotées gazeuses (N_2 et N_2O) à partir de la réduction bactérienne des nitrates se nomme dénitrification (eg. Wang *et al.*, 2003) alors que la production d'ammonium, *via* ce même processus, se nomme ammonification des nitrates ou DNRA (dissimilatory nitrate reduction to ammonium) (par exemple : Gardner *et al.*, 2006). Ces processus peuvent être exprimés schématiquement *via* les réactions suivantes:



Un groupe important de bactéries anaérobies appartenant au genre *Pseudomonas*, capables de synthétiser différents types d'enzymes réductases, peut utiliser les oxydes d'azotes, en occurrence les nitrates, comme accepteurs d'électrons lors de l'oxydation de la MO, en absence d'oxygène (Knowles, 1981). La dénitrification est un processus bactérien possédant un rôle écologique déterminant; en plus de participer au maintient de la biolimitation de l'azote de certains environnements marins côtiers (Howarth, 1988), la dénitrification offre un mécanisme naturel pour atténuer l'effet des apports de nutriments azotés de source anthropique au sein de milieux impactés (Seitzinger, 1988). De ce fait, la dénitrification est en mesure d'agir de façon significative sur le processus d'eutrophisation (par exemple Nowicki *et al.*, 1997) qui gagne inexorablement les zones côtières de part le monde (Cloern, 2001).

1.2 Problématique environnementale

À l'instar du carbone, l'azote est l'un des constituants dont le cycle naturel est le plus modifié par les activités humaines (Boyd, 2001). Alors qu'au cours de la période préindustrielle, la fixation biologique globale était estimée à environ 100 millions de tonnes d'azote par année (Martinez et Béline, 2002), l'activité anthropique est parvenue à niveler voire supplanter ce taux de fixation d'origine naturelle. Pour faire face à une croissance de la population de l'ordre de 1 milliard d'individus tous les 12 ans, la transformation de l'azote moléculaire en formes bio-assimilables se situe désormais à 290 millions de tonnes par an, dont 80 millions de tonnes provenant de la synthèse d'engrais chimiques destinés à des fins agricoles (Galloway, 1998). Dans le but d'alimenter une population toujours grandissante, la production et l'utilisation massive de ces engrais s'est accrue de façon exponentielle (Vezjak *et al.*, 1998), engendrant une importante augmentation des émissions d'oxydes d'azote (NO_x et N_2O) et d'ammoniac (NH_3) qui atteindraient respectivement 31, 15 et 54 millions de tonnes par an (Olivier *et al.*, 1998). Toujours dans le but de pallier à cette croissance démographique, l'industrie agroalimentaire génère chaque année des millions d'animaux d'élevage. Le flux annuel d'azote ingéré par ces animaux est de l'ordre de 110 millions de tonnes, dont seules 10 millions de tonnes sont transformées en produits alimentaires, alors que 100 millions de tonnes d'azote associé aux déjections animales sont rejetées de façon plus ou moins directe dans les écosystèmes (Martinez et Béline, 2002). En plus de contribuer à l'effet de serre (N_2O), ces émissions de produits azotés sont transférées vers les eaux de surfaces et souterraines, puis vers les environnements de transition où elles sont les précurseurs de graves problèmes d'eutrophisation (Cloern, 2001; Flindt *et al.*, 1999; Martinez et Béline, 2002; Livingston, 2001). Bien qu'à l'échelle du globe et sur une échelle temporelle relativement longue, la fixation demeure en équilibre avec les processus de dénitrification (concept de Redfield), la rapidité avec laquelle l'activité anthropique affecte le bilan d'azote global (quelques décennies) laisse présager d'éventuelles perturbations tant au niveau du cycle du carbone que du cycle de phosphore (Falkowsky, 1997).

Parallèlement à la problème agroalimentaire généralement associée aux régions rurales, l'étalement urbain engendre de profonds changements au niveau des écosystèmes

riverains, estuariens et marins côtiers (Nedwell *et al.*, 2002). Ces milieux demeurent largement affectés par les eaux d'égouts municipaux, constituant une source ponctuelle importante d'éléments nutritifs azotés pour ces écosystèmes. Bien que la majorité des municipalités modernisent leurs stations d'épuration (Laurin, 2006), un nombre important d'entre elles rejette toujours leurs effluents dans les eaux côtières. Les champs d'épuration, encore largement utilisés par les particuliers, libèrent aussi de l'azote pouvant être transporté dans les eaux souterraines jusqu'aux eaux côtières. De plus, le développement d'une multitude d'activités industrielles et commerciales associées à l'urbanisation est susceptible d'altérer le cycle de l'azote en milieux côtiers (Verity, 2002; Vitousek *et al.*, 1997). À l'échelle du bassin versant, cette altération se traduit par une mobilisation accrue des espèces azotées tant par les voies terrestres (Nedwell *et al.*, 2002) qu'aériennes (Cornell *et al.*, 2003). À l'échelle du globe, ces mêmes émissions d'azote contribuent au réchauffement planétaire (N_2O) et conséquemment, à la remontée du niveau moyen des océans (Mann et Lazier, 1991; Galloway, 1998).

Le concept d'eutrophisation, généralement employé pour caractériser les environnements riches en nutriments, a été introduit par Nauman dès le début du 20^e siècle (Nauman, 1919). La communauté scientifique s'est ainsi depuis longtemps intéressée aux effets de la charge nutritive dissoute sur les populations d'algues pélagiques en faisant appel à deux concepts antagonistes soit, l'oligothrophie et l'eutrophie. À l'échelle du globe, l'eutrophisation s'accentue de façon dramatique jour après jour et engendre la détérioration de la qualité des eaux côtières (Vezjak *et al.*, 1998; Cloern, 2001; Vitousek *et al.*, 1997 Rabalais et Nixon, 2002; Howarth et Marino, 2006). De façon générale, les milieux estuariens seraient les environnements les plus touchés (Flindt *et al.*, 1999). De plus, la problématique concernant la dispersion massive de produits azotés ne serait pas limitée aux régions chaudes et surpeuplées du globe, mais pourrait avoir des répercussions importantes sur les milieux marins côtiers des hautes latitudes, puisque l'azote agit à titre d'élément biolimitant sur bon nombre de ces environnements (Livingston, 2001). Par conséquent, l'écosystème de l'estuaire du Saint-Laurent ne serait pas à l'abri de ce problème. Les environnements estuariens, plus précisément ceux de type marais côtiers, seraient particulièrement vulnérables à cette problématique, puisqu'ils sont affectés par des

échanges d'eau limités (Herbert, 1999). Ces milieux se trouvant fréquemment à la confluence de rivières, de ruisseaux et d'émissaires variés, voient depuis quelques années leur dynamique profondément perturbée (Page *et al.*, 1995; Herbert, 1999; Mason *et al.*, 2003; Flindt *et al.*, 1999). Menacés par les changements climatiques, par la baisse des apports d'eau douce, par la diminution des apports sédimentaires alluviaux et par la remontée eustatique du niveau marin (Boorman, 1999; Dionne, 1986), leur pérennité jadis assuré par leur recul sur le continent est rendu impossible eu égard à la présence de digues et d'infrastructures de toutes sortes (Mason *et al.*, 2003). Possédant une faible capacité de régénération (Dionne, 1986), ces écosystèmes hautement productifs constituent des espaces importants pour la biodiversité des écosystèmes riverains (Nixon, 1980), une niche écologique de choix pour des centaines d'espèces aquatiques (Boorman, 1999) et un réservoir de nutriments inorganiques pour la production primaire pélagique côtière (Billen et Lancelot, 1988). Occupant la zone de transition entre les environnements continentaux et marins, ces milieux demeurent des environnements dynamiques très complexes, caractérisés par un fort couplage des processus marins/continentaux, pélagiques/benthiques (Davidson-Arnott *et al.*, 2002). Si le rôle biogéochimique de ces milieux, notamment sur le cycle de l'azote en milieu estuaire, demeure méconnu ou mitigé (composante systématiquement négligée en modélisation des systèmes estuariens), il est toutefois clair que la destruction de ces environnements se traduirait par une perte écologique sérieuse. Bien qu'il soit généralement reconnu que les milieux littoraux de type marais côtier jouent un rôle important au niveau des processus de séquestration/dispersion de l'azote dans les estuaires (Tan et Strain, 1979; Walsh, 1991; Boorman, 1999), les processus physiques et les mécanismes biochimiques responsables de cette dynamique demeurent ignorés d'un point de vue quantitatif (Vitousek *et al.*, 1997). Dans la perspective où le problème de l'eutrophisation gagnerait en importance (Galloway, 1998), il devient fort opportun de comprendre la dynamique géochimique de l'azote de la frange littorale de l'estuaire du Saint-Laurent dans le but d'entreprendre des actions concrètes pour assurer son intégrité.

1.3 Objectifs généraux

Bien que les principaux aspects des cycles océanographiques de l'estuaire du Saint-Laurent soit relativement bien connus (par exemple Koutitonsky et Bugden 1991;

Savenkoff *et al.*, 2001) on trouve peu de données empiriques permettant de caractériser les processus saisonniers impliqués dans le cycle de l'azote (Greisman et Ingram, 1977; Coote et Yeats, 1979 ; Vézina *et al.*, 1995; Plourde et Therriault, 2004). Les études traitant des impacts environnementaux engendrés par la dispersion de produits azotés de nature anthropique au sein de cet environnement demeurent tout aussi rares (Howarth *et al.*, 1996; Ro *et al.*, 1998; Painchaud, 1999; Chambers *et al.*, 2001; deBruyn *et al.*, 2003). Au cours des dernières années, l'observation de conditions hypoxiques dans la masse d'eau profonde de l'estuaire, possiblement induite par un accroissement de la proportion d'eau chaude et pauvre en oxygène en provenance de l'océan Atlantique ainsi que par une augmentation du flux de matière organique vers les fond marins (Gilbert *et al.*, 2005) a relancé les efforts de recherche. Ces récents travaux, ainsi que ceux de Thibodeau *et al.* (2006) ont clairement montré les effets croissants de l'eutrophisation sur le milieu estuarien. En revanche, la dynamique saisonnière des nutriments azotés impliqués dans ce phénomène demeure largement inconnue. La caractérisation et la quantification des flux de sources endogènes et exogènes, leurs contributions relative sur les pools d'azote organique et inorganique de l'estuaire ainsi que leurs incidences respective sur les communautés phytoplanctoniques et bactériennes demeurent une question ouverte. De plus, le rôle des milieux intertidaux sur le cycle biogéochimique de l'azote reste à définir, et ce spécialement au cours de la saison hivernale. Ainsi, la dynamique de l'azote dans l'estuaire du Saint-Laurent et l'impact des marais côtiers bordant son littoral sur cette dernière suscitent donc de nombreuses questions. Dans le cadre de cette étude, nous tâcherons de répondre plus spécifiquement à trois d'entre elles énoncées ci-dessous, sous forme d'objectifs généraux :

1. Identifier et quantifier les principaux processus et les mécanismes saisonniers impliqués dans le cycle de l'azote à l'échelle de l'estuaire ainsi que dans les écosystèmes de type marais salant bordant son littoral.
2. Définir le rôle des marais côtiers (en tant que puits/source d'azote) sur la dynamique de l'azote en milieu estuarien.
3. Définir le potentiel de résilience du système estuarien face à l'activité anthropique.

1.4 Objectifs spécifiques

Afin d'atteindre efficacement les objectifs généraux présentés sans souffrir d'un cadre de travail trop vaste, la présente étude a été divisée en plusieurs objectifs spécifiques qui ont chacun donné lieu à un manuscript scientifique. Ces travaux sont présentés aux chapitres 2-8 inclusivement.

1. Mettre au point les techniques analytiques nécessaires à la mesure des espèces azotées (notamment l'ammonium) présentes dans les eaux côtières présentant des caractéristiques physico-chimiques (salinité, charge particulaire et dissoute) variables.
2. Déterminer la variabilité spatiale des espèces de l'azote (NO_2^- , NO_3^- , NH_4^+ , PON) présentes dans la colonne d'eau de l'estuaire au niveau de son axe principal au cours de chacune des saisons de l'année et identifier les processus impliqués. Déterminer la concentration, la signature élémentaire (C/N) et moléculaire (proportion relative des acides aminés hydrolysables) de la matière organique particulaire présente dans les eaux de l'estuaire afin de documenter sa nature, sa source et les processus de génération/dégradation impliqués dans sa dynamique.
3. Identifier les principaux processus biochimiques relatifs au cycle de l'azote impliqués dans le développement des conditions hypoxiques observées dans la masse d'eau profonde de l'estuaire.
4. Déterminer l'abondance des bactéries hétérotrophes présentes dans la colonne d'eau de l'estuaire et identifier quelles sont les variables environnementales (notamment les espèces de l'azote) qui affectent leur distribution.
5. Quantifier les flux advectifs saisonniers (flux tidaux et apports en provenance des tributaires) de nutriments inorganiques dissous (NH_4^+ , NO_2^- , NO_3^- , PO_4^{3-} , Si(OH)_4) affectant les marais de l'estuaire du Saint-Laurent.
6. Quantifier les principaux processus bactériens impliqués dans le cycle de l'azote des marais côtiers (nitrification, denitrification, ammonification) notamment, à l'aide de traceurs isotopiques.

7. Caractériser les communautés microbiennes présentes dans les marais côtiers.

Les informations recueillies dans le cadre de chacune de ces études spécifiques (2 à 7) ont été intégrées à différents modèles présenté au chapitre 9. Dans un premier temps, les données des chapitres 5 à 7 ont été introduites dans un modèle conceptuel appliqué à la dynamique de l'azote au sein d'environnements littoraux, dont un marais impacté par l'activité anthropique (le marais de Pointe-au-Père) et d'un marais non impacté (le marais de Pointe-aux-Épinettes). Proposant un schéma quantitatif des échanges d'azote inorganique dissous (DIN) aux limites d'un réservoir central représentant un marais côtier, ce modèle nous a permis de produire des bilans massiques saisonniers au sein de chacun des milieux étudiés. À l'image des études réalisées par Dame *et al.* (1991), Childers *et al.* (1993) et Brock (2001) sur des environnements de transition similaire de la côte est américaine, ces bilans massiques nous ont permis de mieux comprendre le rôle écosystémique des marais (en terme de puits ou de source d'azote pour le milieu estuaire) et la contribution relative des processus impliqués dans le transfert d'azote entre les différents réservoirs. De façon complémentaire, ces bilans nous ont permis d'évaluer l'incidence des variations saisonnières et de l'activité anthropique (affectant des caractéristiques physico-chimiques intrinsèques du milieu) sur la dynamique de ces milieux intertidaux.

Dans un second temps, nous avons réalisé un bilan annuel d'azote inorganique dissous (DIN) au sein de l'estuaire maritime du Saint-Laurent afin de déterminer le rôle des marais côtiers sur le cycle de l'azote de ce large milieu de transition. En plus d'y intégrer les flux journaliers d'azote associés à la dynamique des marais côtiers, une attention particulière a été portée à la contribution des apports fluviaux, aux processus de transport advectifs verticaux, à l'activité phytoplanctonique et aux processus de recyclage sédimentaire. L'élaboration de ce bilan massique annuel nous a permis de quantifier la dynamique de l'azote dans l'estuaire maritime et d'en déduire le rôle des marais côtiers. De plus, ce même bilan nous a permis de discuter les effets potentiels de l'activité anthropique sur l'estuaire maritime et de façon plus spéculative, de définir son potentiel de résilience.

1.5 Sites à l'étude

1.5.1 Conditions climatiques

Sur le plan climatique, la région de Bic-Rimouski s'apparente à l'ensemble des basses terres de l'estuaire et du golfe du Saint-Laurent : températures fraîches, périodes d'insolations et de précipitations modérées et saison sans gel relativement longue. Toutefois, la position géographique de cette région lui confère des aspects plus continentaux. La température moyenne annuelle enregistrée est comprise dans l'isotherme 2.5–5 °C (minima en janvier de –11 °C et maxima en juillet de 17.4 °C; données issues de la station météorologique de Rimouski moyennées sur un période de vingt ans). L'inertie de la grande masse d'eau estuarienne demeure responsable de ces conditions thermiques clémentes. On peut noter que l'écart entre la température du continent et celle de la masse d'eau estuarienne provoque de fréquents brouillards. La région de Bic-Rimouski est parmi les moins arrosées du Québec méridional, la moyenne des précipitations annuelles étant évaluée à 825 mm. La fraction nivale y contribue pour environ 30%. La période d'ensoleillement est la même pour toute la région côtière du Bas Saint-Laurent, soit 1600–1700 heures/an. Les vents dominants proviennent de l'ouest dans 53% des cas sur un régime annuel et ils atteignent une vitesse moyenne de 22 km/h (Plan directeur Parc du Bic).

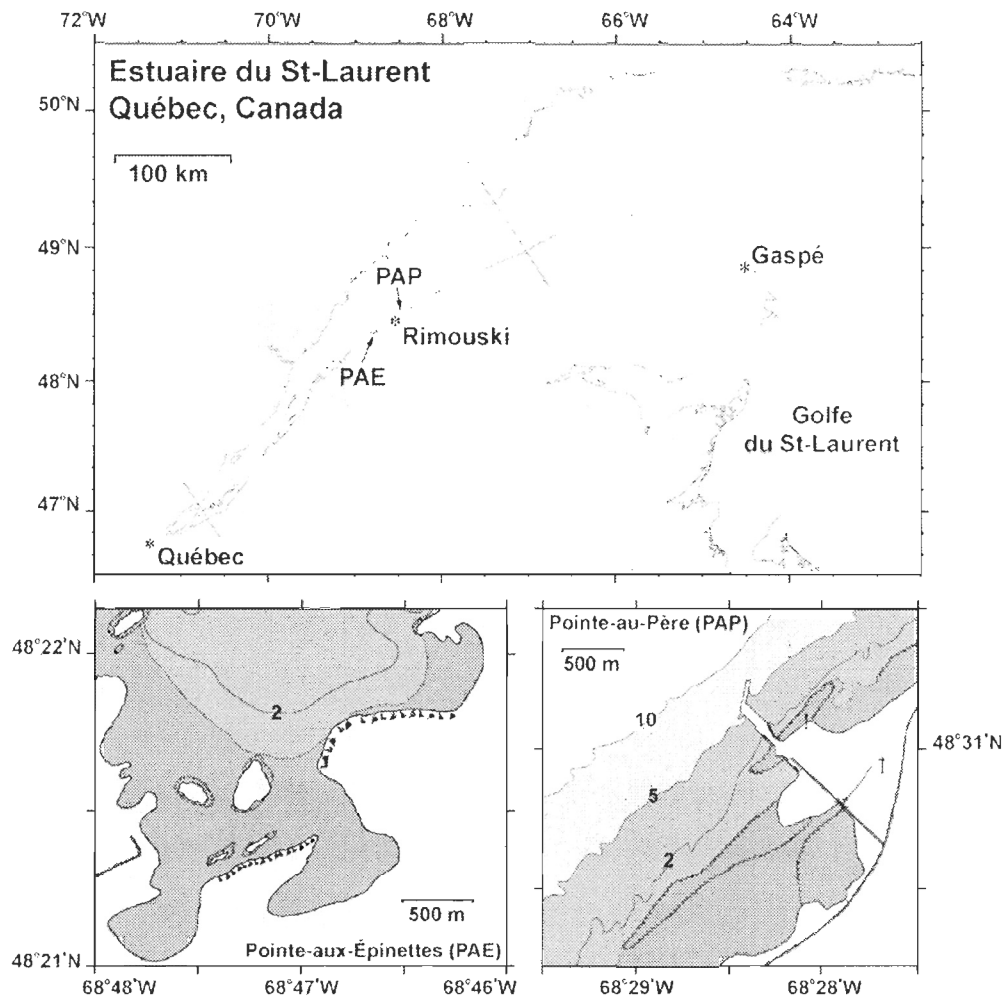


Figure I-2 Sites à l'étude; l'estuaire du Saint-Laurent (en haut), le marais de Pointe-aux-Épinettes (en bas à gauche) et le marais de Pointe-au-Père (en bas à droite).

1.5.2 Description des marais à l'étude

Les sédiments meubles constituant les marais du Saint-Laurent maritime reposent en discordance angulaire sur les métasédiments schisteux de la province géologique des Appalaches. Les contraintes lithosphériques associées à l'orogénie appalachienne ont déformé les strates rocheuses qui constituent le socle régional, leur conférant une structure longitudinale ondulante et plissée orientée NE-SW. Ce socle a été aplani du Primaire au Tertiaire, alors que l'ensemble de l'édifice est soulevé de nouveau et fragmenté par l'érosion différentielle. Au Quaternaire, le retrait de la masse de glace Wisconsinienne, la transgression de la mer de Goldthwait a laissé à la base de la colonne sédimentaire des marais une lentille d'argile massive. La régression progressive de cette mer a engendré la

formation de terrasses dont la plus basse (la terrasse Rimouski) correspond à l'estran actuel sur lequel se sont successivement déposés, sur une puissance de ~ 1 m, des limons, des sables et des graviers. L'unité stratigraphique supérieure, correspondant à la plate-forme herbacée, est plus riche en matière organique que les unités inférieures et forme une rhizosphère colonisée par divers espèces de macrophytes tolérantes aux eaux saumâtres (Dionne, 2004).

Selon Dionne (1972) et Drapeau (1992), la période hivernale serait propice au processus d'édification des marais côtiers du Saint-Laurent. La glace qui se forme en décembre dans l'estuaire, pour y persister jusqu'en avril, joue en effet un rôle déterminant dans la formation des schorres en transportant des sédiments de toutes tailles et en protégeant la côte de l'action érosive des vagues. Au printemps, la fonte des glaces libère une quantité importante de sédiments (moyenne de 100 kg de sédiments par m^2 de glace; Drapeau, 1992) qui contribue localement au processus d'accrétion sédimentaire. Ces processus glaciels engendrent la formation de barres sédimentaires, de dépressions, de cuvettes et de marelles, qui constituent autant de sites d'encrage pour la végétation et de micro-environnements pour les communautés microbiennes.

Le réseau hydrographique interne des deux marais à l'étude n'est pas très élaboré. Tout le territoire s'inscrit dans le bassin versant du fleuve Saint-Laurent. Les eaux s'écoulent directement dans les marais par le biais d'une série de ruisseaux secondaires. Le milieu d'eau douce prend peu d'importance dans les marais contrairement au milieu associé aux eaux salées. Exception faite des micro-environnements situés à l'embouchure des tributaires, l'ensemble de la masse d'eau présente dans les marais présente une salinité moyenne de 21 ppt si on fait abstraction des périodes de crues et de pluies intenses. Les courbes bathymétriques montrent que les baies constituant les marais sont peu profondes, la ligne de 2 m les confinant entièrement (Fig. I-2). Les marées dont l'amplitude moyenne est de 3.1 m avec un maximum d'environ 4.9 m, permettent de dégager une vaste zone intertidale très prisée par la faune et la flore. Cette zone intertidale peut être divisée en 3 sous-environnements caractérisés par la présence de macrophytes spécialisés : 1) la zone médiolittorale inférieure où l'on peut retrouver des algues brunes (par exemple *Fucus bifide*

et vésiculeux), ainsi que la Zostère marine et la Ruppie maritime, 2) la zone médiolittorale intermédiaire principalement caractérisée par la présence de la Spartine à fleurs alternes (*alterniflore*) et la Salicorne d'Europe, 3) la zone médiolittorale supérieure où l'on observe entre autres, la Spartine étalée, la Glauce maritime, le Plantin maritime, la Liminie de nash, l'Arroches hastées, le Carex écailleux et la Troscart maritime.

1.5.3 Description du marais de Pointe-aux-Épinettes

Le marais de Pointe-aux-Épinettes ($48^{\circ} 21.40'N$, $68^{\circ} 46.75'W$), situé dans le parc provincial du Bic, est localisé dans une baie en voie de comblement (l'Anse à l'Orignal) entre deux massifs d'âge Cambrien (bordé à l'ouest par le Mont Chocolat et à l'est par la Montagne du Bûcheron). Ces massifs Cambriens sont constitués d'une formation conglomératique gréseuse appartenant au groupe de Québec. On retrouve en périphérie du marais de nombreux éléments détritiques grossiers, vestiges de l'érosion de ces massifs qui surplombent le marais. À cet effet, un des aspects les plus singuliers de ce marais est son vaste estran sablo-graveleux. L'eau douce s'écoule dans le marais *via* deux tributaires de petite taille (< 1 m de large) situés aux extrémités est et ouest du marais. Puisque le bassin versant de ce marais (s'étendant sur 1.7 km^2) est entièrement conscrit au sein d'un milieu forestier, nous avons considéré ce marais comme non-impacté pour les fins de cette étude (marais témoin propre).

1.5.4 Description du marais de Pointe-au-Père

Le marais de Pointe-au-Père ($48^{\circ} 30.45'N$, $68^{\circ} 28.30'W$) est situé dans la réserve faunique de Pointe-au-Père (sous la responsabilité de Parc Canada), un refuge pour oiseaux migrateurs inauguré en 2002. Ce marais est édifié dans une dépression rocheuse dont l'axe principal est orienté parallèlement à celui du fleuve (NE-SW). Il est abrité des vagues en provenance de l'estuaire par une basse crête; une structure géologique longitudinale associée au flanc immédiat d'une charnière de pli. On peut expliquer la présence, en relief, de cette structure «barrière» en évoquant un processus d'érosion différentiel associé à l'écoulement glaciaire des grands inlandsis quaternaires dans le chenal laurentien. Le marais est ainsi suffisamment isolé de l'estuaire pour permettre la formation d'une structure

microdeltaïque, à la confluence du ruisseau St-Anne et de l'émissaire de la route 132, composée de dépôts sablo-sliteux, par endroit très riche en matière organique. Contrairement au marais de Pointe-aux-Épinettes, le marais de Pointe-au-Père possède un estran vaseux caractérisé par la présence d'un dallage de cailloux glacial. Localisé au sein d'un bassin versant partiellement urbanisé, ce marais reçoit des eaux de ruissellements des égouts pluviaux de la ville de Rimouski, d'installations agricoles et de tourbières *via* 5 tributaires. Ces apports sont à l'origine de nombreux déséquilibres tant de nature sédimentologique que biochimique. On y observe un talus d'érosion, des micro-ravins et micro-falaises en marge des chenaux tidaux ainsi que de plans de glissement engendrés par la solufluxion et la gélifluxion. Pour l'ensemble de ces raisons, nous avons considéré le marais de Pointe-au-Père comme un milieu impacté pour les fins de cette étude.

1.6 Méthodologie

Sans élaborer sur des considérations d'ordre technique, nous présentons ici les travaux d'échantillonnages nécessaires à la réalisation des différents objectifs spécifiques. Ces travaux, menés en parallèle dans l'estuaire du Saint-Laurent ainsi que dans deux marais côtiers (le marais de Pointe-au-Père et le marais de Pointe-aux-Épinettes), sont ici présentés en deux volets.

1.6.1 Procédure d'échantillonnage dans l'estuaire du Saint-Laurent

Au cours de six missions océanographiques ayant eu lieu en mai 2003, juillet 2004, octobre et décembre 2005, février 2006 et mai 2007, correspondant aux différentes conditions saisonnières rencontrées dans ce milieu de transition de haute latitude, nous avons effectué une série de travaux au niveau de la colonne d'eau de l'estuaire du Saint-Laurent. Des échantillons d'eau, prélevées à des profondeurs discrètes, ainsi que des mesures physico-chimiques, réalisées sur des profils continus, ont été recouvrés à bord du N.R. *Coriolis II* et du C.C.G.S. *Admundsen* à l'aide d'une rosette munie de bouteilles à clapet (Niskin[®]) et d'une multi-sonde de type CTD. Dans le but d'obtenir une couverture spatiale représentative, nous avons échantillonné une douzaine de stations situées le long de l'axe principal de l'estuaire soit, entre la ville de Québec et l'île d'Anticosti (Fig. I-3). L'itinéraire nous a permis d'échantillonner des eaux d'une vaste gamme de salinité (0 à 35)

et de température (-1 à 15 °C), caractéristiques des gradients observés en milieu estuarien. Ainsi, pour chacune des stations définies, les masses d'eau en présence (entre 1 et 3) ont été l'objet de prélèvements suivant l'acquisition, en direct, d'un profil CTD. De plus, là où le substrat sédimentaire le permettait, quelques grammes de sédiment de surface ont été prélevés à l'aide d'une benne ou d'un carottier à boîte à des fins d'analyses granulométriques et géochimiques.

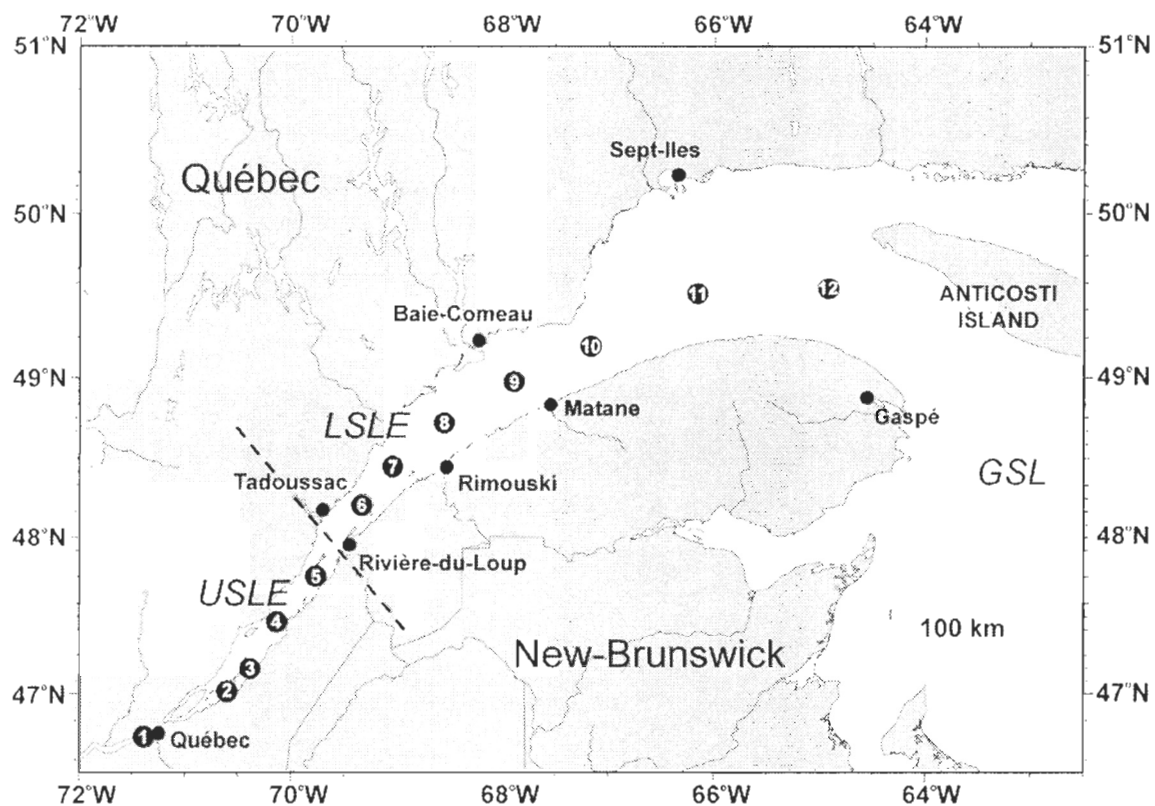


Figure I-3 Situation géographique des stations d'échantillonnage dans l'estuaire et le golfe du Saint-Laurent. USLE représente l'estuaire supérieur, LSLE l'estuaire maritime et GSL le golfe du Saint-Laurent.

1.6.2 Procédure d'échantillonnage dans les marais côtiers

Afin de quantifier adéquatement les différents processus physiques et les mécanismes biochimiques impliqués dans le cycle de l'azote des marais côtiers de l'estuaire du Saint-Laurent, nous avons fait appel à plusieurs stratégies d'échantillonnage. Dans un premier temps, nous nous sommes penchés sur la caractérisation des échanges advectionnels de nutriments azotés entre la masse d'eau estuarienne et les marais côtiers (flux

tidaux) en échantillonnant, sur une base saisonnière, la colonne d'eau des marais suivant un cycle complet de marée. Ces travaux ont été réalisés du 3 mars au 11 novembre 2004 à l'exutoire du marais témoin de Pointe-aux-Épinettes et du marais impacté de Pointe-au-Père (Station I et II, Fig. I-4). Au cours de la même année, des échantillonnages hebdomadaires à marée basse, effectués à plusieurs stations fixes (notamment localisées à l'embouchure des différents tributaires des marais à l'étude; Station A-G, Fig. I-4) ont été réalisés afin de quantifier les apports en azote en provenance des bassins versants et d'évaluer leurs conséquences écosystémiques. Parallèlement à ces prélèvements d'eau, une cartographie à haute résolution (précision ± 1 cm) des marais à l'étude a été réalisée à l'aide d'une station totale, d'un DGPS (zone supra et intertidale) et d'une embarcation légère munie d'un sonar (zone infratidale). Cette cartographie nous a permis de générer les cartes bathymétriques nécessaires à l'élaboration d'un modèle hydrodynamique numérique à partir duquel les échanges tidaux de nutriments azotés ont été calculés. De plus, des échantillons de glace de mer ont été prélevés aux stations I et II ainsi qu'au large des marais afin de procéder à des analyses biochimiques et ainsi mieux comprendre l'incidence de la banquise sur les flux d'azote entre l'estuaire et les marais.

Dans un deuxième temps, une série de carottes de sédiments (entre 10 et 60 cm) a été prélevée dans les marais à l'étude (notamment aux sites marqués d'un carré; Fig. I-4), afin de procéder à des travaux descriptifs. Ces travaux, incluant des descriptions sédimentologiques, des analyses géochimiques ainsi que des identifications microbiologiques, nous ont permis de caractériser le substrat des marais ainsi que de comprendre les mécanismes de nature biogéochimique impliqués dans leur genèse. Enfin, au cours d'un troisième volet, des travaux visant à évaluer l'intensité des processus bactériens les plus pertinents (nitrification, dénitrification, ammonification) ont été réalisés, notamment, en utilisant des enceintes à incubation (suivis en laboratoire ainsi qu'en condition *in situ*). L'évolution temporelle de la concentration des espèces gazeuses et dissoutes de l'azote fut utilisée comme approche indirecte pour quantifier les processus précédemment énumérés (voir Blackburn et Sorensen, 1988). De façon complémentaire, l'utilisation de traceurs isotopiques nous ont permis d'affiner la mesure de ces processus et de comprendre les effets synergiques du couplage de ces derniers.

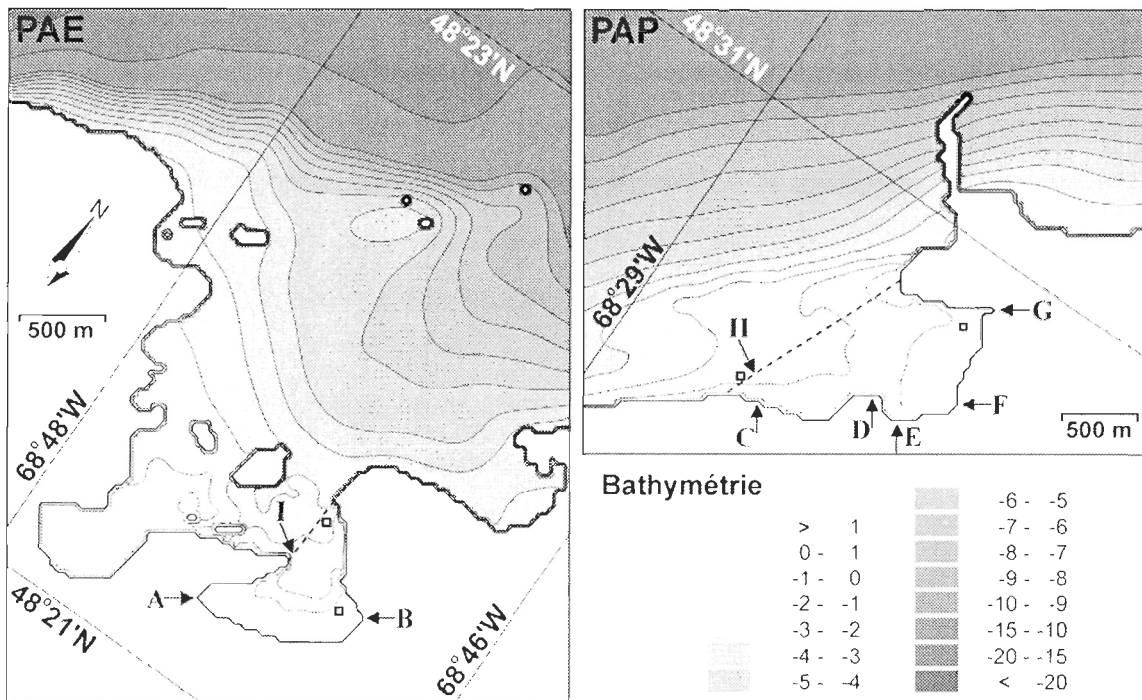


Figure I-4 Sites d'échantillonnage dans les marais côtiers de l'estuaire du Saint-Laurent. La bathymétrie est exprimée en mètre.

1.7 Référence

- Alexander, M. (1977) Introduction to soil microbiology. John Wiley and Sons, Ney-York.
- Billen, G. et Lancelot, C. (1988) Modelling benthic nitrogen cycling in temperate coastal ecosystems. Dans: T.H. Blackburn et Sorensen, J. (Eds) Nitrogen cycling in coastal marine environments. John Wiley and Sons, Ney-York, p. 341-378.
- Blackburn, T.H. et Sorensen, J. (1988) Nitrogen cycling in coastal marine environments. John Wiley and Sons, Ney-York, 451pp.
- Blackburn, T.H., Nedwell, D.B. et Wiebe, W.J. (1994) Active mineral cycling in a Jamaican seagrass sediment. Mar. Ecol. Prog. Ser. 110, 233-239.
- Bock, E., Koops, H.P., Ahlers, B. et Harms, H. (1992) Oxidation of inorganic nitrogen compound. Dans: Balows, A., Truper, H.G., Dworkin, M., Harder, W. et Schleifer, K.H. (Eds) The prokaryotes. A handbook on the biology of bacteria: Ecophysiology, Isolation, Identification, Application. Springer-Verlag, New-York, p. 414-430.
- Boorman, L.A. (1999) Salt marshes – present function and futur change. Mangr. Salt Marsh. 3, 227-241.

- Boyd, S.R. (2001) Nitrogen in future biosphere studies. *Chem. Geol.* 176, 1-30.
- Brock, A.D. (2001) Nitrogen budget for low and high freshwater inflow, Nueces Estuary, Texas. *Estuaries*. 24, 509-521.
- Capone, D.G. et Taylor B.F. (1980) N_2 fixation in the rhizosphere of seagrass *Thalassia testudinum*. *Can. J. Microbiol.* 26, 998-1005.
- Carpenter, E.J. et Capone, D.G. (1983) Nitrogen in the marine environment. Academic Press. Ney-York.
- Carpenter, E.J., Van Raalte, C.D. et Valiela, I. (1978) Nitrogen fixation by algae in a Massachusetts salt marsh. *Limnol. Oceanogr.* 23, 318-327.
- Chambers, P.A., Guy, M., Roberts, E.S., Charlton, M.N., Kent, R., Gagnon, C., Grove, G. et Foster, N. (2001) Nutrients and their impact on the Canadian environment. Agriculture and Agri-Food Canada, Environment Canada, Fisheries and Oceans Canada, Health Canada and Natural Resources Canada, Ottawa.
- Childers, D.L., Mckellar, H.N., Dame, R.F., Sklar, F.H. et Blood, E.R. (1993) A dynamic nutrient budget of subsystem interaction in a salt marsh estuary. *Est. Coast. Mar. Sci.* 36, 105-131.
- Cloern, J.E. (2001) Our evolving conceptual model of the coastal eutrophication problem. *Mar. Ecol. Prog. Ser.* 210, 223-253.
- Coote, A.R. et Yeats, P.A. (1979) Distribution of nutrients in the Gulf of St. Lawrence. *J. Fish. Res. Board Can.* 36, 122-131.
- Cornell, S.E., Jickells, T.D., Cape, J.N., Rowland, A.P. et Duce, R.A. (2003) Organic nitrogen deposition on land and coastal environments: a review of methods and data. *Atmos. Environ.* 37, 2173-2191.
- Dalsgaard, T., Canfield, D.E., Petersen, J., Thamdrup, B. et Acuna-Gonzalez, J. (2003) N_2 production by the anammox reaction in the anoxic water column of Golfo Dulce, Costa Rica. *Nature*. 422, 606-608.
- Dame, R.F., Spurrier, J.D., Williams, T.M., Kjerfve, B., Zingmark, R.G., Wolaver, T.G., Chrzanowski, T.H., Mckellar, H.N. et Vernberg, F.J. (1991) Annual material processing by a salt marsh-estuarine bassin in South Carolina, USA. *Mar. Ecol. Prog. Ser.* 72, 153-166.
- Davidson-Arnott, R.G.D., van Proosdij, D., Ollerhead, J. et Schostak, L. (2002) Hydrodynamics and sedimentation in salt marshes : exemples from macrotidal marsh, Bay of Fundy. *Geomorphology*. 48, 209-231.

- deBruyn, A.M.H., Marcogliese, D.J. et Rasmussen, J.B. (2003) The role of sewage in a large river food web. *Can. J. Fish. Aquat. Sci.* 60, 1332-1344.
- Dionne, J.C. (1972) Caractéristiques des schorres des régions froides, en particulier de l'estuaire du Saint-Laurent. *Z. Geomorphol.* 13, 131-162.
- Dionne, J.C. (1986) Érosion récente des marais intertidaux de l'estuaire du Saint-Laurent. *Géo. Phy. Quat.* 3, 307-323.
- Dionne, J.C. (2004). Âge et taux moyen d'accréation verticale des schorres du Saint-Laurent estuarien, en particulier ceux de Montmagny et de Sainte-Anne-de-Beaupré, Québec. *Géo. Phy. Quat.* 58, 73-108.
- Drapeau, G. (1992) Dynamique sédimentaire des littoraux de l'estuaire du Saint-Laurent. *Géo. Phy. Quat.* 46, 233-242.
- Falkowski, P.G. (1997) Evolution of the nitrogen cycle and its influence on the biological sequestration of the CO₂ in ocean. *Nature*. 387, 272-275.
- Flindt, M.R., Pardal, M.A., Lillebo, A.I., Martins, I. et Marques, J.C. (1999) Nutrients cycling and plant dynamic in estuaries. *Acta Oecol.* 4, 237-248.
- Galloway, J.N. (1998) The nitrogen cycle: changes and consequences. *Env. Poll.* 102, 15-24.
- Gardner, L.R. et Kjerfve, B. (2006) Tidal fluxes of nutrients and suspended sediments at the North Inlet Winyah Bay National Estuarine Research Reserve. *Est. Coast. Shelf Sci.* 70, 682-692.
- Gilbert, D., Sundby, B., Gobeil, C., Mucci, A. et Tremblay, G.H. (2005) A seventy-two-year record of diminishing deep-water oxygen in the St. Lawrence Estuary: The northwest Atlantic connection. *Limnol. Oceanogr.* 50, 1654-1666.
- Greisman, P. et Ingram, G. (1977) Nutrient distribution in the St. Lawrence Estuary. *J. Fish. Res. Board Can.* 34, 2117-2123.
- Herbert, R.A. et Nedwell, D.B. (1990) Role of environmental factors in regulation nitrate respiration in intertidal sediment. Dans: Revsbech, N.P et Sorensen J. (Eds.) Denitrification in soil and sediment. Plenum Press, New York, pp.77-90.
- Herbert, R.A. (1999) Nitrogen in coastal marine ecosystems. *FEMS Micro. Biol. Rev.* 23, 563-590.
- Howarth, R.W. (1988) Nutrient limitation of net primary production in marine ecosystems. *Ann. Rev. Ecol. Syst.* 19, 89-110.

- Howarth, R.W., Billen, G., Swaney, D., Townsend, A., Jarworski, N., Lajtha, K., Downing, J.A., Elmgren, R., Caraco, N., Jordan, T., Berendse, F., Freney, J., Kueyarov, V., Murdoch, P. et Zhao-liang, Z. (1996) Riverine inputs of nitrogen to the North Atlantic Ocean: Fluxes and human influences. *Biogeochemistry*. 35, 75-139.
- Howarth, R.W. et Marino, R. (2006) Nitrogen as the limiting nutrient for eutrophication in coastal marine ecosystems: evolving views over three decades. *Limnol. Oceanogr.* 51, 364-376.
- Jensen, H.M., Lomstein, E. et Sorensen, J. (1990) Benthic NH_4^+ and NO_3^- flux following sedimentation of a spring phytoplankton bloom in Aarhus bight, Denmark. *Mar. Ecol. Prog. Ser.* 61, 87-96.
- Knowles, R. (1981) Denitrification. Dans: Clark, F.E. et Rosswall, T. (Eds.) *Terrestrial Nitrogen Cycle. Processes, Ecosystem Strategies and Management Impact, Ecology Bulletin*, Stockholm, pp. 315-330.
- Koutitonsky, V.G. et Bugden, G.L. (1991) The physical oceanography of the Gulf of St. Lawrence: a review with emphasis on the synoptic variability of the motion. Dans: Therriault, J.-C. (Ed.). *The Gulf of St. Lawrence: Small Ocean or Big Estuary?* Can. Spec. Pub. Fish. Aquat. Sci., pp. 57-90.
- Laurin, M. (2006) Ouvrages de surverse et stations d'épuration : Évaluation de performance des ouvrages municipaux d'assainissement des eaux pour l'année 2005. Ministère des affaires municipales et régionales (MAMR), Québec. 171 pp.
- Livingston, R.J. (2001) Eutrophication processes in coastal systems. Boca Raton, Fla. CRC Press, 327 pp.
- Mackin, J.E. et Aller, R. (1984) Ammonium adsorption in marine sediments. *Limnol. Oceanogr.* 29, 250-257.
- Madigan, M.T., Martinko, J.M. et Parker, J. (2002) *Brock biology of microorganisms*. Pearson Education, NJ, USA.
- Mann, K.H. et Lazier, J.R.N. (1991) *Dynamics of marine ecosystems*, Blackwell publication, Boston, 466 pp.
- Martinez, J. et Béline, F. (2002) Gestion de l'azote en système d'élevage développé. Enjeux scientifiques et environnementaux. *Nat. Sci. Soc.* 10, 52-61.
- Mason, C.F., Underwood, G.J.C., Baker, N.R., Davey, P.A., Davidson, I., Hanlon, A., Long, S.P., Oxborough, K., Paterson, D.M. et Watson, A. (2003) Roles of herbicides in the erosion of salt marshes in eastern England. *Environ. Pollut.* 122, 41-49.
- Mermilliod-Blondin, F., Rosenberg, R., Francois-Carcaillet, F., Norling, K. et Mauclaire, L. (2004) Influence of bioturbation by three benthic infaunal species on microbial

communities and biogeochemical processes in marine sediment. *Aquat. Microb. Ecol.* 36, 271-284.

Nauman (1919) Nagra synpunkter angalnde limnoplanktons økologie. med sarskild hænsyn till fytoplankton. *Svensk Bot. Tidskr.* 13, 129-163.

Nedwell, D.B., Dong, L.F., Sage, A. et Underwood, G.J.C. (2002) Variation of the nutrients load to the Mainland U.K. *Estuaries. Est. Coast. Shelf Sci.* 54, 951-970.

Nishio, T., Koike, I. et Hattori, A. (1983) Estimates of denitrification and nitrification in coastal and estuarine sediment. *Appl. Environ. Microbiol.* 45, 444-450.

Nixon, S.W. (1980) Between coastal marshes and coastal waters: a review of twenty years of speculation and research on the role of salt marsh in estuary productivity and water chemistry. Dans: Hamilton, P. et McDonald, K.B. (Eds.) *Estuarine and wetland Process with emphasis on modeling*, Plenum Press, NY. p. 437-525.

Nowicki, B.L., Requintina, E., van Keuren, D. et Kelly, J.R. (1997) Nitrogen losses through sediment denitrification in Boston Harbour and Massachusetts Bay. *Estuaries.* 20, 626-639.

Olivier, J.G.J., Bouwman, A.F., Van der Hoek, K.W. et Berdowski, J.J.M. (1998) Global air emission inventories for anthropogenic source of NO_x, NH₃ and N₂O in 1990. *Environ. Pollut.* 102, 135-148.

Page, H.M., Petty, R.L. et Meade, D.E. (1995) Influence of watershed runoff on nutrients dynamics in a Southern California salt marsh. *Est. Coast. Shelf Sci.* 41, 163-180.

Painchaud, J. (1999) La production porcine et la culture du maïs. Impacts potentiels sur la qualité de l'eau. *Nat. Can.* 123, 41-46.

Patriquin, D. et Knowles, R. (1972) Nitrogen fixation in the rhizosphere of marine angiosperms. *Mar. Biol.* 16, 49-58.

Plan directeur Parc du Bic.

Plourde, J. et Therriault, J.-C. (2004) Climate variability and vertical advection of nitrate in the Gulf of St. Lawrence. *Canada. Mar. Ecol. Progr. Ser.* 279, 33-43.

Rabalais, N.N. et Nixon, S.W. (Eds) (2002) Preface: Nutrient over-enrichment in coastal waters: global patterns of cause and effect, *Estuaries.* 25, 639-900.

Ro, C., Vet, R., Ord, D. et Holloway, A. (1998) Canadian Air And Precipitation Monitoring Network (CAPMoN) Annual Summary Reports (1983-1996). Air Quality Research Branch. Atmospheric Environment Service. Environment Canada. Downsview, Ontario.

- Savenkoff, C., Vésina, A.F., Smith, P.C. et Han, G. (2001) Summer transport of nutrients in the Gulf of St. Lawrence estimated by inverse modelling. *Est. Coast. Shelf Sci.* 52, 565-587.
- Seitzinger, S.P. (1988) Denitrification in freshwater and coastal marine ecosystems : ecological and geochemical significance. *Limnol. Oceanogr.* 33, 702-724.
- Tan, F.C. et Strain, P.M. (1979) Organic carbon isotope ratio in recent sediments in the St. Lawrence Estuary and the Gulf of the St-Lawrence. *Est. Coast. Mar. Sci.* 8, 213-225.
- Thibodeau, B., de Vernal, A. et Mucci, A. (2006) Recent eutrophication and consequent hypoxia in the bottom waters of the Lower St. Lawrence Estuary: Micropaleontological and geochemical evidence. *Mar. Geol.* 231, 37–50.
- Verity, P.G. (2002) A decade of change in the Skidaway River Estuary. *Estuaries.* 25, 961-975.
- Vezjak, M., Savsek, T. et Stuhler, E.A. (1998) System dynamics of eutrophication process in lake. *Euro. Journ. Opera. Res.* 119, 442-451.
- Vézina, A.F., Gratton, Y. et Vinet, P. (1995) Mesoscale physical-biological variability during summer phytoplankton bloom in the Lower St. Lawrence Estuary. *Est. Coast. Shelf Sci.* 41, 393-411.
- Vitousek, P.M., Aber, J.D., Howarth, R.W., Likens, G.E., Matson, P.A., Schindler, D.W., Schlesinger, W.H. et Tilman, D.G. (1997) Human alteration of the global nitrogen cycle: Sources and consequences. *Ecol. Appl.* 7, 737-750.
- Walsh, J.J. (1991) Importance of continental margins in the marine biogeochemical cycling of carbon and nitrogen. *Nature.* 350, 53-55.
- Wang, F., Juniper, K., Pelegri, S.P. et Macko, S.A. (2003) Denitrification in sediment of the Laurentian Trough, St-Laurent Estuary, Qc., Canada. *Est. Coast. Shelf Sci.* 57, 515-522.
- Whitney, D.E., Woodwell, G.M. et Howarth R.W. (1975) Nitrogen fixation in flax pond: a long island salt marsh. *Limnol. Oceanogr.* 20, 640-643.

CHAPITRE II

Determination of ammonium using a microplate-based fluorescence technique

Patrick Poulin et Émilien Pelletier

Talanta 71 (2007) 1500-1506

2.1 Abstract

The determination of ammonium (NH_4^+) in concentrations ranging from nanomolar to micromolar in fresh and brackish waters often loaded in high suspended particulate matter and dissolved organic acids is presented. The newly described microplate-based fluorometric technique is allowing quick automated readings of different groups of samples with different background fluorescence and matrix effects. The lowest detectable concentration was estimated to 5 nM using the average detected blank \pm 3 SD and the practical detection limit (LOD) determined with successive calibration curves was 50 nM with an excellent repeatability. High loading of suspended particular matter, coloured organic acids, and salinity changes were not interfering with the accurate determination of ammonium. To illustrate its robustness and efficiency, this technique has been applied to water samples taken from rivers, saltmarshes and estuaries, spanning a large range of ammonium levels and chemical properties. Measurements of ammonium on reddish turbid waters sampled in south shore of St. Lawrence Estuary showed ammonium concentrations between $0.05 \pm 0.01 \mu\text{M}$ and $3.89 \pm 0.03 \mu\text{M}$, indicating a significant source of ammonium from terrestrial and saltmarsh ecosystems.

2.2 Introduction

Nitrogen availability is one of the major factors regulating primary production in coastal environments [1]. The marine geochemical cycling of nitrogen and fluxes of inorganic nitrogen species (NO_3^- , NO_2^- , NH_4^+) and dissolved organic nitrogen (DON) in coastal environments are essential to biological processes and marine life in oceans [2]. Easily assimilated and preferentially used by phytoplankton species, ammonium is introduced into coastal systems by bacterial mineralization [3]. In addition, discharge of waste waters increases ammonium in rivers and saltmarshes [4] makes ammonium an efficient marker of anthropogenic pollution in coastal waters. To understand how *in situ* production and terrestrial supplies of ammonium affect aquatic biochemical processes and global nitrogen cycling in coastal environments, accurate determination of ammonium in micromolar or even sub-micromolar concentration is needed. However, precise and accurate determination of ammonium in fresh and brackish waters is often a difficult task because of the high variability of physical and chemical proprieties of coastal waters and related problems resulting from sample conservation and contamination.

In recent years, the use of orthophthaldialdehyde (OPA) reagent which could solve various matrix effects and interference problems often encountered with other methods was developed [5-7]. Considering its excellent sensitivity, low detection limit and ubiquity of applications, the OPA-sulfite- NH_3 reaction is attractive as a reliable method for the measurement of ammonium in nearshore marine environments where salinity, suspended particulate matter and water colour change rapidly from one sample to another. Following a well established mechanism, OPA forms a complex with ammonium which exhibits an intense fluorescent signal [8]. Moreover, the specificity of the reaction has been improved by adding sulphite which contributes to eliminate possible interferences from dissolved amino acids and primary amines [9].

In this paper, we describe an application of the OPA method using a microplate fluorescence reader in an attempt to provide a robust method working in a large range of ammonium concentrations with unfiltered coloured samples showing variable ionic strength and pH. The method has been assessed by determining ammonium in a series of

low salinity and reddish turbid samples from rivers, saltmarshes and estuaries of eastern Canada.

2.3 Experimental

2.3.1 Reagents and solutions

Working reagent (WR) consisting of a solution of OPA and sodium sulphite in a sodium borate buffer is prepared following published instructions [7]. Only freshly ultra-pure deionised water was used to prepare WR, standards and blanks. High purity of water is a determining factor in the success of this method.

The OPA solution is prepared first by dissolving 1.0 g of orthophthaldialdehyde (Sigma, P-1378) into 25 mL of high-grade pure ethanol (BDH, B-90169). The solution has been protected from light and refrigerated in a brown glass bottle due to the light sensitivity of OPA. It is suggested to prepare only the required volume of OPA solution for preparation of the working solution and avoid long-term storage of OPA solution.

The sodium sulphite solution is prepared by adding 1.0 g of sodium sulphite (A.C.S. grade Na₂SO₃ from Sigma, S-4672) to 125 mL deionised water. This solution is stable for at least one month when stored in a dark glass bottle at ambient temperature.

The borate buffer solution is prepared by dissolving 30.0 g of sodium tetraborate hydrate (A.C.S. grade Na₂B₄O₇·10 H₂O from Sigma, S-9640) into 1 L of deionised water. This solution remained stable for months when stored in a glass bottle at ambient temperature.

The working reagent (WR) solution was prepared by mixing 500 mL of sodium borate buffer solution, 2.5 mL of sodium sulphite solution and 25 mL of OPA solution in a carefully pre-cleaned glass bottle. A rest period of at least 24 h is required to optimise the WR complexion ability and decrease the blank response [7]. WR remained stable for months when stored at 4 °C in the dark.

To ensure high sensitivity and low variability within replicates and because the reactivity of the WR changes slowly with time, a new calibration curve is performed for each new series of four samples corresponding to the preparation of one microplate as shown hereafter. Each calibration curve is calculated by using five standard solutions in a range of expected ammonium concentrations (usually between 0.25 and 2.00 μM) from successive dilutions of a 50 μM ammonium solution prepared with freshly deionised water using high purity ammonium hydroxide (Sigma, A-6899) or ammonium salts (Aldrich, 326372)[5].

2.3.2 Instrumentation

All measurements were performed using a microplate fluorescence reader (Spectra Max Gemini[®], Molecular Devices Sunnyvale, California) operated at ambient temperature. The reader is equipped with a dual monochromator allowing a precise selection ($\pm 1 \text{ nm}$) of optimum wavelengths. Ammonium readings in raw fluorescence unit (RFU) were obtained at $\lambda_{\text{ex}} = 360 \text{ nm}$ and $\lambda_{\text{em}} = 430 \text{ nm}$. Microplate-based technique combines fast and automated multiple readings and the use of small samples. Although reacting and transferring small samples increase the analytical error, the possibility of increasing the number of replicates on the same microplate without increasing significantly the working load compensates for the loss of precision on single reading. Preliminary work using 96-well microplates and 200- μL samples showed standard errors $>10 \text{ \%}$ and a practical detection limit above 100 nM which were considered as unsatisfactory for the purpose of our current research on nitrogen cycle in coastal waters. Thus, disposable polystyrene 48-well microplates (Costar[®] type from Corning) allowing larger sample volumes were adopted for all ammonium determinations. Microplates were not reused and fluorescence must be read within 5 minutes after the microplate preparation.

2.3.3 Sample collection and preservation

Small Pyrex bottles (10 mL) with ground-glass joint and glass stopper or ODB type bottles (60-125 mL) were pre-washed with HCl 10 % solution, thoroughly rinsed with

deionised water, and then dried in oven. Bottles were rinsed twice with water to be sampled, fully filled and kept capped in dark on an ice bath until analysis. Such precautions made unnecessary the addition of WR to samples during the field work [7] and simplified the overall field procedure. Dosage has been performed within two hours after sampling to minimize possible effects of bacterial and plankton metabolism. Incubation at 2, 6 and 12 °C of freshly sampled sediment cores collected in the impacted Pointe-au-Père saltmarsh showed a quantitative reduction of labelled $^{15}\text{NO}_3^-$ to $^{15}\text{NH}_4^+$ within a few hours in the overlying water column indicating a rapid change in nitrogen species in these brackish waters (unpublished results). Filtration of samples is not recommended because of inherent well-documented problems resulting from adsorption of ammonium on filters and degassing losses [10, 11]. Since the fluorescence OPA method has been found almost unaffected by suspended particles [12], all samples were analysed without previous filtration.

2.3.4 Sample preparation and incubation with working reagent

The reaction between OPA and ammonium ions is slow at ambient temperature and an optimum incubation period of 4 h has been determined from a kinetic study detailed below (Fig. 1). Attempts of direct incubation in polystyrene microplates indicated a slow but quantitative reaction of WR with plastic surface (Fig. 2). Plastic micro plates could contain additive products rich in terminal reduced nitrogen used as antioxidant compounds to stabilize polymer structure [13]. These products seem to remain available for a slow chemical reaction with WR solution and induce a background fluorescence signal. Thus, incubation has to be carried out in glass tubes.

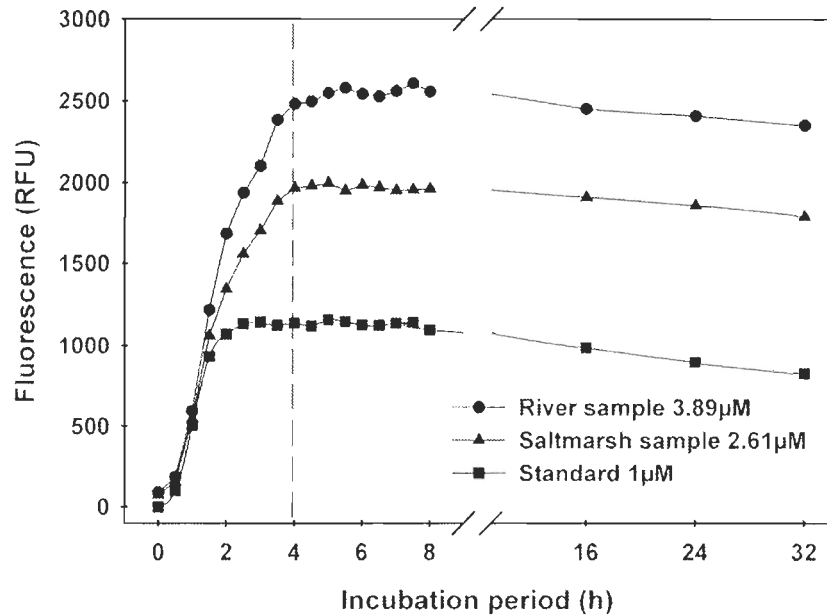


Figure II-1 Time course of the reaction of OPA with ammonium at room temperature (22 °C). Field samples were collected in a small river and a saltmarsh in the provincial park of Bic close to Rimouski. Samples were incubated in 25 mL borosilicate test tubes. Aliquots were transferred into microplate following given time intervals for fluorescence reading.

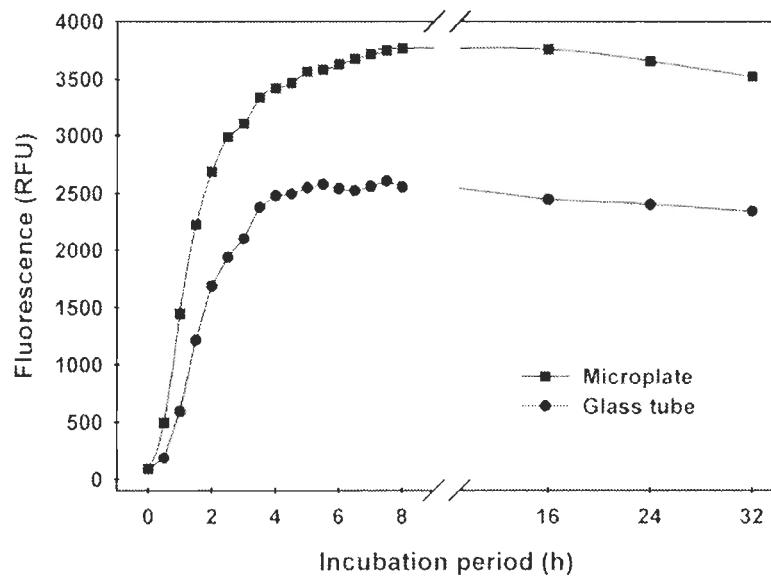


Figure II-2 Time course of the ammonium/OPA reaction at room temperature (22 °C). Incubation carried directly in polystyrene microplates was compared with incubation in glass tubes followed by reading in microplates. Natural freshwater samples were collected from Rimouski River.

Accurate determination of ammonium in natural waters has to take in account background fluorescence and matrix effect from dissolved and particulate organic matter. The matrix effect (ME) is related to unidentified natural substances that may alter the intensity of the fluorescence response of ammonium reacted with OPA whereas background fluorescence is attributed to existing compounds naturally fluorescent at determined wavelengths. Sample replicates doped with known amount of ammonium were prepared to evaluate the matrix effect (ME).

For each natural sample, duplicate 4.00 mL samples were transferred into two disposable 6-mL borosilicate test tubes. In one of the tube, ammonium standard solution (100 µL, 50 µM NH₄⁺) was added as a known surrogate together with 1.00 mL of WR. In the remaining tube only 1.00 mL of WR was added. Tubes were tightly stopped to avoid evaporation and air contamination, manually shaken for a few seconds and incubated in complete darkness for 4 h at 22 °C. To evaluate possible contamination or degradation of reagents, blank determination (4.00 mL of freshly deionised water and 1.00 mL of WR solution) was conducted for each series of four samples. Exposure of standards and samples to the ambient air and light could induce a significant drift of the analytical results.

2.3.5 Microplate preparation

Following the incubation period, samples in glass tubes were transferred into wells of flat-bottomed 48-well microplate for fluorescence determination (Fig. 3). Five standard solutions and four samples (1.00 mL each) were triplicately added into microplate wells. Five wells were left for reagent blank (BK) and four wells for the determination of background fluorescence (BG). Solution used in determining BK was transferred into five consecutive microplate wells whereas BG was evaluated by mixing 200 µL of borate buffer solution with 800 µL of each sample directly in the microplate well without WR addition. Repeated BG readings for the same sample showed a very low variability and thus only one reading was preserved in routine analysis.

Standard 1 0.25 µM	Standard 3 0.75 µM	Standard 5 2.00 µM	BK	Sample A	Sample B	Sample C	Sample D
Standard 1 0.25 µM	Standard 3 0.75 µM	Standard 5 2.00 µM	BK	Sample A	Sample B	Sample C	Sample D
Standard 1 0.25 µM	Standard 3 0.75 µM	Standard 5 2.00 µM	Sample A BG	Sample A	Sample B	Sample C	Sample D
Standard 2 0.50 µM	Standard 4 1.00 µM	BK	Sample B BG	Sample A-add	Sample A-add	Sample A-add	Sample A-add
Standard 2 0.50 µM	Standard 4 1.00 µM	BK	Sample C BG	Sample A-add	Sample A-add	Sample A-add	Sample A-add
Standard 2 0.50 µM	Standard 4 1.00 µM	BK	Sample D BG	Sample A-add	Sample A-add	Sample A-add	Sample A-add

Figure II-3 A typical 48-well microplate scheme showing standards in triplicate on the left side, reagents background blanks (BF in 5 wells) and sample background blanks (BG) in the middle. Samples and samples with surrogate to determine matrix effect (ME) are located on the right side of the plate. The reading of the whole plate takes 30 seconds.

2.3.6 Calculation method (adapted from [7])

The fluorescence signal attributed to the ammonium content in samples (i.e. F_{NH_4} and F_{NH_4ADD}) can be calculated by subtracting blank and background readings (RF_{BK} and RF_{BG}) from raw fluorescence obtained for samples (Eq. 1a and 1b):

$$F_{NH_4} = RF_{NH_4} - RF_{BK} - RF_{BG} \quad (1a)$$

$$F_{NH_4ADD} = RF_{NH_4ADD} - RF_{BK} - RF_{BG} \quad (1b)$$

The matrix effect (ME) can be calculated for each sample with known F_{NH_4} and F_{NH_4ADD} values using Eq. 2, where F_{STD5} and F_{STD4} are fluorescence values of standards 5 and 4, respectively, after subtraction of RF_{BK} :

$$\% ME = \{[(F_{STD5} - F_{STD4}) - (F_{NH_4ADD} - F_{NH_4})] / [F_{STD5} - F_{STD4}]\} \times 100 \quad (2)$$

As the difference in ammonium concentrations between these two standards is 1.0 μmole and the amount of ammonium added to the sample replicate is also 1.0 μmole , a lower reading of F_{NH4ADD} will induce a positive % ME. After F_{NH4} has been corrected for background and the ME contribution has been determined, the accurate concentration of ammonium in the sample (COR_{NH4}) can be calculated from ammonium values (CAL_{NH4}) obtained from the standard curve followed by the correction for ME using as shown in Eq. 3:

$$\text{COR}_{\text{NH4}} = \text{CAL}_{\text{NH4}} + (\% \text{ ME} \times \text{CAL}_{\text{NH4}}) \quad (3)$$

2.4 Results and discussion

2.4.1 Incubation period

The optimum incubation period of 4 h was determined according to the reaction kinetic of a standard solution and field samples with OPA over a 32-h period at ambient temperature (Fig. 1). Fluorescence intensity increases abruptly at the very beginning of the reaction, and then a plateau is reached in approximate 3 h for standards and 4 h for samples. Published instructions from [7] suggested a 2 h-incubation period which is considered not optimal when examining curves of Fig. 1. The reaction between OPA and ammonium is slower in field samples than standard samples. A longer incubation time provides a better reproducibility of the results. The length of the plateau depends on the maximum quantity of fluorescent product and its chemical stability, which extends to about 6 h. Incubations of tubes at 30, 40 and 50 °C in thermostatic bath have been tested and results indicate a good preservation of reproducibility of the method while reducing time to reach the plateau to less than two hours for all temperatures tested. A warm incubation can be a viable option when reaction time has to be drastically reduced, but keeping in mind inconveniences introduced by a temperature regulated device and possible side-reactions modifying the accuracy of the method.

Tableau II-1 Examples of ammonium determination ($n = 3$) in field samples with various physical and chemical properties.

Sample ID	Sampling										
	Temp. (°C)	Salinity	pH	SPM (mg L ⁻¹)	RF _{NH4} (RFU ± SD)	RF _{Bk} (RFU)	RF _{BG} (RFU)	F _{NH4} (RFU ± SD)	ME (% ± SD)	COR _{NH4} (µM ± SD)	Precision (%)
Rimouski River	0.7	0.1	7.64	5.64	302.1 ± 1.6	165.8 ± 3.4	50.0	86.3 ± 3.4	20.0 ± 0.5	0.05 ± 0.01	20.0
Metis River	0.7	0.0	6.66	4.87	1343.5 ± 6.7	98.1 ± 2.0	58.5	1186.9 ± 6.7	24.1 ± 0.7	1.31 ± 0.02	1.4
Bic River	0.6	0.1	7.90	3.24	2571.1 ± 5.5	98.1 ± 2.0	32.3	2113.7 ± 5.5	40.2 ± 0.6	3.89 ± 0.03	0.8
Ste. Anne River	9.8	0.3	7.61	3.78	1619.4 ± 0.8	239.0 ± 3.3	104.2	1366.2 ± 3.3	34.0 ± 0.5	2.25 ± 0.01	0.4
Bic Saltmarsh	9.4	18.0	7.74	12.66	1965.6 ± 4.4	239.0 ± 3.3	19.9	1706.7 ± 4.4	24.9 ± 0.5	2.61 ± 0.02	0.8
Ponté-au-Père Saltmarsh	10.9	15.4	8.04	13.11	784.7 ± 5.4	239.0 ± 3.3	26.2	519.4 ± 5.4	19.6 ± 0.6	0.34 ± 0.01	2.9
St. Lawrence River	8.79	0.8	8.14	15.21	2307.9 ± 4.6	184.6 ± 8.3	9.9	2113.4 ± 8.3	26.7 ± 1.0	3.08 ± 0.04	1.3
St. Lawrence Estuary (10 m depth)	3.3	28.1	8.09	3.12	958.3 ± 1.3	213.3 ± 13.2	37.6	707.4 ± 13.2	9.9 ± 1.9	0.88 ± 0.04	4.5

2.4.2 Background fluorescence (RF_{BG})

The RF_{BG} of natural waters results from the presence of self-fluorescent substances and can be quantitatively evaluated using an aliquot of each sample in which WR solution is replaced by free-OPA borate buffer solution that does not react with ammonium to form the fluorescent complex. The intensity of this signal may be significant and reaches >10 % of the RF signal in some natural waters (Table 1). Highly productive waters containing high levels of chlorophyll and pigments might exhibit high RF_{BG} values. Variation in background fluorescence depends on the origin of the samples and RF_{BG} must be systematically determined and subtracted from measured RF for each sample.

2.4.3 Matrix effect (ME)

Some samples, particularly those from rivers draining peat bogs and saltmarshes, are heavily loaded with reddish humic substances exhibiting a strong ME. These substances reduce the fluorescence intensity produced by the reaction between OPA and ammonium. Unidentified natural dissolved substances have a quenching effect on the fluorescent complex. The ME correction becomes very significant in turbid or strongly coloured water

samples, reaching more than 40 % of the RF signal in some extreme cases (Table 1). Even if ME cannot be eliminated by a chemical reaction, this effect can be adequately corrected by adding a known amount of ammonium to each sample and determining % ME [7].

2.4.4 Influence of salinity

Low salinity effect is a determining factor in the choice of a method dedicated to ammonium determination in nearshore environments. The low ion strength effect (3 %) exhibited by the OPA method compared with other methods has already been discussed [6]. We reassessed this salt effect for the microplate technique by repetitively determining 1.00 µM of ammonium standards prepared with artificial seawater solution of salinity ranging from 0 to 35 over 5 successive days (Fig. 4). Deviation (in %) relative to the response of freshwater reference was calculated and was found not exceeding 1.8 % on average at salinity 35. The deviation is more important in low salinity from 0 to 5 than in the higher salinity range. From a mechanistic point of view, it seems that the fluorescent isoindole formed by the reaction of OPA and ammonium [14] is almost not sensitive to the ionic strength of the solution. Furthermore, the addition of a borate buffer to WR brings the pH value of the reaction medium close to 9.0 which maintains carboxylic acids in neutral forms and reduces surface adsorption on suspended particles and glass tubes. Considering the low deviation observed within the entire salinity range, the present method does not require correction for salt effect as long as the precision of $\pm 2\%$ is acceptable. Thus blank and STD solutions were prepared with pure deionised water and salinity effect was neglected.

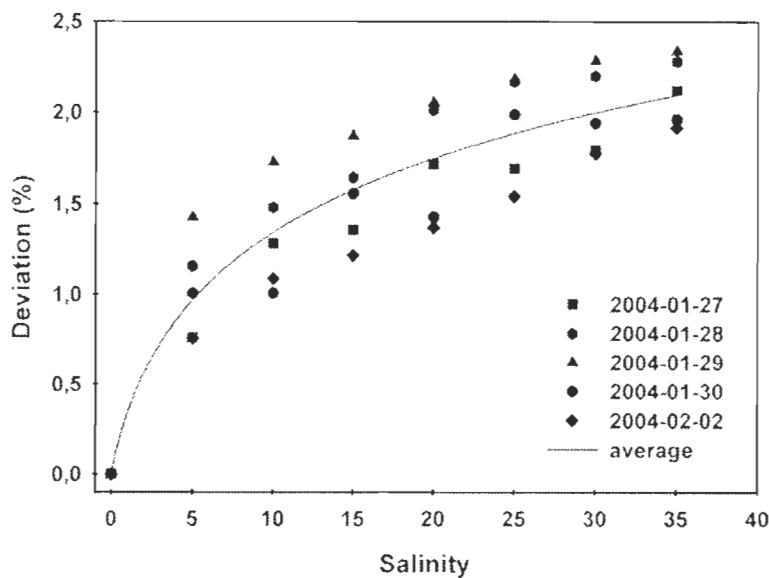


Figure II-4 Influence of salinity on the fluorescence signal obtained for ammonium ($1.00 \mu\text{M}$) in five successive determinations over the entire range of salinity (0–35). Deviation is calculated against the response obtained for the same ammonium concentration in deionised freshwater used as reference.

2.4.5 Limit of detection and analytical reproducibility

The performance of the OPA method heavily relies on the purity of deionised water used for reagent, standard and blank preparations. Moreover, contamination sources from airborne particles and handling are critical factors to be considered in all steps of the protocol, especially in field conditions. Calibration curves calculated with standard solutions from 0 to $10.00 \mu\text{M}$ are shown in Fig. 5. In all cases, the linear regression provided $R^2 = 0.99$ or better and exhibited no significant variability between successive runs over 3 days. The average analytical blank fluorescence contribution was evaluated to $117 \pm 3 \text{ RFU}$. This residual fluorescence seems to correspond to ammonium remaining in deionized water or from handling and air contamination. The lowest detectable concentration was estimated to 5 nM using the average detected blank $\pm 3 \text{ SD}$. This result can be compared to recently published results [15] where a LOD of 7 nM (blank + 3SD) was obtained using a flow-injection apparatus operated at 70°C with OPA reagent. Using the slope of calibration curves instead of the average blank value and following the calculation method recommended by Miller and Miller (1988) [16], the practical limit of

detection (LOD) of the OPA method using a microplate-based technique was $0.05 \mu\text{M}$ (Table 2). A well planned work schedule allows the analysis of 16 samples per hour.

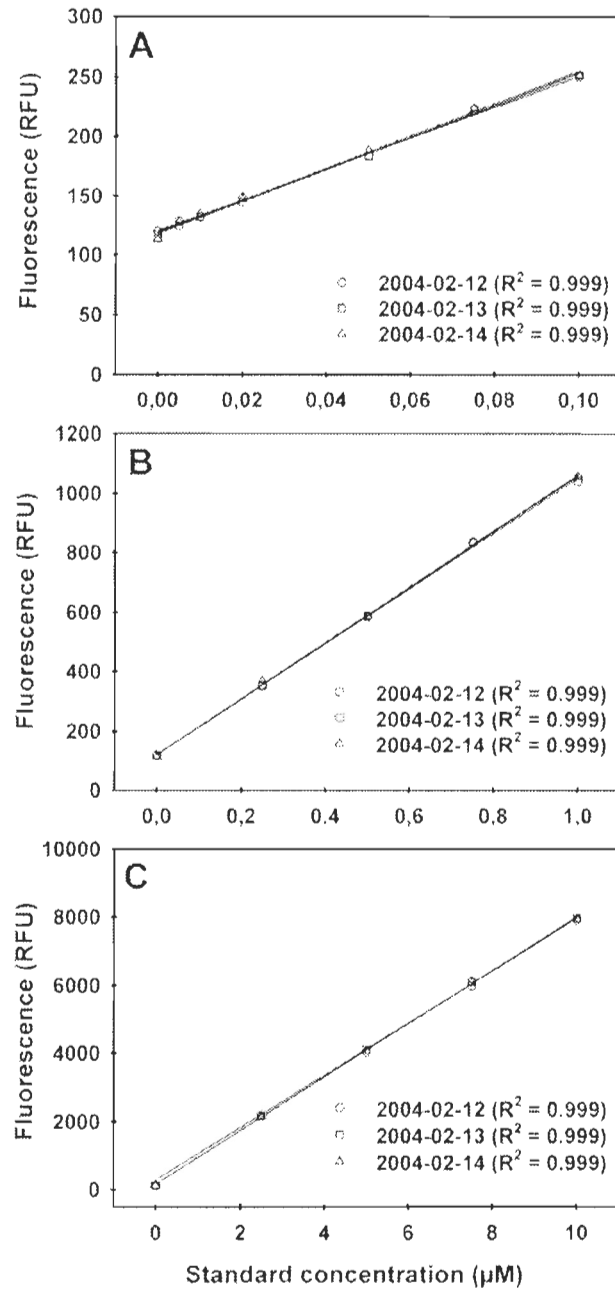


Figure II-5 Standard curves obtained following a 4h-incubation at 22°C . A) low, B) medium, C) high ammonium concentrations. Measurements were repeated in triplicate over three consecutive days.

Tableau II-2 Determination of the practical limit of detection (LOD) of the method according to [16] and using five calibration curves obtained in five successive days.

Standard Curve (0.25 – 2.00 µM)	Correlation coefficient (R ²)	Intercept (a) (RFU)	Slope (b) (RFU µM ⁻¹)	Standard Deviation (S _{y,x})	LOD (y-a = 3S _{y,x}) (µM)
A	1.000	100.45	872.70	9.91	0.03
B	0.999	77.38	891.27	15.81	0.05
C	0.999	59.33	865.62	18.86	0.07
D	1.000	74.17	820.71	10.04	0.04
E	0.999	44.01	880.33	18.80	0.06

Table 3 presents and compares the OPA-microplate-based technique with existing ammonium determination methods using spectrophotometry with idenophenol blue (IPB) [17], voltammetry with ions selective electrodes (ISE) [18] or cathodic stripping techniques (CSV) [19], ion-exclusion chromatography (IEC) [20] and spectrofluorometry with OPA reagent [6, 7, 12, 15]. Most methods can reach a LOD below 0.01 µM, but their common problem is either their lack of applicability to fresh, brackish and marine waters or their excessive sensitivity to coloured waters and suspended particulate matter. Using OPA-based methods, authors [6, 7, 12, 15] developed a sensitive and robust method for ammonium in a very large range of water samples with highly variable properties. The improved OPA technique using microplate reader provides a LOD comparable to the best methods and offers the advantages of a semi-automated method (simple, fast, precise and highly reproducible with almost no interferences). The commercial availability of not expansive microplates using inert material not reacting with OPA would allow the incubation directly in microplates and reduce the work load by 50 %.

Tableau II-3 Comparison of analytical characteristics of ammonium determination procedures.

Method	LOD (μM)	Working range and linearity (μM)	Apparatus	Sample volume (ml)	Toxic Reagents	References
IPB	0.007	0.007 - 0.7	Spectrophotometer UV-VIS	5 ml	Phenol Nitroprusside	[17]
ISE	0.2	0.25 - 10	Electrode	125 ml	n	[18]
CSV	0.004	0.010 - 3	Electrodes Potentiostat	6 ml	n	[19]
IEC	0.125	0.5 - 500	Liquid Chromatograph	0.1 ml	Organic solvents	[20]
Roth's	0.001	Not reported	Fluorometer	0.1 ml	OPA O- Diacetylbenzene 2- Mercaptoethanol	[8]
OPA	0.002	0.005 - 250	Fluorometer	~5 ml	OPA	[6][7][12][15]
Microplate- based OPA	0.005	0.05 - 10	Microplate fluorescence reader	8 ml	OPA	This Paper

2.4.6 Field examples

The microplate technique was tested on water samples collected from rivers, salt marshes along the St. Lawrence Estuary over a period of 24 months providing a large spectrum of different chemical and physical properties (Table 1, Fig 6). In all cases, samples were analysed in triplicate. Standard deviation (SD) with values $< \pm 0.05 \mu\text{M}$ showed the good reproducibility of this technique for determining COR_{NH_4} . The contribution of blank fluorescence under field conditions may be high (30.5 % for Pointe-au-Père saltmarsh) and can reach >50 % of total raw fluorescence when ammonium concentration is particularly low as shown by the Rimouski River sample (Table 1). Fluorescence generated by natural products (RF_{BG} values) cannot be neglected especially for those with sub-micromolar concentrations as illustrated by the samples of Ste Anne

River reaching 104 RFU and the Rimouski River where RF_{BG} represented up to 16 % of the total RF value. The matrix effect remains low for seawater samples (< 15 %) but reaches 30 to 40 % of the fluorescence signal in rivers with a strong background value. The precision, calculated from SD of each field analysis in triplicate, averaged $\pm 2.2\%$ for ammonium concentrations higher than 0.3 μM , but increased to $\pm 20\%$ with concentrations close to the practical LOD in the Rimouski River sample.

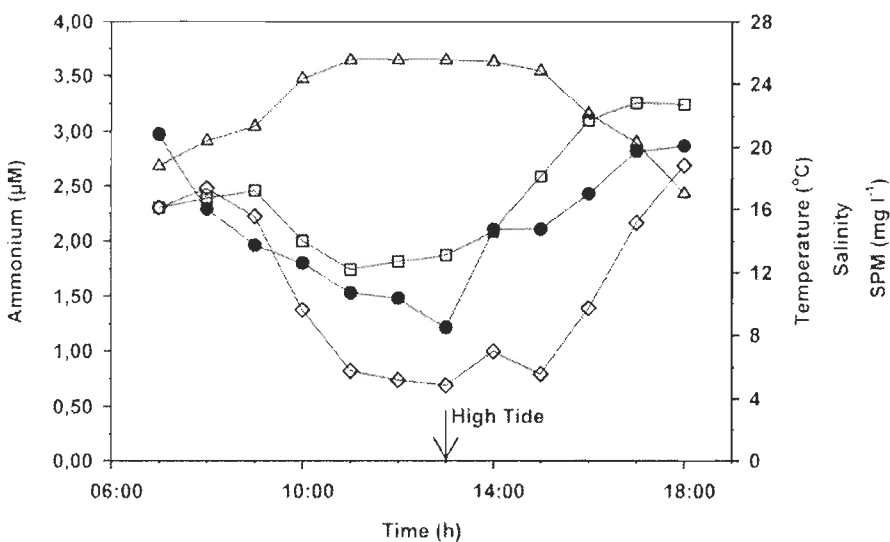


Figure II-6 Ammonium concentration determined during a complete tidal cycle in the Pointe-au-Père saltmarsh. Symbols stand for ammonium (●); temperature (□); salinity (△) and suspended particular matter (◊).

Ammonium concentrations were measured in the Pointe-au-Père saltmarsh over a complete tidal cycle (Fig. 6). This impacted littoral environment dominated by *Spartina alterniflora* is affected by municipal sewage and receives natural reddish turbid waters from surrounding peat bogs. Parameters including temperature, salinity and suspended particular matter concentration (SPM) were measured during one tidal cycle in July 2004 and compared with ammonium measurement. Results show ammonium concentrations vary from 2.97 μM at low tide to 1.21 μM at high tide (Fig. 6) with no particular interferences from salinity, temperature and SPM.

2.5 Conclusion

By adapting the OPA method [6] to a microplate technique, we intended to reduce the sample volume to less than 10 mL, reduce the working load for multiple replicates and increase the robustness of the method for organically loaded samples containing self-fluorescing molecules and humic substances generating a strong matrix effect. As precise and accurate measurements of the reagent blank, sample background and matrix effect are integrated to the automated microplate reading, this technique reduced the variability of the fluorescence signal by using a calibration curve for each group of four samples. Providing an excellent repeatability, low detection limit, low reagent toxicity and waste, this technique was applied with success to natural waters coastal with high contents in particulate and dissolved organic matter and variable salinity.

2.6 Acknowledgements

Authors acknowledge J. Campredon, K. Belzile, and G. Canuel for their technical support during laboratory development of the method and field work. This research was supported by the Canada Research Chairs program (E.P.) and the Natural Sciences and Engineering Research Council of Canada (NSERC Discovery grant).

2.7 Reference

- [1] R.A. Herbert, FEMS Microbiol. Rev., 23 (1999) 563.
- [2] T.H. Blackburn, J. Sorensen, Nitrogen Cycling in Coastal Marine Environment, Wiley, 1988.
- [3] R.M. Maier, I.L. Pepper, C.P. Gerba, Environmental Microbiology. Academic Press, 2000.
- [4] B.D. Nedwell, L.F. Dong, A. Sage, G.J.C. Underwood., Estuar. Coast. Shelf Sci. 54 (2002) 951.
- [5] R. Kérouel, A. Aminot, Mar. Chem. 52 (1996) 173.
- [6] R. Kérouel, A. Aminot, Mar. Chem. 57 (1997) 265.

- [7] M. Holmes, A. Aminot, R. Kérouel, B.A. Hooke, B.J. Peterson, Can. J. Fish. Aquat. Sci. 56 (1999) 1801.
- [8] M. Roth, Anal. Chem. 43 (1971) 880.
- [9] Z. Genfa, P.K. Dasgupta, Anal. Chem. 61 (1989) 408.
- [10] A.D. Eaton, V. Grant, Limnol. Oceanogr. 24 (1979) 397.
- [11] H.-H. Schierup, B. Riemann, Archiv. Hydrobiol. 86 (1979) 204.
- [12] A. Aminot, R. Kérouel, R. D. Birot, Wat. Res. 35 (2001) 1777.
- [13] W.L. Hawkins, Polymer Stabilisation, Wiley-Interscience, 1972.
- [14] P. de Montigny, J.F. Stobaugh, R.S. Givens, R.G. Carlson, K. Srinivasachar, L.A. Sternson, T. Higuchi, Anal. Chem. 59 (1987) 1096.
- [15] R.J. Watson, E.C. Butler, L.A. Clementson, K.M. Berry, J. Environ. Monit. 1 (2005) 37.
- [16] J.C. Miller, J.N. Miller, Statistics for analytical chemistry, 2nd edition., Ellis Horwood, 1988.
- [17] L. Solorzano, Limnol. Oceanogr. 14 (1969) 799.
- [18] C. Garside, G. Hull, S. Murray, Limnol. Oceanogr. 23 (1978) 1073.
- [19] A.-M. Harbin, C.M.G. van den Berg, Anal. Chem. 65 (1993) 3411.
- [20] M. Mori, K. Tanaka, M.I.H. Helaleh, Q. Xu, M. Ikeda, Y. Ogura, S. Sato, W. Hu, K. Hasebe, J. Chromatogr. 977 (2003) 191.

CHAPITRE III

Temporal and spatial variability of ammonium in the St. Lawrence Estuary (Québec, Canada): Significance of allochthonous and autochthonous contributions

Patrick Poulin, Émilien Pelletier, Louis-Charles Rainville et Phill Archambault

Submit to Estuarine, Coastal and Shelf Science

3.1 Abstract

This study presents the results of four oceanographic expeditions carried out in the St. Lawrence Estuary (SLE) in May 2003, July 2004, October 2005 and December 2005. Biogeochemical variables (*i.e.* temperature, salinity, phosphate, silicate, nitrite, nitrate, suspended particulate matter, particulate hydrolysable amino acids (PHAA) and chlorophyll-a) were monitored in the water column and related to spatial and temporal variability of ammonium (NH_4^+). NH_4^+ concentrations measured through the Upper Estuary (USLE) showed a conservative behavior with decreasing seaward concentrations for all sampling periods, except for July 2004 where near constant concentrations were observed. Maximum NH_4^+ concentrations were observed in surface waters in May 2003 and July 2004, and minimum values were recorded in deep layers in October and December 2005. Flux calculations showed that seasonal surface NH_4^+ inputs toward the Lower Estuary (LSLE) were highly variable (Av \pm SE; $980 \pm 434 \text{ T N month}^{-1}$) with the highest seaward transport recorded in October ($2077 \text{ T N month}^{-1}$) while a low landward transport was recorded in July ($-46 \text{ T N month}^{-1}$). As the calculated NH_4^+ contribution to the total USLE dissolved inorganic nitrogen (DIN) flux did not exceed 6% during high productivity periods (*i.e.* May 2003 and July 2004), we estimated that the $\text{N}(\text{NH}_4^+)$ mediated production accounts for probably for less than 2% of the annual phototrophic production in the LSLE area. Thus, land-derived ammonium inputs seem to have a weak effect on the LSLE pelagic productivity, although *in situ* regenerated NH_4^+ production may be more important as a dissolved nitrogen supplier. During the high primary production season (July 2004), low NH_4^+ concentrations were observed in the LSLE surface water ($0.21 \pm 0.07 \mu\text{M}$) while translocation of endogenous particulate organic nitrogen (PON) towards the deep water layers occurred. As NH_4^+ is known to be easily assimilated by phytoplankton, it could

contribute to the increase of labile particulate organic nitrogen (PON) downward flux in the LSLE. Higher NH_4^+ concentrations in the intermediate layer during productivity period coupled to geochemical characteristics of suspended particulate matter suggest a link between phototrophic productivity, grazing and bacterial-mediated mineralization processes such as ammonification in the LSLE. These processes, along with calculated riverine NH_4^+ inputs, provide a first picture of spatial and temporal variations of NH_4^+ loads in the St. Lawrence Estuary.

3.2 Introduction

The anthropogenic nitrogen load from land farming, organic soil erosion, urban and industrial wastes has increased significantly over the last decades, globally affecting the balance between non reactive and reactive nitrogen species (Vitousek *et al.*, 1997). The resulting accumulation of reactive nitrogen is such that it is now considered as the biggest pollution threat in coastal waters (Rabalais and Nixon, 2002; Howarth and Marino, 2006). Estuarine ecosystems are particularly sensitive to this problem since they link land and sea and are active sites of land-based constituent recycling (Flindt *et al.*, 1999). As nitrogen (N) species availability regulates primary and secondary productions in coastal marine environments (Carpenter and Capone, 1983), anthropogenic N inputs are recognized to enhance oxygen consumption by increasing pelagic production process (Duarte, 1995). However, the effects of anthropogenic nitrogen inputs on biogeochemical processes can be highly diversified from one estuary to another one due to complex hydrodynamic regimes of estuarine systems resulting from the interactions between many contributors (e.g. freshwater runoff, marine landward advection, and large scale physical forcing), (Balls, 1994). Although the consequences of these N inputs have been studied in numerous temperate and tropical estuaries there is an important lack of knowledge about the fate of anthropogenic nitrogen in some northern large estuaries such as the St. Lawrence Estuary (Canada).

The St. Lawrence Estuary (SLE) is a naturally eutrophic and permanently stratified estuarine ecosystem. While mechanisms involved in nutrient replenishment of the SLE surface layer, mostly from vertical advection processes (Greisman and Ingram, 1977;

Vézina *et al.*, 1995; Plourde and Therriault, 2004) and upstream riverine inputs (Greissman and Ingram, 1977; Coote and Yeats, 1979; Savenkoff *et al.*, 2001), have been intensively studied in the last decades, seasonal processes implied in ammonium (NH_4^+) distribution remain poorly defined. Among these mechanisms, the potential role of the land-derived NH_4^+ inputs on the SLE ecosystem is not well established. Even though real impacts are still unknown, several authors suggested an increase of the nitrogen load in the St. Lawrence Estuary watershed (Howarth *et al.*, 1996; Ro *et al.*, 1998; Painchaud, 1999; Chambers *et al.*, 2001; deBruyn *et al.*, 2003). Although not yet linked to this N load increase, recent studies demonstrated a contribution of anthropogenic induced eutrophication in the development of hypoxic conditions in St. Lawrence Estuary deep waters (Gilbert *et al.* 2005; Thibodeau *et al.* 2006). New information is thus needed to understand the extent of marine perturbations induced by anthropogenic NH_4^+ inputs and as well as the effects of future changes of these fluxes in relation with global climate change. As NH_4^+ is generally considered to be preferentially used as a N source by autotrophic and heterotrophic plankton species (McCarthy, 1980) and usually represents a significant fraction of the nitrogen pool in estuarine environment (48% in average according to Berman and Brook, 2003), the fate of ammonium in the St. Lawrence Estuary is a cause of concern.

The main objective of this paper is to depict the spatial and temporal distribution of NH_4^+ in the SLE water column in relation with biogeochemical variables (*i.e.* nitrite + nitrate ($\text{NO}_2^- + \text{NO}_3^-$), silicate ($\text{Si}(\text{OH})_4$), phosphate (PO_4^{3-}), chlorophyll-a (Chl-a), particulate organic carbon (POC), particulate organic nitrogen (PON), and particulate hydrolysable amino acids (PHAA)). From May 2003 to December 2005, four oceanographic expeditions were conducted to gather maximum information on NH_4^+ in the SLE water column. Collected data were used to investigate: 1) the relationship between upstream NH_4^+ inputs and hydrologic processes; 2) the biological use of NH_4^+ during high productivity periods; and 3) the occurrence of bacterial N mineralization processes within the whole water column during these high productivity periods.

3.3 Materials and methods

3.3.1 Research area

St. Lawrence Estuary is a transitional 600-km long funnel-shaped macro-tidal environment located in Eastern Canada (Quebec). This large estuary receives freshwater from the catchment's basin of the St. Lawrence River, the second largest freshwater discharge (average $11\ 900\ m^3.s^{-1}$) in North America (El-Sabh and Silverberg, 1990), and the Saguenay River (average $1\ 600\ m^3.s^{-1}$) draining the northern part of Quebec province (Schafer *et al.*, 1983). Watersheds of both St. Lawrence and Saguenay rivers support the activity of about 57 million people, some large industrial zones and important agricultural areas (Chambers *et al.*, 2001). According to El-Sabh, (1979), the estuarine region system begins at the upstream limit of salt intrusion and can be divided into the Upper Estuary (USLE: from Quebec City to the mouth of the Saguenay Fjord near Tadoussac; Fig. 1, stations 1 to 5) and the Lower Estuary (LSLE: from Tadoussac to Pointe-des-Monts; stations 6 to 10). In this study, the LSLE was extended downstream to Anticosti Island (stations 11 to 12) to include upper part of the Gulf of St. Lawrence (Fig. 1). The USLE is a narrow, shallow (< 100 m) and turbid corridor characterised by a rough bottom topography and a maximum turbidity zone (MTZ) near station 2 (D'Anglejan and Smith, 1973). In this area, landward marine water intrusion and seaward freshwater runoff are affected by intense tidal mixing processes (El-Sabh and Silverberg, 1990).

The LSLE is a wider and deeper stratified basin with a 350 m depth clay bottom central valley; the Laurentian Channel. In this area, the combination of fresh and marine waters generates a stratification in three main layers previously described by Bugden (1988): 1) a surface layer (0 - 20 m) displaying seasonal variations in temperature and salinity in response to surface heat fluxes and freshwater runoff, 2) a cold intermediate layer extending from 20 to 150 m depth less affected by environmental changes than the surface layer and 3) a more homogeneous deep water mass (150 m to bottom) that only undergoes long term changes due to a relatively steady inward advection ($0.5\ cm.s^{-1}$) and weak vertical diffusion. Two main processes are responsible for the replenishment of nutrients in the surface water. Over the whole area of the LSLE, seasonal mixing processes, mostly during winter, enable the vertical advection of nutrient-rich waters from

the deeper layer. (Theriault and Lacroix, 1976; Greisman and Ingram, 1977; Vézina *et al.*, 1995; Plourde and Therriault, 2004). Moreover, tidally induced up-welling processes occur near the mouth of the Saguenay Fjord, bringing nutrient-rich bottom waters to the surface and allowing seasonal high biological productivity (El-Sabh, 1979). The LSLE is also strongly affected by an ice cover which begins to form along the shores in late November while complete melting generally occurs in April (El-Sabh, 1979; Saucier *et al.*, 2003).

3.3.2 Sampling strategy

Studying spatial and temporal oceanographic features in a large and deep water body like the St. Lawrence Estuary requires important logistic means and a sea-going oceanographic vessel. As it became clear in early 2003 that it would be impossible to get 4 successive expeditions within the same year, we adapted our sampling strategy and decided to spread over three years our sampling efforts. The first expedition, from May 30 to June 6 2003, corresponded to the second half of the spring flood period with mean freshwater temperature below 5 °C. The second expedition, from 24 to 28 July 2004, corresponded to full summer period with warm air and sunny days. The third expedition, from 5 to 8 October 2005, was typical of the fall period on the estuary with rainy and cold weathers. Finally, the fourth expedition conducted from 15 to 18 December 2005, clearly corresponded to early winter conditions with the beginning of ice formation along seashores. Assuming that large-scale oceanographic features did not change drastically during these three sampling years, we considered each expedition as representative of typical seasonal conditions, but keeping in mind the high seasonal variability often encountered in an estuarine environment.

Water samples were collected at different depths at 12 successive stations located along the main axis of the St. Lawrence Estuary between Quebec City and Anticosti Island (Fig. 1) on oceanographic ships RV *Coriolis II* and CCGS *Amundsen*. Station 1 in front of Quebec City is not affected by saltwater and represents our upstream freshwater station. Vertical profiles of temperature, salinity, and dissolved oxygen (DO) were recorded by a Seabird® SBE 9 multi-probe (temperature accuracy ± 0.01 °C, salinity accuracy ± 0.01 , and

DO accuracy $\pm 0.01 \text{ mg.l}^{-1}$) mounted on a rosette multi-sampler (General Oceanics[®]). Temperature and salinity of samples were validated onboard using a dual temperature and salinity YSI[®] digital probe whereas the probe for DO measurements was validated using Winkler titrations (Strickland and Parson, 1972). Deviations of DO probe compared with onboard chemical titration were always $< 5\%$. Water samples were taken on the upward casts at different depths (between 1 and 6 samples following water depth) using 12-l lever-action Niskin[®] bottles (General Oceanics[®]). Water samples for dissolved nutrients measurements were filtered onto 0.22 μm pore-size Nucleopore[®] membranes and stored in the dark at -80°C in 60 ml polyethylene bottles until analysis. Samples for NH₄⁺ measurement were directly collected from Niskin[®] bottle in clean 250 ml DOB glass bottles and analyzed onboard. Suspended particulate matter (SPM) was collected by filtration on pre-combusted, pre-weighted, 47 mm diameter Millipore[®] glass fiber membranes (until clogging; $< 10 \text{ l}$) and stored at -80°C until analysis. Filters used for elementary analysis were acidified onboard with 10 ml 1% HCl solution (v/v) to remove calcium carbonate. Water samples for Chl-a determination were filtered onboard, in the dark on 25 mm diameter Millipore[®] glass fiber membranes and stored in the dark at -80°C until analysis.

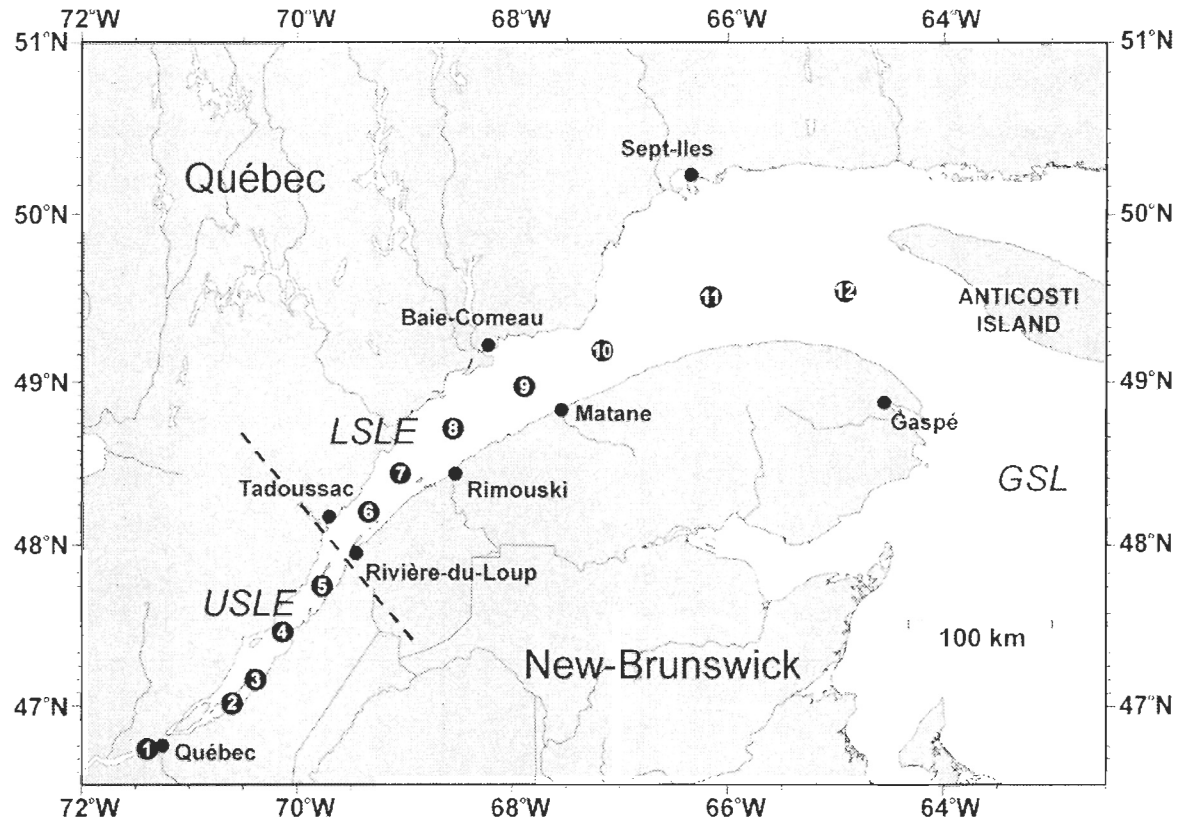


Figure III-1 Sampling area. Numbers in black circle correspond to the sampling station labels. The dotted line represents the virtual geographical separation between the Upper (USLE) and Lower (LSLE) St. Lawrence Estuary. GLS = Gulf of St. Lawrence.

3.3.3 Chemical analyses

Dissolved nutrients ($\text{NO}_2^- + \text{NO}_3^-$, Si(OH)_4 , and PO_4^{3-}) were analyzed by colorimetric techniques (Strickland and Parson, 1972) using automated Technikon® and AA3 Brand+Luebbe® platforms, allowing an overall analytical uncertainty ($\pm 1\sigma$) under $\pm 5\%$. Determination of NH_4^+ concentrations was performed onboard using a spectrofluorometric method described by Poulin and Pelletier (2007). This method provides an analytical uncertainty of $\pm 1\%$ and a detection limit of $0.05 \mu\text{M}$. Elementary analyses (%C_{org}, %N_{tot}) of suspended particulate matter (SPM) were made at the GÉOTOP-UQAM-McGill research center (Université du Québec à Montréal) using a Carlo-Erba® elemental analyzer, and at the ISMER laboratory using an ECS 4010 Costech® instrument, both analyzers equipped with a zero blank auto sampler. Replicates ($n = 10$) of certified

sediment samples (NIST-1941b) were used for quality control of these analyses. The analytical error was determined from replicate measurements of standard material (acetanilide, urea, atropine, nicotinammide) and averaged \pm 5%. POC and PON concentrations were calculated from SPM and quantitative CHN analysis.

Amino acids (PHAA) were extracted from the filters and hydrolyzed with 2 ml of 6 N HCl at 100 °C for 24 h in Pyrex tubes. After hydrolysis, the acid solution was centrifuged and the supernatant was transferred in a glass tube, diluted, and neutralized with 6 N NaOH. Resulting solutions were filtered on 0.22 μ m nylon syringe filters, derivatized with a fluorescent reagent (o-phthaldialdehyde and 2-mercaptoethanol) and then analyzed on a liquid chromatography system (HPLC) following the procedure developed by Lindroth and Mopper (1979) and using a phosphate buffer and methanol gradient. The HPLC system included a Shimadzu® SCL-10A VP controller, a Shimadzu® LC-10AD VP pump unit, a Shimadzu® FCV-10AL VP four mobile phase gradient solvent delivery unit, a Shimadzu® DGU-14A degasser unit, a Shimadzu® CTO-10AC VP column oven unit (using a Agilent® C-18 column [4.6 X 250 mm, 5 μ m]) and a Water® 470 fluorescence detector (using $\lambda_{\text{ex}} = 230$ nm, $\lambda_{\text{em}} = 445$ nm). Amino acid standard was a hydrolyzed protein amino acids mixture produced by Sigma® (A 2908) which contained 21 amino acids and ammonium chloride. The internal standard, aminobutyric acid, was added during the acid treatment of the standard and samples. PHAs were identified by retention times and quantified using sample peaks area, corrected with the internal standard. Relative errors in duplicate analysis were $< 5\%$.

Chl-a was extracted from GFF filters with 10 ml of 90% (v/v) acetone for 24 h at 4 °C in the dark and Chl-a concentrations were determined using a Turner design® spectrophotometer ($\lambda_{\text{em}} = 630$ nm) according to Strickland and Parson (1972) with an overall analytical uncertainty ($\pm 1 \sigma$) averaging $\pm 1\%$.

3.3.4 Water column data analysis

Vertical profiles of dissolved and particulate nutrients at discrete depths were interpolated onto a rectangular grid with the *CTDFGRID EPIC* software (Lukas, R.B., Dept of Oceanography, Univ. of Hawaii), using the method of successive over-relaxation to solve programmed partial differential equations (Ames, 1977).

In an attempt to describe the seasonal influence of the NH_4^+ land-derived inputs to LSLE, the mixing diagram approach was used. Initially developed by Boyle *et al.* (1974), it was frequently used to depict mixing dynamic of transitional environments (e.g. Morris *et al.*, 1995; Kress and Herut, 1998; Kress *et al.*, 2002). As Greisman and Ingram (1977), we postulated that there are only two main sources of nutrients in SLE: freshwater rivers and vertical mixing occurring from Tadoussac upwelling (in the vicinity of station 6, Fig. 1). Assuming the behavior of dissolved salts was conservative in the USLE, measured dissolved inorganic nitrogen (DIN) concentrations ($\text{NO}_2^- + \text{NO}_3^-$, NH_4^+) were plotted against salinity for each sampling period. This approach was not used in the LSLE since dissolved inorganic nutrients presented a non-conservative behavior indicating the presence of significant sinks or sources of DIN in this area. The salinity (PSU) was fixed at 0 for station 1 (freshwater) and at 27 for station 5 which represented the average salinity recorded during our four expeditions. Using these calculated end-members and mean monthly discharges at Québec City, calculated for each sampling period (<http://www.osl.gc.ca/fr/donnees/debits/2000.html>), we estimated NH_4 and DIN fluxes reaching the LSLE surface water via the USLE.

In order to determine if significant seasonal NH_4^+ concentration variations were present in different SLE water masses, the SLE was divided in four specific sections (USLE, LSLE surface (0-20 m), LSLE intermediate (20-150 m) and LSLE bottom (> 150 m)) according to discontinuities observed in the topography and water mass characteristics previously described (El-Sabh, 1977, Bugden, 1988). An ANOVA was carried out to test the surface NH_4^+ concentration variability with sampling locations in the Estuary (USLE and LSLE Surface) and among sampling periods (May 2003, July 2004, October 2005 and December 2005). Normality was verified using the Shapiro-Wilk's test (Zar, 1999) and

homoscedasticity was confirmed by graphical examination of the residuals (Quinn and Keough, 2002). Data were SQRT transformed to achieve homogeneity of variances and normality. When a source of variation was significant, the Tukey-Kramer test (Sokal and Rohlf 1995) was carried out to identify the differences at $\alpha = 0.05$.

Stepwise multiple regressions were used to examine relationships between NH_4^+ concentrations and environmental variables (temperature, salinity, O_2 , $\text{NO}_2^- + \text{NO}_3^-$, PO_4^{3-} , $\text{Si}(\text{OH})_4$, Chl-a, SPM, PON, POC). The salinity was $\log_{10} + 1$ transformed to meet the normality. Based on the Cook's distance (Cook and Weisberg, 1982; Quinn and Keough, 2002), one value was removed from the regression. Normality and homoscedasticity were confirmed by graphical examination of residuals (Quinn and Keough 2002). The variance inflation factor (VIF) to detect collinearity. VIF values were all < 10 (highest value observed was 2.8) indicating no strong collinearity (Quinn and Keough 2002).

Diagenetic alteration of sedimentary amino acids was assessed using the Degradation Index (DI) developed by Dauwe et al. (1999). This index is based on the first axis of a Principal Component Analysis (PCA) of the amino acid composition and summarizes, in one variable, the relative cumulative variation of individual PHAA. DI values were calculated from amino acids average molar ratios, standard deviations and predetermined factor coefficients (i.e. first axis factor coefficients of the PCA from the comprehensive data set of Dauwe et al., 1999). DI value indicates the state of diagenetic alteration of the organic matter; high values corresponding to fresh organic matter while low (negative) values indicating degraded organic mater.

3.4 Results

3.4.1 Temporal and spatial variability of water temperature, salinity and dissolved oxygen

During the four sampling periods, important temperature and salinity changes were observed in SLE surface waters in response to seasonal heat fluxes and variations of riverine freshwater inputs. In the upper estuary (USLE stations 1 to 5; Fig. 1), the shallow water column was well mixed and strong temperature and salinity gradients were observed

year-round with the lowest salinity monitored at station 1 (freshwater) and the highest one at station 5. The mean salinity (all stations and all depths) ranged from 15.77 to 19.77 and was subject to tidal oscillations and freshwater discharges. The lowest mean temperature ($0.15\text{ }^{\circ}\text{C}$) was observed in December 2005 and the highest one ($12.49\text{ }^{\circ}\text{C}$) in July 2004. Only a slight seasonal variability for oxygen concentrations (general mean = $9.64 \pm 0.14\text{ mg O}_2\text{ l}^{-1}$) was observed in LSLE, with the lowest mean concentration appearing in July 2004 and the highest one in December 2005 (Table 1).

In the lower estuary section (LSLE stations 6 to 12; Fig. 1), seasonal variability of salinity and temperature decreased with depth and distance from the channel head. The LSLE water column was stratified during our sampling expeditions. The lowest average temperature in surface water (0 – 20 m) was monitored in December 2005 and the highest one in July 2004. Much less influenced by tides and freshwater discharges, the LSLE-surface average salinity showed little seasonal changes (general mean = 29.10 ± 0.09) while the mean temperature was near zero ($0.40\text{ }^{\circ}\text{C}$) in December 2005 and raised to $7.84\text{ }^{\circ}\text{C}$ in July 2004. LSLE-surface waters were always well oxygenated with values ranging from 9.12 to $11.19\text{ mg O}_2\text{ l}^{-1}$.

LSLE-intermediate waters (20 to 150 m) showed little changes in salinity (32.69 ± 0.05), but some seasonal fluctuations were observed for temperature (ranging from $0.14\text{ }^{\circ}\text{C}$ in May 2003 to $2.39\text{ }^{\circ}\text{C}$ in December 2005) and mean dissolved oxygen which decreased from near saturation ($9.95\text{ mg O}_2\text{ l}^{-1}$) in May 2003 to $6.04\text{ mg O}_2\text{ l}^{-1}$ in December 2005. LSLE-bottom waters (150 m to bottom) showed very stable conditions (mean temperature = $5.25 \pm 0.14\text{ }^{\circ}\text{C}$; mean salinity = 34.52 ± 0.01) indicating no direct influence of seasons on this deep water layer as observed by previous workers. It should be noted that our dissolved oxygen concentrations confirmed stable hypoxic conditions with a general mean value of $2.57 \pm 0.15\text{ mg O}_2\text{ l}^{-1}$ with no significant differences between seasons (Table 1).

Tableau III-1 Average values of the physical and chemical variables measured in SLE during each sampling period and calculated for USLE (0 m to bottom), LSLE-Surface (0 to 20 m), LSLE-Intermediate (20 to 150 m) and LSLE-Bottom (150 m to bottom). AV = Average, SE = Standard error, na = data not available.

Water mass	Expedition	Temperature °C)		Salinity (PSU)		O ₂ (mg l ⁻¹)		NO _x + NO ₃ ⁻ (μM)		NH ₄ ⁺ (μM)		PO ₄ ³⁻ (μM)		Si(OH) ₄ (μM)	
		AV	±SE	AV	±SE	AV	±SE	AV	±SE	AV	±SE	AV	±SE	AV	±SE
USLE	May 2003	4.34	0.75	19.72	3.39	10.10	0.09	25.86	3.85	1.91	0.29	0.82	0.11	14.98	1.96
USLE	July 2004	12.49	1.98	15.77	2.95	8.47	0.12	10.25	0.40	0.59	0.03	0.60	0.10	12.89	1.28
USLE	October 2005	9.00	1.76	16.73	3.87	9.27	0.15	18.28	1.53	2.02	0.69	0.95	0.16	17.13	1.71
USLE	December 2005	0.15	0.26	19.05	3.59	10.71	0.72	21.21	1.60	0.73	0.31	0.96	0.12	21.25	2.63
LSLE-Surface	May 2003	4.20	0.58	29.16	0.41	11.19	0.25	5.96	1.19	0.84	0.20	0.59	0.08	7.15	1.05
LSLE-Surface	July 2004	7.84	1.05	28.13	0.50	9.12	0.13	4.33	0.61	0.47	0.09	0.60	0.08	8.37	1.18
LSLE-Surface	October 2005	4.80	0.67	29.43	0.45	9.74	0.19	9.68	1.14	0.54	0.17	1.00	0.08	8.60	1.05
LSLE-Surface	December 2005	0.40	0.60	29.69	0.45	10.45	0.40	11.51	0.95	0.02	0.09	1.03	0.05	12.65	1.29
LSLE-Intermediate	May 2003	0.14	0.34	32.33	0.14	9.95	0.24	11.88	0.94	0.97	0.19	1.19	0.05	10.89	1.14
LSLE-Intermediate	July 2004	1.09	0.40	32.65	0.22	7.49	0.67	8.51	0.99	0.35	0.13	1.31	0.12	14.84	2.44
LSLE-Intermediate	October 2005	1.88	0.33	32.66	0.29	6.95	0.79	16.69	1.75	0.02	0.00	1.58	0.13	17.14	2.88
LSLE-Intermediate	December 2005	2.39	0.29	33.11	0.26	6.04	0.72	18.18	1.67	0.01	0.00	1.63	0.12	22.29	2.99
LSLE-Bottom	May 2003	5.60	0.20	34.57	0.03	2.96	0.31	26.67	0.19	0.01	0.00	2.16	0.11	37.66	2.76
LSLE-Bottom	July 2004	5.26	0.07	34.54	0.04	2.27	0.17	na	na	0.02	0.01	2.18	0.09	39.44	2.41
LSLE-Bottom	October 2005	5.07	0.11	34.49	0.05	2.38	0.20	25.32	0.10	0.01	0.00	2.35	0.06	38.47	1.66
LSLE-Bottom	December 2005	5.08	0.13	34.49	0.06	3.65	0.24	26.13	0.27	0.01	0.00	2.19	0.04	43.45	0.93

3.4.2 Temporal and spatial variability of dissolved nutrients and SPM

Dissolved nutrient concentrations ($\text{NO}_2^- + \text{NO}_3^-$, PO_4^{3-} , Si(OH)_4) showed important spatial and temporal variations in surface and intermediate SLE water masses (Table 1). Well mixed waters in the upper estuary (USLE) showed high values in silicate and NO_x ($\text{NO}_2^- + \text{NO}_3^-$) in all seasons, except in July 2004, whereas orthophosphate values remained always below 1 μM with a minimum mean value (0.60 μM) also appearing in July 2004. NO_x varied with seasons in both LSLE-surface and intermediate waters indicating important depletion in May 2003 and July 2004. Phosphate and silicate mean values also confirmed a seasonal effect in surface and intermediate layers (Table 1). The LSLE-bottom layer showed a remarkable stability in nutrient concentrations with not significant changes between seasons.

In the upper estuary, SPM and PON concentrations were elevated (reaching 114 mg l⁻¹ and 670 µg l⁻¹ in December 2005 at station 2, detailed results not shown) with highest Chl-a concentration and C/N ratio observed in July 2004 and October 2005, respectively (Table 2). Mean POC concentration was particularly high in December 2005 being almost 3 times higher than in July 2004 and October 2005, and 6 times higher than May 2003. Relatively low C/N (9.46) seems to indicate the presence of fresh marine organic matter in USLE in May 2003. LSLE-surface waters showed SPM values about 10 to 15 times lower than USLE illustrating the important settling of suspended particles in the USLE section and dilution process in the lower estuary. POC and PON concentrations were higher in May 2003 and July 2004 corresponding with the highest Chl-a and C/N values observed for all four expeditions. Chl-a was clearly present in the LSLE-intermediate layer in July 2004 (1.33 µg l⁻¹) and also in May 2003 at a lower level (Table 2). C/N values increased with seasons (from spring to winter) and with depth in the LSLE indicating a gradual change in the quality of the organic matter. Chl-a reached the LSLE-bottom layer in May 2003 (0.07 0.12 µg l⁻¹) and July 2004 (0.12 µg l⁻¹) with a mean C/N value around 9.4. SPM concentrations of the LSLE-bottom layer are comparable to values found in surface and intermediate layers, but 10 to 20 times lower than SPM measured in the USLE where resuspension and freshwater inputs are the main sources of suspended matter.

Particulate amino acids (PHAA) were determined in SPM collected during July 2004, October and December 2005 expeditions in an attempt to reach a better characterization of the particulate organic matter (Table 3). The molar ratio between tyrosine and PHAA (Tyr/PHAA), the contribution of PHAA to total PON (PHAA-N%) and the index DI were also calculated (Table 3). PHAA attained a maximum mean concentration in July 2004 in both USLE (0.47 µmol mg⁻¹) and LSLE (0.94 µmol mg⁻¹) whereas it remained low and almost constant during other sampling seasons (Table 3). The PHAA-N% followed a similar seasonal trend with its highest average contribution recorded in July 2004. All calculated DI were negative and the lowest average DI was observed in December 2005 whereas the highest value was recorded in October 2005 (Table 3). The Thyrosine/PHAA molar ratio was maximum in LSLE – Surface waters for all sampling expeditions (data not available in May 2003) and always very low in bottom waters.

Tableau III-2 Average values of suspended particular matter characteristics measured in SLE during each expedition and calculated for USLE (0 m to bottom), LSLE-Surface (0 to 20 m), LSLE-Intermediate (20 to 150 m) and LSLE-Bottom +(150 m to bottom). AV = Average, \pm SE = Standard error.

Water mass	Expedition	Chl-a ($\mu\text{g l}^{-1}$)		SPM (mg l^{-1})		PON ($\mu\text{g l}^{-1}$)		POC ($\mu\text{g l}^{-1}$)		C/N	
		AV	\pm SE	AV	\pm SE	AV	\pm SE	AV	\pm SE	AV	\pm SE
USLE	May 2003	1.29	0.22	16.97	7.52	59.69	24.87	451.42	177.48	9.46	0.56
USLE	July 2004	7.27	2.23	13.63	8.33	94.07	45.67	964.37	518.10	14.08	2.60
USLE	October 2005	0.11	0.05	21.52	14.08	72.40	22.99	917.34	479.13	13.04	2.42
USLE	December 2005	0.27	0.11	32.10	20.80	214.04	114.88	2752.95	1637.21	13.43	1.02
LSLE-Surface	May 2003	5.20	1.93	2.67	0.38	57.39	16.84	314.37	86.02	7.05	0.66
LSLE-Surface	July 2004	7.55	1.85	1.91	0.12	60.81	14.77	349.26	83.34	6.88	0.32
LSLE-Surface	October 2005	0.64	1.53	1.15	0.08	27.53	5.37	168.37	34.73	7.54	0.73
LSLE-Surface	December 2005	0.13	0.05	1.27	0.19	21.46	2.38	177.90	18.78	8.79	0.73
LSLE-Inter	May 2003	0.36	0.10	1.41	0.29	7.27	1.24	30.50	7.30	8.28	0.43
LSLE-Inter	July 2004	1.33	0.31	1.06	0.07	13.16	2.68	83.33	14.38	8.04	0.84
LSLE-Inter	October 2005	0.06	0.02	0.74	0.10	10.00	0.70	67.95	7.85	8.32	1.06
LSLE-Inter	December 2005	0.03	0.02	0.77	0.09	14.60	1.04	121.39	6.54	9.83	0.60
LSLE-Bottom	May 2003	0.07	0.01	2.08	0.79	5.59	1.44	44.97	12.86	9.35	0.29
LSLE-Bottom	July 2004	0.12	0.02	1.43	0.26	15.19	3.19	100.91	24.34	9.43	0.74
LSLE-Bottom	October 2005	0.02	0.00	1.51	0.12	10.38	0.89	109.21	9.55	12.21	0.90
LSLE-Bottom	December 2005	0.00	0.00	0.77	0.10	12.45	0.68	140.91	8.90	13.19	0.22

Tableau III-3 Average values of tyrosine molar ratio (Tyr/PHAA), PHAA concentration, PHAA-%N and DI measured in SLE during the July 2004, October 2005 and December 2005 expeditions. Values are calculated for USLE (0 m to bottom), LSLE-Surface (0 to 20 m), LSLE-Intermediate (20 to 150 m) and LSLE-Bottom (150 m to bottom). AV = Average, \pm SE = Standard Error and n = number of samples analysed.

Water Mass	Expedition (n)	Tyr/PHAA		PHAA $\mu\text{mol mg SPM}^{-1}$		PHAA-%N %		DI	
		AV	\pm SE	AV	\pm SE	AV	\pm SE	AV	\pm SE
USLE	July 2004 (5)	0.018	0.003	0.47	0.36	28.12	4.84	-0.85	0.01
USLE	October 2005 (5)	0.015	0.002	0.06	0.01	17.6	3.41	-0.63	0.12
USLE	December 2005 (5)	0.014	0.001	0.06	0.02	9.25	0.85	-0.86	0.15
LSLE - Surface	July 2004 (7)	0.033	0.001	0.94	0.07	29.76	3.58	-0.48	0.1
LSLE - Surface	October 2005 (6)	0.022	0.003	0.36	0.09	23.12	2.72	-0.26	0.11
LSLE - Surface	December 2005 (6)	0.018	0.003	0.14	0.03	12.31	1.45	-0.48	0.08
LSLE - Intermediate	July 2004 (7)	0.011	0.003	0.11	0.01	26.71	6.39	-0.55	0.06
LSLE - Intermediate	October 2005 (6)	0.011	0.003	0.12	0.01	21.55	1.46	-0.36	0.18
LSLE - Intermediate	December 2005 (6)	0.009	0.003	0.10	0.01	12.17	1.49	-0.38	0.15
LSLE - Bottom	July 2004 (7)	0.002	0.001	0.08	0.01	17.45	3.68	-0.75	0.03
LSLE - Bottom	October 2005 (6)	<0.001	0.001	0.08	0.01	16.92	1.72	-0.55	0.13
LSLE - Bottom	December 2005 (5)	0.003	0.002	0.07	0.01	9.88	1.84	-0.62	0.11

NH_4^+ concentrations showed variable temporal and spatial distribution patterns among sampling expeditions (Fig.2). The highest concentrations ($>2.5 \mu\text{M}$) were observed in the upper estuary in May 2003 and October 2005. Ammonium was clearly present at concentrations ranging between 0.5 and 2.0 μM in LSLE-surface and –intermediate layers in all seasons, except in December 2005 (Fig. 2). Through the USLE section, NH_4^+ concentrations showed a seaward decrease for all sampling expeditions, except in July 2004 where NH_4^+ presented an almost constant concentration (Table 1, Fig. 2). NH_4^+ concentrations in the LSLE surface water layer showed a distinctive distribution pattern with below detection limit concentration ($< 0.01 \mu\text{M}$) sporadically observed in the first two meters during each sampling period, and the highest concentrations being often found at the thermocline (maximum value of $2.41 \mu\text{M}$ observed in May 2003 at 20 m). The lowest mean NH_4^+ concentration was monitored in December 2005 while the highest one was recorded in May 2003 (Table 1, Fig. 2). In the LSLE intermediate water mass, the mean NH_4^+ concentration remained near the detection limit in October and December 2005, while it reached higher values in May 2003 and July 2004 with the maximum one recorded in May 2003 ($1.73 \mu\text{M}$) (Table 1, Fig. 2). NH_4^+ was below the detection limit in the LSLE bottom layer for all sampling stations and expeditions (Table 1, Fig. 2).

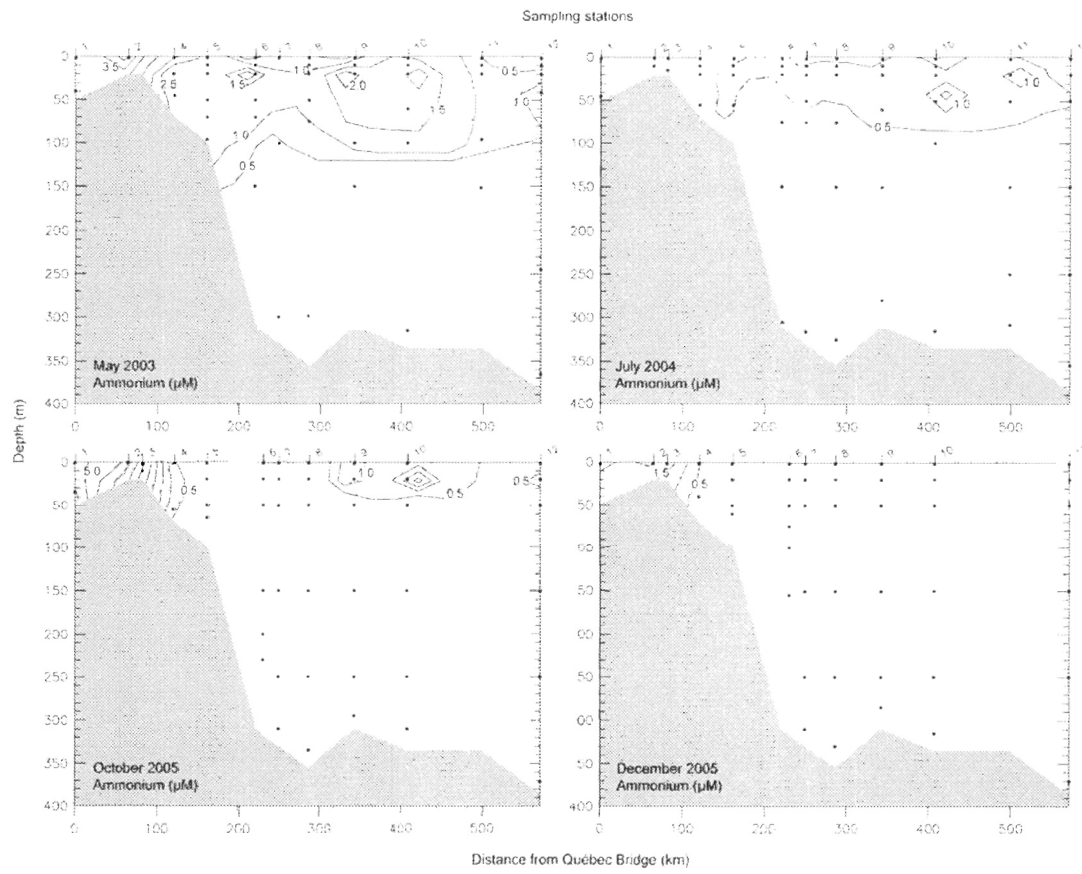


Figure III-2 Vertical profile of ammonium along the main axis of St. Lawrence Estuary between Québec Bridge (station 1) and Anticosti Island (station 12) for the four cruises. Black circles correspond to sampling depth. Note that the scales of the 2 different axes are different.

3.4.3 Statistical analysis of nitrogen species variability

A significant interaction between sampling periods (May 2003, July 2004, October 2005 and December 2005) and the region of the Estuary (USLE Surface and LSLE Surface) for the variable NH_4^+ concentration (Table 4) according the ANOVA results. An *a posteriori* test showed that NH_4^+ concentration was significantly lower in the LSLE in December 2005 and that the highest values were observed in the USLE in May 2003 and October 2005 (Fig. 3). Stepwise multiple regression models ($\log_{10}\text{salinity} + 1$, oxygen concentration, MPS and PON) explained up to 57% of the NH_4^+ concentration. The partial R^2 showed clearly that the salinity explained a very high portion of the variance in NH_4^+ concentrations, the three other variables having a smaller contribution (Table 5).

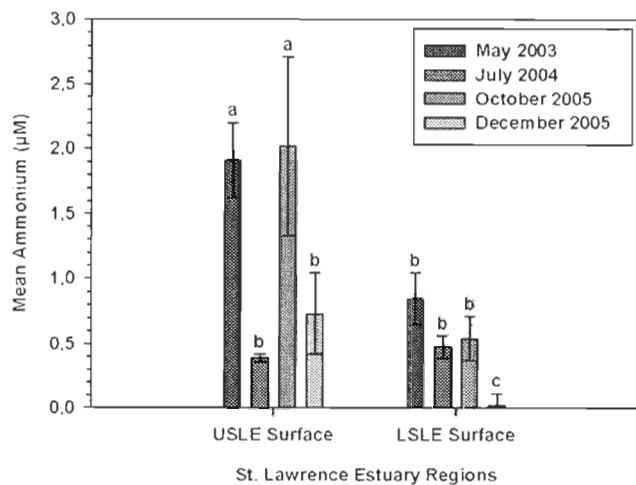


Figure III-3 Mean (\pm SE) of surface (0 - 20 m) ammonium concentration obtained for each sampling period in both St. Lawrence Estuary regions. Different letters indicate a significant difference between regions at a given sampling period ($\alpha = 0.05$).

Tableau III-4 Result of two-way analyses of variance (ANOVAs) testing the effect among the regions of the Estuary (USLE – Surface and LSLE – Surface), and sampling periods (May 2003, July 2004, October 2005 and December 2005) and their interaction on ammonium (NH_4^+).

Variables	Source of variation	df	SS	F	p
Sqrt (NH_4^+)	Region (R)	1	5.061	23.736	< 0.0001
	Sampling Period (SP)	3	6.572	10.274	< 0.0001
	R x SP	3	1.901	2.971	0.035
	Error	99	21.109		

Tableau III-5 Result of multiple stepwise (backward) regression models (stepwise procedure) to estimate the ammonium (NH_4^+) concentration in the Estuary and Gulf of St. Lawrence. Temperature (T , °C), \log_{10} salinity +1 (Sal, PSU), chlorophyll-a (Chl-a, $\mu\text{g l}^{-1}$), oxygen concentration (O_2 , mg l^{-1}), phosphate (PO_4^{3-} , μM), nitrite and nitrate ($\text{NO}_2^- + \text{NO}_3^-$, μM), silicate (Si(OH)_4 , μM), suspended particulate matter (SPM, $\mu\text{g l}^{-1}$), particulate organic nitrogen (PON, $\mu\text{g l}^{-1}$), particulate organic carbon (POC, $\mu\text{g l}^{-1}$) were the tested variables. ns: not significant. Partial R^2 is given below each regression coefficient ($\pm\text{SE}$), total R^2 , and mean squared errors (MSE) are also shown.

	Intercept	T (°C)	\log_{10} Sal	O_2 (mg l^{-1})	Chl-a ($\mu\text{g l}^{-1}$)	PO_4^{3-} (μM)	$\text{NO}_2^- + \text{NO}_3^-$ (μM)	Si(OH)_4 (μM)	SPM (mg l^{-1})	POC ($\mu\text{g l}^{-1}$)	PON ($\mu\text{g l}^{-1}$)	Total R^2 (R^2 adjusted)	MSE
NH_4^+ (μM)	2.9 \pm 0.31	ns	-2.02 \pm 0.18	0.092 \pm 0.014	ns	ns	ns	ns	0.045 \pm 0.008	ns	-0.014 \pm 0.003	0.579 (0.57)	0.379
Partial R^2			0.40	0.052					0.075		0.051		

3.4.4 NH_4^+ transport through the USLE

While a significant linear correlation and comparable negative mixing slopes were observed between NH_4^+ and salinity in May 2003, October 2005 and December 2005, indicating a conservative behavior of this nitrogen species through the whole USLE, NH_4^+ concentrations were poorly correlated with salinity in July 2004. The calculated NH_4^+ riverine end-members show that the USLE upstream input varies in an important way between sampling periods in response to seasonal hydrologic processes which modulate runoff events. Thus, the lowest NH_4^+ riverine end-member was calculated for July 2004 and the highest one for October 2005 (Fig. 4). Despite the high variability of calculated riverine end-members, calculated head-LSLE end-members were more constant with year-around lower values, except for July 2004. NH_4^+ negative mixing slopes suggest that the riverine NH_4^+ load acts as a nitrogen source for the LSLE during every sampling period with the exception of July 2004. The near-zero mixing slope observed in July 2004 indicates that sources may be as important as sinks in the LSLE at this period. As a consequence, the lowest NH_4^+ seaward flux was calculated for July 2004 (with high uncertainty) while the highest value was calculated for October 2005 (Table 6, Fig. 4). As observed with NH_4^+ , the net seaward transport of DIN through the USLE showed important seasonal variations with the lowest flux calculated for July 2004 and the highest for May 2003. The resulting monthly DIN and NO_x fluxes are presented in Table 7. The maximum NH_4^+ contribution to the DIN flux was calculated for October 2005 while a negligible contribution was found for July 2004.

Tableau III-6 Linear regression parameters defined for the mixing diagram of ammonium against salinity. Riverine and LSLE end members as well as nutrient fluxes were calculated from these regression lines. $P < 0.0001$ except for NH_4^+ in May 2003 ($P = 0.0002$) and July 2004 ($P = 0.1748$). Monthly average discharge at Quebec city (Station 1) calculated for each sampling period (<http://www.osl.gc.ca/fr/donnees/debits/2000.html>).

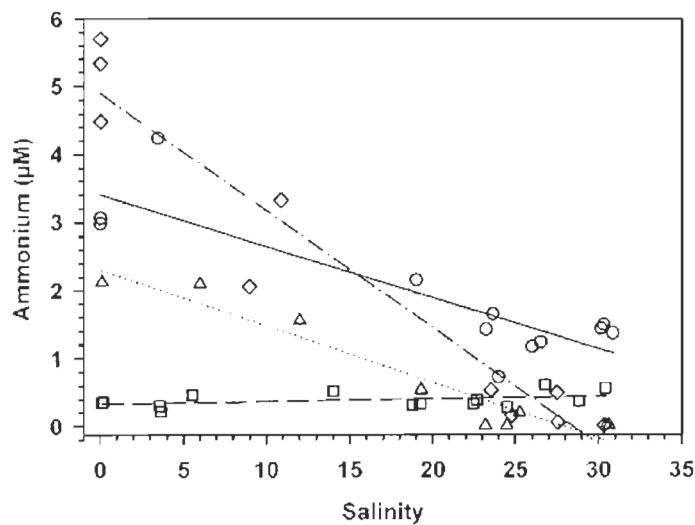
Dissolved nutrient (μM)	Sampling periods	Slope	r^2	Riverine end member $S=0$ Intercept (μM)	LSLE end Member $S=27$ Intercept (μM)	Riverine Discharge $(\text{m}^3 \text{s}^{-1})$	Nutrient Fluxes (mol s^{-1})	Nutrient Fluxes (T N month^{-1})
NH_4^+	May 2003	0.0752	0.7566	3.4012	1.3708	12430.4490	25.2388	946
NH_4^+	July 2004	0.0039	0.1478	0.3318	0.4371	11570.2970	-1.2184	46
NH_4^+	October 2005	-0.1600	0.9384	4.7374	0.4174	12818.9570	55.3779	2077
NH_4^+	December 2005	-0.0827	0.9241	2.3065	0.0736	11241.3890	25.1009	941

Tableau III-7 DIN fluxes through the USLE for each sampling period.

Sampling periods	DIN fluxes (TN month^{-1})	NH_4^+ contribution (%)
May 2003	14888	6
July 2004	1430	0
October 2005	6232	33
December 2005	5858	16
Av	7102	14
SE	1991	7

Tableau III-8 Stoichiometric analyses between Si, N and P in SLE superficial water mass (0 - 2 m) for each sampling period.

# Stations	N/P	May 2003		July 2004		October 2005		December 2005			
		Si/N	Si/P	N/P	Si/N	Si/P	N/P	Si/N	Si/P	N/P	Si/N
1	527.50	0.10	51.45	1167.80	2.01	2343.00	113.23	0.89	100.37	121.15	1.17
2	119.29	0.18	21.37	50.84	0.59	30.22	66.90	0.83	55.68	50.49	1.36
3	n	n	n	42.71	0.81	34.42	33.39	0.86	28.56	34.78	1.31
4	35.61	0.74	26.43	13.37	1.18	15.72	14.93	0.85	12.66	17.22	1.09
5	23.29	0.83	19.32	13.21	1.16	15.36	13.34	0.88	11.75	14.86	1.11
6	11.55	1.48	17.15	9.11	1.90	17.32	10.88	0.91	9.91	12.89	1.22
7	16.04	1.02	16.38	11.50	2.87	33.00	10.73	0.89	9.53	14.13	1.20
8	18.03	1.44	25.89	11.47	3.71	42.55	12.07	0.90	10.89	13.81	1.14
9	2.99	8.24	24.62	10.33	2.41	24.90	9.79	0.71	6.93	12.59	1.25
10	11.46	0.92	10.58	2.60	62.42	162.30	10.89	0.88	9.59	11.39	1.12
11	3.24	7.05	22.87	3.83	1.12	4.30	n	n	n	n	n
12	5.25	1.49	7.84	2.20	21.86	48.10	3.94	0.98	3.87	8.83	0.84

**Figure III-4** Mixing diagram of ammonium concentration against salinity in the USLE. (○ = May 2003, □ = July 2004, ◇ = October 2005 and △ = December 2005).

3.4.5 Variability of nutrient stoichiometric ratios

Stoichiometric analyses between Si, N and P were used to identify a potential nutrient limitation in the SLE superficial water mass (0 to 2 m only) for each sampling period (Table 8). Some divergences of measured dissolved inorganic nutrients ratios from the Redfield ratio ($\text{Si}/\text{N}/\text{P} = 16/16/1$; Redfield *et al.*, 1963), point out to potential limitations for primary production: Dissolved N/P ratio < 10 and Si/N ratio > 1 indicate a potential N limitation, Si/N ratio < 1 and Si/P ratio < 3 indicate a potential Si limitation, whereas a N/P ratio > 30 points out a potential P limitation (e.g. Dortch and Whittlestone, 1992; Justic *et al.*, 1995; Kress *et al.*, 2002). In the upstream part of the USLE (stations 1 to 3), phytoplankton growth was apparently regulated by P limitation during each survey as all N/P values are > 30 . These results might also indicate a large excess of N species. Although no evidence for any nutrient limitation was observed in the LSLE during October and December 2005 expeditions, a potential N limitation was recorded at stations 9, 11 and 12 in May 2003. This potential N limitation was also observed at station 6, 10, 11 and 12 in July 2004 (Table 8).

3.5 Discussion

3.5.1 NH_4^+ transport through the USLE

Our results indicate that an important fraction of the riverine NH_4^+ reaches the LSLE head without being affected by biogeochemical processes occurring in the USLE. Thus, a significant transport of allochthonous NH_4^+ toward the LSLE in May 2003, October 2005 and December 2005 is observed. The poor correlation obtained between NH_4^+ and salinity in July 2004 could be attributed to biotic consumption and regeneration processes (e.g. assimilation, ammonification and nitrification) occurring along the USLE. These processes are probably linked to the high summer primary productivity (high Chl-a) observed in the USLE during the July 2004 survey. This local production led to the accumulation of fresh organic matter, as shown by the low C/N ratio, high PHAA concentration and high PHAA-N%, which was then accessible for *in situ* PON mineralization. As microbial degradation of PON releases ammonium through hydrolysis and deamination processes (Berman and Bronk, 2003), it is likely to observe mineralization

of fresh organic matter leading to a higher NH_4^+ input in the USLE during the July 2004 survey. This PON mineralization, and other N cycling processes, would likely be accelerated by the relatively high temperature observed in the USLE ($12.49 \pm 1.98^\circ\text{C}$), nitrification and denitrification rates being related to temperature (Herbert, 1999).

Even though NH_4^+ showed a conservative behavior for all other sampling periods, the high NH_4^+ flux calculated for October 2005 is an important feature. It illustrates the well documented increase of continental dissolved organic nitrogen (DON) runoff coming from the transport of organic detritus toward rivers and coastal environments (Valiela *et al.*, 1976). For May 2003 and December 2005, the calculated NH_4^+ fluxes through the USLE averaged $940 \text{ T N month}^{-1}$. Because no evidence of NH_4^+ regeneration or consumption processes was observed during these periods, this flux can be considered as a representative value of the continental ammonium input in the LSLE, although a more complete investigation is required to quantify the variability of the continental runoff.

These results are in agreement with early observations by Steven (1974) who was first to suggest that the St. Lawrence River is acting as a significant nutrient source for the LSLE. Later, Cootes and Yeats (1979) estimated the NO_x seaward flux toward the LSLE head at $\sim 6000 \text{ T N month}^{-1}$ whereas Savenkoff *et al.*, (2001) revised that estimation to $\sim 3857 \text{ T N month}^{-1}$ (for summer time only). While our mean calculated NO_x seaward flux ($6120 \text{ T N month}^{-1}$) remained highly variable but comparable to previously published estimates, our study indicates that NH_4^+ can significantly contribute to DIN flux toward the LSLE. NH_4^+ contribution to the DIN seaward flux averaged $\sim 14\%$ ($\sim 990 \text{ T N month}^{-1}$), with minimum contributions registered May 2003 and July 2004, and maximum values observed during low productivity periods (October and December 2005).

3.5.2 Potential nitrogen limitation in the SLE

The low light penetration and low salinity in USLE turbid area may act as potential limiting factors for autotrophic production in the USLE, since bacterial biomass has been observed to largely exceed phytoplankton biomass in this area (Painchaud and Therriault,

1989). The prevalence of vertical advection processes at the head of the LSLE brings P rich bottom water to the surface and a potential N limitation became noticeable during high productivity periods. However, a potential co-limitation of N and Si could have been present during the May 2003 and July 2004 campaigns following Redfield ratios.

These results are in agreement with Levasseur and Therriault (1987) who reported such a pattern at the head of the Laurentian channel. Although no evidence for any nutrient limitation was observed during the October 2005 and December 2005 cruises, N limitation was recorded in the LSLE surface water in May 2003 and July 2004. Therriault and Levasseur (1985) assessed that nitrate is most likely the limiting nutrient in the LSLE when sufficient external radiation energy penetrates the surface layer. The high Si/P and Si/N ratios recorded in the LSLE in July 2004 might indicate the existence of a phytoplankton growth event generating an important pool of Si and Chl-a and decreasing the pool of DIN in surface waters. A similar production event was also observed in May 2003. Even if previous studies reported that phytoplankton growth was not initiated before June in the LSLE (Sinclair, 1978; Therriault and Levasseur, 1985), Our results indicate that conditions were favourable to phytoplankton growth at the end of May 2003 in the LSLE. These observations reinforce the idea that increased phytoplankton productivity, first stimulated by favourable water column conditions, may contribute to the decrease of DIN concentrations in the LSLE surface layer.

3.5.3 Endogenous NH_4^+ production in the SLE

The low Chl-a concentrations observed in USLE and LSLE surface waters during December 2005 expedition indicate a very low primary production during that period. This low productivity is characteristic of winter time in the SLE, as low surface temperatures (often $< 0^\circ\text{C}$) induce sea ice formation, reducing light penetration in surface layer. Primary production being barely absent, it is assumed that the formation of endogenous PON during this period is negligible. This assumption is supported by the high SPM C/N and low PHAA concentrations observed in the whole SLE water column and by the fact that no sign of pelagic NH_4^+ uptake or regeneration processes is present in the whole SLE. Our data clearly show a conservative behavior of NH_4^+ in the USLE in December, while NH_4^+

concentrations remained below the detection limit in the whole LSLE water column. This NH_4^+ distribution pattern is characteristic of low productivity periods when physical mixing processes are dominant over biotic processes in the SLE.

The picture was very different for May 2003 and July 2004. The high Chl-a concentrations measured in both USLE and LSLE waters are indicative of high productivity events as previously described for summer period (Sinclair, 1978; Therriault and Levasseur, 1985, Levasseur and Therriault, 1987). Concomitant low N/P and high Si/N and Si/P ratios observed in the LSLE surface water suggest that the phytoplankton bloom, which is usually initiated in early June, reached an advanced maturation stage in July 2004. Typical phytoplankton succession patterns may be divided into three maturation stages (Margalef, 1958) characterized by a progressive depletion of surface nutrients. The low NH_4^+ concentrations observed in the LSLE sub-surface in May 2003 and July 2004 may be caused by consumption by phototrophic organisms. The geochemical signature of SPM in the LSLE water column provides evidence for the occurrence of production events generating an important pool of newly produced and recycled endogenous organic matter. In addition, the statistical analyses confirmed the occurrence of an important labile SPM downward transfer in May 2003 and July 2004 in the LSLE, as significant changes were observed in the vertical profiles of Chl-a and PON concentrations as well as for the SPM C/N ratio. This last observation is in accordance with the results of Levasseur and Therriault (1987) and Colombo *et al.*, (1996) who demonstrated that large autochthonous particles, mostly diatom theca and copepod fecal pellets, were produced in the LSLE during phytoplankton growth events.

As only 30% of the autochthonous production of the LSLE was estimated to settle down in the LSLE or seaward exported (Lucotte *et al.*, 1991), a significant proportion of the autochthonous particles should be recycled within the LSLE water column. While particles sink, a gradual break down takes place, releasing DOM in the surrounding waters (Smith *et al.*, 1992). Such processes might be important in regard to organic matter dynamic, as the turnover time of amino acids in sinking particles might be a few hours only (0.2 – 2.1 days) (Smith *et al* 1992). Colombo *et al.* (1996) have shown that grazing activity

(predominantly important at 0 – 50 m depth; Roy *et al.*, 2000) has an important influence on the composition of autochthonous sinking particles. Zooplankton, in addition to produce fecal pellets, breaks down a portion of the particulate matter into smaller particles, colloids and DOM. Such zooplankton related DOM has been described by Lampitt *et al.* (2000) and Berman and Bronk (2003). This newly formed DOM pool is assumed to be preferentially consumed and mineralized by heterotrophic bacteria (Smith *et al.* 1992; Davey *et al.*, 2001). This process might occur in the whole water column, as total bacterial abundance is little influenced by depth in the LSLE (Lemarchand K., unpublished results.).

Direct NH_4^+ production by phytoplankton excretion (Brezinski, 1988), photochemical release (Koopmans and Bronk, 2002) or viral algae lysis (Bratbak *et al.*, 1998), is likely to occur in the LSLE surface water. Solubilization and recycling of labile POM by both zooplankton and microbial activities can probably explain increased concentrations of NH_4^+ observed in the intermediate layer in May 2003 and July 2004, as fresh autochthonous POM sinks from the productive euphotic zone. Bacterial respiration being directly related to primary production in aquatic environments (del Giorgio *et al.*, 1997), it is likely that ammonification follows a similar trend in estuarine environments. However, new information is needed to determine if there is a coupling between ammonification rates and autotrophic biomass production in the SLE.

3.5.4 Significance of PHAA pattern

Since hydrolysable amino acids (PHAA) can be used as an indicator of POM source as well as a marker to study early diagenetic processes occurring in estuarine water and sediment (Chen *et al.*, 2004), our SPM amino-acid analysis may provide more information on processes involved in NH_4^+ spatial and temporal distribution in the LSLE. PHAA concentrations showed a clear decrease with depth (by a factor of about 10 times) between surface and the bottom deep layer. Surprisingly, the calculated DI did not give a clear indication of the decreasing POM lability with depth which would normally be induced by differential mineralization (Dauwe *et al.*, 1999). DI values registered in the SLE during July 2004 expedition are relatively similar throughout the water column and are not significantly higher than those found during low productivity periods (October and

December 2005). This result might be explained by a greater heterotrophic activity during summer, the labile organic compounds being quickly recycled while the more refractory amino acid containing compounds remained in the water column. Low DI might also be an effect of dilution with land-derived allochthonous organic matter which would have a low DI.

A detailed examination of the molar ratio of individual amino acids with total PHAA did not allow to discern a clear spatial or temporal pattern. Only the molar ratio of tyrosine (Tyr) showed a significant decrease with depth, similar to the trend observed for PHAAs. As Tyr is known to be quickly degraded by bacteria in marine environment (Dauwe *et al.*, 1999), the variation of its molar ratio in the LSLE is less sensitive to dilution with refractory allochthonous POM than DI. Because Tyr concentrations measured in SPM collected in LSLE surface water during a high productivity period are higher than those measured in the USLE for the same period, we suggest that Tyr may be a marker of fresh organic matter in cases where the dynamic of SPM diagenesis can not be clearly assessed by DI values. The steep decrease in tyrosine molar ratios with depth is thus a good indicator that autochthonous SPM is mineralized with depth in the LSLE water column.

Chl-a concentrations measured in fall 2005 were significantly lower than in July 2004 in both the upper and lower SLE surface waters, indicating a much lower primary production. As the labile SPM concentration was low in the LSLE water column (based on the average SPM C/N ratio and PHAA concentration), a concomitant low NH_4^+ mean concentration was also observed in the LSLE superficial layer. The relatively high NH_4^+ concentrations observed at stations 9, 10 and 12 in October 2005 are associated with higher than the average Chl-a concentrations ($1.13 \pm 0.18 \mu\text{g l}^{-1}$) for this water mass. Mechanisms involved in elevated NH_4^+ concentrations measured during this period appears to be related to previously described process observed in spring and summer, but may also be linked to vertical advection processes which have brought rich nutrient water to the surface layer and stirred primary production event as previously observed by Mcguillicuddy *et al.*, (1998) in the Atlantic Ocean. Available data did not allow to decide what could be the favored mechanism.

3.6 Main findings and conclusion

The seasonal distribution of dissolved and particulate nutrients in the SLE described in this paper provides a first snapshot of spatial variations of NH_4^+ loads. Our results indicates that upstream NH_4^+ inputs to SLE are highly variable, with the highest seaward transport occurring during fall and the lowest one during summer, illustrating the strong effect of the seasonal variability of freshwater discharge. Although no potential nutrient limitation was observed during fall and winter times, N has been identified as the probable limiting nutrient in spring and summer. As NH_4^+ is known to be preferentially consumed by phytoplankton, allochthonous NH_4^+ supply is assumed to have a significant effect on the LSLE phototrophic productivity. This hypothesis is supported by the small changes in NH_4^+ concentrations registered in May 2003 and July 2004 which seem to indicate that NH_4^+ uptake and production processes are closely balanced, and suggest an important recycling of NH_4^+ in the LSLE. Low NH_4^+ concentrations are observed during the phytoplankton growing season in the LSLE surface water while translocation of endogenous PON towards the deep water layers occurred. As phytoplankton biomass assimilates NH_4^+ , it contributes to the increase of the downward labile PON flux in the LSLE. The observed increase of NH_4^+ concentrations in the LSLE intermediate layer during the productive period suggests a coupling between phototrophic productivity, grazing and bacterial-mediated mineralization processes, such as ammonification. Further investigations based on interdisciplinary researches are needed to better understand multi-scale processes related to NH_4^+ distribution.

3.7 Acknowledgements

This research was supported NSERC (Natural Science and Engineering Research Council), ISMER grant, and by Canada Research Chair in Ecotoxicology (E. Pelletier) with a contribution of the Quebec-Ocean network. The authors gratefully acknowledge the captain and crew of the R/V *Coriolis II* and CGGS *Amundsen* for their support and enthusiasm.

3.8 References

- Ames, W.F., 1977. Numerical methods for partial differential equation. 2nd ed. Academic Press, New York.
- Balls, P.W., 1994. Nutrient inputs to estuaries from nine Scottish east coast rivers: Influence of estuarine processes on inputs to the North Sea. *Estuarine, Coastal and Shelf Science* **39**, 329-352.
- Berman, T. and Bronk, D.A., 2003. Dissolved organic nitrogen: a dynamic participant in aquatic ecosystems. *Aquatic Microbial Ecology* **31**, 279-305.
- Boyle, E., Collier, R., Dengler, A.T., Edmond, J.M., Ng, A.C. and Stallard, R.F., 1974. On the chemical mass-balance in estuaries. *Geochimica et Cosmochimica Acta* **38**, 1719-1728.
- Bratbak, B., Heldal, M., Jacobsen, A., Nagasaki, K. and Thingstad, F., 1998. Virus production in *Phaeocystis pouchetii* and its relation to host cell growth and nutrition. *Aquatic Microbiological Ecology* **16**, 1-9.
- Brezinski, M.Z., 1988. Vertical distribution of ammonium in stratified oligotrophic water. *Limnology and Oceanography* **33**, 1176-1182.
- Bugden, G.L., 1988. Oceanographic conditions in the deeper water of the Gulf of St. Lawrence in the relation to the local and oceanic forcing. NAFO SCR Doc. 88/87.
- Carpenter, E.J. and Capone, D.G., 1983. Nitrogen in the marine environment. Academic Press, New-York.
- Chambers, P.A., Guy, M., Roberts, E.S., Charlton, M.N., Kent, R., Gagnon, C., Grove, G. and Foster, N., 2001. Nutrients and their impact on the Canadian environment. Agriculture and Agri-Food Canada, Environment Canada, Fisheries and Oceans Canada, Health Canada and Natural Resources Canada, Ottawa.
- Chen, J., Li, Y., Yin, K. and Jin, H., 2004. Amino acids in the Pearl River Estuary and adjacent water: origins, transformation and degradation. *Continental Shelf Research* **24**, 1877-1894.
- Colombo, J.C., Silverberg, N. and Gearing, J.N., 1996. Biogeochemistry of organic matter in the Laurentian Trough, I. Composition and vertical fluxes of rapidly settling particles, *Marine Chemistry* **51**, 277-293
- Cook, R.D. and Weisberg, S., 1982. Residuals and influence in regression. Chapman and Hall, New York.
- Coote, A.R. and Yeats, P.A., 1979. Distribution of nutrients in the Gulf of St. Lawrence. *Journal of Fisheries Research Board Canada* **36**, 122-131.

- D'Anglejan, B.F. and Smith, E.C., 1973. Distribution, transport and composition of suspended matter in the St. Lawrence Estuary. Canadian Journal of Earth Science **10**, 1380-1396.
- Davey, K.E., Kirby, R.R., Turley, C.M., Weightman, A.J. and Fry, J.C., 2001. Depth variation of bacterial extracellular enzyme activity and population diversity in the northeastern North Atlantic Ocean. Deep-Sea Research II **48**, 1003-1917.
- Dauwe, B., Middelburg, J.J., Herman, P.M.J. and Heip, C.H.R., 1999. Linking diagenetic alteration of amino acids and bulk organic matter reactivity. Limnology and Oceanography **44**, 1809-1814.
- deBruyn, A.M.H., Marcogliese, D.J. and Rasmussen, J.B., 2003. The role of sewage in a large river food web. Canadian Journal of Fisheries and Aquatic Science **60**, 1332-1344.
- del Giorgio, P.A., Cole, J.J. and Cimberis, A., 1997. Respiration rates in bacteria exceed phytoplankton production in unproductive aquatic system. Nature **385**, 148-151.
- Dortch, Q. and Whittlestone, T.E., 1992. Does nitrogen or silicon limit phytoplankton production in the Mississippi river plume and nearby regions? Continental Shelf Research **12**, 1293-1309.
- Duarte, C.M., 1995. Submerged aquatic vegetation in relation to different nutrient regimes. Ophelia **41**, 87-112.
- El-Sabh, M.I., 1979. The Lower St. Lawrence Estuary as a physical oceanographic system. Naturaliste Canadien, **106**, 55-73.
- El-Sabh, M.I. and Silverberg, N. (1990) The St. Lawrence Estuary: introduction. In: El-Sabh, M.I. and Silverberg, N. (Eds.), Oceanography of a Large-scale Estuarine System. Springer-Verlag, New York, pp. 1-9.
- Flindt, M.R., Pardal, M.A., Lillebo, A.I., Martins, I. and Marques, J.C., 1999. Nutrients cycling and plant dynamic in estuaries. Acta Oecologica **20**, 237-248.
- Gilbert, D., Sundby, B., Gobeil, C., Mucci, A. and Tremblay, G.H., 2005. A seventy years record of diminishing deep-water oxygen levels in the St. Lawrence Estuary – the northwest Atlantic connection. Limnology and Oceanography **50**, 1654-1666.
- Greisman, P. and Ingram, G., 1977. Nutrient distribution in the St. Lawrence Estuary. Journal of Fisheries Research Board Canada **34**, 2117-2123.
- Herbert, R.A., 1999. Nitrogen cycling in coastal ecosystems. FEMS Microbiology Reviews **23**, 563-590.
- Howarth, R.W., Billen, G., Swaney, D., Townsend, A., Jarworski, N., Lajtha, K., Downing, J.A., Elmgren, R., Caraco, N., Jordan, T., Berendse, F., Freney, J., Kueyarov, V., Murdoch,

- P. and Zhao-liang, Z., 1996. Riverine inputs of nitrogen to the North Atlantic Ocean: Fluxes and human influences. *Biogeochemistry* **35**, 75-139.
- Howarth, R.W. and Marino, R., 2006. Nitrogen as the limiting nutrient for eutrophication in coastal marine ecosystems: evolving views over three decades. *Limnology and Oceanography* **51**, 364-376.
- Justic, D., Rabalais, N.N. and Turner, R.E., 1995. Stoichiometric nutrient balance and origin of coastal eutrophication. *Marine Pollution Bulletin* **30**, 41-46.
- Kress, N., Coto, S.L., Brenes, C.L., Brenner, S. and Arroyo, G., 2002. Horizontal transport and seasonal distribution of nutrients, dissolved oxygen and chlorophyll-a in the Gulf of Nicoya, Costa Rica: a tropical estuary. *Continental Shelf Research* **22**, 51-66.
- Kress, N. and Herut, B., 1998. Hypernutrification in the oligotrophic eastern Mediterranean. A study in Haifa Bay (Israel). *Estuarine, Coastal and Shelf Science* **46**, 645-656.
- Lampit, R.S., Noji, T. and von Bodungen, B., 2000. What happens to zooplankton faecal pellets? Implications for material flux. *Marine Biology* **104**, 15-23.
- Levasseur, M. and Therriault, J.-C., 1987. Phytoplankton biomass and nutrient dynamics in a tidally induced upwelling: the role of the $\text{NO}_3 : \text{SiO}_4$ ratio. *Marine Ecology Progress Series* **39**, 87-97.
- Lindroth, P. and Mopper, K., 1979. High performance liquid chromatographic determination of subpicomole amounts of amino acids by precolumn fluorescence derivatization with o-phthalodialdehyde. *Analytical Chemistry* **51**, 1667-1674.
- Lucotte, M., Hillaire-Marcel, C. and Louchouarn, P., 1991. First-order organic carbon budget in the St-Lawrence Lower Estuary from ^{13}C data. *Estuarine, Coastal and Shelf Science* **32**, 297-312.
- Margalef, R., 1958. Temporal sucession and spatial heterogeneity in phytoplankton. In: Buzzati-Traverso, A.A. (Ed.), *Perpective in marine biology*. University of California Press, Berkeley and Los Angeles, pp.323-349.
- McCarthy, J.J., 1980. Nitrogen and phytoplankton ecology. In: Moris, I. (Ed.), *The physical ecology of phytoplankton*. Blackwell. pp.191-233.
- McGillicuddy Jr, D.I., Robinson, A.R., Siegel, D.A., Jannasch, H.W., Johnsonk, R., Dickey, T.D., McNeil, J., Michaels, A.F. and Knapk, A.H., 1998. Influence of mesoscale eddies on new production in the Sargasso Sea. *Nature* **394**, 263-265.

- Morris A.W., Allen, J.I., Howland, R.J.M. and Wood, R.G., 1995. The estuary plume zone: source or sink for land-derived nutrient discharges? *Estuarine, Coastal and Shelf Science* **40**, 387-402.
- Painchaud, J. and Therriault, J.-C., 1989. Relation between bacteria, phytoplankton and particulate organic carbon in the Upper St. Lawrence Estuary. *Marine Ecology Progress Series* **56**, 301-311.
- Painchaud, J., 1999. La production porcine et la culture du maïs. Impacts potentiels sur la qualité de l'eau, *Le Naturaliste Canadien* **123**, 41-46.
- Plourde, J. and Therriault, J.-C., 2004. Climate variability and vertical advection of nitrate in the Gulf of St. Laurence, Canada. *Marine Ecology Progress Series* **279**, 33-43.
- Poulin, P. and Pelletier, E., 2007. Determination of ammonium using a microplate-based fluorometric technique. *Talanta* **71**, 1500-1506.
- Quinn, G. P. and Keough, M. J., 2002. Experimental design and data analysis for biologists. Cambridge University Press. Cambridge.
- Rabalais, N.N. and Nixon, S.W. EDS., 2002. Preface: Nutrient over-enrichment in coastal waters: global patterns of cause and effect. *Estuaries* **25**, 639-900.
- Redfield, A., Ketchum, B.H. and Richards, F.A., 1963. The influence of organisms on the composition of sea water. In: Hill, M.N. (Ed.), *The sea*. John Wiley, New-York. vol. 2, pp. 26-77.
- Ro, C., Vet, R., Ord, D. and Holloway, A., 1998. Canadian air and precipitation monitoring network (CAPMoN). Annual summary reports (1983-1996). Air quality research branch. Atmospheric environment service. Environment Canada. Downsview. Ontario.
- Roy, S., Silverberg, N., Romero, N., Deibel, D., Klein, B., Savenkoff, C., Vésina, A.F., Tremblay, J.-É. and Rivkin, R.B., 2000. Importance of mesozooplankton feeding for the downward flux of biogenic carbon in the Gulf of St. Lawrence (Canada). *Deep-Sea Research II* **42**, 519-544.
- Saucier, F.J., Roy, F. and Gilbert, D., 2003. Modeling the formation and circulation processes of water masses and the sea ice in the Gulf of St. Lawrence, Canada. *Journal of Geophysical Research* **108**, 3269-3289.
- Savenkoff, C., Vézina, A.F., Smith, P.C. and Han, G., 2001. Summer transport of nutrients in the Gulf of St. Lawrence estimated by inverse modelling. *Estuarine, Coastal and Shelf Science* **52**, 565-587.
- Schafer, C.T., Smith, J.N. and Seibert, B., 1983. Significance of natural and anthropogenic sediment input to the Saguenay Fjord, Québec. *Sedimentary Geology* **36**, 177-194.

- Sinclair, M., El-Sabh, M. and Brindle, J.-R., 1976. Seaward nutrient transport in the Lower St. Lawrence Estuary. *Journal of Fisheries Research Board Canada* **33**, 1271-1277.
- Sinclair, M., 1978. Summer Phytoplankton Variability in the Lower St. Lawrence Estuary. *Journal of Fisheries Research Board Canada* **35**, 1171-1185.
- Smith, D.C., Meinhard, S., Alldredge, A.L. and Azam, F., 1992. Intense hydrolytic enzyme activity on marine aggregates and implications for rapid particle dissolution. *Nature* **359**, 139-142.
- Sokal, R.R. and Rohlf, F.J., 1995. *Biometry*, 3^r ed, W.H. Freeman and Company, New York.
- Steven, D.M., 1974. Primary and secondary production in the Gulf of St. Lawrence. McGill University. Marine Science Center, MS Rep., n° 26.
- Strickland, J.D.H. and Parson, T.R., 1972. A practical Handbook of seawater Analysis, 2nd ed. Bulletin of the Fisheries Research Board of Canada, Ottawa, n° 167.
- Theriault, J.-C. and Lacroix, G., 1976. Nutrients, chlorophyll, and internal tides in the St. Lawrence Estuary. *Journal of Fisheries Research Board Canada* **33**, 2747-2757.
- Theriault, J.-C. and Levasseur, M., 1985. Control of phytoplankton production in the lower St. Lawrence Estuary: light and freshwater runoff. *Naturaliste Canadien* **112**, 77-96.
- Thibodeau, B., de Vernal, A. and Mucci, A., 2006. Recent eutrophication and consequent hypoxia in the bottom waters of the Lower St. Lawrence Estuary: Micropaleontological and geochemical evidence. *Marine Geology* **231**, 37-50.
- Valiela, I., Teal, J.M. and Persson, N.Y., 1976. Production and dynamics of experimentally enriched salt marsh vegetation, belowground biomass. *Limnology and Oceanography* **21**, 245-252.
- Vézina, A.F., Gratton, Y. and Vinet, P., 1995. Mesoscale physical-biological variability during summer phytoplankton bloom in the Lower St. Lawrence Estuary. *Estuarine, Coastal and Shelf Science* **41**, 393-411.
- Vitousek, P.M., Aber, J.D., Howarth, R.W., Likens, G.E., Matson, P.A., Schindler, D.W., Schlesinger, W.H. and Tilman, D.G., 1997. Human alteration of the global nitrogen cycle: Sources and consequences. *Ecology Applied* **7**, 737-750.
- Zar, J.H., 1999. Biostatistical analysis. Prentice-Hall, Inc., Englewood Cliffs, New Jersey.

CHAPITRE IV

Evidence for nitrate assimilation and respiration in hypoxic deep waters of the Lower St. Lawrence Estuary

Patrick Poulin, Émilien Pelletier

Submit to Marine Chemistry

4.1 Abstract

This study reports seasonal changes in dissolved inorganic nitrogen (DIN), dissolved oxygen (DO) and other chemical and biological parameters measured in the water column of Lower St. Lawrence Estuary (LSLE), a large and deep northern estuary already affected by hypoxic conditions. Data from a series of five oceanographic cruises between spring 2003 and winter 2006 allowed the observation of seasonal fine-scale changes in DO, DIN, and C/N ratio of suspended particulate organic matter (SPOM) profiles. A transient but remarkable DIN depletion appeared in the entire water column during summer 2004. The hypothesis of a dual assimilation/respiration process in the hypoxic deep water layer is discussed. The presence of important chlorophyll-a concentrations with low C/N ratio in SPOM far below the photic zone are indicative of a large reservoir of labile organic carbon available to biodegradation by aerobic bacteria with regeneration of nitrate in surface and intermediate layers, but could be the source of a nitrification/denitrification uncoupling process taking place in the deep layer due to DO depletion. Following calculations of N* (deficit in nitrate), dN (aerobic partial nitrification) and dN'' (anaerobic denitrification), our results provide evidences of bacterial oxidation of organic matter by simultaneous oxygen (nitrification) and nitrate (denitrification) use in the deep water column. As much as 42-61% of nitrate deficit is attributed to denitrification whereas the rest is due to partial nitrification (35-47%) with a possible minor contribution from phytoplankton darkness assimilation (4-11%). A denitrification response within the water column leading to a seasonal nitrate deficit, but leaving DO saturation levels almost unchanged between seasons; this might be seen as a «protective mechanism» that kept DO level within hypoxic

conditions ($65 \pm 10 \mu\text{M}$) and prevented the development of anoxic conditions in deep LSLE at least for the last 15-20 years.

4.2 Introduction

Examining historical record of water temperature and dissolved oxygen in St. Lawrence Estuary, Gilbert *et al.* (2005) observed a severe decline of deep-water oxygen over the last seven decades and the rise of hypoxic conditions (O_2 below $65 \mu\text{M}$ level) in the lower section of the estuary between the mouth of Saguenay Fjord and Pointe-des-Monts area. Authors attributed a large part of the deep-water oxygen depletion (up to two thirds) to changes in properties of water mass entering the Gulf of St. Lawrence leaving at least one third of oxygen losses unexplained by coastal circulation and tentatively attributed to an increasing oxygen demand in the estuary. Historical record also revealed an apparent stabilization in the oxygen regime in the last 15-20 years (Gilbert *et al.*, 2005). A two-dimensional model of dissolved oxygen (DO) levels in deep Lower St. Lawrence Estuary (LSLE) using a benthic-pelagic coupling approach confirmed that mineralization of organic carbon plays a determining role in generating hypoxic conditions in LSLE, but author found inconsistency between calculated and measured sediment oxygen demand in their attempt to explain observed DO depletion in the deepest layer of the water column (Benoit *et al.*, 2006).

DO depletion has been identified as a critical problem in many coastal and estuarine ecosystems supporting fisheries (Falkowski *et al.*, 1980; Rosenberg, 1985; Vitousek *et al.*, 1997). Hypoxia is operationally defined as DO concentration under 2 mg.l^{-1} ($65 \mu\text{M}$), a level not fully supporting biological diversity. It has been observed that bottom trawls fail to capture demersal fish, shrimp or crab when operated in areas under 2 mg.l^{-1} of DO (Renaud, 1986). Although this phenomenon can naturally occur in marine coastal areas (Helly and Levin, 2004), hypoxia development next to urbanised coastal zones appears to be directly related to anthropogenic modification of tributaries (Cloern, 2001). Estuarine and coastal waters often receive important nutrient inputs originating from various terrestrial sources such as industrial and municipal wastewater, dredged material, agricultural and urban runoffs. Recent studies conducted in Gulf of Mexico (Turner *et al.*,

2005), Gulf of California (Beman *et al.*, 2005), Chesapeake Bay (Alderson *et al.*, 2001) and Pearl River Estuary (Yin *et al.*, 2004) demonstrated a positive relationship between nutrient increase in the water column and hypoxia development. Authors pinpointed a direct increase of autochthonous photosynthetic production in response to nutrient loads generating an accumulation of organic material in the bottom layer, which in turn increases biodegradation activities. As most decomposers are aerobic, oxygen consumption often becomes greater than oxygen renewal, creating a continuous depletion in DO concentrations (Duarte, 1995). The study of Wolgast *et al.* (1998) on Pacific Ocean in presence of high particulate organic matter flux showed that concomitant oxygen and nitrate respiration occurred in microzones of aggregates in oxygenated bottom waters and caused loss of fixed nitrogen through denitrification.

This paper aims to examine fine scale seasonal changes in dissolved inorganic nitrogen (DIN), DO, and C/N profiles in intermediate and bottom water layers of LSLE in an attempt to identify main chemical and biological processes that could influence hypoxic conditions in this large estuary.

4.3 Materials and Methods

4.3.1 Study area

The lower St. Lawrence Estuary (LSLE) is a stratified 370-km long funnel-shaped tidal environment reaching a 350 m depth central glacial valley along the Laurentian Channel. This estuary is the catchment basin of the St. Lawrence River (flow rate $11900 \text{ m}^3.\text{s}^{-1}$) taking its origin in North American Great Lakes (El-Sabh and Silverberg, 1990), and the Saguenay River ($1600 \text{ m}^3.\text{s}^{-1}$) draining the northern part of Quebec (Schafer *et al.*, 1983). Watersheds of both St. Lawrence and Saguenay rivers support the activity of about 57 millions people, some large industrial zones and important agricultural areas (Chambers *et al.*, 2001; Painchaud, 1999). The LSLE is strongly influenced by the Atlantic Ocean regime through winds, tides, landward bottom water intrusions as well as by surface seaward freshwater runoff (Koutitonsky and Bugden, 1991) The mixing between fresh and salt waters generates a stratification in three main layers: 1) a surface layer displaying

seasonal variations in temperature and salinity. 2) a cold intermediate layer extending from 50 to 200 m depth, and 3) a more consistent deep water mass (below 200 m) that only undergoes long term changes due to relatively steady inward advection (0.5 cm.s^{-1}) and weak vertical diffusion (Bugden, 1988).

This naturally eutrophic system is influenced by seasonal dependant mixing processes which contribute to replenish surface water nutrients via the vertical advection of nutrient-rich deep layers (Theriault and Lacroix, 1976; Greisman and Ingram, 1977; Vézina *et al.*, 1995; Plourde and Therriault, 2004). In addition, tidally induced up-welling processes, occurring at the head of Laurentian Channel, bring bottom waters to the surface allowing seasonal high biological productivity (El-Sabh, 1979). While LSLE surface water may reach 15°C during summer time, ice cover is observed during winter period; the ice begins to form along the shore in late November while complete melting generally occurs in April (El-Sabh, 1979; Saucier *et al.*, 2003).

4.3.2 Data collection and sampling

Water samples were collected at different depths at four successive stations located along the main LSLE axis (Fig. 1). Five seasonal surveys (1-3 June 2003, 25-26 July 2004, 6-7 October and 17-18 December 2005, and 8-9 February 2006) were carried out onboard *Admunsen* and *Coriolis II* oceanographic vessels, both equipped with the same sampling devices and similar laboratory accommodation. Vertical profiles of temperature, salinity, and DO were recorded using a Seabird[®] SBE 9 multi-probe (temperature accuracy $\pm 0.01^{\circ}\text{C}$, salinity accuracy ± 0.01 , and DO accuracy $\pm 0.01 \text{ mg.l}^{-1}$) mounted on a rosette multi-sampler (General Oceanics[®]). In addition, water samples were taken on the up casts at 6 different depths using 12 l lever-action Niskin[®] bottles (General Oceanics[®]). Temperature and salinity of samples were validated onboard using dual temperature and salinity YSI[®] digital probe whereas probe for DO measurements were assessed using Winkler titrations (Strickland and Parson, 1972). Deviations of DO probe compared with onboard chemical titration were always below 5%. Samples for $\text{NO}_2^- + \text{NO}_3^-$ and PO_4^{3-} determinations were filtered onto 0.22 μm pore-size Nucleopore[®] membrane and stored in the dark at -80°C in

60 ml polyethylene bottles while samples for NH_4^+ were directly collected from Niskin® bottle in clean 250 ml BOD glass bottles and analysed onboard. Samples for suspended particulate organic matter (SPOM) characterisation were collected by filtration on pre-combusted, pre-weighted, 47 mm diameter Millipore® glass fibre membranes, acidified with 10 ml of 1% HCl solution (v/v) and stored at -80 °C. Samples for chlorophyll-a (Chl-a) determination were filtered in dark on 25 mm diameter Millipore® glass fibre membranes and stored at -80 °C. DIN was calculated as the sum of $\text{NO}_2^- + \text{NO}_3^-$ and NH_4^+ , and is given in μM .

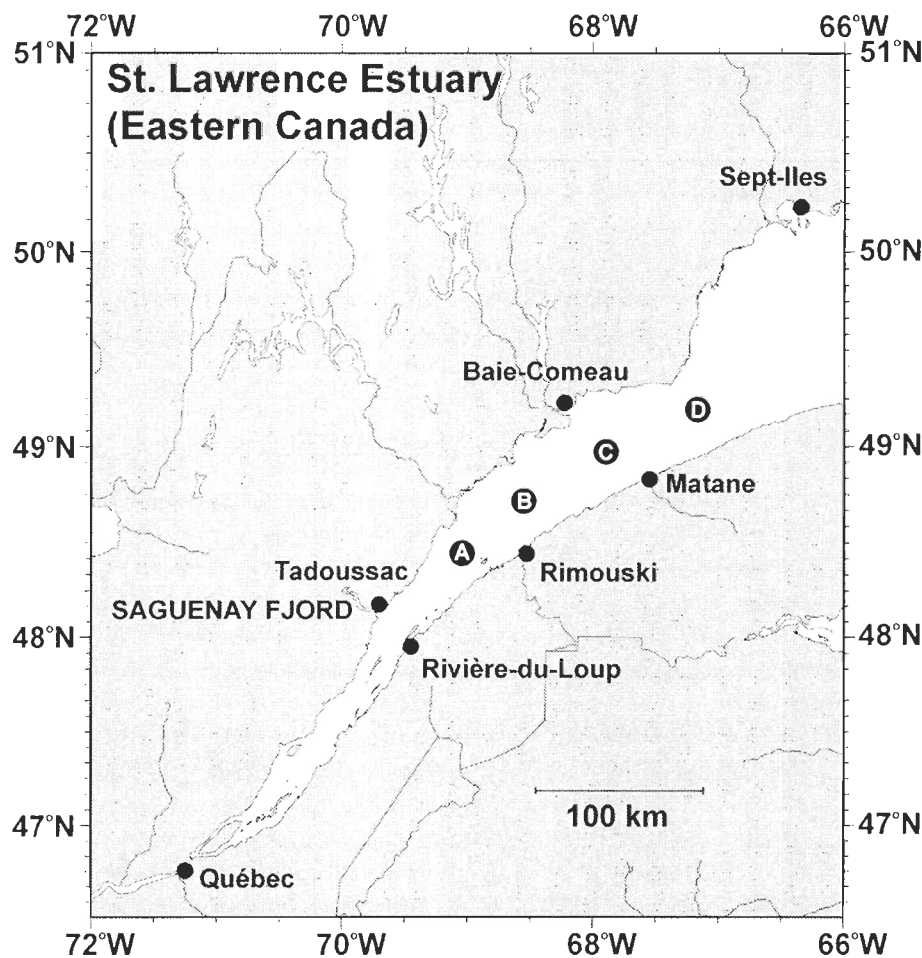


Figure IV-1 Sampling area in Lower St. Lawrence Estuary. Letters in black circle correspond to the sampling stations.

4.3.3 Chemical analyses

Dissolved nutrients ($\text{NO}_2^- + \text{NO}_3^-$ and PO_4^{3-}) were analysed by colorimetric techniques (Strickland and Parson, 1972) using automated analytic Technikon® and AA3 Brand+Luebbe® platforms, allowing an overall analytical uncertainty ($\pm 1 \sigma$) under $\pm 5\%$. Determination of NH_4^+ concentrations was performed onboard, using a microplate-based spectrofluorometric method described by Poulin and Pelletier (2007), which provided an analytical uncertainty ($\pm 1 \sigma$) of $\pm 1\%$. SPOM elementary analyses were made at both the GÉOTOP-UQAM-McGill research centre at Université du Québec at Montréal and ISMER using a Carlo-Erba® elemental analyser and a ECS 4010 Costech® instrument equipped with a zero blank auto sampler. Replicate analysis ($n = 10$) of certified sediment sample (NIST-1941b) was used as quality control for these analyses. Analytical error ($\pm 1 \sigma$) was determined from replicate measurements of standard material (acetanilide, urea, atropine, nicotinamide) and averaged $\pm 5\%$. Particulate organic carbon (POC) was calculated from SPOM and quantitative CHN analysis. Pigments (Chl-a) were extracted from GFF filters with 10 ml of 90% (v/v) acetone for 24 h at 4 °C in the dark and concentration of Chl-a was determined using a Turner design® spectrophotometer ($\lambda = 630 \text{ nm}$) according to Strickland and Parson (1972) with an overall analytical uncertainty ($\pm 1 \sigma$) averaged $\pm 1\%$.

4.4 Results

DO profiles of the four stations sampled in different seasons are presented in Figure 2 and confirm the sharp decrease of oxygen saturation (%) from the intermediate water layer (50 to 200 m) to the deep layer (from 200 m to the bottom) for all stations at all seasons. Fine scale changes can be observed in the intermediate layer, particularly in station C where the lowest saturation levels are observed in December 2005 followed by October 2005. Profiles in July 2004 and February 2006 show very similar shapes and are generally indiscernible. DO profiles in deep layer show very few seasonal changes: although the percent of saturation in February 2006 was usually slightly higher than the others, a phenomenon particularly visible in downstream station D where the supply of more oxygenated deep waters from the Gulf of St. Lawrence is expected.

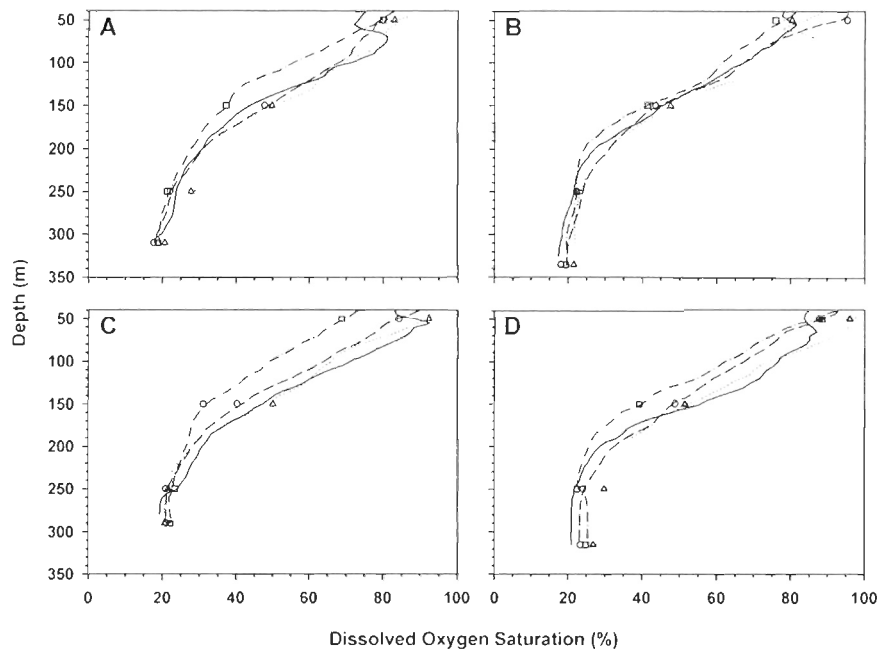


Figure IV-2 Dissolved oxygen profiles of the four stations sampled in different seasons. Lines state for in situ CTD profiles whereas forms indicate the depth at which Winkler titrations were performed (\diamond = July 2004, \circ = October 2005, \square = December 2005 and \triangle = February 2006).

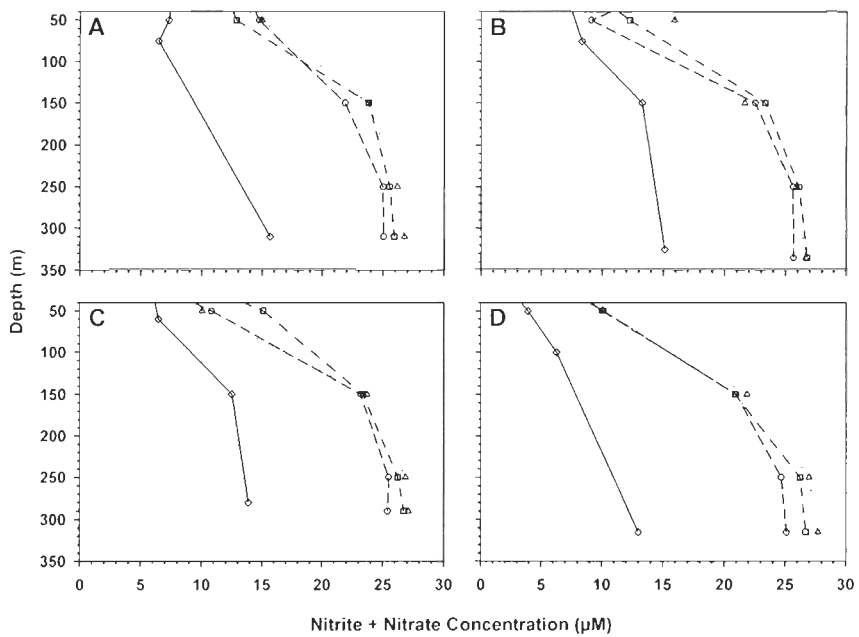


Figure IV-3 Nitrate + nitrite profiles of the four stations sampled in different seasons. Forms indicate analysed samples.

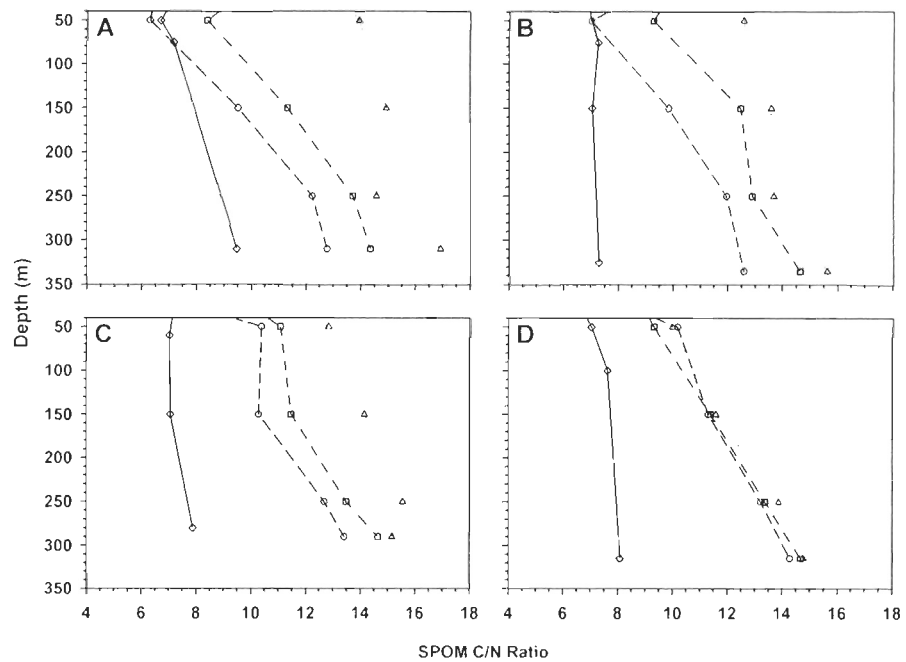


Figure IV-4 Suspended particulate organic matter C/N ratio profiles of the four stations sampled in different seasons. Forms indicate analysed samples.

DIN profiles (Fig. 3) illustrate similarities between stations and seasons with a progressive increase of DIN concentrations in intermediate and deep layers from about 15 μM at 50 m depth to about 25-27 μM at 300 m, except for the summer profile showing a major depletion of DIN for all stations. In July 2004, DIN measured in bottom waters (near or below 300 m) averaged $14.4 \pm 0.6 \mu\text{M}$ (Av \pm SD) which represents an apparent loss of about 50% of DIN when compared with observed values in other seasons. NH_4^+ was present only in surface waters and barely absent ($< 0.02 \mu\text{M}$) in deep waters for all stations and seasons (results not shown).

C/N ratios in SPOM (Fig. 4) show distinct profiles for each season, best illustrated at station C where C/N profiles progressively move towards higher values from July 2004 to February 2006 in both intermediate and deep layers. Only downstream station D shows a different pattern with July 2004 profile clearly different from others.

Seasonal changes in chemical composition of the deep water layer (using only data between 250 and 330 m to minimize possible mixing effects with the intermediate layer) of LSLE are summarized in Table 1. The first striking feature of this deep water mass is its temporal and spatial homogeneity illustrated by only very tiny changes in salinity (34.54 ± 0.09) and temperature (5.18 ± 0.35 °C) around the year and even amongst the stations. The upstream station A is generally slightly cooler and less salty than downstream station D. However, chemical parameters driven by biological activities show remarkable changes with seasons. As expected, POC concentrations are quite low in early June 2003 before summer high production peak, increased in July 2004, and stayed relatively high in fall and winter months. C/N increased steadily from July 2004 to February 2006. Values of C/N ratio around 9-10 are observed in early June 2003. Chl-a was clearly present in deep waters in July 2004 (up to $0.22 \mu\text{g l}^{-1}$ in upstream station A) and decreased sharply in fall and winter. As previously observed in seasonal profiles, DIN was much lower in bottom layer in July 2004 than in all the other seasons. Orthophosphate concentrations averaged $2.2 \pm 0.2 \mu\text{M}$ and showed few changes between stations and seasons.

Table 2 reports DO/DIN ratios ranging between 2.41 and 3.48 for all stations and all seasons, except for July 2004 where higher values (3.65 and 5.10) are observed. In an attempt to identify and quantify processes leading to nitrate deficits (including possible presence of NO_2^-) in LSLE deep waters, we adopted the approach recently proposed by Li *et al.* (2006) to calculate empiric parameters deficit in nitrate (N^*), aerobic partial nitrification (dN) and anaerobic denitrification (dN **).

Tableau IV-1 Mean values of particulate organic carbon (POC, µg/l), C/N, chlorophyll-a (Chl-a µg/l), total dissolved inorganic nitrogen (DIN, µM), dissolved orthophosphate (P µM), dissolved oxygen (DO, µM), salinity and temperature (°C) in bottom waters of lower St. Lawrence Estuary. Otherwise stated, numbers are average values of 2 samples collected between 250 and 330 m following station depth.^a NA = data not available.

	Early June 2003	End of July 2004	Early October 2005	Mid-December 2005	Early February 2006
Station A					
POC	83 (300 m)	220 (315 m)	121	187	197
C/N	10.28	9.47	12.50	14.03	15.75
Chl-a	0.080	0.220	0.025	0.006	< 0.001
DIN	27.1	15.7	25.0	25.7	26.5
P	2.5	2.4	2.5	2.4	2.1
DO	90.63	58.34	63.44	62.50	74.94
Salinity	34.60	34.44	34.48	34.41	34.37
Temperature	6.40	5.08	5.07	4.84	4.66
Station B					
POC	29 (300 m)	107 (325 m)	64	161	14.64
C/N	9.07	7.30	12.27	13.78	< 0.001
Chl-a	0.030	0.090	0.010	0.003	26.7
DIN	26.6	15.1	25.6	26.8	2.1
P	2.4	2.4	2.5	2.3	68.44
DO	64.31	55.16	62.50	66.41	34.55
Salinity	34.53	34.48	34.53	34.48	4.95
Temperature	5.23	5.18	4.99	4.98	144
Station C					
POC	NA ^a	109 (280 m)	117	158	15.35
C/N		7.68	13.05	14.06	< 0.001
Chl-a		0.090	0.030	< 0.001	27.0
DIN		13.9	25.4	26.5	2.2
P		2.3	2.4	2.2	65.51
DO		60.44	66.88	72.41	34.54
Salinity		34.46	34.53	34.62	5.12
Temperature		5.17	5.23	5.24	98
Station D					
POC	37 (315 m)	50 (315 m)	128	150	14.32
C/N	9.28	8.10	13.75	14.03	< 0.001
Chl-a	0.060	0.140	0.020	< 0.001	27.3
DIN	26.8	13.0	24.9	26.5	2.1
P	2.0	2.1	2.3	2.1	88.86
DO	93.09	66.88	69.06	77.81	34.62
Salinity	34.67	34.56	34.64	34.70	5.02
Temperature	5.49	5.37	5.21	5.34	115

Tableau IV-2 DO/DIN ratio, N* (nitrate deficit), dN (partial nitrification, $\mu\text{mol l}^{-1}$) and dN'' (denitrification, $\mu\text{mol l}^{-1}$) defined for the bottom waters of lower St. Lawrence Estuary using the average values of 2 samples collected between 250 and 330 m following station depth.^a When Na > N > Nb, denitrification (dN'') is not contributing to the deficit. ^b Data not available.

	Early June 2003	End of July 2004	Early October 2005	Mid-December 2005	Early February 2006
Station A					
DO/DIN	3.34 (300 m)	3.72 (315 m)	2.54	2.43	2.84
N*	-9.28	-20.59	-12.27	-9.77	-4.95
dN	7.00	9.69	9.72	7.78	4.18
dN''	n.c. ^a	8.67	n.c.	n.c.	n.c.
Station B					
DO/DIN	2.41 (300 m)	3.65 (325 m)	2.44	-7.88	-4.73
N*	-8.74	-20.98	-11.97	6.12	3.97
dN	6.77	9.55	9.31	n.c.	n.c.
dN''	n.c.	9.24	n.c.		
Station C					
DO/DIN	NA ^b	4.35 (280 m)	2.63	-5.27	-5.48
N*		-19.85	-9.48	4.39	4.39
dN		7.71	7.65	n.c.	n.c.
dN''		10.67	n.c.		
Station D					
DO/DIN	3.48(315 m)	5.14 (315 m)	2.77	-4.41	-3.30
N*	-3.12	-18.45	-8.19	3.80	2.76
dN	2.81	6.49	6.91	n.c.	n.c.
dN''	n.c.	11.17	n.c.		

A relationship between observed nitrate + nitrite concentration (N) and N* is shown in eq. 1, where $\check{N} = 16(P - 0.181)$ and P is the measured orthophosphate concentration as defined by Gruber and Sarmiento (1997).

$$N^* = N - \check{N} \quad \text{eq. 1}$$

For dN and dN'' calculations, the expected concentration of N for a complete nitrification (N_a) and the expected concentration of N during a partial nitrification (N_b) are firstly illustrated in eq. 2 and eq. 3 respectively.

$$N_a = m(P - P_o) \quad \text{eq. 2}$$

$$N_b = C_0 + C_1P + C_2P^2 + C_3P^3 \quad \text{eq. 3}$$

Value m and P_0 in eq. 2 can be obtained from the linear least square fitting of P versus N plot of all deep layer data points, where P_0 is the value of intercept at $N = 0$ and m is the value of slope. Based on our fitting curve, P_0 and m are -0.6051 and 11.1460 respectively, where $R^2 = 0.8186$. A cubic least-square fitting of P versus N plot of all deep layer data points gives $C_0 = 1.7354$, $C_1 = 1.7673$, $C_2 = 14.2610$ and $C_3 = -3.9905$ with $R^2 = 0.8399$, which provide the four constants for eq. 3.

For a given P value, when $N_a > N > N_b$, it is assumed that the nitrate deficit is only caused by the partial nitrification (dN) but not denitrification ($dN^{''}$). Therefore, the calculation of dN in eq. 4 gives the nitrate deficit.

$$dN = N_a - N \quad \text{eq. 4}$$

For a given P value, when $N < N_b$, it is assumed that the nitrate deficit is caused by both partial nitrification (dN) and denitrification ($dN^{''}$), which can be calculated by eq. 5 and eq. 6 respectively.

$$dN = N_a - N_b \quad \text{eq. 5}$$

$$dN^{''} = N_b - N \quad \text{eq. 6}$$

Table 2 shows a loss of nitrate (negative N^*) for all stations and seasons but especially in July 2004 with N^* values often 4 to 5 times lower than February 2006. As nitrate deficit can be caused by both partial nitrification and denitrification, Li *et al.* (2006) proposed to used dN as a measurement of partial nitrification (which increases with nitrification) and $dN^{''}$ as a measure of denitrification. These results show a partial nitrification process occurring year-round at all stations with the lowest dN values observed in February 2006 ($3.82 \pm 0.73 \mu\text{mol l}^{-1}$) and the highest ones obtained in October 2005 ($8.40 \pm 1.34 \mu\text{mol l}^{-1}$). In general, partial nitrification can explain a substantial fraction of nitrate deficit registered in the LSLE bottom layer (35-90%). Although the average nitrate

loss by partial nitrification measured in July 2004 ($8.36 \pm 1.54 \mu\text{mol l}^{-1}$) was similar to the one observed in October 2005, the nitrate deficit induced by denitrification process was found more important. High dN^{**} values ($9.94 \pm 1.18 \mu\text{mol l}^{-1}$) were observed only in July 2004 at all stations whereas this process was estimated to be negligible for other sampling periods because we observed $N_a > N > N_b$ for determined P values. In addition, partial nitrification and denitrification processes explained from 89 to 96% of nitrate deficit recorded in July 2004 whereas denitrification alone accounted for 42-61% [$(dN^{**} / -N^*) \times 100$].

4.5 Discussion

Physical properties and chemistry of the deep water layer (below 200 m) of the Gulf of St. Lawrence have been closely examined during Phase I of the Canadian Joint Global Ocean Flux Study (CJGOFs) in 1992-1994 (Savenkoff *et al.*, 1996). The Anticosti Gyre station located about 200 km eastward our station D showed average salinity and temperature of 34.4 ± 0.1 and $4.8 \pm 0.1^\circ\text{C}$, respectively, which are slightly lower than mean values reported here for LSLE. Gilbert *et al.* (2005) reported a mean temperature of 4.98°C for the deepest layer of LSLE using data collected from 1984 to 2003 which is again slightly lower but not significantly different from our average value ($5.18 \pm 0.35^\circ\text{C}$) for years 2003 to 2006. All these data confirm the high stability of the deep LSLE layer which is only subject to a slow upward advection process with properties varying on a decadal time scale only (Gilbert *et al.*, 2005).

Detailed oxygen profiles between July 2004 and February 2006 (Fig. 2) illustrate some fine scale changes not previously reported as the intermediate layer (50 to 200 m) are subject to some seasonal fluctuations apparently related to carbon and nitrogen cycling with lowest DO saturation levels observed in December 2005. This temporary loss of DO is attributed to respiration of marine organic matter produced in the surface layer and terrestrial SPOM (vascular plant debris) imported from the St. Lawrence River watershed. C/N profiles support this assumption and exhibit higher values in fall and winter indicating a progressive decay of particulate organic matter in the water column. This simple and

expected pattern is not observed in the deepest water layer where DO saturation levels remained almost unchanged with seasons with saturation values very close to 20% (63-65 µM) for stations A, B and C and slightly higher in downstream station D. SPOM sampled in LSLE deep waters during July 2004 shows high Chl-a content while C/N ratio gives evidence for an endogenic source of SPOM sinking through the water during summer time (Table 1 and Fig. 4). As SPOM sampled in July 2004 appears to be only partly affected by pelagic degradation processes, we suggest that very low temperature of the intermediate layer (Saucier *et al.*, 2003) coupled to rapid sinking of these particles through the water column are factors leading to only a partial degradation by bacterial activity during the sedimentation process. This hypothesis is supported by a previous study carried by Levasseur and Therriault (1987) showing that large autochthonous particles, mostly under the form of diatom theca and copepod fecal pellets are produced in the LSLE during phytoplankton growth events.

The most striking feature of our results is the loss of DIN in the whole water column sampled in July 2004 when compared with other sampling periods. Such a difference can not be explained by advection or mixing processes involving a mixing of surface or intermediate nitrate depleted water masses with deep waters, because salinity and temperature should have been affected the same way, and it is obviously not the case. The LSLE deep waters are very stable all around the year at all stations (Table 1) and are not diluted with less dense and warmer waters during summer (Gilbert *et al.*, 2005). Only two basic biological mechanisms can consume nitrate in marine environment: photosynthesis and nitrate respiration. The euphotic zone depth was determined at 26-29 m in the Gulf of St. Lawrence (Savenkoff *et al.*, 1996) and is assumed to be thinner in the LSLE due to the presence of fine suspended particles derived from the St. Lawrence River drainage basin. Photosynthesis can not be responsible for carbon fixation in the LSLE deep layer although Chl-a was present at all stations in July 2004 (Table 1). However, nitrate uptake by phytoplankton cells can occur in darkness and this process might be part of the explanation for missing DIN in summer.

The ability of diatoms and flagellates to assimilate nitrogen in darkness, the cost/benefit ratio for uncoupling nitrogen and carbon uptake (Clark *et al.*, 2002), and the advantages for some diatoms to engage vertical migration have been roughly discussed when surface layers become nutrient-depleted (Kanda *et al.*, 1989; Richardson *et al.*, 1998; Watanabe *et al.*, 1991). The partial decoupling of carbon fixation and nitrate assimilation by fast growing diatoms is considered as a typical situation in the temperate spring bloom when N assimilation in light phase alone may be rate limiting (Kanda *et al.*, 1989). Vertical migration and dark nitrogen uptake are expected to occur in LSLE in late spring and summer when the thin euphotic surface layer becomes DIN-depleted by phytoplanktonic activity ($[Chl-a] = 20.00 \pm 7.52 \mu g^{-1}$; $[DIN] = 3.2 \pm 2.0 \mu M$; $N/P \approx 9$) at 2 m depth observed in July 2004 (results not shown). Assuming that a portion of these phytoplankton cells are not ingested by zooplankton in surface layer because of the abundant primary production during that period, we suggest that the ability of cells to N assimilation in darkness is preserved while cells fall toward deep water layer. Although our data do not allow quantification of the proposed process, we suggest this mechanism might contribute in DIN depletion particularly in the intermediate layer (50 to 150 m) since this layer is subject to an intense mixing process in summer and can sequester cells for a while. For the deep layer, Li *et al.* (2006) have already mentioned in their conclusion that parameters N^* , dN and dN^{**} are roughly related by $-N = dN + dN^{**}$. The difference, if any, might be attributed to another consuming process such as dark assimilation. We suggest that 4 to 11% of missing nitrate in July 2004 in the LSLE deep layer may be induced by dark biotic assimilation.

Nitrate respiration or denitrification is a well documented process taking place in DO depleted marine organic matter-rich sediment (see Herbert, 1999 for a review). As denitrification is recognised to be limited by nitrate and organic matter availability, coupled nitrification/denitrification process is commonly observed in surface coastal sediments (Jenkins and Kemp, 1984). Denitrification is also well documented in anoxic water masses particularly in tropical regions where the bacterial community can supply to the lack of DO by consuming nitrate (Condispoti and Packard, 1980). Nitrate respiration was also mentioned as a plausible mechanism in aerobic bottom waters of NE Pacific Ocean

(Wolgast *et al.*, 1998). Authors observed a simultaneous use of nitrate and oxygen in respiration and postulated that denitrification occurred in microzones of aggregated particles in oxygenated waters ($\text{DO} = 135 \mu\text{M}$). LSLE deep layer seems to offer favourable conditions for nitrate respiration in hypoxic bottom waters ($65 \mu\text{M}$) when rich organic particles from surface layer high productivity are exported to the bottom. According to our data, July 2004 DIN and DO profiles seem both influenced by the abundance of sinking organic matter characterized by a low C/N and the presence of preserved Chl-a. Following Li *et al.* (2006) calculations, our results provide evidences of bacterial oxidation of organic matter by simultaneous oxygen (nitrification) and nitrate (denitrification) use (Table 2) in the water column. Savenkoff *et al.*, (1996) proposed bacterial respiration as an important benthic organic matter mineralization process along the Laurentian channel in the Gulf of St. Lawrence. However, nitrate respiration had never been reported in the LSLE water column and only available data on denitrification rate in LSLE sediment (1.8 to $3.3 \mu\text{mol N}_2 \text{ m}^{-2} \text{ h}^{-1}$) have been proposed by Wang *et al.*, (2003). According to this study, it is unlikely that surface sediment nitrate respiration can explain the low DIN concentrations by itself throughout the LSLE water column in July 2004 because sediment denitrification rate appears too low and DIN profiles do not show a consumption gradient near the bottom. To explain nitrate missing from the deep Bering Sea without involving a water column nitrate respiration, Lehmann *et al* (2005) calculated a very high denitrification rate of $9.6 \mu\text{mol N m}^{-2} \text{ h}^{-1}$ which is obviously not the case in the LSLE. Nitrate deficit in deep LSLE is a transient phenomenon appearing and disappearing within a few weeks. While low DO concentrations may have contributed to limit nitrification, high summer labile organic matter supply and high DIN availability have stimulated denitrification within sinking particles. This assumption was first developed by Wolgast *et al.*, (1998) as these authors observed denitrification in deep ocean waters with $\text{DO/DIN ratios} \geq 3.8$. Our DO/DIN ratios in LSLE deep waters in July 2004 ranged from 3.65 to 5.14 and always higher than other seasons.

Historical DO levels reported by Gilbert *et al* (2005) show an apparent stability of %DO saturation ($20 \pm 3\%$) from early 1990s up to 2003 although water temperature increased rapidly by about 0.7°C in the same period. Our own DO values taken from 2003

to 2006 show saturation between 18 and 25% and are in perfect accordance with previous data. Following the model of Gilbert *et al* (2005), DO levels should have been sensitive to such an important change in water temperature due to a reduction of oxygen solubility. We suggest that decoupling between nitrification and denitrification processes within labile SPOM in high DIN and low DO environment may contribute to stabilise DO concentrations in the LSLE bottom layer. It seems that $\text{DO} = 65 \pm 10 \mu\text{M}$ (corresponding to about 20% saturation in deep LSLE) acts as a threshold where denitrification becomes a favoured mechanism and «protect» deep waters against a further development of anoxia. Such a threshold might be governed by biodynamic factors (energy requirement for using DIN versus DO and carbon lability) but our data do not allow further calculations.

4.6 Conclusion

Our results bring evidences that uncoupled nitrification/denitrification process can occur in hypoxic estuarine deep waters when favourable conditions are present. A massive downward exportation of freshly produced organic matter during summer induced an unexpected denitrification response within the deep water column leading to a nitrate deficit, but leaving DO saturation levels almost unchanged between seasons. No evidence of a significant contribution to nitrate loss by sedimentary denitrification was observed. Denitrification in the water column during episodic massive input of labile organic carbon might be seen as a «protective mechanism» that kept DO level within hypoxic conditions ($65 \pm 10 \mu\text{M}$) and prevented the development of anoxic conditions at least for the last 15-20 years. This hypothesis offers an interesting framework to better understand the processes involved in hypoxia development in the LSLE and furthermore, to understand how this environment will be affected by increasing eutrophication. A number of studies showed an increase of total organic matter concentration in St. Lawrence Estuary sediment (Louchouarn *et al*, 1997; St-Onge *et al*, 2003; Thibodeau *et al*, 2006). An increasing proportion of marine SPOM reaching bottom sediments in the last three decades (Louchouarn *et al*, 1997; St-Onge *et al*, 2003) was observed. In addition Thibodeau *et al*. (2006) showed a ten-fold increase in the accumulation rate of dinoflagellate cysts and benthic foraminifera in the LSLE sediment over the last four decades which can be interpreted as a recent increase in pelagic and benthic production. Warmer surface waters

induced by climate changes coupled to increasing nutrient import from St. Lawrence River drainage basin might trigger this «apparent hypoxic steady-state» and push the system toward a complete consumption of available dissolved oxygen within a few decades.

4.7 Acknowledgements

This research was funded by Natural Science and Engineering Research Council (NSERC-Discovery grant E.P.) and the Canada Research Chair in Ecotoxicology (E.P.). The authors gratefully acknowledge the captain and the crew of the R/V Coriolis II and CCGS Amundsen for their support. This paper is a contribution to Quebec-Ocean network (FQRNT).

4.8 References

- Alderson, J.M., Helz, G.R. and Miller, C.V. 2001. Reconstructing the rise of recent coastal anoxia; molybdenum in Chesapeake Bay sediments. *Geochim. Cosmochim. Acta.* 65: 237-252.
- Beman, J.M., Arrigo, K.R. and Matson, P.A. 2005. Agricultural runoff fuels large phytoplankton blooms in vulnerable areas of the ocean. *Nature.* 434: 211-214.
- Benoit P., Gratton, Y. and Mucci, A.. 2006. Modeling the dissolved oxygen levels in the bottom waters of the Lower St. Lawrence Estuary: Coupling of benthic and pelagic processes. *Mar. Chem.* 102: 13-32.
- Bugden G.L. 1988. Oceanographic conditions in the deeper water of the Gulf of St. Lawrence in the relation to the local and oceanic forcing. *NAFO SCR Doc.* 88/87.
- Chambers, P.A., Guy, M., Roberts, E.S., Charlton, M.N., Kent, R., Gagnon, C., Grove, G. and Foster, N. 2001. Nutrients and their impact on the Canadian environment. Agriculture and Agri-Food Canada, Environment Canada, Fisheries and Oceans Canada, Health Canada and Natural Resources Canada. Ottawa.
- Clark, D.R., Flynn, K.J. and Owens, N.J.P. 2002. The large capacity for dark nitrate-assimilation in diatoms may overcome nitrate limitation of growth. *New Phyto.* 155: 101-108.
- Cloern, J.E. 2001. Our evolving conceptual model of the coastal eutrophication problem. *Mar. Ecol. Prog. Ser.* 210: 223-253.

- Condispoti, L.A. and Packard, T.T.. 1980. Denitrification rates in the eastern tropical South Pacific. *J. Mar. Res.* 38:453-477.
- Duarte, C.M. 1995. Submerged aquatic vegetation in relation to different nutrient regimes. *Ophelia.* 41: 87-112.
- El-Sabh, M.I. 1979. The Lower St. Lawrence Estuary as a physical oceanographic system. *Naturaliste Can.* 106: 55-73.
- El-Sabh, M.I. and Silverberg, N. (Eds) 1990. Oceanography of a large scale estuarine system: The St. Lawrence. Coastal and Estuarine Studies. Springer-Verlag. New-York. n° 39.
- Falkowski, P.G., Hopkins, T.S. and Walsh, J.J. 1980. An analysis of factors affecting oxygen depletion in the New York Bight. *J. Mar. Res.* 38: 479-506.
- Gilbert, D., Sundby, B., Gobeil, C., Mucci, A. and Tremblay, G.H. 2005. A seventy-two-year record of diminishing deep-water oxygen in the St. Lawrence Estuary: The northwest Atlantic connection. *Limnol. Oceanogr.* 50: 1654-1666.
- Greisman, P. and Ingram, G. 1977. Nutrient distribution in the St. Lawrence Estuary. *J. Fish. Res. Board Can.* 34: 2117-2123.
- Gruber, N. and Sarmiento, J.L. 1997. Global patterns of marine nitrogen fixation and denitrification. *Glob. Biogeochem. Cycles.* 11: 235-266.
- Helly, J.J. and Levin L.A. 2004. Global distribution of naturally occurring marine hypoxia on continental margins. *Deep Sea Res. Part I.* 51: 1159-1168.
- Herbert, R.A. 1999. Nitrogen in coastal marine ecosystems, FEMS Microb. Biol. Rev. 23: 563-590.
- Jenkins, M.C. and Kemp, W.M. 1984. The coupling of nitrification and denitrification in two estuarine sediments. *Limnol. Oceanogr.* 29: 609-619.
- Kanda, J., Xiemann, D.A., Conquest, L.D. and Bienfang, P.K. 1989. Light-dependency of nitrate uptake by phytoplankton over the spring bloom in Auke Bay, Alaska. *Mar. Biol.* 103: 563-569.
- Koutitonsky, V.G. and Gugden, G.L. 1991. The physical oceanography of the Gulf of St. Lawrence: A review with emphasis on the synoptic variability of the motion. In Therriault J.C. (Ed) The Gulf of St. Laurence: small or big estuary? *Can. Spec. Publ. Fish. Aquat. Sci.* p.57-90.
- Lehmann, M.F., Sigman, D.M., McCorkle, D.C., Bunelle, B.G., Hoffmann, S., Kienast, M., Canbe, G and Clement, J. 2005. Origin of the deep Bering sea natrate deficit : Constraints

from the nitrogen and oxygen isotopic composition of water column nitrate and benthic nitrate fluxes. *Glob. Biogeochem. Cycles.* doi:10.1029/2005GB002508.

Levasseur, M. and Therriault, J.-C. 1987. Phytoplankton biomass and nutrient dynamics in a tidally induced upwelling: the role of the $\text{NO}_3 : \text{SiO}_4$ ratio. *Mar. Ecol. Prog. Ser.* 39: 87-97.

Li, Y-H., Menviel, L. Peng, T-H. 2006. Nitrate deficits by nitrification and denitrification processes in the Indian Ocean. *Deep-Sea Res. I.* 53: 94-110.

Louchouarn, P., Lucotte, M., Canuel, R., Gagné, J.-P. and Richard, L.-P. 1997. Sources and early diagenesis of lignin and bulk organic matter in the sediments of the Lower St. Lawrence Estuary and the Saguenay Fjord. *Mar. Chem.* 58: 3-26.

Painchaud, J. 1999. La production porcine et la culture du maïs. Impacts potentiels sur la qualité de l'eau. *Naturaliste Can.* 123: 41-46.

Plourde, J. and Therriault, J.-C. 2004. Climate variability and vertical advection of nitrate in the Gulf of St. Lawrence, Canada. *Mar. Ecol. Prog. Ser.* 279: 33-43.

Poulin P. and Pelletier E. 2007. Determination of ammonium using a microplate-based fluorometric technique. *Talanta.* doi:10.1016/j.talanta.

Renaud, M. 1986. Hypoxia in Louisiana coastal water during 1983: Implication for the fisheries. *Fish. Bull. (Washington, D. C.)* 84: 19-26.

Richardson, T.L., Cullen, J.J., Kelley, D.E., and Lewis, M.R. 1998. Potential contributions of vertically migrating *Rhizosolenia* to nutrient cycling and new production in the open ocean. *J. Plank. Res.* 20:219-241.

Rosenberg, R. 1985. Eutrophication: the future marine coastal nuisance? *Mar. Pollut. Bull.* 16: 227-231.

Saucier, F.J., Roy, F. and Gilbert, D. 2003. Modeling the formation and circulation processes of water masses and the sea ice in the Gulf of St. Lawrence, Canada. *J. Geophysic. Res.* 108: 3269-3289.

Savenkoff, C., Vézina, A.F., Packard, T.T., Silverberg, N., Therriault, J.-C., Chen, W., Bérubé, C., Mucci, A., Klein, B., Mesplé, F., Tremblay, J.-E., Legendre, L., Wesson, J. and Ingram, R.G. 1996. Distributions of oxygen, carbon, and respiratory activity in the deep layer of the Gulf of St. Lawrence and their implications for the carbon cycle. *Can. J. Fish. Aquat. Sci.* 53: 2451-2465.

Schafer, C.T., Smith, J.N., and Seibert, B. 1983. Significance of natural and anthropogenic sediment input to the Saguenay Fjord, Québec. *Sediment. Geol.* 36: 177-194.

- St-Onge, G., Stoner, J.S., and Hillaire-Marcel, C.. 2003. Holocene paleomagnetic records from the St. Lawrence Estuary, eastern Canada: centennial to millennial-scale geomagnetic modulation of cosmogenic isotopes. *Earth Planet. Sci. Lett.* 209: 113-130.
- Strickland, J.D.H. and Parson, T.R. 1972. A practical handbook of seawater analysis, 2nd ed. Fisheries Research Board of Canada. Ottawa. n° 167.
- Theriault, J.-C. and Lacroix, G., 1976. Nutrients, chlorophyll, and internal tides in the St. Lawrence Estuary. *J. Fish. Res. Board Can.* 33: 2747-2757.
- Thibodeau, B., de Vernal, A. Mucci, A. 2006. Recent eutrophication and consequent hypoxia in the bottom waters of the Lower st. Lawrence estuary: Micropaleontological and geochemical evidence. *Mar. Geol.* 231: 37-50.
- Turner, R.E., Rabalais, N.N., Senson, E.M., Kasprzak, M., Romaire, T. 2005. Summer hypoxia in the northern Gulf of Mexico and its prediction from 1978 to 1995. *Mar. Environ. Res.* 59: 65-77.
- Vézina, A.F., Gratton, Y. and Vinet, P. 1995. Mesoscale physical-biological variability during summer phytoplankton bloom in the Lower St. Lawrence Estuary. *Est. Coast. Shelf Sci.* 41: 393-411.
- Vitousek, P.M., Aber, J.D., Howarth, R.W., Likens, G.E., Matson, P.A., Schindler, D.W., Schlesinger, W.H., and Tilman, D.G. 1997. Human alteration of the global nitrogen cycle: Sources and consequences. *Ecol. Appl.* 7: 737-750.
- Wang, F., Juniper, S.K., Pelegri, S.P. and Macko, S.A. 2003. Denitrification in sediment of the Laurentian Trough, St. Lawrence Estuary, Québec, Canada. *Est. Coast. and Shelf Sci.* 57: 515-522.
- Watanabe, M., Kohata, K., and Kimura, T. 1991. Diel vertical migration and nocturnal uptake of nutrients by *Chattonella antiqua* under stable stratification. *Limnol. Oceanogr.* 36: 593-602.
- Wolgast, D.M., Carlucci, A.F., and Bauer, J.E. 1998. Nitrate respiration associated with detrital aggregates in aerobic bottom waters of the abyssal NE Pacific. *Deep-Sea Res. II.* 45: 881-892.
- Yin, K., Lin Z. and Ke., Z. 2004. Temporal and spatial distribution of dissolved oxygen in the Pearl River Estuary and adjacent coastal waters. *Cont. Shelf Res.* 24: 1935-1948.

CHAPITRE V

Bacterioplankton distribution in the St. Lawrence Estuary during ice-free and ice-covered periods: Proportion of high and low nucleic acid content cells

Karine Lemarchand, Patrick Poulin, Philippe Archambault and Emilien Pelletier

Submit to FEMS Microbiology Ecology

5.1 Abstract

In sub-Arctic estuaries subject to the presence of seasonal sea ice, how bacterial communities development is intertwined with environmental variables is still poorly understood during the ice-covered period. The aim of this study was to determine the seasonal and intra-water mass variability in the abundance and structure (proportion of high nucleic acid cells, %HNA) of total heterotrophic bacteria (TB) along the main axis of the St. Lawrence Estuary (SLE) during ice-free and ice-covered periods. No significant differences were observed in the upper SLE for both sampling periods. In contrast, the distribution of bacterioplankton in the lower SLE showed a decrease of TB with depth in ice-free period whilst, during the ice-covered period, TB were homogeneously distributed throughout the water column. This variance could be explained at 81 % by combined effects of temperature, salinity, dissolved oxygen (DO), suspended particulate matter (SPM), Chlorophyll *a* (Chla) and C:N ratio. On the other hand, the %HNA variance could be explained at 51 % by the combination of ammonium (NH_4^+), salinity, SPM and nitrite + nitrate ($\text{NO}_2^- + \text{NO}_3^-$) concentrations. %HNA and TB variations indicate that the structure and abundance of bacterial communities respond in different ways to external forcing and that low nucleic acid cells may be favored in low productive waters. Moreover, nitrogen concentration appeared to be the main factor influencing the %HNA, with no significant influence of temperature, whereas distribution of TB appeared to be driven by multiple physical and chemical variables.

5.2 Introduction

Heterotrophic bacteria constitute a large and essential component of marine food webs (Gasol et al. 1997), playing pivoting roles in major biogeochemical cycles (Legendre & Rassoulzadegan 1995) and sharing with phytoplankton the capacity to take up dissolved carbon and incorporate it into particulate organic carbon (POC) (Revilla et al. 2000). In oceanic systems not receiving allochthonous inputs of carbon, bacterial production is ultimately supported by the supply of organic carbon from primary producers. However, in coastal and estuarine waters, allochthonous inputs of carbon can be important and lead to bacteria-dominated areas where no coupling with primary production can be observed (Findlay et al. 1991, Azam 1998, Del Giorgio & Duarte 2002).

Sub-Arctic estuaries are highly dynamic aquatic systems where bacterial communities are still poorly characterized. In contrast with temperate estuaries, sub-Arctic estuaries, such as the St. Lawrence Estuary (SLE, Quebec, Canada), are strongly influenced by the seasonality and by the formation of a sea ice cover during winter time. This seasonal cycling leads to important changes in hydrodynamic and chemical conditions and, as a consequence, in biological populations and communities that inhabit year around the Estuary. In 2005, Gilbert *et al.* reported a significant decrease of oxygen concentrations in the bottom waters of the Lower St. Lawrence Estuary (LSLE) in the last seventy years (from 125 µmol l⁻¹ in the 1930's to an average of 65 µmol l⁻¹ for the 1984–2003 period). Although this depletion can be, to some extent, explained by changes in physical and chemical characteristics of the LSLE bottom water mass, one third to one half of the oxygen loss cannot be attributable to physical causes and needs to be better understood (Gilbert et al. 2005). Moreover, it has been suggested that cold winters in the Gulf of St. Lawrence associated with a thick ice cover would result in high nitrate replenishment and high spring phytoplankton bloom, whereas warm winters associated with a thin ice cover would result in a low nitrate replenishment, a low spring phytoplankton bloom and a dominance of heterotrophs (Plourde & Therriault 2004). Given the dominance of bacteria in communities and ecosystem processes (Azam 1998, Cotner & Biddanda 2002), a high heterotrophic activity in surface waters may lead to a higher oxygen demand in the water column after warm winters. Considering the rise of hypoxia in the bottom layer of the

LSLE since the 1930s, a better characterization of the heterotrophic bacteria dynamic in the whole water column during the ice-covered period is needed to improve our understanding the response of sub-Arctic estuaries to environmental changes related to direct and indirect anthropogenic activities.

Most of the heterotrophic bacterial measurements previously conducted in the SLE have focused on the euphotic zone (between 0-50 m) during productivity peak periods (late spring and summer) and only scarce data are available on the abundance and composition of bacterial communities in this sub-Arctic Estuary (Siron et al. 1993, Painchaud et al. 1995, Lovejoy et al. 2000) under winter conditions. As temperature was demonstrated to be the major factor affecting bacterial growth rate in resource unlimited temperate estuaries (Revilla et al. 2000), it is important to understand the behavior of the bacterial compartment during the ice-covered period to assess the significance of heterotrophic bacteria in biogeochemical processes involved year-around in carbon and nitrogen cycles of SLE.

The main objective of this study was to assess the seasonal and intra-water mass variability of abundance and structure of total heterotrophic bacterial community in the main axis of the St. Lawrence Estuary during ice-free (October 2005) and ice-covered (December 2005) periods. Nucleic acid content of marine bacterial populations has received considerable attention during the last decade (Lebaron et al. 2001, Longnecker et al. 2005, Nishimura et al. 2005, Sherr et al. 2006). Even if the ecological significance of high nucleic acid content cell (HNA) and low nucleic acid content cell (LNA) subgroups is still a controversial matter (Gasol et al. 1999, Longnecker et al. 2006, Sherr et al. 2006, Moràn et al. 2007, Scharek & Latasa 2007), the proportion of HNA cells (%HNA) within the total heterotrophic bacteria appears to be a valuable tool for distinguishing the assemblages and/or the physiological status of the total population. Two sampling campaigns were conducted to (1) describe the spatial distribution of the total heterotrophic bacterial community in the SLE, (2) investigate the structure of this community through the distribution of HNA and LNA cells and (3) investigate how the heterotrophic bacterial community, including differences in %HNA, responds to the presence of an ice cover in

relation with variations of environmental variables (*i.e.* temperature, salinity, dissolved oxygen, dissolved inorganic nutrients, suspended particular matter, and chlorophyll *a*).

5.3 Material and Methods

5.3.1 Study site

The St. Lawrence Estuary (Quebec, Canada) is a transitional 600-km long funnel-shaped macro-tidal environment beginning at the upstream limit of the salt intrusion (eastern tip of Ile d'Orléans) and divided into two distinct zones: the Upper Estuary (USLE) and the Lower Estuary (LSLE) (Fig. 1). The geographical limit between the USLE and the LSLE is set near the mouth of the Saguenay Fjord (between stn5 and stn6), where the Estuary floor rises from 350 m to 25 m generating a tide induced up-welling process and allowing a high biological productivity (Koutitonsky & Bugden 1991).

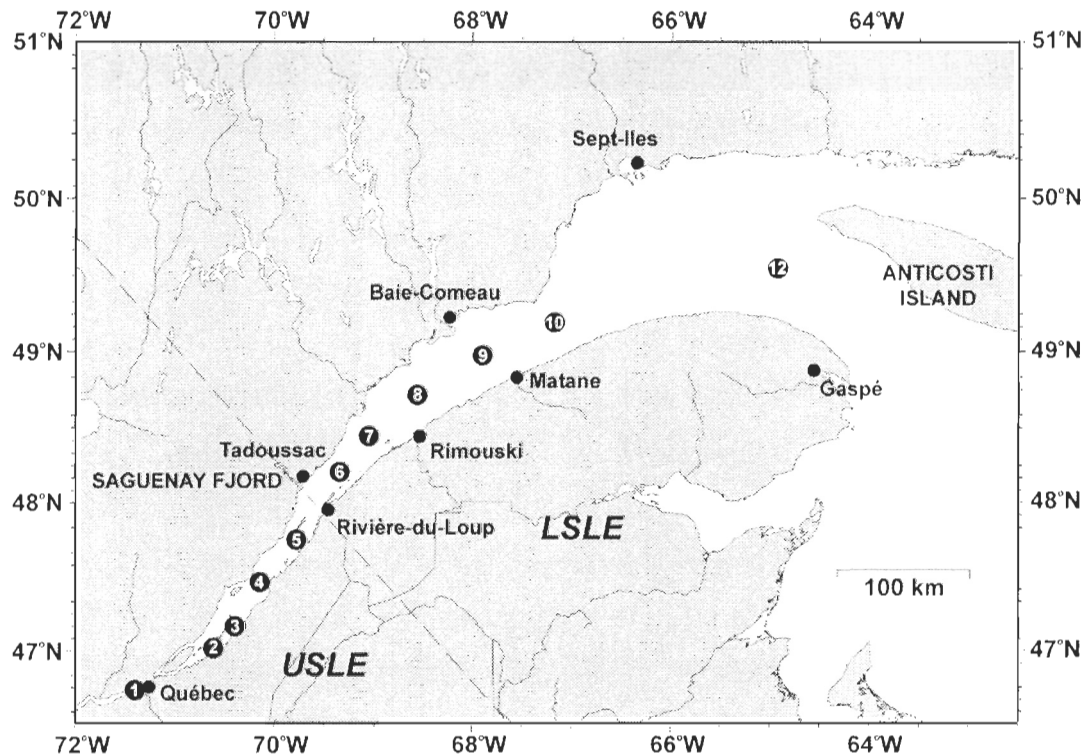


Figure V-1 Sampling area and location of the sampling stations. The dotted line represents the geographical separation between the Upper (USLE) and Lower (LSLE) St. Lawrence Estuary.

The USLE is a narrow, shallow and turbid corridor characterized by rough bottom topography where landward marine water intrusions and seaward freshwater runoff are affected by intense tidal mixing processes. This vigorous mixing process contributes to a vertical homogeneity in distribution of dissolved and particulate constituents through the entire water column and promotes the formation of a maximum turbidity zone around stn2 (Lucotte & D'Anglejan 1986). The LSLE is a deep stratified basin featuring a 350 m depth smooth bottom central valley; the Laurentian Channel, which is strongly influenced by the Atlantic Ocean through winds, tides, landward bottom water intrusions and surface seaward freshwater runoff coming from the watershed (Koutitonsky & Bugden 1991). The vertical distribution of biological and chemical variables responds to changing stratification characteristics imposed by the ice-free and ice-covered periods (El-Sabh & Silverberg 1990). The ice formation usually starts in December in the USLE, producing ice floes that are pushed downstream by tidal currents and prevailing winds and quickly reaching the LSLE and the Gulf in late December – early January. Spring flood and a complete melting of the ice cover generally occur in April (El-Sabh 1979, Saucier et al. 2003). During the ice-free period from May to November, the combination of fresh and marine waters generates in the LSLE a stratification in three layers: (1) a surface layer (0 to 20 m) displaying high seasonal variations in temperature and salinity, (2) a cold intermediate layer (20 to 150 m) less affected by environmental changes than the surface layer, (3) a deep layer (150 m to the bottom) that only undergoes long term changes due to relatively steady inward advection (0.5 cm s^{-1}) and weak vertical diffusion (Koutitonsky & Bugden 1991). Under ice-covered conditions, water freezing temperature and very low freshwater inputs contribute to homogenize surface and intermediate layers leaving only two thick layers: a surface layer corresponding to the first 150 m in depth and the year-around stable deep layer.

5.3.2 Sampling scheme

Water samples were collected at 11 stations located along the main axis of the SLE during two multidisciplinary oceanographic cruises (Fig. 1). The first sampling cruise was conducted onboard the *RV Coriolis II* in October 2005 (from 2005/10/05 to 2005/10/10) while the second sampling campaign was carried on the Canadian Research Icebreaker

CCGS *Amundsen* in December 2005 (from 2005/12/05 to 2005/12/18). At each sampling station, vertical profiles of temperature, salinity, and dissolved oxygen (DO) were recorded using a Seabird® SBE 9 multi-probe (temperature accuracy $\pm 0.01\text{ }^{\circ}\text{C}$, salinity accuracy ± 0.01 , and DO accuracy $\pm 0.01\text{ mg l}^{-1}$) mounted on a rosette multi-sampler (General Oceanics®). Sample temperature and salinity were validated onboard using a dual temperature and salinity YSI® digital probe whereas DO measurements were assessed using Winkler titration (Strickland & Parson 1968). Deviations of DO probe compared with onboard chemical titration were always below 5 %. Water samples were taken from 1 to 6 depths depending upon the total depth of the water column using 12 L lever-action Niskin® bottles (General Oceanics Inc., USA). Water samples for the determination of bacterioplankton abundance and structure were poured into 5 ml Cryovials® tubes and fixed with formaldehyde (final concentration = 2 % v/v) before storage at $-80\text{ }^{\circ}\text{C}$. Water samples for dissolved inorganic nutrient concentrations (DIN; ammonium [NH_4^+], nitrite and nitrate [$\text{NO}_2^- + \text{NO}_3^-$]), suspended particulate matter (SPM), C and N contents in SPM and chlorophyll *a* (Chla) were processed as following: (1) samples for $\text{NO}_2^- + \text{NO}_3^-$ analyses were filtered onto 25 mm, 0.22 μm pore-size Nucleopore® membrane and filtrates stored in the dark at $-80\text{ }^{\circ}\text{C}$ in clean 60 ml polyethylene bottles until analysis; (2) samples for NH_4^+ determination were collected in clean 250 ml DO glass bottles and analyzed onboard; (3) samples for Chla determination were collected on 25 mm Whatman® GF/F filters and stored frozen at $-80\text{ }^{\circ}\text{C}$ while (4) SPM samples were filtered on pre-combusted, pre-weighted, 47 mm diameter Millipore® glass fibber membranes, until clogging (maximum 10 liters). Filters were acidified (to remove carbonates) with 10 ml of 10 % v/v HCl solution and stored at $-80\text{ }^{\circ}\text{C}$ for further laboratory analyses.

5.3.3 DIN, SPM and Chla analyses

Determination of NH_4^+ concentrations was performed onboard, using a microplate-based spectrofluorometric method which provides an analytical uncertainty ($\pm 1\sigma$) of $\pm 1\%$. Determination of $\text{NO}_2^- + \text{NO}_3^-$ concentrations was made by classical colorimetric technique (Strickland & Parson 1968) using an automated analytic AA3 Brand+Luebbe®

platform and allowing an overall analytical uncertainty ($\pm 1 \sigma$) under $\pm 5\%$ (Poulin & Pelletier 2007).

SPM elementary analysis (POC and PON) was performed using a ECS 4010 Costech® instrument equipped with a zero blank autosampler. Quality of sample analysis was controlled by replicate analysis ($n = 10$) of a certified sediment sample (NIST-1941b). Analytical error ($\pm 1 \sigma$) was determined from replicate measurements of standard material (acetanilide, urea, atropine, nicotinamide) and averaged $\pm 5\%$. Filters for Chla determination were extracted in 3 ml of 95 % methanol and sonicated on an ice bath. The extract was cleared by centrifugation and filtration through a 0.22 μm Gelman Acrodisc filter. A 50 μl aliquot was then injected in a reversed-phase C8 Waters Symmetry column thermostated at 25 °C. Gradient elution was controlled by a Thermo Separation P4000 pump and used Zapata et al.'s (Zapata et al. 2000) mobile phases A and B1, with A varying from 100 % to 60 % in 22 min then decreasing to 5 % at 28 min and stabilizing. Peaks were detected using a Spectroflow 980 fluorescence detector in line with a Spectra Focus fast scanning absorbance detector. Peaks were identified and quantified using external pigment standards with an accuracy of $\pm 0.001 \mu\text{M}$, from DHI Water and Environment (Denmark) as detailed in Roy et al. (Roy et al. 1996) and extinction coefficients were taken from Jeffrey et al. (Jeffrey et al. 1997).

5.3.4 Flow cytometry analyses for bacterial abundance and %HNA

Frozen samples were thawed and two subsamples were half diluted in TE 10X buffer (100 mM Tris-HCl, 10 mM EDTA, pH 8.0). One ml of the resulting dilution was stained with SYBR® Green I nucleic acid gel stain at a dilution of 1/5,000 of the commercial solution (Invitrogen, Inc), incubated for 15 min at room temperature in the dark (Lebaron et al. 2001) and analyzed during 180 s with a EPICS® ALTRA™ cell sorting flow cytometer (Beckman Coulter® Inc.) equipped with a laser emitting at 488 nm. Fluorescent beads (Fluoresbrite YG microspheres 1 μm , Polysciences™) were systematically added to each sample as an internal standard to normalize cell fluorescence emission and light scatter values. Heterotrophic bacteria (TB) were detected in a plot of green fluorescence

recorded at 530 ± 30 nm (FL1) versus side angle light scatter (SSC). A plot of green fluorescence versus red fluorescence was used to differentiate between photosynthetic and non-photosynthetic prokaryotes. The volume analyzed was calculated by weighing each sample before and after each run to calculate cell abundance. HNA and LNA subgroups were discriminated by gating the FL1-versus-SSC plot and respective abundances of both subgroups were determined. The %HNA was determined by the ratio of HNA cells on TB. Vertical profiles of TB and %HNA at discrete depths were interpolated onto a rectangular grid using the *CTDFGRID EPIC* program (Lukas, R.B., Dept of Oceanography, Univ. of Hawaii), with the method of successive over-relaxation to solve programmed partial differential equations.

5.3.5 Statistical analyses

Spearman's rank correlations were used to test the correlation between bacterial population characteristics (*i.e.* TB and %HNA) and environmental variables. The hypotheses related to seasonal and intra-water mass variability in bacterial abundance and %HNA in the St. Lawrence Estuary were tested with analyses of variance. The St. Lawrence Estuary water mass was subdivided in four distinct sections (USLE, LSLE surface [LSLE Surf.; 0 – 20 m], LSLE intermediate [LSLE Int.; 20 – 150 m] and LSLE bottom [LSLE Bot.; >150 m]) as previously described and according to CTD profiles. Two-way ANOVAs were carried out to test if the TB abundance and %HNA differ between the location in the Estuary (USLE and LSLE Surf.) and among seasons (October and December 2005). Other two-way ANOVAs we performed to compare the same variables among the season and the three water layers in the LSLE. The assumptions of homoscedasticity and normality were verified by the spread of residuals as suggested by Quinn and Keough, (Quinn & Keough 2002) and confirmed by the Shapiro-Wilk's test (Zar 1999). A transformation was used to respect the statistical assumptions when necessary. Furthermore, two outlier values were removed for the two ANOVAs comparing seasons and stations in the Estuary. Four outlier values were removed from the ANOVA comparing the bacterial abundance for the three layers of water and seasons. When a source of variation was significant, Tukey-Kramer test was carried out to identify the differences at $\alpha = 0.05$ (Sokal & Rohlf 1995).

Multiple regression analyses were used to link the environmental parameters (NH_4^+ , $\text{NO}_3^- + \text{NO}_2^-$, water temperature, salinity, Chla, DO, SPM and C:N ratio) to TB abundance and %HNA variations. We used Akaike's Information Criteria adjusted for sample size (AICc) and adjusted coefficients of determination (r^2 adjusted) for model selection (Quinn & Keough 2002). The regression model with the smallest AICc value was considered the most parsimonious model explaining variability in bacterial abundance and %HNA. Normality was verified using the Shapiro-Wilk's test (Zar 1999) and homoscedasticity was confirmed by graphical examination of the residuals (Montgomery 1991). Based on the Cook's distance (Cook & Weisberg 1982, Quinn & Keough 2002) three values were removed from the TB abundance data and one value from the %HNA data.

5.4 Results

5.4.1 Physical variables

Water column mean temperature in the USLE was 7 °C higher in October than in December whereas salinity and DO concentrations remained at similar values during both sampling periods (Table 1). As expected from general oceanographic conditions described earlier for LSLE, temperature changes were greater between the three layers present during the ice-free period, while only two water layers can be distinguished during the ice-covered period. Temperature, salinity and DO concentration recorded in these different layers at both sampling periods are reported in (Table 1). Temperature and salinity increased with depth in both cases, while DO concentrations decreased with depth.

5.4.2 SPM, Chla and DIN distributions

The SPM concentrations recorded in the SLE indicate the presence of a highly turbid area in the USLE between stn2 and stn3, with concentrations reaching $\sim 100 \text{ mg l}^{-1}$ at stn2. The SPM concentrations for the upper Estuary ranged from 1.52 to 77.46 mg l^{-1} and from 3.71 to 114.44 mg l^{-1} in October and December, respectively. SPM concentrations in the LSLE were lower than in the USLE (Table 1) and a weak variability was monitored

during the two sampling periods with concentration values ranging from 0.42 (intermediate layer, Oct.) to 1.77 mg l⁻¹ (surface layer, Dec.).

Chla concentrations were very low during in October as well as in December with numerous samples under the detection limit (Table 1). The highest Chla concentration in the ULSE was observed in October (0.370 µg l⁻¹) while this maximum in December sampling was only 0.254 µg l⁻¹. In the LSLE, Chla concentrations observed in surface water reached 1.710 µg l⁻¹ in October and 0.422 µg l⁻¹ in December. As expected, Chla concentrations determined in intermediate and bottom waters were lower than in surface waters and never exceeded 0.240 µg l⁻¹.

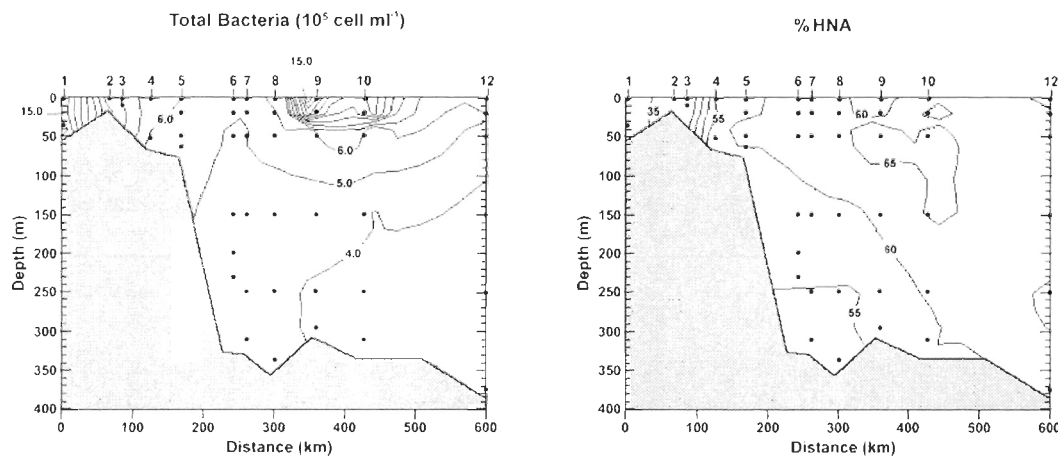
Tableau V-1 Comparison of environmental and biological variables in the USLE and in the LSLE during October and December 2005. The LSLE water column was analyzed as a three layer water mass, presenting a surface layer (0 to 20 m), and intermediate layer (20 to 150 m) and a bottom layer (>50 m). <DL: under the detection limit.

	Temperature °C	Salinity	DO mg l ⁻¹	SPM µg l ⁻¹	Chla µg l ⁻¹	NH ₄ ⁺ µM	NO ₂ ⁺ + NO ₃ µM	C:N	10 ⁵ TB cell ml ⁻¹	% HNA
ULSE										
<u>October 2005</u>										
<i>n = 9</i>	7.23 (4.83)	20.44 (10.98)	9.54 (0.54)	14.44 (25.81)	0.11 (0.19)	1.24 (1.66)	17.57 (4.39)	10.57 (5.07)	6.38 (1.50)	52 (10)
<u>December 2005</u>										
<i>n = 8</i>	0.24 (0.79)	21.42 (8.66)	10.51 (1.89)	24.15 (37.55)	0.20 (0.24)	0.56 (0.82)	20.27 (4.14)	13.55 (1.94)	6.25 (2.49)	54 (5)
LSLE										
<u>October 2005</u>										
<i>0 - 20 m</i> <i>(n = 12)</i>	4.80 (1.64)	29.43 (1.36)	9.74 (0.67)	1.09 (0.25)	0.63 (0.61)	0.54 (0.73)	9.68 (4.56)	7.43 (1.38)	8.25 (3.70)	61 (4)
<i>20 - 150 m</i> <i>(n = 12)</i>	1.88 (1.13)	32.66 (0.99)	6.95 (2.74)	0.76 (0.19)	0.06 (0.07)	0.02 (0.01)	16.69 (6.08)	9.21 (2.17)	4.44 (0.72)	63 (5)
<i>> 150 m</i> <i>(n = 12)</i>	5.07 (0.37)	34.49 (0.17)	2.38 (0.68)	1.24 (0.30)	0.02 (0.01)	< DL	25.32 (0.33)	12.60 (1.78)	3.92 (0.54)	57 (4)
<u>December 2005</u>										
<i>0 - 20 m</i> <i>(n = 12)</i>	0.40 (1.08)	29.69 (1.67)	10.45 (1.37)	1.09 (0.41)	0.15 (0.16)	0.02 (0.02)	11.51 (3.64)	9.92 (1.56)	3.85 (0.33)	57 (3)
<i>20 - 150 m</i> <i>(n = 13)</i>	2.39 (1.04)	33.19 (0.95)	6.04 (2.59)	0.91 (0.56)	0.05 (0.06)	< DL	18.18 (6.00)	10.58 (2.52)	3.48 (0.46)	58 (3)
<i>> 150 m</i> <i>(n = 11)</i>	5.08 (0.45)	34.49 (0.20)	2.65 (0.81)	1.07 (0.39)	< DL	< DL	26.22 (0.88)	11.24 (1.87)	3.38 (1.18)	55 (2)

Higher NH₄⁺ concentrations were observed in the USLE than in the LSLE for both sampling periods (Table 1). NH₄⁺ concentrations reached 4.48 µM in the USLE in October and 2.10 µM in December while in the LSLE surface layer NH₄⁺ reached 2.23 µM in October and a very low 0.05 µM in December. In intermediate and bottom waters, NH₄⁺

never exceeds 0.05 μM in October whereas it remained under our detection limit in December. In the USLE, $\text{NO}_2^- + \text{NO}_3^-$ concentrations ranged from 13.80 to 27.74 μM in October and from 17.24 to 28.78 μM in December. In the LSLE, $\text{NO}_2^- + \text{NO}_3^-$ concentrations increased with depth and decreased with salinity and were similar in October and in December (Table 1).

A)



B)

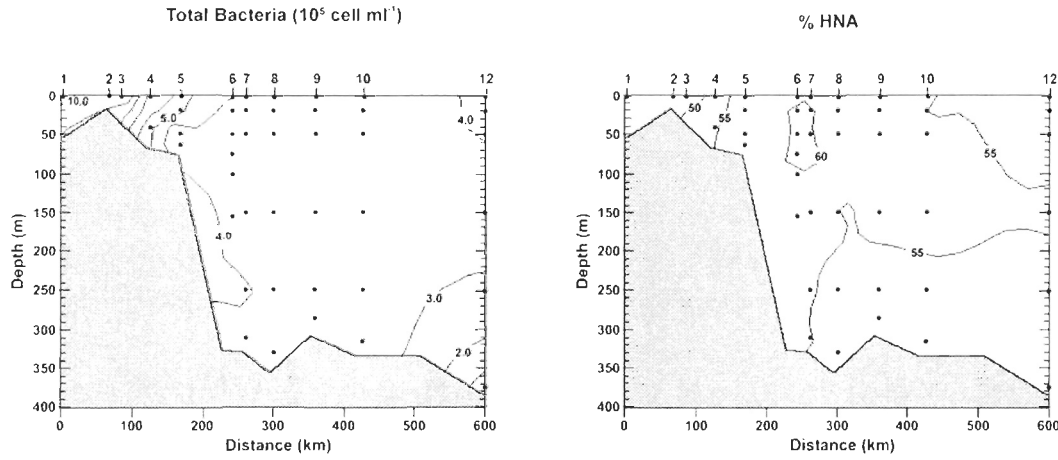


Figure V-2 Longitudinal profiles of total bacteria (TB) abundance and %HNA with depth along the sampling area during (A) October 2005 and (B) December 2005. Sampling depths are indicated by black dots. The produced 2D figures present a compressed vertical scale magnitude x1450 compared to the horizontal scale.

5.4.3 Heterotrophic bacteria abundance and structure

No significant differences were observed in the USLE within both sampling periods. TB abundance remained around 6.3×10^5 cell ml $^{-1}$ with a contribution of 53 % of HNA cells (Table 1). The TB maxima were recorded at the head of the USLE and reached 1.7×10^6 cell ml $^{-1}$ in October and 1.05×10^6 cell ml $^{-1}$ in December (Fig. 2). According to the ANOVAs, TB abundance and %HNA varied significantly between locations and seasons (Table 2). The results of the *a posteriori* Tukey-Kramer test showed that TB abundance was significantly lower in the LSLE in December (TB $\sim 3.6 \times 10^5$ cell ml $^{-1}$) than in October in both locations (*i.e.* LSLE and USLE; TB $\sim 6.1 \times 10^5$ cell ml $^{-1}$) (Table 2). %HNA did not vary in the same way (Table 2). The %HNA was significantly greater in the LSLE area in October than in the USLE in October (LSLE $\sim 60\%$; USLE $\sim 52\%$) and than in both sections of the Estuary in December ($\sim 55\%$) (Table 2).

Tableau V-2 Results of two-way analyses of variance (ANOVAs) testing the effect among the position in the Estuary (USLE Suf. and LSLE Suf.) and seasons (October 2005 and December 2005) and their interaction on bacterial abundance and % HNA. Transformations are mentioned when necessary to achieve the assumptions of the ANOVA. Note: LSLE = Lower St. Lawrence Estuary, USLE = Upper St. Lawrence Estuary.

Variables	Source of variation	df	SS	F	p
Log (Bacterial abundance)	Position (P)	1	0.3012	4.533	0.0403
	Season (Se)	1	0.9389	14.133	0.0006
	P x Se	1	0.554	8.339	0.0066
	Error	38	4.4297		
% HNA	Position (P)	1	405.155	11.836	0.0015
	Season (Se)	1	26.182	0.765	0.3878
	P x Se	1	144.533	4.222	0.0474
	Error	38	1771.744		
<i>A posteriori</i> Tukey-Kramer test					
Log (Bacterial abundance)	LSLE-Oct = USLE-Oct = USLE-Dec > LSLE-Dec				
% HNA	LSLE-Oct > LSLE-Dec = USLE-Dec = USLE-Oct				

The results of the second ANOVAs testing the effect among the water layers in the LSLE and the seasons showed a significant interaction for TB abundance in this stratified part of the SLE (Table 3). The *a posteriori* Tukey-Kramer test showed in October a

bacterial abundance maximum in the surface layer and a minimum in the bottom layer. The high mean TB value observed in the LSLE surface waters was the result of two high recordings at stn9 (1.6×10^6 cell ml $^{-1}$) and stn10 (1.1×10^6 cell ml $^{-1}$), with respect to other stations that showed average abundances of 5.9×10^5 cell ml $^{-1}$ (Fig. 2). In contrast, bacterial abundances in December were similar in the three layers ($\sim 3.6 \times 10^5$ cell ml $^{-1}$) and did not significantly differ from the abundance observed in October in the deep layer (3.9×10^5 cell ml $^{-1}$). Even if FL1 and SSC signatures of LNA and HNA subgroups were similar for the two sampling periods at each depth (Fig. 3), the two main factors (season and depth) of the ANOVAs were significant for the %HNA (Table 3). There was no difference between surface and intermediate layers, but both presented a significant higher %HNA contribution than the bottom layer whatever the season (Table 1). Finally, the mean %HNA was significantly greater in October than in December (Table 3).

Tableau V-3 Results of two-way analyses of variance (ANOVAs) testing the effect among the water layers in the Lower St. Lawrence Estuary (0-20 m, 20-150 m and 150 m- bottom) and the seasons (October 2005, December 2005) and their interaction on bacterial abundance and % HNA. Transformation was not necessary to achieve the assumptions of the ANOVA. Note: Surf = Surface = 0 - 20m, Int = Intermediate = 20-150 m, Bot= Bottom = 150 m to the bottom.

Variables	Source of variation	df	SS	F	p
Bacterial abundance	Depth (D)	2	1.40×10^{11}	23.542	<0.0001
	Season	1	1.98×10^{11}	66.657	<0.0001
	(Se)				
	D x Se	2	8.28×10^{10}	13.913	<0.0001
	Error	67	5.41×10^{11}		
% HNA	Depth (D)	2	420.85	17.255	<0.0001
	Season	1	340.70	27.938	<0.0001
	(Se)				
	D x Se	2	12.32	0.505	0.6058
	Error	71	1560.44		

A posteriori Tukey-Kramer test

Bacterial abundance Surf-Oct >Int-Oct > Bot-Oct = Surf-Dec = Bot-Dec = Int-Dec

% HNA Depth: Intermediate = Surface > Bottom

Season: October > December

5.4.4 Relationship between TB, %HNA and environmental variables

Multiple linear regressions of bacterial abundances and %HNA distributions along the estuarine gradient were performed to determine the major factors affecting these two variables. The variance of bacterial abundance was explained at 81 % by the combination of temperature, salinity, DO, SPM, Chla and C:N ratio (r^2 adjusted = 0.807, $p < 0.0001$, root mean square error [RMSE] = 71494, $n = 85$). In addition, %HNA variance could be explained at 51 % by the combination of NH_4^+ , salinity, SPM and $\text{NO}_2^- + \text{NO}_3^-$ concentrations (r^2 adjusted = 0.514, $p < 0.0001$, RMSE = 3.899, $n = 87$). As previously observed with the Spearman rank correlation (Table 4), DIN appeared to be the main factor influencing the proportion of HNA cells in the bacterial population, with no significant influence of temperature, whereas distribution of TB appeared to be driven by multiple physical and chemical variables. In addition, Spearman rank correlation showed a negative relation between TB and NH_4^+ ($p < 0.01$) and a positive one between %HNA and NH_4^+ ($p < 0.05$); traducing the discrepancy between total abundance and population structure (Table 4).

Tableau V-4 Spearman rank correlation coefficients between bacterial abundances (cell mL^{-1}) and %HNA ratios and environmental variables. The number of pair values in each data set is 88. Values** are significant at a level of $p < 0.01$ whereas values* are significant at a level of $p < 0.05$.

Depth (m)	Temperature (°C)	Salinity	DO (mg L^{-1})	NH_4^+ (μM)	$\text{NO}_2^- + \text{NO}_3^-$ (μM)	SPM (mg L^{-1})	Chla ($\mu\text{g L}^{-1}$)	C/N ratio
-0.516**	0.166	-0.604**	0.428**	0.646**	-0.270*	0.310**	0.534**	-0.286**
-0.101	-0.200	-0.043	0.055	-0.215*	-0.406**	-0.205	0.006	-0.329**

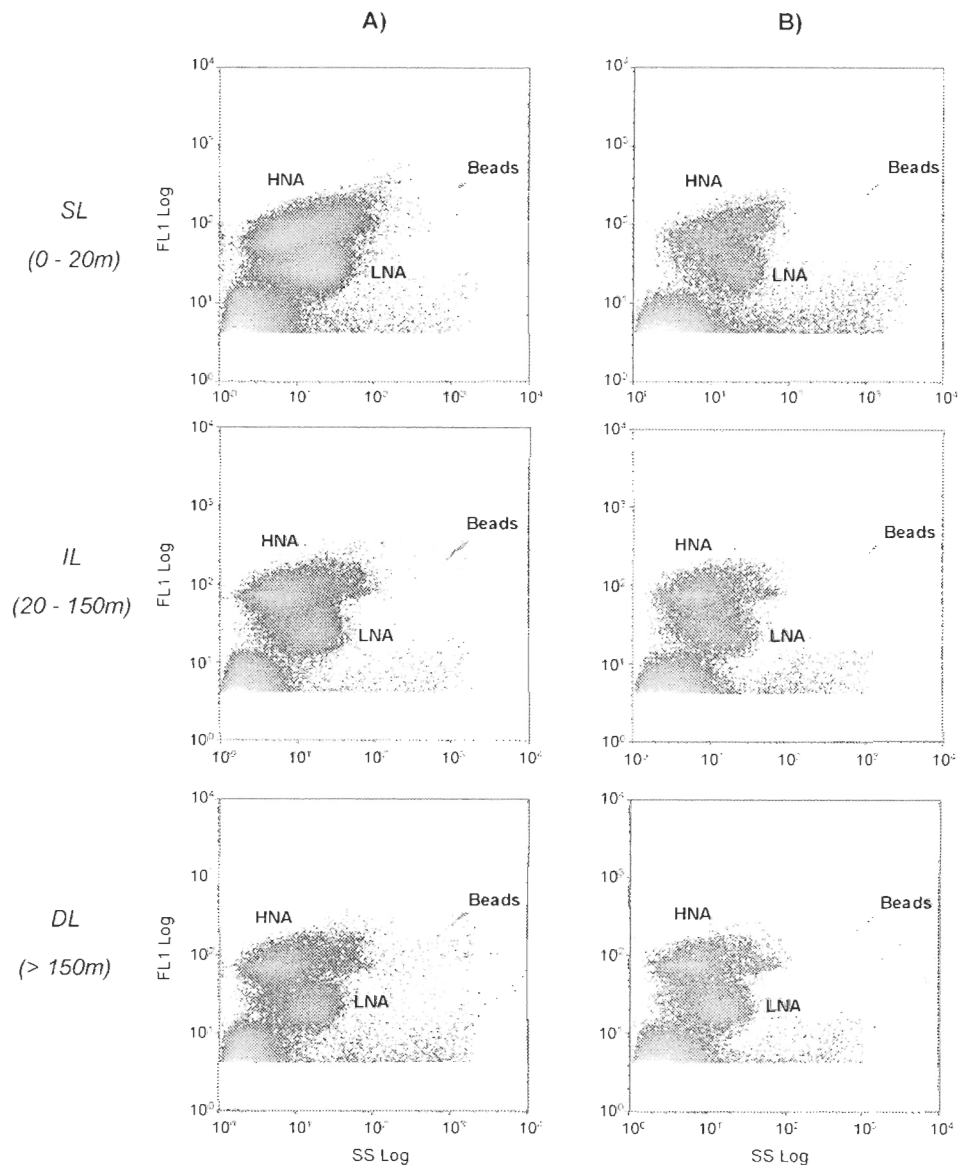


Figure V-3 Distribution of HNA and LNA cells at station 9 in the surface (SL), intermediate (IL) and deep (DL) layers of LSLE in (A) October and (B) December 2005. Bacteria were detected in a plot of green fluorescence recorded at 530 ± 30 nm (FL1) versus side angle light scatter (SSC) and were presented on logarithmic scales on the cytograms. Fluorescent beads were added as an internal standard to normalize cell fluorescence emission and light scatter values of each sample.

5.5 Discussion

In the context of current climate changes, one of the main challenges in microbial ecology is to understand how bacterial populations are intertwined with environmental variables in marine systems. Heterotrophic bacteria are responsible for the ultimate decomposition of organic matter, and for the production of regenerated nutrients in marine

waters. Sub-Arctic coastal environments, such as the St. Lawrence Estuary, are of specific interest since the presence of an ice cover during about one-third of the year slows down gas exchange at the air/water interface, reduces light penetration and consequently decreases photosynthesis while respiration of heterotrophs persists around the year. In addition, the extend of the ice cover during winter time was suggested to play a major role on nitrate replenishment of surface waters and, as a consequence, on the intensity of the phytoplankton spring bloom (Plourde & Therriault 2004). Since bacteria are the most abundant heterotrophic organisms in marine waters, they are active consumers of DO and nitrate throughout the water column. A recent study demonstrated that distribution and abundance of bacterial taxa in surface coastal waters were strongly influenced by abiotic and biotic factors and that their patterns could be highly predictable from environmental variables (Fuhrman et al. 2006). As modifications in abundance, activity and composition of bacterial assemblages may lead to important variations of biogeochemical processes throughout the water column (Rivkin & Legendre 2002), their variations during winter time need to be consider as important factors to accurately model the biogeochemical processes that take place in cold estuaries on a seasonal scale.

During this study, the ice-free (October 2005) and ice-covered (December 2005) periods were characterized by low Chla concentrations in the surface layer (*i.e.* between 0.11 and 0.64 $\mu\text{g l}^{-1}$). Despite these low Chla values, TB abundances recorded in late fall were in the same order of magnitude than those reported in the Gulf of St. Lawrence during the summer 1994 (Lovejoy et al. 2000). TB abundance and %HNA did not vary significantly in the USLE during the two sampling periods. TB values are in agreement with those previously reported in the upper part of the SLE (Painchaud & Therriault 1989). The USLE is a well mixed area mostly influenced by freshwater inputs coming from the St. Lawrence River. The absence of significant differences between October and December records suggest that the presence of the ice cover did not limit the growth of heterotrophic bacteria compartment where nutrients are abundant year around. In contrast, greater variations in the LSLE were observed with and without the presence of an ice cover. TB abundance was higher in late fall than in winter whereas the reverse relationship was observed for the %HNA. These results suggest that environmental conditions encountered

during the ice-covered period act differently on bacterial abundance than on population structure, in terms of HNA and LNA cells proportion within the whole population. During the ice-covered period, bacteria were homogenously distributed in the LSLE water column and persisted deep into the aphotic zone where they are assumed to play a dominant role in the organic matter cycling. These abundances observed in a cold northern estuary were in concordance with the large and relatively constant number of bacterial cells normally found in surface and deep ocean waters (*i.e.* 6.0×10^5 cell ml $^{-1}$ at 0 - 50 m deep and 3.3×10^5 cell ml $^{-1}$ at > 50 m depth) (Li et al. 2004), and were significantly lower in December than in October. Multiple linear regressions of bacterial abundance distribution along the estuarine gradient demonstrated that 81 % of the variance of TB abundances can be explained by the combination of temperature, salinity, DO, SPM, Chla and C:N ratio. These results support the hypothesis that the reduction of TB abundance in December could be related to the presence of an ice cover limiting the phytoplanktonic production of dissolved organic matter in surface waters and the sink of particulate organic matter toward deep water layers.

HNA and LNA bacterial subpopulations have been identified in various aquatic environments and have been used to characterize free pelagic communities (Li et al. 1995, Zubkov et al. 2001, Nishimura et al. 2005, Sherr et al. 2006). Both subpopulations were observed everywhere along the Laurentian Channel and the subpopulation signatures were similar to those previously observed in different aquatic environments (Gasol et al. 1999, Lebaron et al. 2001, Servais et al. 2003). Despite their similar FL1 and SSC signatures their relative contribution (%HNA) to the heterotrophic bacterial population was variable. Unfortunately, direct comparison with other seasons is impossible since no report of HNA and LNA cell distributions has been produced until now in the studied area. In the present study, lower percentages of HNA cells were monitored in the deep waters of the Estuary (Table 3). This observation is in agreement with Zubkov et al. (2001) who showed that the contribution of LNA bacteria to the total bacterioplankton activity in the surface mixed layer of the Celtic Sea did not exceed 15 %, but represented up to 30 % of total bacterial activity in deeper waters. For a long time, the proportion of HNA cells within the total bacterial population has been considered as an index of the relative growing activity of bacterial assemblages (Gasol et al. 1999) or of metabolically active cells (Lebaron et al.

2001, Servais et al. 2003). Nevertheless, recent studies tend to demonstrate that LNA cells could exhibit high growth-specific rates, especially the smallest ones, and that their specific activity could be major in some marine environments (Zubkov et al. 2001, Longnecker et al. 2005, Scharek & Latasa 2007). Interestingly, significant differences were observed between the two sampling periods featuring higher %HNA in October than in December. This variation could be explained at 51 % by the combination of NH_4^+ , salinity, SPM and $\text{NO}_2^- + \text{NO}_3^-$ concentrations, suggesting a greater role of nitrogen on HNA cells distribution than on TB distribution in the LSLE. The divergence between TB and %HNA variations is concordant with the existence of various bacterial communities within marine systems which may respond to an external biotic or abiotic forcing in many ways resulting in biomass and growth rate differences (White et al. 1991, Schafer et al. 2001, Benlloch et al. 2002, DeLong 2002, Bowman & McCuaig 2003, Giovannoni & Stingl 2005). In this study, TB abundances recorded in the whole water column under the ice cover were in the same order of magnitude than the one recorded in the deep water layer during the ice-free period suggesting that heterotrophic bacteria abundance remained relatively constant in winter despite the seasonal lower primary organic matter production and the low temperatures.

St. Lawrence Estuary data recorded in 2005 under fall and winter conditions clearly indicated that TB abundance was negatively correlated with depth, salinity C:N ratio ($p < 0.01$, Table 4) and $\text{NO}_2^- + \text{NO}_3^-$ ($p < 0.05$, Table 4) and positively correlated with DO, NH_4^+ , SPM and Chla ($p < 0.01$, Table 4), whereas %HNA was negatively correlated with $\text{NO}_2^- + \text{NO}_3^-$, C:N ratio ($p < 0.01$, Table 4) and NH_4^+ ($p < 0.05$, Table 4) without significant correlation with physical variables, DO, SPM and Chla. These observations confirm that TB and %HNA are not regulated by the same process and that the variation of total bacterial abundance is not sufficient to understand the progression of the bacterial compartment composition year around in our sub-Arctic Estuary. The availability of nitrogen, especially NH_4^+ , appeared to play an important and antagonistic role on the repartition of TB and HNA subgroup in the SLE. The positive correlation of NH_4^+ , SPM and Chla (proxy of primary production) with TB confirms that ammonium is a crucial nitrogen compound for primary production, and as a consequence for bacterial production. Nitrogen limitation was proposed to explain the end of HNA cell growth phase and the

decline of TB after a phytoplankton bloom (Wetzel & Wheeler 2004). The negative relationship observed between HNA and DIN during our study is in disagreement with this finding and could be explained by the fact that even if bacteria account for roughly 40 % of the total uptake of inorganic N in the water column, they also contribute to ammonium regeneration in marine waters (Kirchman 2000). The absence of relationship between %HNA and Chla during the two sampling periods suggests that in low primary production conditions where heterotrophic organisms are dominant, LNA cells may be favored compared to HNA cells as it was demonstrated in nutrient limited waters by Zubkov *et al.* (2001). This result is contrasting with the correlation observed between TB and Chla and confirms that total bacteria, HNA cells, and LNA cells respond differently to the composition of the phytoplankton stocks and that abundance and proportion of HNA bacteria may be a useful indicator of relative bacterial activity only in high phytoplankton biomass area. We caution that cell mortality due to biotic factors (e.g. predation by heterotrophic flagellates, viral infection) may play a role in the observed distribution of TB, HNA and LNA cells during winter and need to be investigated (Gasol *et al.* 1999, Lovejoy *et al.* 2000, Sherr *et al.* 2006).

Our results clearly demonstrate that the distribution of bacterioplankton in the SLE during fall and winter was independent of the water column temperature and stratification in the LSLE and that TB abundances were homogeneously distributed throughout the water column during the ice-covered period. TB abundances were similar to the one recorded in most oceanic systems and were mostly affected by the combination of temperature, salinity, DO, SPM, Chla and C:N ratio. %HNA and TB abundance varied in the opposite way in response to variations of DIN concentrations in the water column during our sampling periods characterized by low Chla concentrations. Even if the ecological significance of HNA and LNA subgroups is still a controversial matter the proportion of HNA and LNA cells within the total heterotrophic bacteria could represent an interesting tool for distinguishing the progression of bacterial assemblages within the total population in cold sub-Arctic estuaries. %HNA and TB variations in the SLE during fall and winter indicate that bacterial communities were mostly determined by nitrogen availability and phytoplankton stocks and suggest that LNA cells may be favored in low productive waters

characterized by low phytoplankton concentrations. As a consequence, the presence of an ice cover limiting light penetration and primary production during three to four months in the St. Lawrence Estuary seems to play a greater role on bacterial diversity than on bacterial abundance. Further investigations, particularly during exponential phytoplankton blooms, will be conducted to confirm these findings. Further developments are presently under progress to highlight the diversity of the dominant bacteria throughout the water column of the Estuary in order to better understand the relationship between the diversity of the bacterial community and environmental variables. These data are crucial to determine the functional role of these communities and to adequately model their impact on biogeochemical cycles in sub-Arctic estuaries in the light of increasing loads of nutrients by anthropogenic activities and climate warming.

5.6 Acknowledgement

This research was financially supported by ISMER, by the Natural Sciences and Engineering Council of Canada (NSERC) through the Canada Research Chair in Ecotoxicology, and ship time awarded to Drs E.P. and J.-P. Gagné. This paper is a contribution to the Quebec Ocean network. The authors wish to thank the captain and crew of the *R/V Coriolis II* and *CCGS Amundsen* for their assistance and enthusiasm and C. Belzile for his assistance during flow cytometry analyses. A special thank is addressed to J.-C. Therriault and M. Chénier for their attentive review of this paper and to the anonymous reviewers for their attention and comments.

5.7 References

- Azam F (1998) Microbial control of oceanic carbon flux: the plot thickens. *Science* 280:694-696
- Benlloch S, Lopez-Lopez A, Casamayor EO, Ovreas L, Goddard V, Daae FL, Smerdon G, Massana R, Joint I, Thingstad F, Pedros-Alio C, Rodriguez-Valera F (2002) Prokaryotic genetic diversity throughout the salinity gradient of a coastal solar saltern. *Environ Microbiol* 4:349-360

- Bowman JP, McCuaig RD (2003) Biodiversity, community structural shifts, and biogeography of prokaryotes within Antarctic continental shelf sediment. *Appl Environ Microbiol* 69:2463-2483
- Cook RD, Weisberg S (1982) Residuals and Influence. In: Hall Ca (ed) Regression, New York
- Cotner JB, Biddanda BA (2002) Small players, large role: microbial influence on biogeochemical processes in pelagic aquatic ecosystems. *Ecosystems* 5:105-121
- Del Giorgio PA, Duarte CM (2002) Respiration in the open ocean. *Nature* 420:379-384
- DeLong EF (2002) Microbial population genomics and ecology. *Curr Opin Microbiol* 5:520-524
- El-Sabh MI (1979) The lower St. Lawrence Estuary as a physical oceanographic system. *Naturaliste can.* 106:55-73
- El-Sabh MI, Silverberg N (1990) The St. Lawrence Estuary: introduction. In: El-Sabh MI, Silverberg N (eds) *Oceanography of a Large-scale Estuarine System*. Springer-Verlag, New York, p 1-9
- Findlay S, Pace ML, Lints D, Cole JJ, Caraco NF, Peierls B (1991) Weak coupling of bacterial and algal production in a heterotrophic ecosystem: The Hudson River Estuary. *Limnol Oceanogr* 36:268-278
- Fuhrman JA, Hewson I, Schwalbach MS, Steele JA, Brown MV, Naeem S (2006) Annually reoccurring bacterial communities are predictable from ocean conditions. *Proc Natl Acad Sci U S A* 103:13104-13109
- Gasol JM, Del Giorgio PA, Duarte CM (1997) Biomass distribution in marine planktonic communities. *Limnol Oceanogr* 42:1353-1363
- Gasol JM, Zweifel UL, Peters F, Fuhrman JA, Hagstrom A (1999) Significance of size and nucleic acid content heterogeneity as measured by flow cytometry in natural planktonic bacteria. *Appl Environ Microbiol* 65:4475-4483
- Gilbert D, Sundby B, Gobeil C, Mucci A, Tremblay GH (2005) A seventy-two-year record of diminishing deep-water oxygen in the St. Lawrence estuary: The northwest Atlantic connection. *Limnol Oceanogr* 50:1654-1666
- Giovannoni SJ, Stingl U (2005) Molecular diversity and ecology of microbial plankton. *Nature* 437:343-348
- Jeffrey SW, Mantoura RFC, Wright SW (1997) *Phytoplankton pigments in oceanography: guidelines to modern methods*, Vol 10. UNESCO Publishing, Paris

Kirchman DL (2000) Uptake and regeneration of inorganic nutrients by marine heterotrophic bacteria. In: Kirchman DL (ed) *Microbial Ecology of the Oceans*. Wiley-Liss, Inc., New York, p 261-288

Koutitonsky VG, Bugden GL (1991) The physical oceanography of the Gulf of St. Lawrence: a review with emphasis on the synoptic variability of the motion. In: Therriault J-C (ed) *The Gulf of St. Lawrence: Small Ocean or Big Estuary?*, Vol 113. Canadian Special Publication of Fisheries and Aquatic Sciences, p 57-90

Lebaron P, Servais P, Agogue H, Courties C, Joux F (2001) Does the high nucleic acid content of individual bacterial cells allow us to discriminate between active cells and inactive cells in aquatic systems? *Appl Environ Microbiol* 67:1775-1782

Legendre L, Rassoulzadegan F (1995) Plankton and nutrient dynamics in marine waters. *Ophelia* 41:153-172

Li WKW, Head EJH, Glen Harrison W (2004) Macroecological limits of heterotrophic bacterial abundance in the ocean. *Deep Sea Res Part I Oceanogr Res Pap* 51:1529-1540

Li WKW, Jellet JF, Dickie PM (1995) DNA distributions in planktonic bacteria stained with TOTO or TO-PRO. *Limnol Oceanogr* 40:1485-1495

Longnecker K, Sherr BF, Sherr EB (2005) Activity and phylogenetic diversity of bacterial cells with high and low nucleic acid content and electron transport system activity in an upwelling ecosystem. *Appl Environ Microbiol* 71:7737-7749

Longnecker K, Sherr BF, Sherr EB (2006) Variation in cell-specific rates of leucine and thymidine incorporation by marine bacteria with high and low nucleic acid content off the Oregon coast. *Aquat Microb Ecol* 43:113-125

Lovejoy C, Legendre L, Therriault J-C, Tremblay J-E, Klein B, Ingram RG (2000) Growth and distribution of marine bacteria in relation to nanoplankton community structure. *Deep Sea Res Part II Top Stud Oceanogr* 47:461-487

Lucotte M, D'Anglejan B (1986) Seasonal control of the Saint-Lawrence maximum turbidity zone by tidal-flat sedimentation. *Estuaries* 9:84-94

Montgomery DC (1991) *Design and analysis of experiments*, John Wiley & Sons, Toronto
 Morán XAG, Bode A, Suárez LÁ, Nogueira E (2007) Assessing the relevance of nucleic acid content as an indicator of marine bacterial activity. *Aquat Microb Ecol* 46:141-152

Nishimura Y, Kim C, Nagata T (2005) Vertical and seasonal variations of bacterioplankton subgroups with different nucleic acid contents: possible regulation by phosphorus. *Appl Environ Microbiol* 71:5828-5836

- Painchaud J, Therriault J (1989) Relationships between bacteria, phytoplankton and particulate organic carbon in the upper St. Lawrence Estuary. *Mar Ecol Prog Ser* 56:301-311
- Painchaud J, Therriault J, Legendre L (1995) Assessment of salinity-related mortality of freshwater bacteria in the Saint Lawrence Estuary. *Appl Environ Microbiol* 61:205-208
- Plourde J, Therriault J-C (2004) Climate variability and vertical advection of nitrates in the Gulf of St. Lawrence, Canada. *Mar Ecol Prog Ser* 279:33-43
- Poulin P, Pelletier E (2007) Determination of ammonium using a microplate-based fluorometric technique. *Talanta* 71:1500-1506
- Quinn GP, Keough MJ (2002) Experimental design and data analysis for biologists, Cambridge University Press, Cambridge
- Revilla M, Iriarte A, Madariaga I, Orive E (2000) Bacterial and phytoplankton dynamics along a trophic gradient in a shallow temperate estuary. *Estuar, coast shelf sci* 50:297-313
- Rivkin RB, Legendre L (2002) Roles of food web and heterotrophic microbial processes in upper ocean biogeochemistry: Global patterns and processes. *Ecol Res* 17:151-159
- Roy S, Chanut J-P, Gosselin M, Sime-Ngando T (1996) Characterization of phytoplankton communities in the Lower St. Lawrence Estuary using HPLC-detected pigments and cell microscopy. *Mar Ecol Prog Ser* 142:55-73
- Saucier FJ, Roy F, Gilbert D, Pellerin P, Ritchie H (2003) Modeling the formation and circulation processes of water masses and sea ice in the Gulf of St. Lawrence, Canada. *J Geophys Res C* 108:3269-3289
- Schafer H, Bernard L, Courties C, Lebaron P, Servais P, Pukall R, Stackebrandt E, Troussellier M, Guindulain T, Vives-Rego J, Muyzer G (2001) Microbial community dynamics in Mediterranean nutrient-enriched seawater mesocosms: changes in the genetic diversity of bacterial populations. *FEMS Microbiol Ecol* 34:243-253
- Scharek R, Latasa M (2007) Growth, grazing and carbon flux of high and low nucleic acid bacteria differ in surface and deep chlorophyll maximum layers in the NW Mediterranean Sea. *Aquat Microb Ecol* 46:153-161
- Servais P, Casamayor EO, Courties C, Catala P, Parthuisot N, Lebaron P (2003) Activity and diversity of bacterial cells with high and low nucleic acid content. *Aquat Microb Ecol* 33:41-51
- Sherr EB, Sherr BF, Longnecker K (2006) Distribution of bacterial abundance and cell-specific nucleic acid content in the Northeast Pacific Ocean. *Deep Sea Res Part I Oceanogr Res Pap* 53:713-725

- Siron R, Pelletier E, Delille D, Brochu C (1993) Réponse de la flore bactérienne de l'estuaire du Saint-Laurent à un déversement éventuel de pétrole. *Water Pollution Research Journal of Canada* 28:385-414
- Sokal RR, Rohlf FJ (1995) Biometry: the principles and practice of statistics in biological research, New York
- Strickland JDH, Parsons TR (1968) A practical handbook of seawater analysis. *Fish Res Bd Can Bull* 167
- Wetz MS, Wheeler PA (2004) Response of bacteria to simulated upwelling phytoplankton blooms. *Mar Ecol Prog Ser* 272:49-57
- White PA, Kalff J, Rasmussen JB, Gasol JM (1991) The effect of temperature and algal biomass on bacterial production and specific growth rate in freshwater and marine habitats. *Microl Ecol* 21:99-118
- Zapata M, Rodriguez F, Garrido JL (2000) Separation of chlorophylls and carotenoids from marine phytoplankton: a new HPLC method using a reversed phase C8 column and pyridine-containing mobile phases. *Mar Ecol Prog Ser* 195:29-45
- Zar JH (1999) Biostatistical analysis, Prentice-Hall, Inc., Englewood Cliffs, New Jersey
- Zubkov MV, Fuchs BM, Burkill PH, Amann R (2001) Comparison of cellular and biomass specific activities of dominant bacterioplankton groups in stratified waters of the Celtic Sea. *Appl Environ Microbiol* 67:5210-5218

CHAPITRE VI

Seasonal nutrient fluxes variability of northern salt marshes: Examples from the lower St. Lawrence Estuary

Patrick Poulin, Émilien Pelletier, Vladimir G. Koutitonski and Urs Neumeier

Submit to Estuaries and Coasts

6.1 Abstract

This study presents the tidal exchange of ammonium, nitrite + nitrate, phosphate and silicate between two St. Laurence salt marshes and adjacent estuarine waters. Marshes nutrient fluxes were evaluated for Pointe-au-Père and Pointe-aux-Épinettes salt marshes, both situated on the south shore of the lower St-Lawrence Estuary in Rimouski area (Québec, Canada). Using field nutrients samples, high precision bathymetric records and a hydrodynamic numerical model (MIKE21-NHD) forced with predicted tides, nutrients fluxes were estimated through salt marshes outlet cross-sections at four different periods of the year 2004 (March, May, July and November). Calculated marshes nutrient fluxes are discussed in relation with stream inputs, biotic and abiotical marsh processes and the incidence of sea ice cover. In both marshes, the results show the occurrence of year-round and seaward NH_4^+ fluxes and landward $\text{NO}_2^- + \text{NO}_3^-$ fluxes (ranging from 9.39 to 30.48 mg N d⁻¹ m⁻² and from -32.07 to -9.59 mg N d⁻¹ m⁻², respectively) as well as variable PO_4^{3-} and Si(OH)_4 fluxes (ranging from -3.73 to 6.34 mg P d⁻¹ m⁻² and from -29.19 to 21.91 mg Si d⁻¹ m⁻², respectively). These results suggest that $\text{NO}_2^- + \text{NO}_3^-$ input to marsh can be a significant source of NH_4^+ through dissimilatory nitrate reduction to ammonium (DNRA). This NH_4^+ , accumulating in marsh sediment rather than being removed through coupled nitrification–denitrification or biological assimilation, is exported toward estuarine waters. From average P and Si tidal fluxes analysis, both salt marshes act as a sink during high productivity period (May and July) and as a source, supplying estuarine water during low productivity period (November and March).

6.2 Introduction

Salt marshes are considered as major features of macro-tidal estuaries. They are recognised as dynamic and complex environments that perform many functions valued by human coastal communities. They provide critical functions such as coastal defence against large storms, wildlife conservation, organic material burying and nutrient cycling (Boorman, 1999). Recently, this high recognition and appreciation of the salt marsh importance aroused the interest of the scientific community because there is a need to understand general mechanisms governing salt marsh formation and shrinking. The health and the stability of salt marshes are linked to a delicate balance between deposition and erosion of sediment. This balance may come under threat due to climate change, concomitant to sea-level rise and storm-frequency increase, and coastal urbanisation (Fagherazzi *et al.*, 2004). Like in other parts of the world, northern salt marshes located in St. Lawrence Estuary are subjected to erosion due to direct and indirect anthropogenic pressures (Dionne, 1986; Dionne, 2004). Exposed to freezing 4 to 5 months each year, littoral sea ice action of St. Lawrence salt marshes (e.g.; Allard and Champagne, 1980; Dionne, 1968; Dionne, 1989) and sediment dynamics (e.g.; Sérodes and Dubé, 1983; Drapeau, 1992; Dionne 2004) were extensively investigated, but our understanding of the dynamic of northern marsh environments is still incomplete, especially during winter season when sea ice covers the littoral area. There is still a lack of knowledge about biogeochemical processes in these icy environments, especially concerning the nitrogen (N), phosphorus (P) and silica (Si) cycles. Nutrient turnover is cause of concern as concentrations of dissolved N and P have increased substantially in many rivers world-wide over the last decades, mostly as a consequence of the intensive use of fertilizers and detergents (Rabouille *et al.*, 2001). These increases have occasionally been held responsible for increased phytoplankton growth and the development of toxic algal blooms in estuaries and neighbouring coastal regions (Riegman *et al.*, 1992). Therefore, it is essential to determine rates of nutrients exchange in northern salt marshes as a first step toward predicting long term behaviour of cold coastal ecosystems under the expected scenario of a global coastal eutrophication (Jickells, 2005). The complex question of nutrient cycling needs to be addressed in the St. Lawrence River system since eutrophication has been

shown to be partially responsible of hypoxia development in the Lower St. Lawrence Estuary bottom layer (Thibodeau *et al.*, 2006).

Since early seventies, nutrients exchange between coastal and marine environments attracted the interest for many researchers (Odum and de la Cruz, 1967; Heinle and Flemer, 1976. Valiela *et al.*, 1978; Dame *et al.*, 1991; de la Lanza Espino and Medina, 1993; Baldwin and Mitchell, 2000; Valiela *et al.*, 2000; Struyf *et al.*, 2005; Gardner and Kierfve, 2006). While contributing to improve our understanding of coastal dynamics, some of these studies have also been subject of discussion. Nutrient flux measurement in coastal zone remains a difficult task because material exchanges in intertidal areas are regulated by numerous environmental factors interacting at different time and space scales (Fan and Jin, 1989). *In situ* or laboratory sediment incubations using isotopic tracers or microelectrode techniques may provide interesting information about local nutrient fluxes, however the high spatial heterogeneity of salt marshes restrains the significance of punctual measurements and consequently, the validity of any extrapolation to the whole marsh. Despite the large assortment of factors defining coastal environment dynamics, hydrodynamic simulation combined with geochemical field measurements at some key locations remains an efficient tool to characterize and furthermore compare littoral ecosystems.

In an attempt to improve our understanding of biogeochemical processes of northern salt marshes with a long wintering period and estimate their contribution to nutrients cycling in adjacent coastal waters, a one-year sampling program has been conducted in two nearby salt marshes exposed to similar hydrodynamic conditions, but submitted to different anthropogenic pressures. This study describes the exchange of ammonium (NH_4^+), nitrite + nitrate ($\text{NO}_2^- + \text{NO}_3^-$), phosphate (PO_4^{3-}), and silicate (Si(OH)_4) between two St. Lawrence salt marshes and adjacent estuarine waters. The seasonal nutrient fluxes were estimated for a low impacted site (Pointe-au-Père salt marsh) and for a pristine site (Pointe-aux-Épinettes salt marsh) by using field nutrients samples, high precision bathymetric records and a hydrodynamic numerical model. The calculated seasonal nutrient fluxes were used (1) to define the functional role of salt marsh environment in term of nutrient buffering capacity

and (2) to determine whether northern salt marshes can act as a sink or as a source of nutrients for adjacent estuarine waters.

6.3 Site description

Pointe-aux-Épinettes (PAE) and Pointe-au-Père (PAP) salt marshes are both located on the south shore of St. Lawrence Estuary near Rimouski (Québec, Canada) (Fig. 1). The St. Lawrence Estuary is a long funnel-shaped tidal environment (400 km), forged by late Holocene glacial events, reaching 70-km width and 300-m depth in its outer portion. The large dimension of this stratified estuary induces typically marine hydrodynamic conditions in the Rimouski area. Coastal environments are strongly affected by large-scale physical forcing such as tides, winds, and waves reaching up to 4 m during exceptional storms (Drapeau, 1992). Semi-diurnal tidal movement induced up-welling occurs near the mouth of the Saguenay Fjord and brings nutrient-rich bottom waters to the surface. The mean tidal range is 3.3 m and the mean spring tidal range is 4.8 m. The St. Lawrence ecosystem is subject to important seasonal variations affecting estuarine water temperature, salinity, nutrient concentrations and phytoplanktonic activity. One of the main features is the sea ice formation that begins in December and persists until April (Saucier *et al.*, 2003). Floating ice can erode the intertidal area by ice-scouring and ice-rafting, but it also contributes to marsh accretion by importing sediment with a large grain-size range. Floating ice reduces wave energy and land-fast ice protects marshes from both tidal currents and waves (Drapeau, 1992). By limiting atmosphere/sediment heat exchanges, sea ice reduces the sediment desiccation and stabilizes underneath water temperature slightly over the freezing point, allowing the maintenance of biological processes.

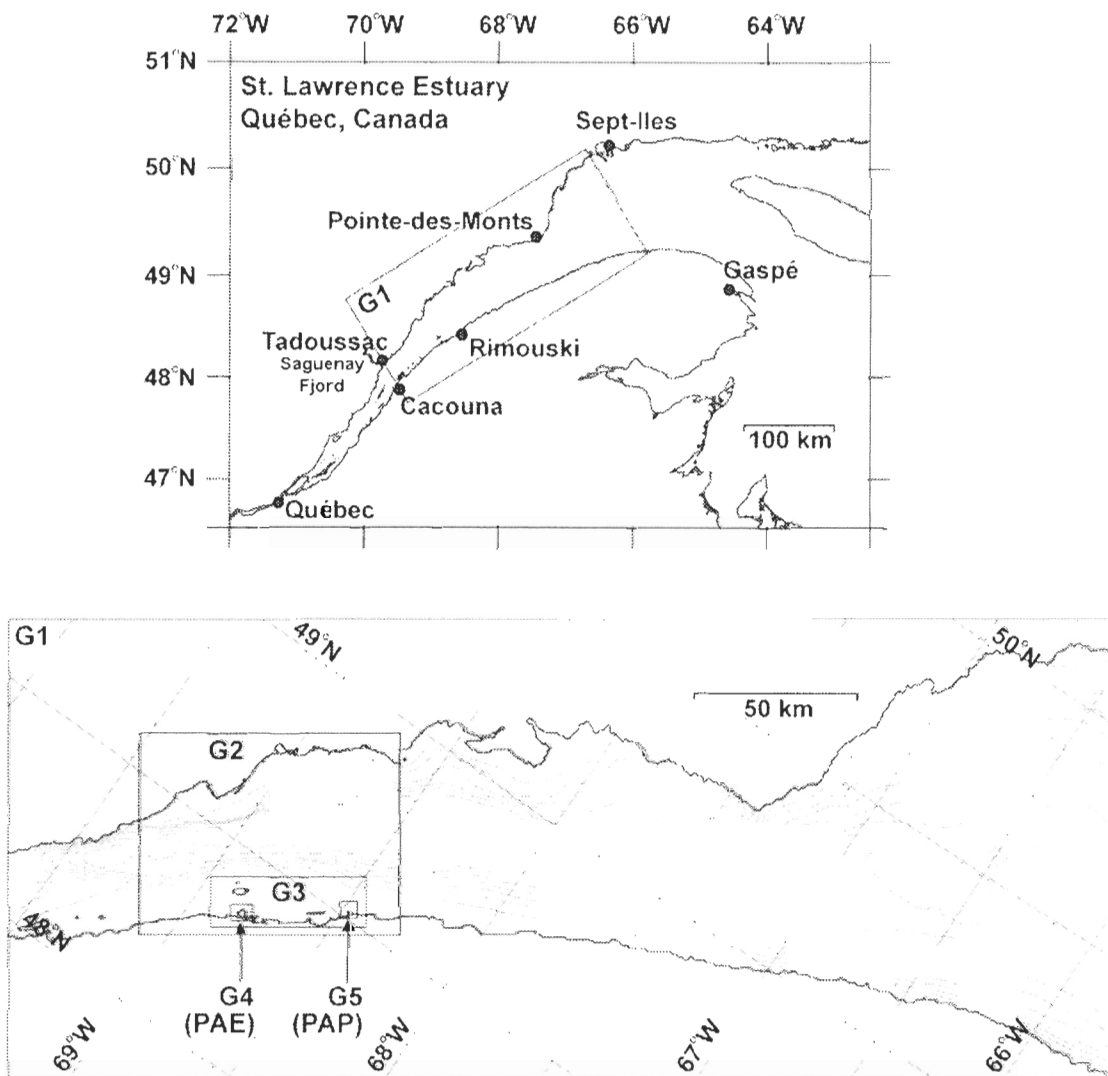


Figure VI-1 The Lower St. Lawrence estuary (G1) nested grid set-up used to compute tidal volume fluxes at the seaward boundaries of each Pointe-aux-Épinettes (PAE; G4) and Pointe-au-Père (PAP; G5) marshes, with intermediate grids G2 and G3. On grid G1, contour interval is 50 m.

The PAE salt marsh ($48^{\circ} 21.40'N$, $68^{\circ} 46.75'W$) is located in the Bic Provincial Park, a protected area created in October 1984. The marsh is situated at the far end of a protected bay (Anse à l'Orignal) between two steep hills composed of Cambrian claystone/sandstone. The marsh is dominated by areas with homogenous emergent macrophyte communities (*Spartina alterniflora* in the lower part, *Spartina patens* and other halophytes in the upper part) surrounded by shallow vegetation-free creeks. The marsh

receives freshwater runoff by two small streams that serve also as main drainage channels (A, B, Fig. 2a). Since its 1.7-km² watershed is completely within the Park and mainly forested, the PAE marsh can be considered as a pristine environment for the aim of this study.

The PAP salt marsh (48° 30.45'N, 68° 28.30'W) is part of the Pointe-au-Père National Wildlife area, a protected site under the responsibility of the Canadian Wildlife Service since September 2002. It is confined in a shallow elongated basin parallel to the main St. Lawrence estuary axis and sheltered from wave actions by a low, partially submerged ridge made of Palaeozoic claystone. The lower marsh is also dominated by *Spartina alterniflora* growing between numerous three-quarter buried boulders while the higher marsh presents a more diversified halophyte community. The upper marsh is nearly a flat platform which terminates seaward with a steep slope or a micro-cliff of 0.5 m. Unlike PAE, the PAP coastline is formed by roads and residential areas. Located in a partly urbanised watershed, this marsh receives nutrient inputs from both agricultural and urban runoff. These freshwater supplies enter the marsh by two small rivers (E and G, Fig. 2) as well as by three pluvial and urban sewage overflow drains, (C, D, and F, Fig. 2). Erosion structures, such as micro-cliff, micro-ravine and high marsh collapse, occur along drainage channel edges. From our point of view, this marsh can be considered as a low impacted environment.

Located 29 km apart, the two studied salt marshes are affected by similar natural forcing and large-scale processes. As their relative elevation toward the mean sea level is similar, we could assume that both studied areas are comparable in term of their developmental stage (late Holocene deposit; Dionne, 2004). However, the PAP marsh is more exposed to wave action than the PAE marsh. The sedimentary characteristics of both marshes are comparable, featuring three superposed facies: 1) basal post-glacial silty-clay deposited in the Goldthwait Sea, which is exposed on mud flats; 2) low-marsh sandy-silt locally enriched in plant detritus; and 3) high-marsh facies with fine sediments that are rich in organic matter and characterised by the presence of a reduce clayey rhizosphere composed of macrophyte roots and stalks (Dionne, 2004). Ice-raftered boulders and cobbles

are sprinkled over the whole intertidal area, but are especially concentrated at the outer edge of the marshes. The upper marshes are characterised by numerous scour-pits (called *marelles* in French) that are 10-30 cm deep and 1-5 m large. They were formed by a combination of ice-scouring and biogeochemical processes and they remain stable over several years (Gauthier and Goudreau, 1983).

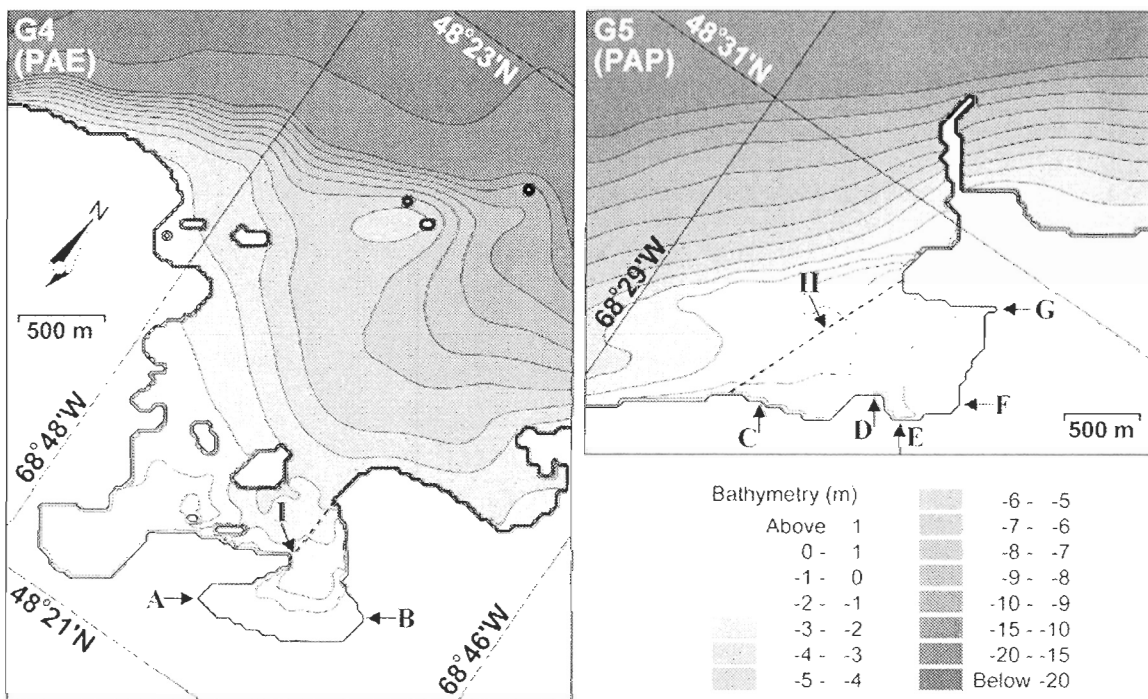


Figure VI-2 The G4 and G5 grids enclosing the Pointe-aux-Épinettes (PAE) and Pointe-au-Père (PAP) marshes. A, B, C, D, E, F and G represent sampled tributaries, I and II represent marshes outlet sampling sites and the dashed lines represent the virtual limit between marshes and estuary used for flux calculations. Bathymetries are in meter and the zero contour is the mean sea level. Stations I and II are both 0.5 m below the map zero. The lower marsh is located between -0.5 and + 1.0 m and upper marsh is landward of the 1.0 m contour line. Bathymetry of the study areas comes from high resolution field survey while bathymetry from deeper area is taken from marine chart.

6.4 Material and Methods

6.4.1 Water sampling

Both studied salt marshes were regularly sampled from June 2003 to November 2004. The first sampling campaign was carried out weekly from 16 June 2003 to 16 June 2004. Water samples (6 L) were collected at low tide at the mouth of every natural and man-made tributaries (Stations A, B, C, D, E, F, G) as well as at station I and II, located at the outer marsh limit of PAE and PAP salt marshes, respectively (Fig. 2). These last stations were both located at the deepest part of the drainage channels, where water fluxes are the highest. Sampling was carried out on both marshes the same day to facilitate further comparisons between studied areas.

The second sampling campaign was conducted seasonally in March, May, July, and November 2004. Water samples (6 L) were taken hourly through a complete tidal cycle (12 h) at stations I and II. Seasonal sampling was carried out under favourable meteorological conditions, (wind < 5 km h⁻¹, no rain or snow) on two consecutive days. Using a moored light boat, the shallow well-mixed water column was sampled just under surface for 12 consecutive hours. Water samples were collected in triplicate within 10 minutes to determine nutrient concentrations variability. A graduated perch and a YSI temperature, salinity, dissolved oxygen multi-probe were used to measure tide level and *in situ* physical and chemical properties. During winter time (March 2004 sampling), holes were drilled through the sea ice cover (30-35 cm) to sample the water column beneath the ice. Marshes sites were found frozen only during March 2004 sampling.

All samples were collected in pre-cleaned glass and polypropylene bottles. Samples for dissolved nutrients determination (PO_4^{3-} , $\text{NO}_2^- + \text{NO}_3^-$, and $\text{Si}(\text{OH})_4$) were filtered on 0.22 µm nitrocellulose membrane and kept frozen (-80 °C) until analysis. Samples for NH_4^+ determination were kept on an ice bed and analysed the same day. Water samples for Chlorophyll-*a* (Chl-*a*) determination were filtered in the field on 25 mm diameter Millipore GF/F glass-fiber filters, then stored in the dark at -80 °C until analysis.

6.4.2 Flow measurements, water and nutrients fluxes calculations

During the first sampling series, tributary water velocity was measured using a digital impeller flow meter (#GO2030R, General Oceanic). Stream water fluxes were calculated by multiplying the current velocity by the stream cross-section area at measurement location, while nutrient fluxes were calculated by multiplying water flux by measured nutrient concentration. Monthly averages were computed from the weekly measurements of nutrient and fresh water fluxes.

For the second sampling series, preliminary tests in fall 2003 showed practical difficulties in using flow meters to measure current speed and direction at the outer marsh limit. To offset the uncertainty generated by important tidal current instability and lateral variability, water fluxes through the outlet cross sections of both marshes were computed from hydrodynamic simulations using the MIKE21-NHD numerical model (Abbott *et al.*, 1981), a commercially available model that is commonly used for coastal studies. This model is a vertically integrated finite difference model, calculating elevations and currents at each computational grid cell of a rectangular domain. One of the useful feature of the MIKE21-NHD model is that it allows shallows cells to dry during ebbing tides. For the present study, a nested-grid approach was used to scale down tidal boundary conditions for the marsh grids from a much larger tidal model of the lower St. Lawrence Estuary. The nested-grid approach (NHD module) provides the capability to compute regional large grid and local fine grid flow fields in a single model setup and simulation. In this case, the nested set up starts with a 390×200 grid G1 of the Lower St. Lawrence Estuary with a cell dimension of 810 m (Fig. 1). A second 277×211 grid G2 is then nested in G1 with a cell dimension of 270 m, a third 496×157 grid G3 is nested in G2 with a cell dimension of 90 m, and finally the marshes grids G4 and G5 are nested in the G3 grid, both with cell dimensions of 30 m. The bathymetric features of the Lower St. Lawrence Estuary (G1) and intermediate (G2 and G3) grids were extracted from Canadian Hydrographic Service maps. The bathymetric characteristics of the PAE and PAP marshes grids (G4 and G5) were interpolated from high resolution bathymetric surveys produced in the framework of this study (Fig. 2). A Leica total station TC 605 was used for mapping intertidal and supratidal

areas, whereas a Raytheon sonar DE-719C (208 kHz) and a Trimble DGPS NT-300 installed on a light boat were used for mapping subtidal areas of both marshes systems.

The large G1 grid was forced by tidal predictions interpolated between Cacouna on the south shore and Tadoussac on the north at its upstream open boundary and by interpolated tidal predictions between Sept-Iles on the north shore and Ste-Anne-des Monts on the south shore at its downstream open boundary. Tidal forcing along both open boundaries was obtained by interpolating results from harmonic analysis of hourly sea levels recorded at the four corner stations by the Canadian Hydrographic Service. More details about the set up can be found in a similar MIKE21 nested set-up used by Koutitonsky and Gidas (1996) to study the dilution of urban waste waters discharged in the coastal zone some 3 km southwest of the PAP marsh. The numerical simulation outputs of sea levels and currents were computed at each hour in each cell of the G4 and G5 grids as well as water volume exchanges between salt marshes and the estuary (across the dashed lines shown on Fig. 2). An example of sea level and current time series produced by the numerical simulation is shown in Fig. 3.

Nutrients fluxes between St. Lawrence Estuary and studied marsh ecosystems (Outlet Flux) were defined as:

$$\text{Outlet Flux} = (\text{Marsh Flux} \cdot \chi) + \text{Watershed Flux} \quad (1)$$

Where Marsh Flux ($\text{mg d}^{-1} \text{m}^{-2}$) is nutrients uptake and release at the marsh sediment/water interface, Watershed Flux (kg d^{-1}) is the tributaries nutrients inputs and χ the flooded marsh area (m^2). Nutrients exchanges through marsh cross sections (Outlet Flux; kg d^{-1}) were calculated using the following equations, considering semi-diurnal tide cycling:

$$\alpha = \sum_{f1}^{f2} (\bar{Q} \cdot T) \cdot C \quad (2)$$

$$\beta = \sum_{e1}^{e2} (\bar{Q} \cdot T) \cdot C \quad (3)$$

$$\text{Outlet Flux} = 2(\beta - \alpha) \quad (4)$$

Where α is the amount nutrient in flooding tide (kg), β is the nutrient amount in ebb tide, $f1$ and $f2$ are the first and last sampling times during the flooding tide, $e1$ and $e2$ are the first and last sampling times during the ebb tide, Q is the tidal water flux, T is the time interval

between two samplings and C is the nutrient concentration. Negative nutrient marsh fluxes indicate marsh uptake whereas positive fluxes indicate a marsh release.

Pearson correlations were performed to assess the relationship between pairs of variables considering correlation significance at $p < 0.05$. A One-Way Analysis of Variance (ANOVA) was performed to test if there is a significant difference between measured seasonal fluxes within studied marshes as well as between marshes. To isolate groups that differed from the others, a Tukey post-hoc test was performed. When ANOVA assumptions were not respected, a Kruskal-Wallis One-Way Analysis of Variance on Ranks was performed followed by a Dunn's post-hoc test. Differences between groups were considered significant at the $p < 0.05$ level. Statistical computations were performed with Sigma Stat® version 3.11.

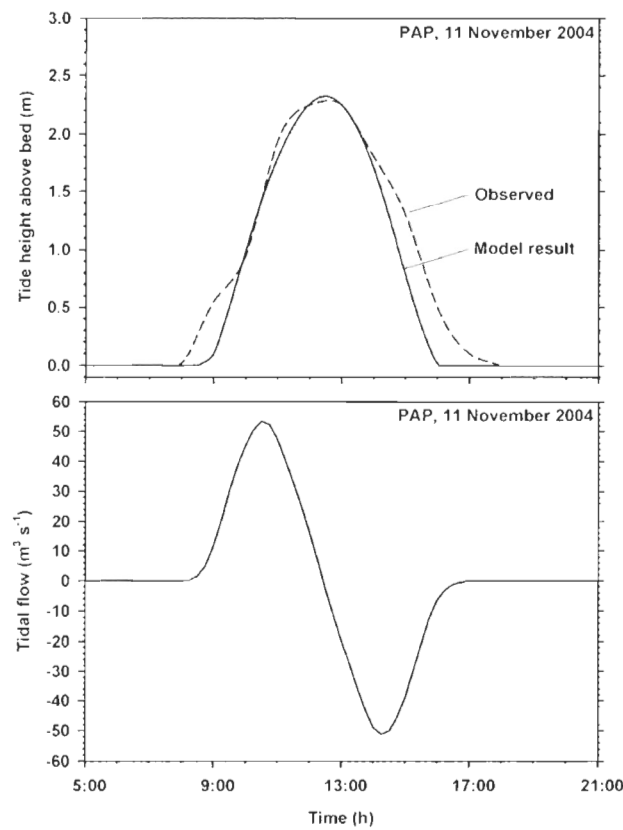


Figure VI-3 Typical example of tide cycle (tide height above marsh surface at site II) with associate temporal patterns of modeled tide level (top) and flow (bottom). Dashed line stand for field observation and solid line for numerical simulation. The asymmetry of observed tide curve is induced by wind effects, barometric pressure changes, marsh roughness (small scale irregularities) and sediment porosity.

6.4.3 Ice cores collection and processing

Sea ice samples were collected in triplicate in February 4, 2005, from one reference pelagic site located 400 m offshore ($48^{\circ} 31.20'N$, $68^{\circ} 28.30'W$) and at the outer edge of both studied marshes (i.e., near stations I and II, Fig. 2). Sampling was done during the coldest period of the winter when air temperature ranged typically between -15 and -25 °C. Ice cores were taken at high tide using a 7.5 cm ice auger. Cold conditions were carefully maintained during transportation and sub-sampling. Three ice sections corresponding to top, middle, and base of the ice sheet were cut from the cores using an ice saw. Ice sections were thoroughly rinsed with deionised water (melting ~2 mm of the exterior surface), and then placed in heat-sealed plastic bag and slowly melted in darkness at 4 °C.

6.4.4 Chemical Analysis

Dissolved nutrients (PO_4^{3-} , $\text{NO}_2^- + \text{NO}_3^-$, and Si(OH)_4) were analysed by standard colorimetric techniques (Strickland and Parson, 1972) with automated Technicon® and AA3 Bran+Luebbe® platforms, allowing an overall analytical uncertainty ($\pm 1 \sigma$) under $\pm 5\%$. Ammonium (NH_4^+) concentrations were determined with a spectrofluorometric method previously described in Poulin and Pelletier (2007). This automated method for microplate reader provides an analytical uncertainty ($\pm 1 \sigma$) of $\pm 1\%$. Pigments (Chl-*a*) were extracted from the glass-fibre filters in 10 ml of 90% (v/v) acetone for 24 h at 4 °C in the dark, and then Chl-*a* concentrations were determined using a Turner Design® spectrophotometer ($\lambda = 630$ nm) according to Strickland and Parson (1972), allowing an overall analytical uncertainty ($\pm 1 \sigma$) of $\pm 1\%$.

6.5 Results

6.5.1 Tributaries freshwater and dissolved inorganic nutrient inputs

Compared to PAE salt marsh which received low freshwater and nutrient inputs from its forested watershed, PAP salt marsh received a larger volume of freshwater enriched in dissolved inorganic nutrients (Fig. 4). In both pristine and low impacted marsh environments, the smallest freshwater fluxes (average \pm standard deviation of weekly

measurements) were observed during winter period (December 2003 to March 2004; PAE = frozen inlets; PAP = $0.034 \pm 0.058 \text{ m}^3 \text{ s}^{-1}$) whereas the highest ones were measured in April 2004 (PAE = $0.035 \pm 0.031 \text{ m}^3 \text{ s}^{-1}$; PAP = $1.933 \pm 0.665 \text{ m}^3 \text{ s}^{-1}$) during spring snow melting. PAE marsh tributaries showed similar average freshwater flux through summer and fall (June-November 2003; $0.008 \pm 0.003 \text{ m}^3 \text{ s}^{-1}$), whereas PAP marsh freshwater inputs showed more variability during the same period ($0.241 \pm 0.479 \text{ m}^3 \text{ s}^{-1}$), which can be related to input of urban sewage. In addition, this urban sewage has an important effect on stream nutrient concentrations. On average, ammonium, phosphate and nitrate concentrations were 120, 380 and 770 times greater in tributaries flowing into PAP than those discharging into PAE while silicate concentrations were only 2 times greater in PAP marsh streams. In both environments, tributaries nutrient concentrations showed an important seasonal variability. In PAE, the highest mean ammonium, nitrate and silicate concentration was observed during summer period ($\text{NH}_4^+ = 0.22 \mu\text{M}$; $\text{NO}_2^- + \text{NO}_3^- = 0.46 \mu\text{M}$ in June 2003 and $\text{Si(OH)}_4 = 48.79 \mu\text{M}$ in July 2003) whereas phosphate concentration remained low all year around ($< 0.1 \mu\text{M}$). In PAP, the highest mean ammonium and phosphate concentrations were registered during winter time ($\text{NH}_4^+ = 14.97 \mu\text{M}$ in February 2004 and $\text{PO}_4^{3-} = 0.78 \mu\text{M}$ in March 2004) while maximum mean silicate and nitrate concentration was observed in autumn period ($\text{Si(OH)}_4 = 78.38$ in September 2003 and $\text{NO}_2^- + \text{NO}_3^- = 115.37$ in October 2003).

Affluent nutrient flux followed a similar trend with highest mean fluxes observed in April 2004 in both marshes (Fig. 5). Although mean Si(OH)_4 fluxes from PAE streams remained almost constant through the sampling period ($1.158 \pm 0.841 \text{ kg Si d}^{-1}$), very low PO_4^{3-} fluxes ($< 0.001 \text{ kg P d}^{-1}$) as well as low NH_4^+ and $\text{NO}_2^- + \text{NO}_3^-$ fluxes were observed (from not detected (ND) to $0.001 \text{ kg N d}^{-1}$ and from ND to $0.006 \text{ kg N d}^{-1}$, respectively). On the other hand, PAP marsh affluent fluxes showed an important seasonal variability with lowest nutrient fluxes measured in February 2004 and highest ones in April 2004 with mean fluxes varying from 0.095 to $4.766 \text{ kg N d}^{-1}$ for NH_4^+ , 0.014 to $0.946 \text{ kg P d}^{-1}$ PO_4^{3-} , 0.195 to $55.893 \text{ kg N d}^{-1}$ $\text{NO}_2^- + \text{NO}_3^-$, and 0.474 to $8.822 \text{ kg Si d}^{-1}$ Si(OH)_4 .

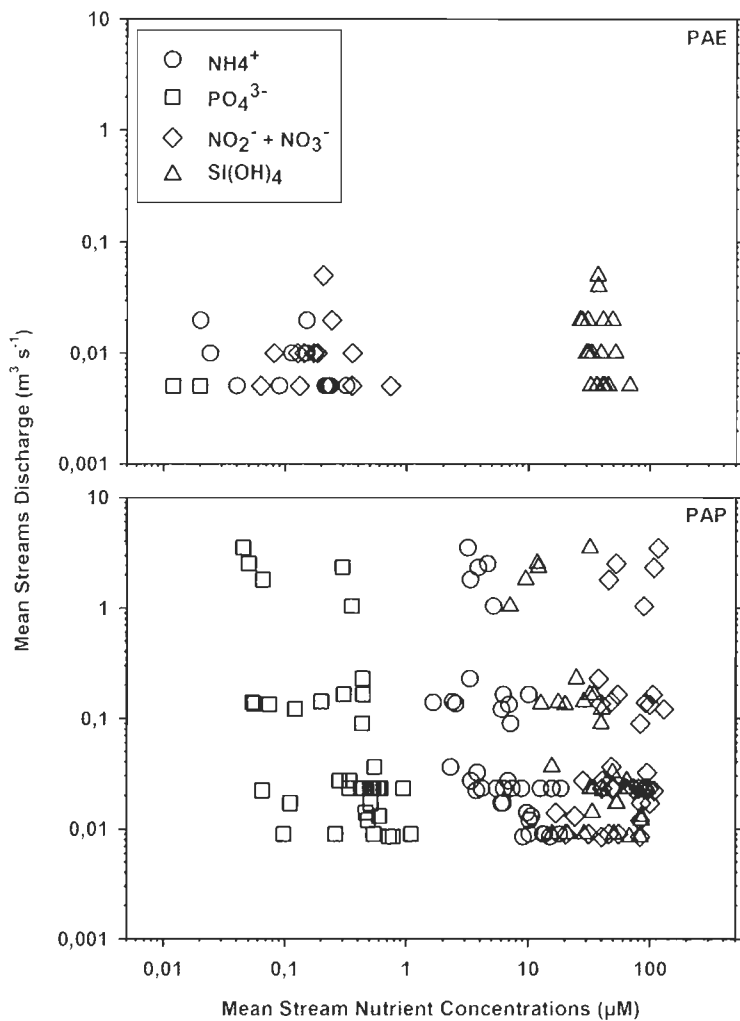


Figure VI-4 Mean monthly streams discharge vs mean monthly stream nutrient concentrations showed for Pointe-aux-Épinettes marsh (PAE) and Pointe-au-Père marsh (PAP) on a log/log scale.

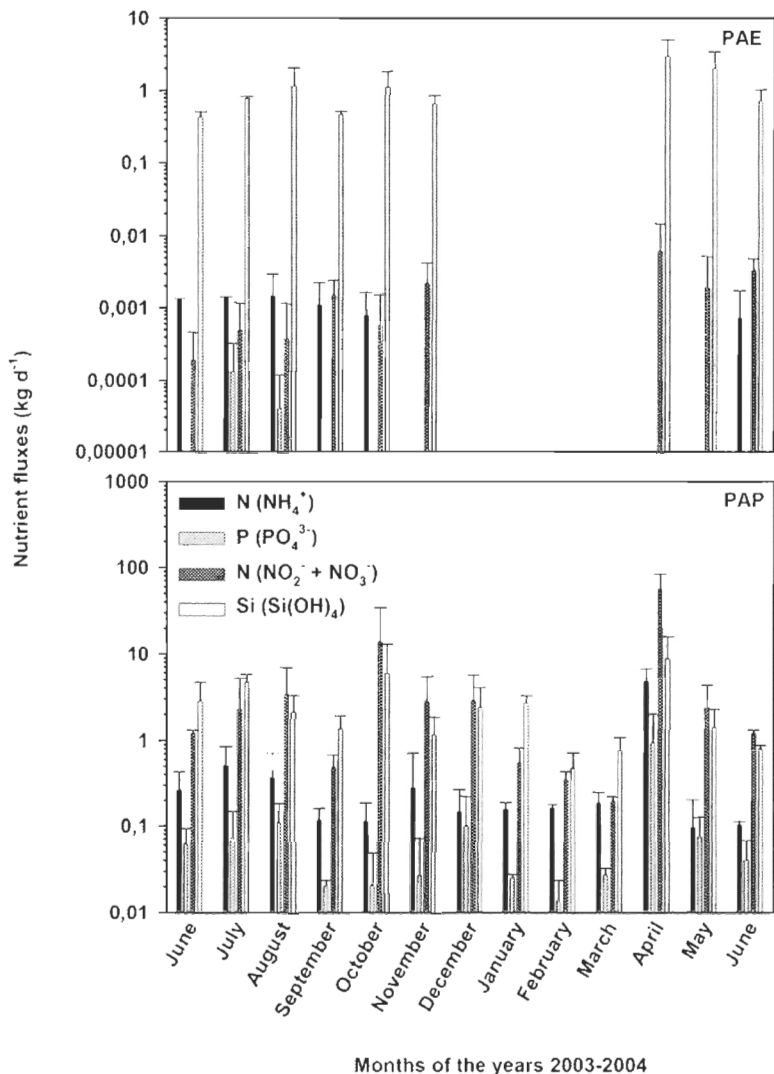


Figure VI-5 Affluent nutrient fluxes from Pointe-aux-Épinettes (PAE) and Pointe-au-Père (PAP) marshes (monthly average \pm standard deviation from weekly measurements taken from 17 June 2003 to 18 June 2004). From December to March, there is no data in PAE since streams are turned to ice. Nutrients fluxes are presented in a log scale.

6.5.2 Tides

Although tide level time series given by the hydrodynamic model are not corrected for wind effects, barometric pressure change, marsh roughness (small scale irregularities) and sediment porosity (inducing asymmetry in tidal level time series), a good match was observed between modeled tide level and field measurements carried out at stations I and II (Fig. 3 and Table 1). In PAE marsh, the maximal tide height above marsh surface observed during studied tide cycles varied from 1.30 m (14 July 2004) to 2.25 m (11 November

2004) whereas, it ranged from 1.40 m (13 July 2004) to 2.50 m (3 May 2004) in PAP (Fig. 6 and Table 1).

The flooded marsh areas (submerged area according to the numerical simulation landward of the dashed lines on Fig. 2) varied between 0.16 and 0.26 km² and 0.32 and 0.45 km² in PAE and PAP marshes, respectively. The resulting tidal flux given by the model reached a maximum of 50.9 m³ s⁻¹ in November 2004 and 53.5 m³ s⁻¹ in May 2004 in PAE and PAP marshes, respectively.

Tableau VI-1 Outputs of hydrodynamic numerical model used for Outlet Flux calculation. Maximum tide heights observed at sites I and II (Max Tide Obs) and maximum tide heights computed by the model (Max Tide Model) for these sites are give according to the marsh surface (-0.5 m). The flooded marsh area (Flood Area) is the submerged area landward of the marshes cross section (dashed lines on Figure 2) at high tide. Max Tidal Flux stand for maximum tidal flux computed through the marshes cross section of Pointe-aux-Épinettes (PAE) and Pointe-au-Père (PAP) salt marshes.

Sampling time	PAE					PAP				
	Max Tide Obs (m)	Max Tide Model (m)	Flood Area (km ²)	Flood Area (%)	Max Tidal Flow (m ³ s ⁻¹)	Max Tide Obs (m)	Max Tide Model (m)	Flood Area (km ²)	Flood Area (%)	Max Tidal Flow (m ³ s ⁻¹)
March 2004	1.75	1.8	0.18	64	31.4	2.00	2.0	0.41	87	49.7
May 2004	2.00	2.0	0.24	86	39.3	2.50	2.5	0.45	95	53.5
July 2004	1.30	1.3	0.16	57	19.0	1.40	1.4	0.32	68	29.1
November 2004	2.25	2.3	0.26	93	50.9	2.25	2.3	0.44	93	53.4

6.5.3 Salt-marsh water-column characteristics

Water temperature, salinity and Chl-*a* concentration ranged over sampling seasons from -0.2 to 23.5 °C, from 11.4 to 31.2 and from 1.02 to 31.65 µg L⁻¹, respectively (Fig 6). The lowest temperature and Chl-*a* concentration, and the highest salinity were recorded in PAP marsh in March 2004, under sea ice condition. The lowest water salinity was recorded in PAP marsh in May 2004 due to a significant contribution of affluent freshwater input to the marsh water budget (0.12 ± 0.14 m³ s⁻¹) while the highest temperature and Chl-*a* concentration were observed in PAE marsh in July 2004.

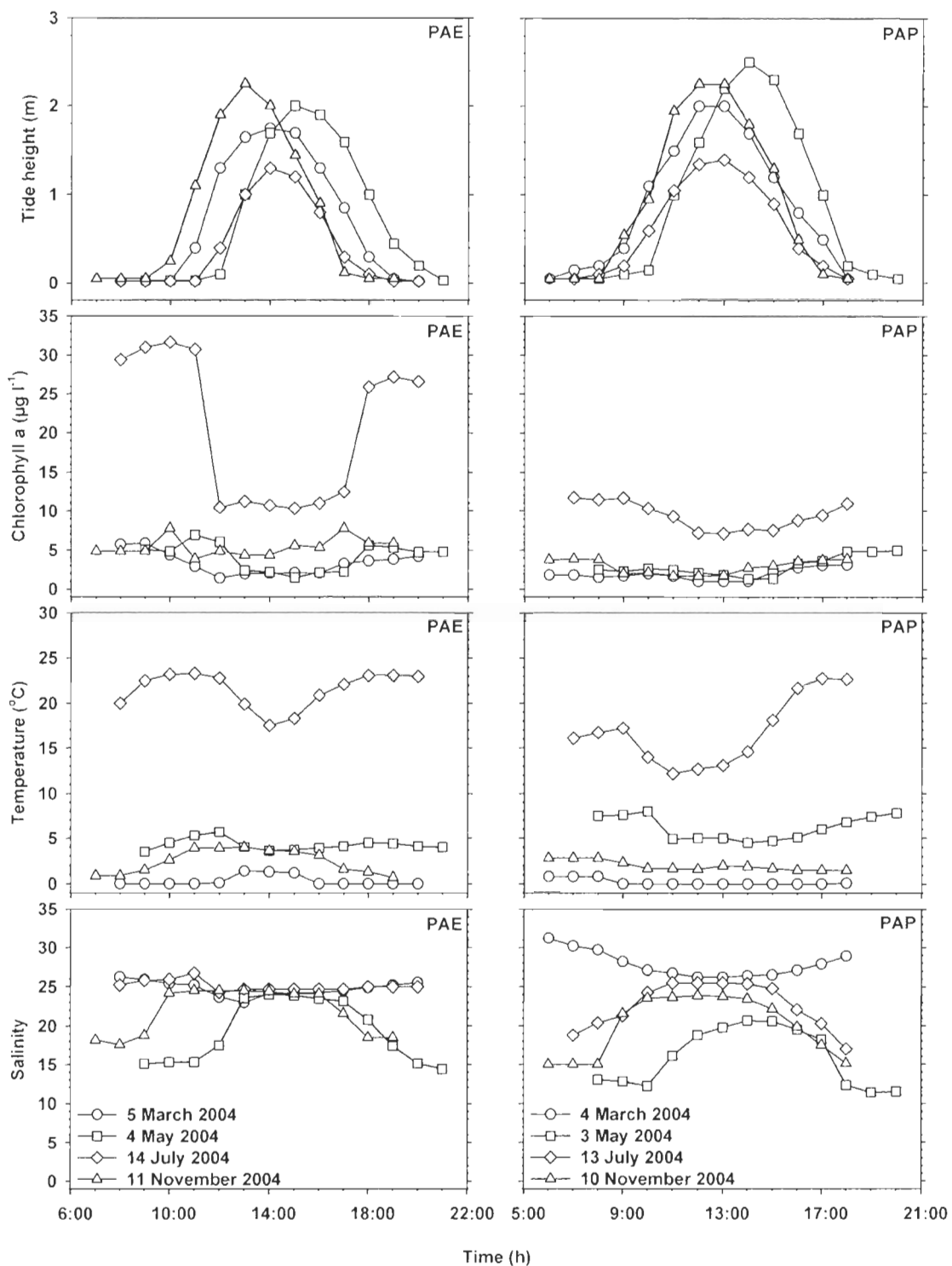


Figure VI-6 Diurnal variations of tide height above marsh surface, Chl-*a* average concentration, temperature and salinity monitored at station I (Pointe-aux-Épinettes, PAE) and II (Pointe-au-Père, PAP) during the four seasonal surveys.

Average nutrient concentrations monitored during seasonal sampling, through complete tidal cycles at stations I and II are illustrated in Figure 7. Before tide flooding (i.e. during the first hour of sampling), nutrient concentrations measured in marsh runoff showed an important seasonal and inter-site variability with the lowest values recorded in July 2004 and highest ones in March 2004. Monitored NH_4^+ , PO_4^{3-} , $\text{NO}_2^- + \text{NO}_3^-$ and Si(OH)_4 concentrations ranged from 2.87 μM (PAP) to 30.74 μM (PAP), from 0.79 μM (PAP) to 1.73 μM (PAE), from 0.37 μM (PAE) to 17.81 μM (PAE) and from 6.47 μM (PAE) to 35.49 μM (PAP), respectively. These values were similar to mean dissolved nutrient concentrations obtained from weekly survey carried at low tide, at station I and II (Fig. 8). Only silicate concentrations from PAE marsh registered in March 2004 showed a noticeable difference. At high tide, nutrient concentrations presented similar seasonal variations (with lowest nutrient concentrations recorded in July 2004 and highest ones in March 2004) and were found very comparable for both studied areas. Observed NH_4^+ , PO_4^{3-} , $\text{NO}_2^- + \text{NO}_3^-$ and Si(OH)_4 concentrations ranged from 1.11 μM (PAP) to 5.76 μM (PAP), from 0.57 μM (PAP) to 1.30 μM (PAE), from 1.75 μM (PAP) to 18.72 μM (PAE) and from 11.55 μM (PAP) to 23.36 μM (PAE), respectively.

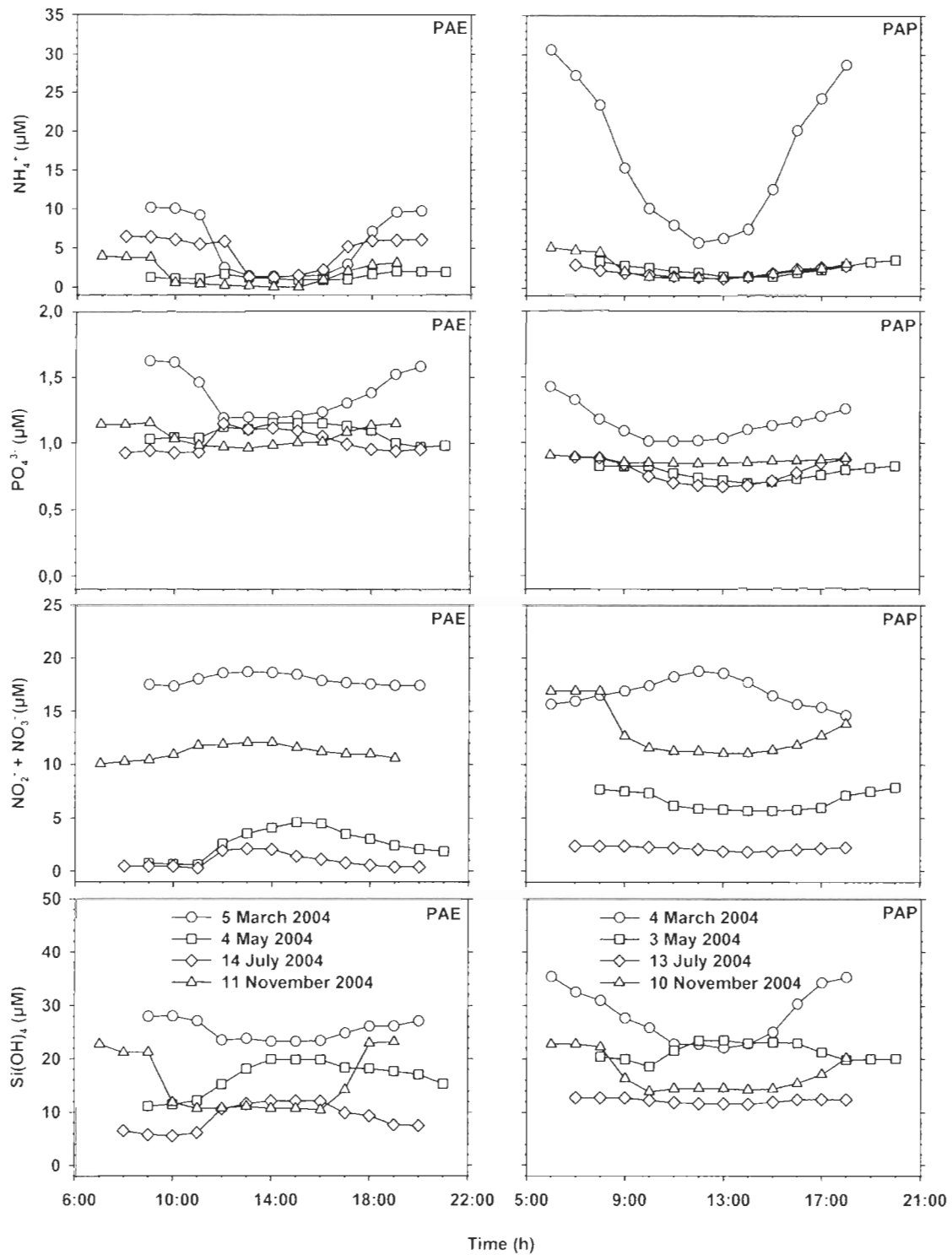


Figure VI-7 Diurnal variations of ammonium (NH_4^+), phosphate (PO_4^{3-}), nitrite + nitrate ($\text{NO}_2^- + \text{NO}_3^-$) and silicate ($\text{Si}(\text{OH})_4$) average concentrations monitored at station I (Pointe-aux-Épinettes, PAE) and II (Pointe-au-Père, PAP) during the four seasonal surveys.

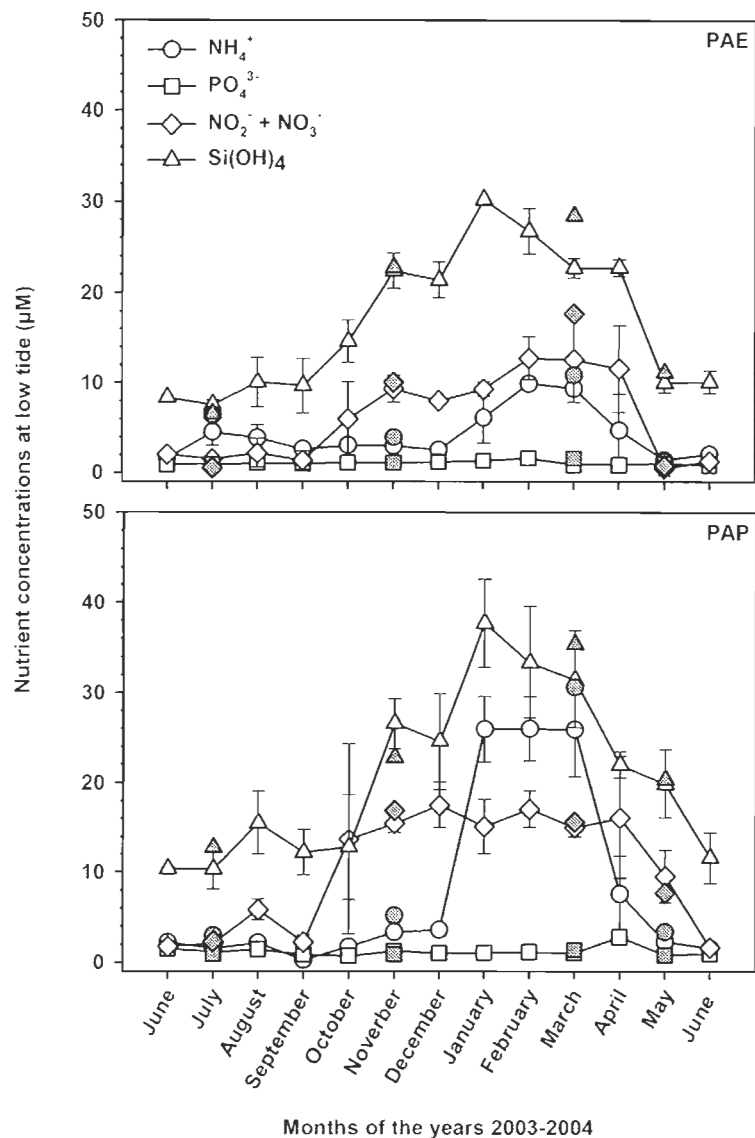


Figure VI-8 Runoff nutrient concentrations from Pointe-aux-Épinettes (PAE) and Pointe-au-Père (PAP) marshes registered at low tide at station I and II (monthly average \pm standard deviation from weekly measurements taken from 17 June 2003 to 18 June 2004). Filled symbols indicate nutrient concentrations registered during seasonal survey.

6.5.4 Seasonal nutrient tidal fluxes

Marshes fluxes of dissolved inorganic nutrients through the outer marsh limits are illustrated in Figure 9. Both marshes released NH_4^+ in all seasons, with the lowest average flux measured in May 2004 ($4.53 \pm 5.84 \text{ mg N d}^{-1} \text{ m}^{-2}$ in PAP) and the highest one in March 2004 ($37.56 \pm 10.89 \text{ mg N d}^{-1} \text{ m}^{-2}$ in PAE). There is no significant differences ($p <$

0.05) between NH_4^+ seasonal fluxes measured within PAE and PAP marshes individually, neither between marshes. Monthly averages of PO_4^{3-} tidal fluxes show that both studied marshes may act as a phosphate source for estuarine waters in March and November 2004. The data also suggest that marshes may act as a phosphate sink in May and July 2004. However, this trend is not statistically significant because of the high variability of measurements. Seasonal PO_4^{3-} fluxes, varying from $-7.29 \pm 12.70 \text{ mg P d}^{-1} \text{ m}^{-2}$ (PAE; July 2004) to $8.07 \pm 24.09 \text{ mg P d}^{-1} \text{ m}^{-2}$ (PAE; March 2004), and were not statistically different from one marsh to the other. There is an important $\text{NO}_2^- + \text{NO}_3^-$ marsh uptake in all sampled seasons, with average fluxes ranging from $-7.60 \pm 10.22 \text{ mg N d}^{-1} \text{ m}^{-2}$ (PAE; November 2004) to $-38.32 \pm 10.89 \text{ mg N d}^{-1} \text{ m}^{-2}$ (PAE; March 2004). However, there is no significant differences between $\text{NO}_2^- + \text{NO}_3^-$ seasonal fluxes measured within PAE and PAP marshes individually, neither between marshes. As observed for phosphate, measured average Si(OH)_4 fluxes showed that both marshes may act as a silicate source for estuarine water in March and November 2004 and as a silicate sink in May and July 2004. Although seasonal Si(OH)_4 fluxes were not statistically different in PAP marsh, a significant change is observed PAE marsh ($p = 0.03$) with significant differences noticed between Si(OH)_4 fluxes measured in March and July 2004. However, there is no statistical difference between Si(OH)_4 seasonal fluxes measured in PAE and in PAP marshes. Measured seasonal Si(OH)_4 fluxes ranged from $-44.40 \pm 11.52 \text{ mg Si d}^{-1} \text{ m}^{-2}$ (PAE, July 2004) to $35.90 \pm 21.85 \text{ mg Si d}^{-1} \text{ m}^{-2}$ (PAE, March 2004).

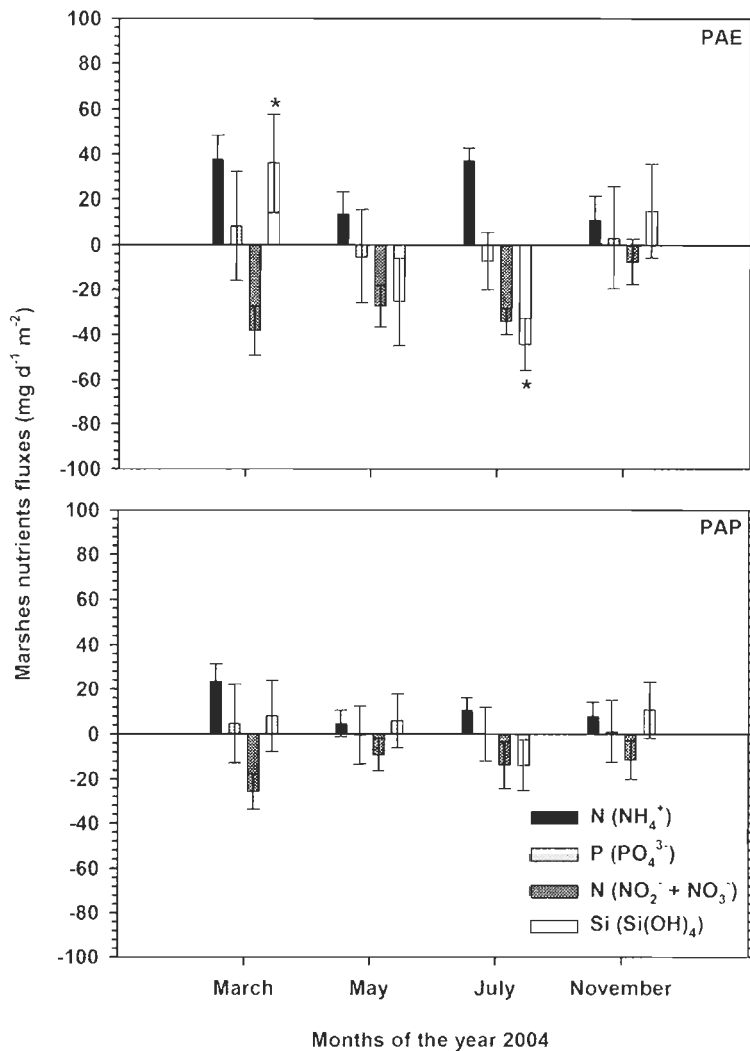


Figure VI-9 Estimated marsh nutrients fluxes for Pointe-aux-Épinettes (PAE) and Pointe-au-Père (PAP) marshes. Average \pm standard deviation values are given for the four seasonal surveys. Error bars represent variability in nutrient concentration between the triplicate nutrient samples.

Since seasonal nutrient fluxes were statistically similar in both studied sites, respective marsh fluxes were averaged to calculate mean seasonal tidal nutrient fluxes per flooded marsh area, which can probably be considered as representative of south shore marshes of the lower St. Lawrence Estuary. Figure 10 shows clearly the previously described seasonal pattern with important NH_4^+ release (ranging from $9.06 \pm 11.02 \text{ mg N d}^{-1} \text{ m}^{-2}$ (May) to $30.48 \pm 13.43 \text{ mg N d}^{-1} \text{ m}^{-2}$ (March)) and $\text{NO}_2^- + \text{NO}_3^-$ uptake (ranging from $-9.59 \pm 13.36 \text{ mg N d}^{-1} \text{ m}^{-2}$ (November) to $-32.07 \pm 13.43 \text{ mg N d}^{-1} \text{ m}^{-2}$ (March)). In

addition, highly variable PO_4^{3-} and $\text{Si}(\text{OH})_4$ fluxes (ranging $-3.73 \pm 17.43 \text{ mg P d}^{-1} \text{ m}^{-2}$ (May) to $6.34 \pm 29.70 \text{ mg P d}^{-1} \text{ m}^{-2}$ (March) and from $-29.19 \pm 16.18 \text{ mg Si d}^{-1} \text{ m}^{-2}$ (July) to $21.91 \pm 26.95 \text{ mg Si d}^{-1} \text{ m}^{-2}$ (March), respectively) were observed.

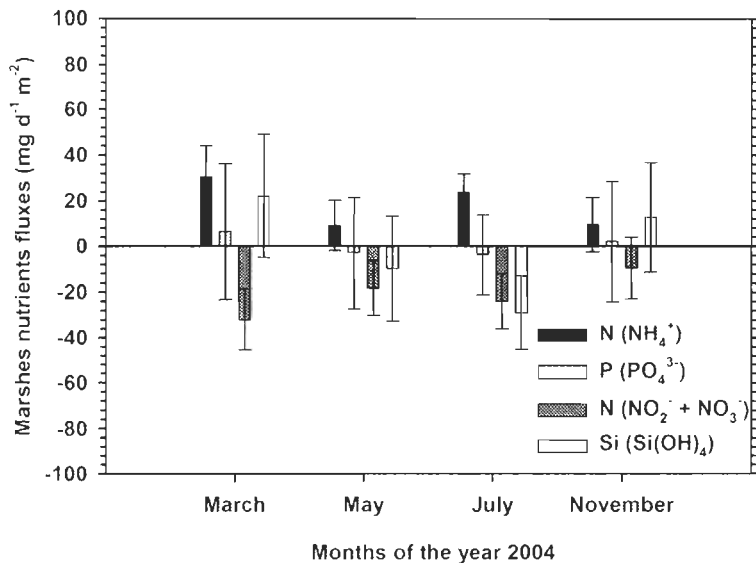


Figure VI-10 Estimated marsh nutrients fluxes in the lower St. Lawrence Estuary marshes. Average \pm standard deviation values are given for the four seasonal surveys.

6.5.5 Ice cores segments characteristics

The ice cores collected at the offshore site near Rimouski, at station I (PAP marsh) and station II (PAE marsh) measured 30, 39, and 42 cm, respectively. Their chemical characteristics are presented in Table 2. For each site, the surface, intermediate, and bottom sections of the core presented similar characteristics. However, inter-site variability are observed with highest salinity, PO_4^{3-} , $\text{NO}_2^- + \text{NO}_3^-$ and $\text{Si}(\text{OH})_4$ concentrations observed in the offshore ice core. The highest NH_4^+ concentrations were measured in PAP while, the highest Chl-*a* concentrations monitored in PAE.

Tableau VI-2 Characteristics (average, AV, and standard deviation, SD) of ice core sections. Ice cores were collected the 4 February 2005 from one control pelagic site located offshore in the Saint-Lawrence estuary (SLE) as well as in the Pointe-aux-Épinette (PAE) and Pointe-au-Père (PAP) salt marshes.

	Length (cm)	Salinity		NH_4^+ (μM)		PO_4^{3-} (μM)		$\text{NO}_2^- + \text{NO}_3^-$ (μM)		Si(OH)_4 (μM)		$\text{Chl-}a$ ($\mu\text{g l}^{-1}$)	
		AV	SD	AV	SD	AV	SD	AV	SD	AV	SD	AV	SD
SLE Surface	10	11.70	1.35	0.01	0.00	0.68	0.06	6.65	1.33	8.78	1.26	0.05	0.03
SLE Intermediate	10	8.20	0.26	0.01	0.00	0.58	0.02	4.13	0.28	6.78	0.25	0.04	0.03
SLE Bottom	10	6.37	0.67	0.21	0.35	0.52	0.01	3.34	0.71	8.84	0.42	0.29	0.10
PAE Surface	13	5.20	0.53	0.43	0.48	0.43	0.02	3.28	0.51	5.54	0.34	3.22	3.16
PAE Intermediate	13	4.93	0.06	0.13	0.04	0.41	0.03	2.39	0.26	5.30	0.10	2.92	1.18
PAE Bottom	13	5.13	0.21	0.45	0.11	0.40	0.02	2.31	0.15	5.35	0.20	3.46	1.26
PAP Surface	14	7.20	0.17	1.52	0.21	0.58	0.08	4.61	0.42	8.40	0.08	1.21	1.24
PAP Intermediate	14	5.90	0.56	1.43	0.08	0.52	0.02	3.12	0.43	7.60	0.69	1.58	0.44
PAP Bottom	14	5.00	0.26	2.67	0.14	0.53	0.03	2.80	0.19	7.27	0.48	2.60	1.51

6.6 Discussion

This paper is first to report around-the-year nutrient fluxes in northern salt marshes exposed to severe winter conditions inducing a four-month ice cover. We found surprisingly active salt marshes even during winter with a sizable production of ammonium and a consumption of $\text{NO}_2^- + \text{NO}_3^-$. Seasonal nutrient fluxes measured in both studied marshes revealed to be statistically similar within studied sites (with the exception of Si(OH)_4 in PAE) as well as between marshes. This similarity is possibly related to the dominance of constant year-round biogeochemical processes weakly affected by temperature and light, but not as much as expected by human activities. These finding are discussed hereafter in regard to each flux of dissolved nutrients.

6.6.1 Validity of marshes nutrient fluxes calculations

The numerical hydrodynamic model used to characterise nutrient fluxes between St. Lawrence Estuary marshes and coastal waters provided new insights for understanding the seasonal dynamic of northern salt marshes. For all simulations, the hydrodynamic model reproduces well the observed water levels (Table 1). Therefore, the hydrodynamic model used in this study is probably as well adapted than similar models which have been used for other geochemical studies in coastal area (e.g. Zheng *et al.*, 2004).

In ideal conditions, the weekly and seasonal data sets should have overlapped for the whole study period. However, for practical reasons, the data sets overlapped only for a portion of the study period. Both data sets covered a full year but the weekly sampling started earlier and stopped before the third and fourth seasonal tidal sampling event occurred. Although this complication may weaken the significance of calculated marsh fluxes, we argue that it won't changes the main conclusions of this study. Because marshes fluxes calculated for the two studied sites remain statistically similar despite the very distinct watershed fluxes, we think that inter annual variability of precipitation (which modulate watershed nutrients fluxes) have a weak effect on marshes systems nutrients fluxes. Nevertheless, historical weather data obtained from Meteorological Service of Canada for Rimouski area show similar total precipitation volume for July 2003 and 2004 (117.6 and 138.8 mm) and in November 2003 and 2004 (104.6 and 105.0 mm, respectively) which should strength the validity of this study. In addition, the similitude observed between nutrient concentrations measured at low tide during weakly and seasonal sampling survey (Fig. 8) confirms the significance of seasonal based interpretation of marshes nutrients fluxes.

6.6.2 Incidence of tributaries

The geomorphology of PAP marsh is characterized by a drainage channel network deeply incised in a vegetated platform. Field observations showed that a large portion of flushed water from the major affluents is directly evacuated to the Estuary by these channels without being in contact with the marsh surface, limiting the possibility of nutrient uptake or transformation by plants and microbiota. Therefore, we suggest that elevated affluent discharges measured in PAP marsh (Fig. 4) promoted active erosion processes and contributed little to eutrophication. Flood events induced by rain storms and snow melting coupled with a reduced sediment upload (due to upstream sediment retention by artificial obstacles) have increased channel flow and general marsh vulnerability to erosion processes. Erosion structures often observed in PAP include channel edge slumping, cliff formation, and displacement of *Spartina* rafts. However, as nutrients can be a limiting factor in coastal environment productivity (Justic *et al.*, 1995), affluent inputs may induce significant modification of the balance between autotrophic and heterotrophic activities in

marsh areas as well as in adjacent coastal waters. While PAE marsh streams correspond to < 0.1% of N($\text{NO}_2^- + \text{NO}_3^-$) and P(PO_4^{3-}) and between 11-34% of Si(Si(OH)_4) marsh uptake, these tributaries account for negligible 0.02% of N(NH_4^+) and less than 17% of Si(Si(OH)_4) marsh release through tidal cycle (as defined by the relative contribution of Watershed Flux on Marsh Flux). Assuming that this pattern is representative of pristine marsh areas along the south shore of the St. Lawrence Estuary, it turns out that the only noticeable contribution of natural affluent runoff to nearby coastal waters resides in the silicate budget. On the other hand, the potential contribution of impacted affluents to salt marsh nutrient budget shows to be considerably different. PAP marsh streams provide from 2 to 58% of N($\text{NO}_2^- + \text{NO}_3^-$), 32 to 124% of P(PO_4^{3-}), and up to 65% of Si(Si(OH)_4) marsh uptake. In addition, PAP marsh tributaries account for up to 15% of N(NH_4^+), 6% of P(PO_4^{3-}) and 55% of Si(Si(OH)_4) of marsh nutrient releases. More investigations are needed to clearly relate anthropogenic nutrient load, microbial diversity and productivity in northern salt marsh environments, since these environments are light limited most part of the year due to either their high water turbidity in spring and fall or the presence of a ice cover in winter. Because streams input does not generally exceed PAP marsh total N and P potential demand (as defined by Marsh flux), we can conclude that anthropogenic activities have not induced an important nutrient pollution problem in this particular case. According to our field observation, elevated tributaries discharge measured in PAP marsh has promoted erosion processes rather than other types of alteration, which could modify the ecosystem function in term of nutrient regeneration capacity. However, this suggests that there is a potential impact of watershed runoff on estuarine water as runoff had minimal contact with the PAP marsh platform itself at low tide.

6.6.3 Seasonal processes potentially implied in tidal nutrient fluxes

In agreement with the classical study of Nixon (1980) about coastal marshes, the results presented here show that south shore St. Lawrence Estuary (SLE) marshes act as an important year-round $\text{NO}_2^- + \text{NO}_3^-$ sink and a NH_4^+ source in spite of a four-month ice cover (Fig. 10). This dissolved inorganic nitrogen exchange pattern has been reported in many temperate salt marsh environments (Dame and Gardner, 1993; Groszkowski, 1995; Campana, 1998; Ziegler *et al.*, 1999; Valiela *et al.*, 2000; Neubauer *et al.*, 2005).

Using labelled nitrogen (^{15}N), Poulin *et al.* (2007) recently showed that among possible nitrate consumption mechanisms in SLE marshes, denitrification (bacterial reduction of NO_3^- to N_2) and DNRA (Dissimilatory Nitrate Reduction to Ammonium) represent the most obvious bacterial processes. Although the relative contribution of bacterial processes to nitrate uptake is not well defined in SLE marshes, denitrification is estimated to remove 19-31% of NO_3^- marsh uptake (with no clear temperature dependence). The remaining fraction is assumed to be removed by DNRA, Mn^{2+} oxidation (Luther *et al.*, 1997), Fe^{2+} oxidation (Straub *et al.*, 1996), N_2O production (via incomplete denitrification; Robinson *et al.*, 1998) as well as by biological assimilation (Dugdale and Goering, 1967). From a seasonal point of view, $\text{NO}_2^- + \text{NO}_3^-$ assimilation by autotrophic community appeared to be weak compared with bacterial consumption since significantly higher $\text{NO}_2^- + \text{NO}_3^-$ uptake has been observed in PAE during winter sampling (when sea ice cover restraint autotrophic activity, low chlorophyll in water samples) compared to ice-free seasons. Even if this picture might constitute a plausible explanation, more investigations are needed to better understand the role of autotrophic activity in winter-freezing marshes in regard to specific nutrient requirements and fine scale temporal assimilation patterns.

DNRA is widely recognized as an important NH_4^+ source in shallow coastal environments (An and Gardner, 2002) and seems also play an important year-round role in SLE marshes as shown by the significant negative correlation between $\text{NO}_2^- + \text{NO}_3^-$ and NH_4^+ fluxes ($r^2 = 0.84$, $p = 0.05$; calculated with data presented on Fig. 10). This correlation is indicative of a coupling between $\text{NO}_2^- + \text{NO}_3^-$ retention and NH_4^+ production in cold salt marsh sediment. Ammonification (NH_4^+ bacterial production from nitrogenous macromolecule such as polyamino-sugar, protein, peptide, nucleic acid, amino acids) should also be considered here as a possible significant mineralization process in coastal vegetated sediment (Blackburn *et al.*, 1994). Ammonification generally increases with temperature, labile vegetative material deposition, sewage (as in PAP marsh), and oxygen availability (Herbert, 1999). Thus, it could represent a substantial seasonal NH_4^+ source for SLE tidal marshes, especially during summer and fall when higher water temperature and high evapotranspiration (promoting dewatering and oxygen penetration in sediment) occur

(Rocha, 1998). However, this contribution may be hidden by biological assimilation because NH_4^+ is known to be preferentially used by phytoplanktonic species (Maier *et al.*, 2000), and high Chl- a concentration was observed in the marsh water column. Finally, coupled nitrification–denitrification process (bacterial oxidation of NH_4^+ to NO_3^- followed by the reduction of NO_3^- to N_2), which is recognized as an important process under the previously described summer conditions (Herbert, 1999), may play an additional role in term of NH_4^+ consumption, but lack of results preclude from more specific conclusion.

In opposition to the complex inter-relationship of nitrogen species, average PO_4^{3-} tidal fluxes show a simple seasonal trend with PO_4^{3-} release in March and November and uptake in May and July. Some authors have reported a similar seasonal pattern in temperate marsh environments (Reimold and Daiber, 1970; Wolaver and Spurrier, 1988) and a number of biogeochemical mechanisms have been proposed to explain this behaviour. For example, macrophyte species (such as *Spartina alterniflora*) may act as an important PO_4^{3-} sink in marsh environment when the community is well established (i.e. in summer). In addition to autotrophic activity, P dynamic remains closely related to Fe cycle (Roden and Edmonds, 1997). Generally, PO_4^{3-} is sequestered by Fe^{3+} in both oxic sediment and water column whereas PO_4^{3-} is released from anoxic sediment during the reduction of Fe^{3+} to Fe^{2+} . Even if iron redox processes might be driven by abiotic processes alone, bacterial activity (such as iron-reducing and sulphate-reducing bacteria using Fe^{3+} and SO_4^{2-} as the terminal electron acceptor for anaerobic respiration) is recognized as predominantly responsible of PO_4^{3-} release (Boström *et al.*, 1988). In addition, some authors have proposed that bacteria containing polyphosphates as P storage compounds can hydrolyse these products to PO_4^{3-} under anaerobic conditions (Wentzel *et al.*, 1986; Gächter and Meyer, 1993) while PO_4^{3-} may be released from the hydrolysis of organic matter by bacteria which own enzymes like nucleotidases (Azam and Hodson, 1979). Since organic matter availability increase during autumn period, bacterial uptake of low molecular weight organic compounds such as proteins and fatty acids may promote PO_4^{3-} release during fall and winter. Moreover, Vepraskas and Faulkner (2001) have shown that PO_4^{3-} may precipitate as calcium phosphate or co-precipitate with carbonates in sediment with $\text{pH} > 7$. Since all these mechanisms may be involved in the marsh P cycle, additional studies are

needed to better understand the synergic effects of mineral reaction on tidal flux in cold marshes.

Both marshes acted as a Si(OH)₄ sink during high productivity period (May and July) and as a supplier of Si to the estuarine water during low productivity period (November and March). Biological uptake has a notable incidence on seasonal marsh silicate fluxes. Benthic diatoms identified in both marshes (eg. *Achnanthes delicatula*, *Navicula cryptocephala*, *Cocconeis disculus*; unpublished results) colonising marsh surface sediments during summer, incorporate Si(OH)₄ to produce biogenic silicate tests (SiO₂), which can be buried when new sediment is deposited on the marsh. In addition, marsh graminea (e.g. *Spartina alterniflora* and *Spartina paten*) abundant along the St. Lawrence Estuary coastline, may act as a potential sink during growing season (Si content from 5-15% of total dry weight in graminea; Struyf *et al.*, 2005). After the growing season, the decay of vegetal material in marsh areas is considered as a significant source of amorphous silica (Willey and Spivack, 1997).

6.6.4 Role of sea ice

Our results support the hypothesis that sea ice has many direct and indirect effects on marsh nutrient fluxes in winter in spite of low water temperature and low light energy. From an ecosystem point of view, the most obvious effect of the ice cover is related to pelagic phytoplanktonic productivity. Because autotrophic production is limited by light availability during winter time in the St. Lawrence Estuary (Theriault and Levasseur, 1985), nutrient-rich deep waters brought to the surface by vertical advection processes are not depleted by biological activity. Surface water samples collected offshore Rimouski city in February 2006 showed concentrations of NH₄⁺, PO₄³⁻, NO₂⁻ + NO₃⁻ and Si(OH)₄ averaging 0.28, 0.94, 13.47 and 12.61 μM, respectively, while Chl-*a* concentration remained near the limit of detection (0.01 μg L⁻¹) (data not shown). High nutrient concentrations measured in marsh flooding water during the March 2004 survey (Fig. 7) most probably stimulated microbial nutrient transformation processes in the marsh. As observed by Jungle *et al.* (2004) in the Arctic environment, it can be assumed that SLE

marshes are colonised by cold-adapted microbial communities contributing significantly to the marsh nutrient budget, even under winter conditions.

In addition to elevated nutrient concentrations in estuarine waters, sea ice induces several physical and chemical modifications in water column and sediments of SLE marshes which in turn affect tidal nutrient fluxes. In marine coastal environment, sea ice grows via fractionated crystallisation. This process increases underneath water salinity (see Fig. 6) and the pool of exchangeable nutrients in marsh sediments by decreasing their sorption capacity (Liu *et al.*, 2002; Hou *et al.*, 2003). Moreover, sea ice cover reduces sediment exposure to atmospheric oxygen by limiting sediment dewatering which usually occurs between tidal inundations via evaporation and drainage. This process enhances anoxic conditions in marsh sediments and anaerobic processes such as DNRA, PO_4^{3-} and Si(OH)_4 mineralization. Sea ice mechanical action on marsh platforms like compaction (Argow and FitzGerald, 2006), ice drifting, and rafting (Drapeau, 1992; Pejrup and Andersen, 2000) may enhance these biochemical processes by changing the redox gradient of the sediments and by increasing migration of pore water and colloidal matter through water/sediment interface. These ice-induced perturbations may promote benthic turnover rate of organic matter as well as tidal nutrient exchange in SLE marshes.

Sea ice contributes also to the nutrient budget by storing seawater nutrients through winter time and releasing them during spring (Brooks *et al.*, 1999). Although nutrient concentrations measured in the sampled ice cores were relatively low compared to underneath water (Table 2), ice could act as an additional nutrient source in the early spring for marsh environment. However, ice may be accumulated on marshes or transported toward open waters during melting event, therefore the relative contribution of melt waters remain difficult to define. In addition, sea ice is a favourable environment for a wide range of cold adapted phytoplanktonic and bacterial species (Sullivan and Palmisano, 1984; Junge *et al.*, 2004). Even if significant Chl- α concentration was observed in ice cores samples, the pheopigment/Chl- α ratio (5.24 ± 1.53 , $n = 27$; data not shown) remained high and argues for the presence of senescent phytoplanktonic cells incorporated to ice during its formation. Coming both from water column and surface sediment, this old production is

assumed not to deplete nutrient concentrations within sea ice interstitial water. Total bacterial abundance was important in ice cores (5.24×10^5 cell ml $^{-1}$ ± 0.86 , n = 27; data not shown), but the activity of this bacterial community is still unknown at temperature well below 0 °C. Although bacterial mineralization/consumption process occurring in icy environment may affect temporal evolution of ice nutrient concentrations and consume organic carbon as already observed in Antarctic fast ice (Delille *et al.*, 2002), data are not available for St. Lawrence Estuary. Using Trousselier *et al.* (1997) bacterial biomass conversion index (i.e. 60 fg C cell $^{-1}$) and applying it to our total cells measurement, we observed that bacterial biomass found in St. Lawrence Estuary ice cores (~30 mg C m $^{-3}$) is comparable to other icy environment such Arctic (2.4-220 mg C m $^{-3}$; Gradinger and Zhang, 1997) and Antarctic (10-200 mg C m $^{-3}$; Delille *et al.*, 2002) sea ice. Nevertheless, new information are needed to better understand the relationship between total biomass, diversity and activity of the bacterial community implied in nutrients cycles and pinpoint a possible structure/function link in this cold environment.

6.7 Conclusion

Nutrient fluxes measured in this study argue for a significant role of northern salt marshes in the estuarine annual nutrient budget. As most of measured seasonal nutrient fluxes were statistically comparable in both studied marshes, it can be concluded that south shore SLE marsh environments are year-round active nutrient processors. A series of interrelated biogeochemical changes involved in biotic and abiotic organic-matter mineralization processes generated by daily shifting between atmospheric exposure and tidal inundation have been illustrated. Among these processes, denitrification, DNRA, and ammonification, are pinpointed as the most significant ones since important landward NO $_2^-$ + NO $_3^-$ flux and seaward NH $_4^+$ were observed. These transformation processes by marsh microbial community are ecologically essential to estuarine nutrient cycling, as denitrification contributes to remove excess of anthropogenic nitrogen loads; DNRA and ammonification supply the estuarine autotrophic activity as NH $_4^+$ is the preferential nitrogen form used by phytoplanktonic species (McCarthy, 1980).

This importance of salt marshes should be brought even more sharply into focus because of the threats posed by the predicted global warming, rise of sea level, and urban expansion along the coastline (Boorman, 1999). Because they reached an advanced stage of development, the lower St. Lawrence Estuary marshes are becoming more vulnerable to increased erosive forces since many years (Morisette, 2006; Bernatchez and Dubois, 2008) and they represent no more than 90 km² (Dionne, 1986). These marshes possess a strong nutrient regeneration potential even during wintertime and need restoration efforts to recover their significant contribution to the whole St. Lawrence estuarine system.

6.8 Acknowledgements

This research was funded by Natural Science and Engineering Research Council (NSERC-Discovery grant E.P.) and the Canada Research Chair in Ecotoxicology (E.P.). The authors gratefully acknowledge ISMER technician for their support as well as Karine Lemarchand and Michèle Desève for biological data acquisition. This paper is a contribution to Quebec-Ocean network (FQRNT).

6.9 References

- Abbott, M.B., McCowan, A.D. and Warren, I.R. 1981. Numerical modelling of free-surface flows that are two-dimensional in plan. In: Fischer, H.B. (Ed) Transport models for inland and coastal waters, Academic Press, New York.
- Allard, M. and Champagne, P. 1980. Dynamique glacielle à la pointe d'Argentenay, île d'Orléans, Québec. Géographie Physique Quaternaire 34: 159-174.
- An, S. and Gardner, W.S. 2002. Dissimilatory nitrate reduction to ammonium (DNRA) as a nitrogen link, versus denitrification as a sink in a shallow estuary (Laguna Madre/Baffin Bay, Texas). Marine Ecology Progress Series 237: 41–50.
- Argow, B.A. and FitzGerald, D.M. 2006. Winter processes on northern salt marshes: Evaluating the impact of in-situ peat compaction due to ice loading, Wells, ME. Estuarine, Coastal and Shelf Science 69: 360-369.
- Azam, F. and Hodson, R.E. 1977. Dissolved ATP in the sea and its utilization by marine bacteria. Nature 267: 696–697.

- Baldwin, D.S. and Mitchell, A.M. 2000. The effect of drying and re-flooding on sediment and soil nutrient dynamics of lowland river-floodingplain systems: a synthesis. *Regulated Rivers Research and Management* 16: 457-567.
- Blackburn, T.H., Nedwell, D.B. and Wiebe, W.J. 1994. Active mineral cycling in a Jamaican seagrass sediment. *Marine Ecology Progress Series* 110: 233-239.
- Bernatchez, P. and Dubois, J.-M. 2008. Seasonal quantification of coastal processes and cliff erosion on fine sediment shoreline in a cold temperate climate, north shore of the St. Lawrence maritime Estuary. *Journal of Coastal Research* 24: 169-180.
- Boorman, L.A. 1999. Salt marshes – present function and future change. *Mangroves and Salt Marsh* 3: 227-241.
- Boström, B., Andersen, J.M., Fleischer, S. and Jansson, M. 1988. Exchange of phosphorus across the sediment–water interface. *Hydrobiologia* 170: 229–244.
- Brooks, P.D., Campbell, D.H., Tonnessen, K.H and Heuer, K. 1999. Natural variability in N export headwater catchments: snow cover controls on ecosystem N retention. *Hydrological Processes* 13: 2191-2201.
- Campana, M.L. 1998. The effect of *Phragmites australis* invasion on community processes in a tidal freshwater marsh. M.S. Thesis, College of William and Mary, Virginia Institute of Marine Science, Gloucester Point, Virginia.
- Dame, R.F., Spurrier, J.D., Williams, T.M., Kjerfve, B., Zingmark, R.G., Wolaver, T.G., Chrzanowski, T.H., Mckellar, H.N. and Vernberg, F.J. 1991. Annual material processing by a salt marsh-estuarine basin in South Carolina, USA. *Marine Ecology Progress Series* 72: 153-166.
- Dame, R.F. and Gardner, L.R. 1993. Nutrient processing and the development of tidal creek ecosystems. *Marine Chemistry* 43: 175-183.
- de la Lanza Espino, G. and Medina, M.A.R. 1993. Nutrient exchange between subtropical lagoons and the marine environment. *Estuaries* 16: 273-279.
- Delille, D., Fiala, M., Kuparinen, J., Kuosa, H. and Plessis, C. 2002. Seasonal changes in microbial biomass in the first-year ice of the Terre Adélie area (Antarctica). *Aquatic Microbial Ecology* 28: 257-265.
- Dionne, J.C. 1968. Action of shore ice on tidal flats of the St. Lawrence estuary. *Maritime Sedimentology* 4: 113-115.
- Dionne, J.C. 1986. Érosion récente des marais intertidaux de l'estuaire du Saint-Laurent. *Géographie Physique et Quaternaire* 50: 307-323.

- Dionne, J.C. 1989. An estimate of shore ice action in a Spartina tidal marsh, St. Lawrence Estuary, Quebec, Canada. *Journal of Coastal Research* 5: 281-295.
- Dionne, J.C. 2003. Observations géomorphologiques sur les méga-blocs du secteur sud-est de la batture argileuse de la Baie à l'Orignal, au Parc du Bic, dans le Bas-Saint-Laurent (Québec). *Géographie Physique et Quaternaire*. 57 : 95-101.
- Dionne, J.C. 2004. Âge et taux moyen d'accréation verticale des schorres du Saint-Laurent estuaire, en particulier ceux de Montmagny et de Sainte-Anne-de-Beaupré, Québec. *Géographie Physique et Quaternaire* 58: 73-108.
- Drapeau, G. 1992. Dynamique sédimentaire des littoraux de l'estuaire du St-Laurent. *Géographie Physique et Quaternaire* 46: 233-242.
- Dugdale, R.C. and Goering, J.J. 1967. Uptake of new and regenerated forms of nitrogen in primary productivity. *Limnology and Oceanography* 12: 196-206.
- Fagherazzi, S., Marani, M. and Blum, L.K. 2004. Introduction: The coupled evolution of geomorphological and ecosystem structure in salt marshes. In: Fagherazzi, S., Marani, M. and Blum, L.K. (Eds) *The ecogeomorphology of tidal marshes*, American Geophysical Union, USA.
- Fan, A. and Jin, X. 1989. Tidal effect on nutrient exchange in Xiangshan Bay, China. *Marine Chemistry* 27: 259-281.
- Gächter, R. and Meyer, J.S. 1993. The role of microorganisms in mobilization and fixation of phosphorus in sediments. *Hydrobiologia* 253:103–121.
- Gardner, L.R. and Kjerfve, B. 2006. Tidal fluxes of nutrients and suspended sediments at the North Inlet Winyah Bay National Estuarine Research Reserve. *Estuarine Coastal and Shelf Science* 70: 682-692.
- Gauthier, B. and Goudreau, M. 1983. Mares glacielles et non glacielles dans le marais salé de l'Isle-Verte, Estuaire du Saint-Laurent, Québec. *Géographie Physique et Quaternaire* 37: 49-66.
- Gradinger, R. and Zhang, Q. 1997. Vertical distribution of bacteria in Arctic sea ice from the Barents and Laptev Seas. *Polar Biology*, 17: 448-454.
- Groszkowski, K.M. 1995. Denitrification in a tidal freshwater marsh. Senior Thesis, Harvard College, Cambridge, Massachusetts.
- Heinle, D.R. and Flemer, D.A. 1976. Flows of material between poorly flooded tidal marshes and an estuary. *Marine Biology* 35: 359-373.
- Herbert, R.A. 1999. Nitrogen cycling in coastal ecosystems. *FEMS Microbiology Reviews* 23: 563-590.

- Hou, L.J., Liu, M., Jiang, H.Y., Xu, S.Y., Ou, D.N., Liu, Q.M. and Zhang B.L. 2003. Ammonium adsorption by tidal flat surface sediments from the Yangtze Estuary. *Environmental Geology* 45: 72-78.
- Jickells, T. 2005. External inputs as a contributor to eutrophication problems. *Journal of Sea Research* 54: 58-69.
- Junge, K., Eicken, H. and Deming, J.W. 2004. Bacterial activity at -2 to -20°C in Arctic sea ice. *Applied and Environmental Microbiology* 70: 550-557.
- Justic, D., Rabalais, N.N. and Turner, R.E. 1995. Stoichiometric nutrient balance and origin of coastal eutrophication. *Marine Pollution Bulletin* 30: 41-46.
- Koutitonsky, V.G. and Gidas, N.K. 1996. Real-time management of sewage disposal in the Coastal zone. In: *The global ocean-towards operational oceanography*. Proceedings of Oceanology International 96, Vol. 1, 5-8 March, Brighton, UK.
- Liu, M., Hou, L., Xu, S., Ou, D., Yang, Y., Zhang, B. and Liu, Q. 2002. Adsorption of phosphate on tidal flat surface sediments from the Yangtze Estuary. *Environmental Geology* 42: 657-665.
- Luther, G.W., Sundby, B., Lewis, B.L., Brendel, P.J., Silverberg, N. 1997. Interactions of manganese with nitrogen cycle: alternative pathways to dinitrogen. *Geochimica et Cosmochimica Acta* 61: 4043-4045.
- McCarthy, J.J. 1980. Nitrogen and phytoplankton ecology. In: Moris, I. (Ed.), *The physical ecology of phytoplankton*. Blackwell, pp.191-233.
- Maier, R.M., Pepper, I.L. and Gerba, C.P. 2000. *Environmental microbiology*. Academic Press. San Diego. 604 pp.
- Morisette, A. 2006. Évolution côtière haute résolution de la région de Longue-Rive-Forestville, Côte Nord de l'estuaire maritime du Saint-Laurent. Mémoire de maîtrise, Université du Québec à Rimouski, Québec.
- Neubauer, S.C., Anderson, I.C. and Neikirk, B.B. 2005. Nitrogen cycling and ecosystem exchanges in a Virginia tidal freshwater marsh. *Estuaries* 28: 909-922.
- Nixon, S.W. 1980. Between coastal marshes and coastal waters-a review of twenty years of speculation and research in the role of salt marshes in estuarine productivity and water chemistry. In *Estuarine and Wetland Processes*. Plenum, New York, pp. 437-525.
- Odum, E.P. and de la Cruz, A.A. 1967. Particulate organic detritus in a Georgia salt-marsh-estuarine ecosystem. In Lauff, G. H. (Ed) *Estuaries*. American Association for the Advancement of Science, pp. 383-388.

- Pejrup, M and Andersen, T.J. 2000. The influence of ice on sediment transport, deposition and reworking in a temperate mudflat area. the Danish Wadden Sea. *Continental Shelf Research* 20: 1621-1634.
- Poulin, P. and Pelletier, E., 2007. Determination of ammonium using a microplate-based fluorometric technique. *Talanta* 71: 1500-1506.
- Poulin, P. Pelletier, E. and St-Louis, R. 2007. Seasonal variability of denitrification efficiency in northern salt marshes: An example form the St. Lawrence Estuary. *Marine Environmental Research* 63: 490-505.
- Rabouille, C., Mackenzie, F.T. and Ver, L.M. 2001. Influence of the human perturbation on carbon, nitrogen and oxygen biogeochemical cycles in the global ocean. *Geochimica Cosmochimica Acta* 65: 3615-3641.
- Riegman, R., Noordeloos, A.A.M. and Cadee, G.C. 1992. Phaeocystis blooms and eutrophication of the continental coastal zones of the north-sea. *Marine Biology* 112: 479-484.
- Reimold, R.J. and Daiber, F.C. 1970. Dissolved phosphorus concentrations in a natural salt-marsh of Delaware. *Hydrobiologia* 36: 361-371.
- Robinson, A.D., Nedwell, B.D. Harrison, R.M. 1998. Hypernutrified estuaries as a source of N₂O emission to the atmosphere: the estuary of the River Colne. Essex, UK. *Marine Ecology Progress Series* 164: 59-71.
- Rocha, C. 1998. Rhythmic ammonium regeneration and flushing in intertidal sediment of the Sado estuary. *Limnology and Oceanography* 43: 823-831
- Roden, E.E. and Edmonds, J.W. 1997. Phosphate mobilization in iron-rich anaerobic sediments: microbial Fe(III) oxide reduction versus iron-sulfide formation. *Archiv für Hydrobiologie* 139: 347-378.
- Saucier, F.J., Roy, F. and Gilbert, D., 2003. Modeling the formation and circulation processes of water masses and the sea ice in the Gulf of St. Lawrence, Canada. *Journal of Geophysical Research* 108: 3269-3289.
- Sérodes, J.-B. and Dubé, M. 1983. Dynamique Sédimentaire d'un estran à spartines. *Naturaliste Canadien* 110:11-26.
- Sullivan, C.W. and Palmisano, A.C. 1984. Sea ice microbial communities – distribution, abundance, and diversity of ice bacteria in McMurdo Sound, Antarctica, in 1980. *Applied and Environmental Microbiology* 47: 788-795.
- Straub, K.L., Benz, M., Schink, B., and Widdel, F. 1996. Anaerobic, nitrate-dependent microbial oxidation of ferrous iron. *Applied Environmental Microbiology* 62: 1458-1460.

- Strickland, J.D.H., Parson, T.R. 1972. A practical handbook of seawater analysis. Fisheries Research of Canada, Ottawa, 310 pp.
- Struyf, E., Van Damme, S., Gribsholt, B. and Meire, P. 2005. Freshwater marshes as dissolved silica recyclers in an estuarine environment (Schelde Estuary, Belgium). *Hydrobiologia* 540:69–77
- Theriault, J.-C. and Levasseur, M. 1985. Control of phytoplankton production in the lower St. Lawrence Estuary: light and freshwater runoff. *Naturaliste Canadien* 112: 77-96.
- Thibodeau, B., de Vernal, A. and Mucci, A. 2006. Recent eutrophication and consequent hypoxia in the bottom waters of the Lower St. Lawrence Estuary: Micropaleontological and geochemical evidence. *Marine Geology* 231: 37–50.
- Trousselier, M., Bouvy, M., Courties, C., Dupuy, C. 1997. Variation of carbon content among bacterial species under starvation condition. *Aquatic Microbial Ecology* 13:113–119.
- Valiela, I., Teal, J.M., Volkmann, S., Shafer, D. and Carpenter, E.J. 1978. Nutrient and particulate fluxes in a salt marsh ecosystem: Tidal exchange and inputs by precipitation and ground water. *Limnology and Oceanography* 23: 798-812.
- Valiela, I., Cole, M.L., McClelland, J., Hauxwell, J., Cebrian, J. and Joye, S.B. 2000. Role of salt marshes as part of coastal landscapes. In: Weinstein MP, Kruger DA (eds) Concepts and Controversies in Tidal Marsh Ecology. Kluwer Academic Publishers, Dordrecht, 23-38.
- Vepraskas, M.J. and Faulkner, S.P. 2001. Redox chemistry of hidrics soils. In: Richardson, J.L., Vepraskas, M.J. (Eds) Wetland soils. Florida: Lewis Publishers; p. 85-107.
- Wentzel, M.C., Lötter, L.H., Loewenthal, R.E. and Marais, G.R. 1986. Metabolic behaviour of *Acinetobacter* spp. in enhanced biological phosphorus removal—a biochemical model. *Water SA* 12: 209–224.
- Willey, J.D. and Spivack, A. 1997. Dissolved silica concentrations and reactions in pore waters from continental slope sediments offshore from Cape Hatteras, North Carolina, USA. *Marine Chemistry* 56: 227-238.
- Wolaver, T.G. and Spurrier, J.D. 1988. The exchange of phosphorus between a euhaline vegetated marsh and the adjacent tidal creek. *Estuarine, Coastal and Shelf Science* 28: 203-214.
- Zeng, L., Chen, C. and Zhang, F.Y. 2004. Development of water quality model in the Satilla River Estuary, Georgia. *Ecological modeling*, 178: 457-482.

Ziegler, S., Velinsky D.J., Swarth, C.M. and Fogel, M.L. 1999. Sediment-water exchange of dissolved inorganic nitrogen in a freshwater tidal wetland. Technical report of the Jug Bay Wetland Sanctuary, Lothian, Maryland.

CHAPITRE VII

Seasonal variability of denitrification efficiency in northern salt marshes: An example from the St. Lawrence Estuary

Patrick Poulin, Emilien Pelletier and Richard Saint-Louis

Marine Environmental Research 63, 490-505

7.1 Abstract

In coastal ecosystems, denitrification is considered as a key process in removing excess dissolved nitrogen oxides and participating in the control of eutrophication process. Little is known about the role of salt marshes on nitrogen budget in cold weather coastal area. Although coastal salt marshes are known as important sites for organic matter degradation and nutrient regeneration, bacterial mediated nitrogen processes, such as denitrification, remain unknown in northern and sub-arctic regions, especially under winter conditions. Using labelled nitrogen (^{15}N), denitrification rates were measured in an eastern Canadian salt marsh in August, October and December 2005. Freshly sampled undisturbed sediment cores were incubated over 8 h and maintained at their sampling temperatures to evaluate the influence of low temperatures on the denitrification rate. From 2 to 12 °C, average denitrification rate and dissolved oxygen consumption increased from 9.6 to 25.5 $\mu\text{mol N}_2 \text{ m}^{-2} \text{ h}^{-1}$ and from 1.3 to 1.8 $\text{mmol O}_2 \text{ m}^{-2} \text{ h}^{-1}$, respectively, with no statistical dependence of temperature ($p > 0.05$). Nitrification has been identified as the major nitrate source for denitrification, supplying more than 80% of the nitrate demand. Because no more than 31 % of the nitrate removed by sediment is estimated to be denitrified, the presence of a major nitrate sink in sediment is suspected. Among possible nitrate consumption mechanisms, dissimilatory reduction of nitrate to ammonium (DNRA), metal and organic matter oxidation processes are discussed. Providing the first measurements of denitrification rate in a St. Lawrence Estuary salt marsh, this study evidences the necessity of preserving and restoring marshes. They constitute an efficient geochemical filter against an excess of nitrate dispersion towards coastal waters even under cold northern conditions.

7.2 Introduction

Denitrification is the dissimilatory reduction of nitrogen oxides (NO_2^- ; NO_3^-) to gaseous nitrogen (N_2). A large group of anaerobic bacteria of the genus *Pseudomonas*, synthesizing different types of reductases, can use reduced nitrogen oxides as electron acceptors in the absence of oxygen (Knowles, 1981). Denitrification is recognised as the key process to maintain nitrogen limitation in coastal waters (Howarth, 1988). It removes excess dissolved inorganic nitrogen loads (Seitzinger, 1988), decreasing the amount of fixed nitrogen available to the primary producers (Nixon, 1981). As a consequence, denitrification is important in controlling the eutrophication level in coastal environments (eg. Nowicki *et al.*, 1997) that are increasingly affected by anthropogenic nutrient inputs (Cloern, 2001). The exposure of terrestrial organic matter and nutrient inputs to estuaries (Gearing and Pocklington, 1990) leads to high primary productivity and high organic matter deposition, and therefore results in high bacterial mineralization, which causes a depletion of oxygen supplies in the sedimentary compartment (Duarte, 1995). Formed in the upper littoral zone of mid and high latitudes, coastal salt marshes are known as a major feature of macrotidal estuaries (Jickells and Rae, 1997). Affected strongly by tidal flooding and by riverine runoff, marsh areas are recognised to act as an important bioprocessor of nitrogen species (Aziz and Nedwell, 1986) which play many critical roles of ecological and economical values (Boorman, 1990). Although the nitrogen cycle in North-West Atlantic Coast and Western Europe temperate salt marshes (Kaplan *et al.*, 1979; Aziz and Nedwell, 1986; Koch *et al.*, 1992; Thompson, 1995; Eriksson *et al.*, 2003) has been studied extensively, our understanding of the dynamic of sub-arctic marsh environments is still incomplete, specially during winter time when sea ice covers littoral area. There is still lack of knowledge about biogeochemical processes in these icy environments, especially the nitrogen cycle and the rate of microbial-mediated nitrogen transformations such as denitrification. As the first step toward predicting decennial behaviour of cold coastal ecosystems under the actual scenario of global coastal eutrophication (Cloern, 2001; Jickells, 2005), it is essential to determine rates and pathways via which fixed nitrogen is metabolised by bacteria.

The main objective of this study is to evaluate seasonal denitrification rates in a northern salt marsh subject to frozen conditions for four months of year. Using labelled nitrate ($^{15}\text{NO}_3^-$) (Nielsen, 1992), denitrification rates were measured in Pointe-au-Père salt marsh sediment (St. Lawrence Estuary, Québec, Canada) in August, October and December 2005; with weather conditions corresponding to summer, fall and winter, respectively. Freshly sampled intact cores were incubated under *in situ* temperatures to evaluate the influence of temperature on N_2 , dissolved inorganic nitrogen (DIN) and O_2 fluxes resulting from denitrification and mineralization processes. During the late experiment in December, sediment cores were collected under a thin ice cover to quantify denitrification rates under the coldest conditions occurring in this coastal region. The quantitative significance of denitrification as well as relative contribution of biochemical processes, such as organic matter mineralization to the cold salt marsh nitrogen cycle, has been discussed. It is the first time to directly measure the denitrification rate in a St. Lawrence Estuary salt marsh and estimate the relative importance of denitrification as a nitrate removal process in northern estuaries.

7.3 Materials and methods

7.3.1 Studied site

The Pointe-au-Père salt marsh ($48^\circ 30.30'\text{N}$, $68^\circ 28.30'\text{W}$) is located on the south shore of the St. Lawrence Estuary in the city of Rimouski (Québec, Canada) (Fig. 1). This marsh has been part of the Pointe-au-Père National Wildlife Area protected by Canadian Wildlife Service (Environment Canada) since September 2002. Confined in an elongated basin parallel to the main Estuary axis and sheltered from wave actions by a longitudinal Palaeozoic structure, this 22.6 ha marsh is dominated by areas with homogenous emergent macrophyte (*Spartina alterniflora*) communities surrounded by vegetation-free network creeks. Due to its low slope, the floodwater complexly spreads over marsh area during semi-diurnal cyclic tidal excursion; tidal water enters by a large inlet at the western border, progresses laterally and smoothly over mud flats, as energy of the incoming tide is dissipated by friction on the inner bay. Located in a partly urbanised watershed, this marsh receives nitrogenous inputs in micro-molar concentrations from both agricultural and urban

runoff (Av \pm SD; 7.29 ± 16.43 kg DIN d $^{-1}$). This freshwater runoff enters the salt marsh by two main drainage channels along the south-east border (0.28 ± 0.59 m 3 s $^{-1}$). In addition, the St. Lawrence coastal zone is subject to important seasonal variations, which affects water temperature and salinity in response to heat flux and freshwater discharge. One of the main features of Saint-Lawrence cold salt marshes is the formation of sea ice that begins in early December and persists until April. This ice cover plays an important role in littoral ecosystems. Although sea ice erodes tidal flats, it protects the intertidal zone from wave action and generates singular sedimentary structures (Dionne, 1998; Drapeau, 1992; Serodes and Dubé, 1983).

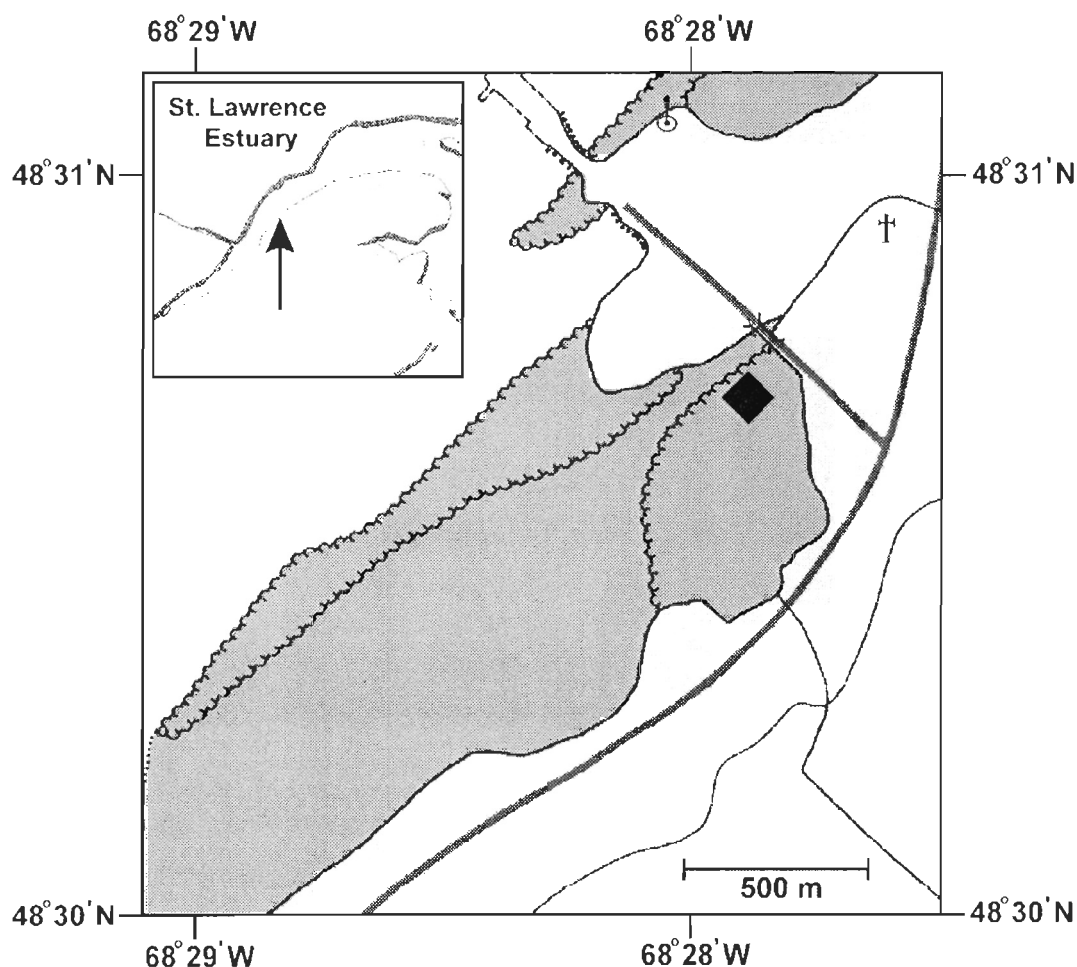


Figure VII-1 Map of Pointe-au-Père salt marsh located along the St-Lawrence Estuary south shore in Rimouski. The white area represents the infra-littoral zone, dark grey area the inter-tidal zone and light grey area the supra-littoral zone. The black square represents the 10-m 2 sampling area.

7.3.2 Sampling procedure

For each experiment (carried out in August, October and December 2005), 18 sediment cores (5 to 10 cm long x 9.8 cm i.d.) were collected at low tide in the same 10 m² area showing homogenous and specific surface characteristics (Fig. 1) using a tubular aluminium corer (100 cm long x 9.8 cm i.d.). To minimize perturbation of superficial sediment, the corer was slowly pushed into the sediment and the core was recovered using a small shovel. Each sediment core was delicately truncated at 3 cm below the sediment surface, to obtain a 3-cm long x 9.8 cm i.d. core, and was carefully transferred to a Plexiglas tube (14.5 cm long x 9.8 cm i.d.) later used as incubation chambers. Tubes with cores were transported to the laboratory within 30 minutes to minimize alteration of natural biogeochemical equilibria, and wrapt in aluminium foil to avoid photochemical reactions. In addition, 50 L of surface sea water was collected from the Pointe-au-Père biological station pier (Fig. 1) and stored in an acid pre-cleaned polypropylene bottle to perform incubation; whose salinity, dissolved oxygen and nitrate level is 25 ± 2 , 10 ± 2 mg l⁻¹ and 1.8 µM (August) ~ 14.7 µM (December), respectively.

7.3.3 Laboratory incubations

In the laboratory, tubes were placed in a temperature controlled room set at the temperature measured in sediment cores at the sampling site (i.e. 12, 6, and 2 °C for August, October and December, respectively). The tubes were labelled from 1 to 18 and sealed at the bottom with rubber stoppers. Tubes 1 to 8 were used for denitrification measurements, tubes 9 to 12 were used for nitrate (NO₃⁻) and ammonium (NH₄⁺) flux measurements whereas tubes 13 to 16 were used for dissolved oxygen (O₂) flux measurements. These 16 capped tubes (named incubation chambers) were incubated in the dark, using a large temperature-controlled water bath equipped with a stirring system (shaking table type), set at the temperature corresponding to the sampling season. The incubation period was fixed at 8 h to avoid expected development of hypoxic conditions ([O₂] < 2 mg l⁻¹) in the overlying water layer, since preliminary data obtained over the last three years showed that Pointe-au-Père salt marsh water column is year around well oxygenated. The remaining two sediment cores, kept in tubes 17 to 18, were freeze-dried

and homogenised for determination of sediment characteristics, including carbon and nitrogen element, particle size, trace metal and total hydrolysable amino acid (THAA).

7.3.4 Denitrification activity

For the denitrification rate determination, seawater (500 ml) enriched with 35 to 45 μM K^{15}NO_3 (98 atom % $^{15}\text{NO}_3$, Aldrich) was transferred in tubes 1 to 8, giving a water layer of about 7 cm height and an air head-space of \sim 2 cm (281 ml). The concentration of NO_3^- in typically impacted salt marsh water was \sim 20 μM . Tubes were capped with rubber stoppers equipped with gas-tight sampling ports and stirred for 10 min using a stirring table set at \sim 60 RPM to ensure homogenization of spiked nitrate. Then, a 5-ml water sample was sampled and replaced by ambient air (using 5-ml gas-tight syringe) to measure the initial concentration of NO_3^- and therefore the initial concentration of $^{15}\text{NO}_3^-$ was calculated. Tube air head-space was sampled (using a 10 μl gas-tight syringe) to measure the initial N_2 isotopic composition. After an 8-h incubation period, sediment cores were manually shaken for 2 min in order to equilibrate pore water gases with the overlying water. Air head-space of each chamber was sampled once again to measure final N_2 isotopic composition. Before each sampling, the gas-tight syringe and the GC-IRMS injection port were flushed with helium. After collection, air samples were immediately introduced in the GC gas port for isotopic composition determination to avoid a gas storage step and contamination risks.

7.3.5 Nitrogen species and dissolved oxygen fluxes

The procedure described previously was applied to the 8 remaining incubation tubes, but labelled K^{15}NO_3 was replaced by unlabelled KNO_3 . These chambers were incubated without gas head-space and were sampled hourly during 8 h, using 5 and 25 ml gas-tight syringes. For NO_3^- flux measurements, water samples (5 ml) were taken from tubes 9 to 12, transferred into 5-ml cryovials and stored at -80°C for further analysis. The same procedure was applied to measure NH_4^+ fluxes except that water samples were analysed immediately after sampling. The remaining four chambers (13 to 16) were used for O_2 flux measurements as 25-ml water samples were transferred in volumetric glass

bottles and analysed without delay. To avoid depressurisation in chambers, sampled water was replaced by an identical volume of ambient air.

Using denitrification rate measurement via direct determination of air head-space N₂ isotopic enrichment from immersed sediments (Nielsen, 1992) can avoid some of the problems associated with indirect approaches (e.g. Sorensen, 1978). However, despite their advantages, the labelled N₂ flux technique suffers of some artefacts mainly caused by the non-equilibrium conditions imposed by closed chambers (Hammersley and Howes, 2005), particularly for O₂. Since sediment cores were incubated without considering diurnal tidal inundation and dewatering cycle, photosynthetic O₂ production as well as atmospheric advection, sedimentary O₂ supply was blocked. This artefact could alter chamber chemical conditions (affecting the redox structure of sediment core and the equilibrium between dissolved ionic compounds in the pore water and onto sedimentary particles), and affects the balance between aerobic and anaerobic heterotrophy as well as the overall measured nitrification-denitrification rates (Risgaard-Petersen, 2003). By opting for an experimental design including short incubation period, relatively large gas headspace and water thicknesses, we minimised measurement errors and artefacts linked to closed incubation chambers.

7.3.6 Analyses

Isotopic composition of air head-space N₂ (¹⁴N¹⁴N, ¹⁴N¹⁵N and ¹⁵N¹⁵N) was determined using a gas chromatograph/combustion/isotope ratio mass spectrometer system (GC/C/IRMS Delta XP Plus[®], Thermo Finnigan equipped with a Conflo III interface). Gas samples (10 µl) were injected manually in the GC inlet and nitrogen species were separated isothermally at 125 °C by gas chromatography using a DB5 30 m capillary column (0.25 mm i.d.) with helium as the vector gas and were combusted in an oxidation and reduction furnace at 850 and 650 °C respectively. The gas samples were then passed through a cryogenic trap (liquid nitrogen) to remove water vapour and condensable gases followed by the alternative introduction of pure N₂ reference gas and N₂ samples into the mass spectrometer for ¹⁴N¹⁴N, ¹⁴N¹⁵N and ¹⁵N¹⁵N peaks area determination. The retention time for N₂ was 150 sec and mass peaks were integrated over 120 sec.

Dissolved O₂ was measured using the standard Winkler titration method (Strickland and Parson, 1968). NO₃⁻ dosages were made by classical colorimetric technique (Strickland and Parson, 1968) using an automated analytic Bran+Luebbe AA3® platform whereas NH₄⁺ concentrations were determined using a micro-plate base fluorometric technique (Poulin and Pelletier, 2006). Sediment core elementary analyses for carbon and nitrogen (C_{org}/N_{tot}) were performed with a ECS 4010 Costech® instrument equipped with a zero blank auto sampler, using certified sediment sample ($n = 10$) NIST-1941b as a reference, whereas granulometric analyses were done with Coulter® counter model LS13320C. Trace metals (Mn and Fe) were measured in 0.5 g dry sediment samples according to Anschutz *et al.*(2000). Extraction was carried with 35 ml of 1 N HCl for 6 h. The solutions were centrifuged, surnatant was diluted in 1 % HCl and analysed in normal mode with an inductively coupled plasma mass spectrometer (ICP-MS Agilent® 7500c) equipped with a micro-nebulizer. Metals were quantified with an external linear calibration curve established from standard solutions (Multielements standards solution IV. Fluka Chemie, Sigma-Aldrich). Total hydrolysable amino acids (THAA) were measured in 0.5 g freeze-dried, homogenised sediment samples. After hydrolysis with 10 ml of 6 N HCl at 100 °C for 24 h, the supernatant acid solution was centrifuged, diluted and neutralized with 2 N NaOH. The solutions were analysed on a Shimadzu® LC 10AD VP HPLC system using a Agilent® C-18 column (4.6 X 250 mm, 5 µm) and a Water® 470 fluorescence detector ($\lambda_{\text{ex}} = 230$ nm. $\lambda_{\text{em}} = 445$ nm) after derivatisation with o-phthaldialdehyde and 2-mercaptoethanol (Lindroth and Mopper, 1979) using phosphate buffer and methanol gradient. Individual amino acids were identified and quantified using amino acid standard solution (Sigma®) which contained 21 amino acids and ammonium chloride.

7.3.7 Calculations

Total denitrification rates (Dt) were calculated from chamber air-space ¹⁵N enrichment according to Nielsen (1992). The labelled ¹⁵N concentration was estimated by multiplying its isotopic ratios (¹⁴N/¹⁵N/total N₂ and ¹⁵N/¹⁵N/total N₂) by the calculated N₂ concentration in the air trapped in the head-space and in water layer knowing the

distribution coefficient of N₂ in sea water as a function of temperature (Weiss, 1970). NO₃⁻ denitrification rates coming from overlying water (Dw) and denitrification rates of NO₃⁻ produced within the sediment by nitrification (Dn) were calculated using equations below. These equations require three main assumptions: 1) the total amount of ¹⁴N¹⁴N inside the incubation chamber does not change during the sample collection period, 2) the ¹⁵N labelling of the NO₃⁻ in the sediment is uniform, 3) ¹⁴N¹⁵N and ¹⁵N¹⁵N constitute 0.7299 % and 0.001 % of total N₂ in the air (Nielsen, 1992).

$$D15 = (^{14}\text{N}^{15}\text{N}) + 2(^{15}\text{N}^{15}\text{N}) \quad (1)$$

$$D14 = D15 \times (^{14}\text{N}^{15}\text{N}) / 2(^{15}\text{N}^{15}\text{N}) \quad (2)$$

$$Dw = D15 \times [^{14}\text{NO}_3^-] / [^{15}\text{NO}_3^-] \quad (3)$$

$$Dt = D15 + D14 \quad (4)$$

$$Dn = Dt - Dw \quad (5)$$

The ¹⁴NO₃⁻ concentrations were determined in overlying water in incubation chambers before ¹⁵NO₃⁻ addition whereas ¹⁵NO₃⁻ concentrations were measured as a concentration increase in water after the addition.

Diagenetic alteration of sedimentary amino acids was assessed using the Degradation Index (DI) developed by Dauwe and Middelburg (1998) and Dauwe et al. (1999). This index is based on the first axis of a Principal Component Analysis (PCA) of the amino acid composition and summarizes, in one variable, the relative cumulative variation of 14 amino acids (aspartic acid, glutamic acid, serine, histidine, threonine, arginine, glycine, tyrosine, alanine, methionine, valine, phenylalanine, isoleucine and leucine). DI values were calculated from amino acids average molar concentration, standard deviation and predetermined coefficient factors (i.e. first axis of the Principal

Component Analysis from the comprehensive data set of Dauwe et al., 1999). The DI sign indicates a depletion (-) or an enrichment (+) of labile organic nitrogen protein in sediment.

Pearson correlations were performed in first instance to assess the relationship between pairs of variables considering correlation significance at $p < 0.05$ level. Thereafter a One-Way Analysis of Variance (ANOVA) was performed to test the significant effect of a fixed factor (temperature) on dependant variables (denitrification, oxygen and nitrate consumptions and ammonification). To isolate groups that differed from the others, a Tukey post-hoc test was performed. When ANOVA assumptions were not respected, a Kruskal-Wallis One-Way Analysis of Variance on Ranks was performed followed by a Dunn's post-hoc test. Differences between groups were considered significant at the $p < 0.05$ level. Comparisons of means were performed with Sigma Stat[®] version 3.11 from SyStat Software Inc.

7.4 Results

Sediment analysis revealed that all cores exhibited quite uniform characteristics with organic carbon abundance ranging from 6.5 to 9.0 %, C/N values ranging from 13.2 to 19.4, average particle size ranging from 109 to 198 μm , manganese and iron concentrations ranging from 0.04 to 0.08 $\mu\text{mol g}^{-1}$ (d.w.) and from 4.17 to 4.84 $\mu\text{mol g}^{-1}$ (d.w.), respectively (Table 1).

Total denitrification rates ($Dt = Dw + Dn$) measured in Pointe-au-Père salt marsh sediment varied from 5.73 to 15.01 $\mu\text{mol N}_2 \text{ m}^{-2} \text{ h}^{-1}$ at 2 °C, from 11.18 to 24.62 $\mu\text{mol N}_2 \text{ m}^{-2} \text{ h}^{-1}$ at 6 °C, and from 18.36 to 42.24 $\mu\text{mol N}_2 \text{ m}^{-2} \text{ h}^{-1}$ at 12 °C. Measured Dt rates increased with temperature but this trend is not statistically significant ($p > 0.05$) (Fig. 2) due to a large range of values observed for each series of measurements. For the same initial nitrate addition, Dt rates remained important even under the lowest temperature since the average rate at 2 °C was only 2.6 fold lower than the one determined at 12 °C. Denitrification coming from overlying water (Dw) averaged 15, 6 and 2 % of Dt rates at 2, 6 and 12 °C, respectively. Although representing a minor contribution to Dt rates, Dw values were statistically correlated to temperature ($p = 0.001$). Denitrification produced

within the sediment by nitrification (D_n) represented the main contribution to D_t rates. Statistically correlated to temperature ($p = 0.038$), D_n contributed for 85, 94 and 98 % of D_t rates at 2, 6 and 12 °C, respectively.

Tableau VII-1 Geochemical characteristics (mean values) of sediment samples collected in St. Lawrence Estuary salt marsh in 2005.

Sample size	Grain (y/m/d)	N (μm)	C (%)	C/N	[Mn] (μmol g ⁻¹)	[Fe] (μmol g ⁻¹)	[AA] (μmol g ⁻¹)	DI
2005-08-10	109.6	0.55	6.53	13.96	0.04	4.34	58.28	-0.66
2005-08-10	109.5	0.54	9.00	19.35	0.04	4.36	49.27	-0.69
2005-08-10	ND ¹	ND	ND	ND	ND	ND	59.58	-0.66
2005-10-04	198.5	0.61	6.91	13.19	0.07	4.17	ND	ND
2005-10-04	167.4	0.56	8.18	17.01	0.04	4.52	ND	ND
2005-12-06	156.5	0.55	6.96	14.86	0.08	4.63	ND	ND
2005-12-06	145.3	0.56	7.67	16.11	0.08	4.84	ND	ND

Dissolved oxygen sediment consumption rates also showed an increasing trend with temperature, which ranged from 1.25 to 1.43 mmol O₂ m⁻² h⁻¹ at 2 °C, from 1.59 to 1.70 mmol O₂ m⁻² h⁻¹ at 6 °C, and from 1.63 to 1.94 mmol O₂ m⁻² h⁻¹ at 12 °C; but this was not statistically significant ($p > 0.05$) (Fig. 3). However, sediment nitrate consumption and ammonium generation rates were both statistically correlated to temperature ($p = 0.001$ and 0.04, respectively). Between 2 and 6 °C, nitrate and ammonium fluxes remained statistically identical (ranging from 59.25 to 139.41 μmol NO₃⁻ m⁻² h⁻¹ and 2.61 to 69.70 μmol NH₄⁺ m⁻² h⁻¹) whereas they significantly increased at 12 °C (215.52 to 296.79 μmol NO₃⁻ m⁻² h⁻¹ and 205.56 to 248.62 μmol NH₄⁺ m⁻² h⁻¹) (Fig. 4). This observation is expected

to be closely linked to the increase of microbial activity with the temperature (Sundback *et al.*, 2000). In addition, a significant linear correlation was observed between nitrate consumption and ammonium generation rates ($r = 0.90$), which indicated a possible mechanistic relationship between these two processes in salt marsh sediment.

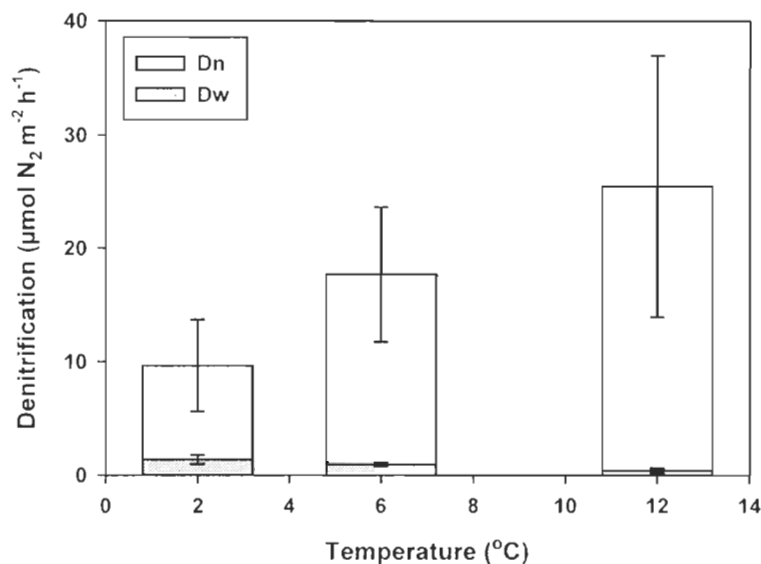


Figure VII-2 Contribution of denitrification rates produced within the sediment cores by nitrification (Dn in grey) and denitrification rates coming from overlying water (Dw in black) to total denitrification (Dt) as a function of incubation temperatures. Values represent mean \pm SD ($n = 8$).

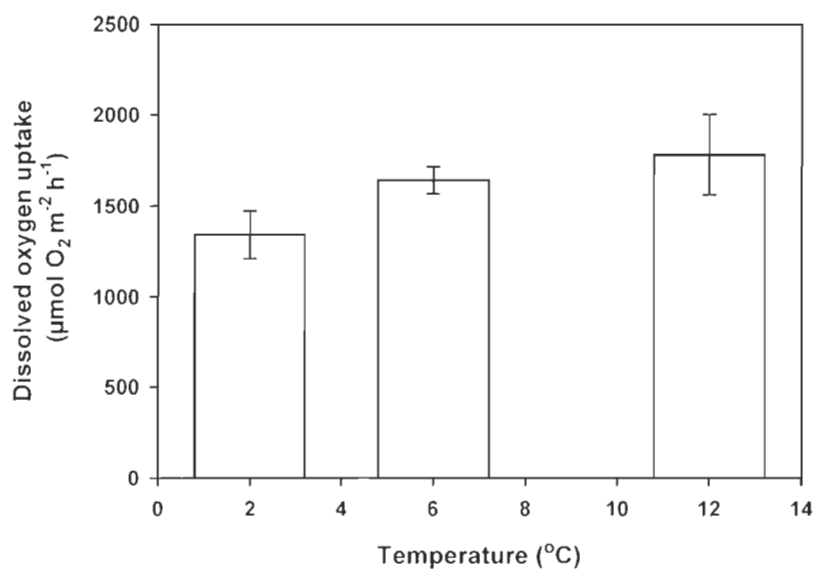


Figure VII-3 Dissolved oxygen uptake rates as a function of incubation temperatures. Values represent mean \pm SD ($n = 4$).

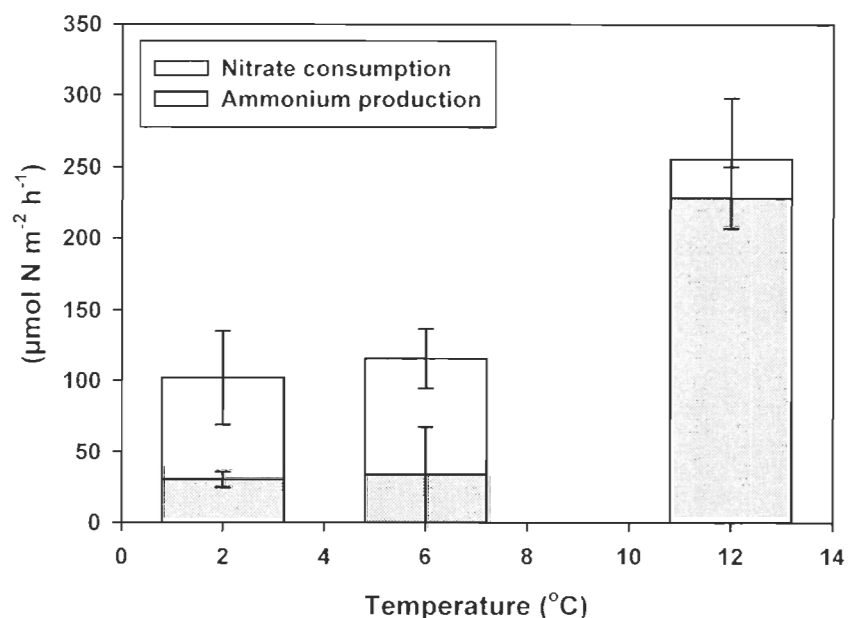


Figure VII-4 Nitrate consumption rates (in grey) and ammonium production rates (black) as a function of incubation temperatures. Values represent mean \pm SD ($n = 4$).

A typical HPLC profile of total hydrolysable amino acids (THAA) is given in figure 5 showing the dominance of aspartic and glutamic acids, serine, threonine and alanine in salt marsh sediment. THAA concentrations measured in triplicate on one core sampled during summer time (early in August 2005), reached $55.71 \pm 5.61 \mu\text{mol g}^{-1}$ ($n = 3$). The average DI value calculated for Pointe-au-Père salt marsh sediment (-0.67 ± 0.02 ; $n = 3$) was below the range of values usually obtained for coastal sediments (from -0.35 to 1.01) as reported by Dauwe *et al.* (1999) indicating that organic matter in sediment was in an advanced decomposition state (Table 1).

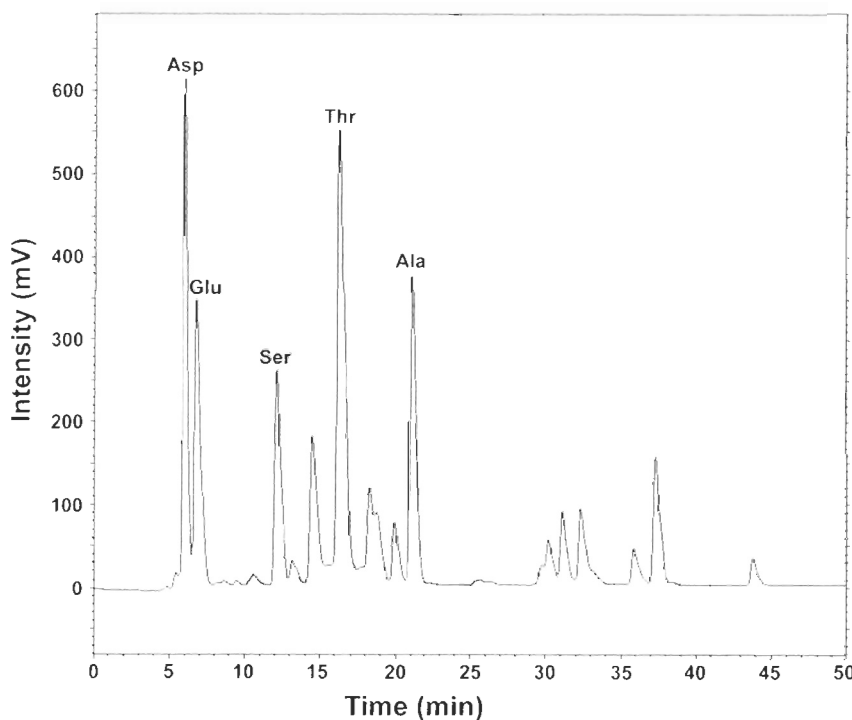


Figure VII-5 Typical HPLC chromatogram of THAA extracted from Pointe-au-Père salt marsh sediment sampled in August 2005. main identified amino acids are aspartic acid (Asp), glutamic acid (Glu), serine (Ser), threonine (Thr) and alanine (Ala).

7.5 Discussion

A large body of information is available on factors influencing denitrification in coastal marine environments (see review by Herbert, 1999). The three main factors influencing benthic denitrification are temperature, supplies of NO_3^- and availability of organic carbon (Smith *et al.*, 1985; Yoon and Benner, 1992; Tuominen *et al.*, 1998). Despite these factors, denitrification rates values measured in our cold salt marsh sediments are comparable with those obtained by other workers along the North-West Atlantic Coast and in Western Europe temperate salt marshes (e.g. Great Sippewissett Marsh (New England, USA) 0-357 $\mu\text{mol N}_2 \text{ m}^{-2} \text{ h}^{-1}$, Kaplan *et al.*, 1979; Colne Point Marsh (England) 2.6-6.4 $\mu\text{mol N}_2 \text{ m}^{-2} \text{ h}^{-1}$, Aziz and Nedwell, 1986; Torridge Marsh (England) 2.51-59.0 $\mu\text{mol N}_2 \text{ m}^{-2} \text{ h}^{-1}$, Koch *et al.*, 1992; New Port Marsh (North Carolina, USA) 0-14.6 $\mu\text{mol N}_2 \text{ m}^{-2} \text{ h}^{-1}$, Thompson., 1995; Lagoon of Venise (Italia) 0-160 $\mu\text{mol N}_2 \text{ m}^{-2} \text{ h}^{-1}$, Eriksson *et al.*, 2003). Although a part of the variation in published denitrification rates could be related to differences in experimental designs, values reported here indicate that the

denitrifying process is efficient in cold salt marsh sediments, even under winter conditions. Due to the lack of a significant relationship between mean Dt rate and temperature of incubation, the direct effect of temperature was difficult to assess when dissolved oxygen and nutrient concentration variations in the overlying water were taken in account. Temperature effects were weak since mean Dt rate at 2 °C was only 2.6 fold lower than during incubation at 12 °C (Fig. 2). Although the high variability of measured denitrification rates needs to be considered to explain the lack of significant relationship between mean Dt rates and temperature, the incidence of coupled bacterial processes and favourable chemical conditions such as high NO_3^- availability should be considered. In addition, this result could indicate the combined contribution of a cold-adapted microbial population, which dominated winter time moderate denitrification activity, with a higher temperature optimum population being active during summer (Blackburn and Sorensen, 1988). However, no information is available on bacterial population succession in the study area.

Denitrification is recognised to be limited by NO_3^- supplies and hence by nitrification in coastal sediments (Jenkins and Kemp, 1984). In our study, nitrification is the main source of NO_3^- for denitrification, with an average Dn rate contribution reaching 98 % of Dt rate at 12 °C. Since Dn was statistically correlated to temperature, this result suggests that the coupling between nitrification and denitrification is thermo-dependant and consequently could be more important under summer than winter conditions in a cold salt marsh environment. The relative contribution of Dw to Dt could therefore explain the observed seasonal trend of denitrification rates. Dw rates, expected to increase with the *in situ* NO_3^- concentration, was negatively related to temperature ($p = 0.001$). Because *in situ* NO_3^- concentration was higher in December (14.7 μM) than in August (1.8 μM) in the St. Lawrence Estuary surface water, due to the incidence of sea ice on primary producers (data not shown), Dw contribution to Dt tends to mask seasonal denitrification variation (since the same $^{15}\text{NO}_3^-$ amendment was used for each experiment). These results indicate a control of Dw by NO_3^- concentrations and suggest that NO_3^- could play a substantial role in Dt limitation in cold salt marsh environment.

Aerobic respiration is related to temperature in coastal sediment (Thamdrup *et al.*, 1998; Silverberg *et al.*, 2000). However, no statistical relationship can be demonstrated ($p > 0.05$) between oxygen consumption rates and temperature in our study (Fig. 3). We hypothesize that aerobic microbial mineralization processes, predominantly responsible for oxygen consumption, are affected mainly by the quality and quantity of sedimentary organic matter and much less by temperature. Even if elementary analysis revealed no significant trend in organic carbon content with seasons (Table 1), more organic matter is available in salt marsh sediment during fall than at the end of summer (Valiela *et al.*, 1976). Since available organic matter may increase during autumn period when dead vegetation is added to marsh, it could have increased the overall sediment oxygen consumption during incubation carried in October as well as in December. Thus, carbon availability is low in summer but potential oxygen consumption rates are high because of warmer temperatures, while in fall/winter, carbon availability is high but potential rates are limited by colder temperatures. Alternatively, a greater proportion of carbon degradation could take place during the warmer months via alternative oxidation pathways such as sulphate, iron or manganese reduction.

Average NO_3^- consumption (molecular ratio) represented 46, 42 and 86 % of O_2 respiration rates at 2, 6 and 12 °C, respectively, showing that NO_3^- plays a determining role as a terminal electron acceptor for organic matter mineralization. On the other hand, we estimated that no more than 31 % of NO_3^- removed by salt marsh sediment at 6°C was subsequently denitrified (based upon the highest Dt/NO_3^- consumption ratio). Because nitrate consumption largely exceeded denitrification, alternative NO_3^- reduction pathways in sediment are suspected. Dissimilatory NO_3^- reduction to NH_4^+ (DNRA) by heterotrophic bacteria has been reported as very important NO_3^- reduction pathway in shallow coastal environments (An and Gardner, 2002). On a molar ratio basis, NH_4^+ average flux reached 89 % at 12 °C and 29 % at 6 and 2 °C of the average NO_3^- consumption (Fig. 4). This result and the observed significant positive correlation between nitrate consumption and ammonium generation rates ($r = 0.90$) could indicate that a coupling exists between these two processes in cold salt marsh sediment. However, before considering this coupling, we need to evaluate the relative contribution of both ammonification processes (NH_4^+ bacterial

production from organic matter and DNRA processes) on NH_4^+ generation rates. Although we did not measure $^{15}\text{NH}_4^+$ enrichment from $^{15}\text{NO}_3^-$ amendment in this study (to determine DNRA rates), the calculated DI (-0.67) from THAA measurement as well as the C/N ratio (13.2-19.4) of organic matter suggest that marsh sediment possessed only a small amount of labile organic material readily available for biologic mineralization (Table 1).

Mainly related to bacterial, phytoplanktonic and zooplanktonic cell plasma material (Dauwe and Middelburg, 1998), aspartic acid, glutamic acid, serine, threonine and alanine stand for this labile organic matter pool (Fig. 5). Although amino acids from proteins are the major organic nitrogen source to microbial ammonification (Pantoja and Lee, 2003), the quantitative mineralization of THAA present in marsh sediment ($55.71 \pm 5.61 \mu\text{mol g}^{-1}$) can not be used to explain the observed NH_4^+ flux ($228.51 \pm 21.67 \mu\text{M NH}_4^+ \text{ m}^2 \text{ h}^{-1}$). Thus, we suggest DNRA constitute a significant nitrogen recycling process in this sedimentary environment. This assumption is supported by a study carried by King and Nedwell (1985) which shows that NO_3^- concentration contributed to determine either how much NO_3^- is lost to N_2 or preserved as NH_4^+ in anaerobic salt marsh sediment. These authors demonstrated that a low NO_3^- concentration ($[\text{NO}_3^-] < 236 \mu\text{M}$) can enhance DNRA whereas a high NO_3^- concentration promoted denitrification. In addition, Joye and Hollibaugh, (1995) showed that sulphur compounds can inhibit denitrification and enhance DNRA. Since only a low $^{15}\text{NO}_3^-$ concentration was used in this study (corresponding to natural level) and particularly because the presence of sulphur compounds was suspected in our salt marsh samples (presence of hydrogen sulphide odour during sampling) DNRA should be investigated in cold salt marsh sediment as a key NO_3^- removal process.

Another NO_3^- sedimentary sink that can be invoked in this study is the NO_3^- reduction by Mn^{2+} . In anoxic sediment, dissolved oxidants present in pore water are recognised to be actively used by heterotrophic bacteria as terminal electron acceptor for OM oxidation, leading to the reduction of oxidized metals. Partially reduced metal, such as Mn^{2+} , can be re-oxidised to MnO_2 by NO_3^- in the absence of oxygen (Luther *et al.*, 1997). Although this abiotic process could contribute to nitrogen cycling, reduced Mn likely played a marginal contribution in measured NO_3^- flux considering low Mn^{2+} concentration

(0.04-0.08 $\mu\text{mol g}^{-1}$) measured in salt marsh sediment (Table 1) compared to St. Lawrence Estuary surface sediment (13.4- 92.8 $\mu\text{mol g}^{-1}$; Anschutz *et al.*, 2000).

Results based on field and laboratory studies (Simek and Cooper, 2002) assessed that denitrification processes measured in cold salt marshes would not be a significant source of N_2O . These authors showed that denitrification end products were mostly determined by sediment pH with low $\text{N}_2\text{O}/\text{N}_2$ production ratios in more neutral sediment. Because pH of flooding estuarine water in the Pointe-au-Père marsh varied from 6.5 to 8.5 (data not shown), denitrification should mostly produce N_2 . Although both environments might be different, dinitrogen was the exclusive product of denitrification in the Tagus Estuary salt marsh sediment (Cartaxana and Lloyd, 1999). High organic content and low oxygen concentration were assumed to increase the demand for electron acceptors in salt marsh sediment, preventing N_2O emission by denitrification. In addition, a recent study on a coastal embayment located in Eastern Canada reported very low N_2O production from denitrification ranging from undetectable to 40 $\text{pmol N}_2\text{O l}^{-1} \text{d}^{-1}$ (Punshon and Moore, 2004).

The relatively high microbial organic matter degradation propensity observed in salt marsh surface sediment (Table 1) coupled with high nitrate uptake capacity measured in this study argue for a significant role of salt marsh in estuarine annual N and C budget. The reduced vascular plant canopy and coarse salt marsh sediment favour the development of benthic microbial communities involved in N and C biochemical cycles (Aspen *et al.*, 2004). Nevertheless, since St. Lawrence Estuary marshes are affected strongly by erosion (Dionne, 1986), these areas actually might appear insignificant in regard to estuarine bottom sediment surface ($\sim 3000 \text{ km}^2$). While they represented only 90 km^2 in 1986 (Dionne, 1986), these marsh areas are becoming more vulnerable to increased erosive forces (Morisette, 2006). Thus, it is clear that marsh areas need restoration effort to recover a significant contribution to the whole St. Lawrence estuarine system because these ecosystems possess a strong nutrient regeneration potential. Concerning the nitrogen cycle, measured sedimentary denitrification and NO_3^- consumption rates on this study were, in average, ~ 6 times higher than rates measured in deep sediments of the St. Lawrence

marine system ($1.8\text{-}3.3 \mu\text{mol N}_2 \text{ m}^{-2} \text{ h}^{-1}$; and $13.9\text{-}25.5 \mu\text{mol NO}_3^- \text{ m}^{-2} \text{ h}^{-1}$; Wang *et al.*, 2003). In addition, assuming that 2.4 mol of N_2 are produced through the mineralization of 6 g of elemental carbon (Gottschalk, 1979), we can estimate the denitrification contribution to the carbon salt marsh cycle at $< 64 \mu\text{g C m}^{-2} \text{ h}^{-1}$ (using average summer time denitrification rate value). This carbon mineralization rate resulting from denitrification is 16 times higher than the one defined for the Laurentian Through by Wang *et al.* (2003) evaluated at $4.125 \mu\text{g C m}^{-2} \text{ h}^{-1}$ (based on a denitrification rate of $3.3 \mu\text{mol N m}^{-2} \text{ h}^{-1}$).

Because this study focused only on one specific site, we cannot extrapolate our results to the whole St-Lawrence Estuary intertidal system. On the other hand, these results combined to those of Wang *et al.*, (2003) support the idea that cold salt marsh environments appear to be an efficient year-round sinks for nitrate, which could contribute to the whole St. Lawrence estuarine denitrification capacity if actions are taken to increase substantially their surface. This study shows that denitrification accounts for a variable fraction of NO_3^- reducing processes and alternative pathways, such as DNRA, appear important in salt marsh sediment, especially during summer. Further investigations should be undertaken to explain the relative contribution of these two processes as well as seasonal changes in NO_3^- reducing bacterial population in this area. Considering that coastal wetlands are being lost worldwide (Boorman, 1999), our results highlight the importance of preserving and restoring northern salt marsh areas, as they are part of an efficient geochemical filter against nitrate dispersion towards coastal waters.

7.6 Acknowledgement

Authors acknowledge G. Drouin and G. Canuel for their technical support during laboratory and field works and reviewers for helpful suggestions. This research was supported by the Canada Research Chair program (E.P.) and the Natural Sciences and Engineering Research Council of Canada (NSERC Discovery grant). This paper is a contribution of Quebec-Ocean network.

7.7 References

- An, S.. Gardner, W.S.. 2002. Dissimilatory nitrate reduction to ammonium (DNRA) as a nitrogen link, versus denitrification as a sink in a shallow estuary (Laguna Madre/Baffin Bay, Texas). *Marine Ecology Progress Series*, 237, 41-50.
- Anchutz, P., Sundby, B., Lefrançois, L., Luther III, G.W., Mucci, A., 2000. Interactions between metal oxides and species of nitrogen and iodine in bioturbated marine sediments. *Geochimica et Cosmochimica Acta*, 64, 2751-2763.
- Aspen, R.J., Vardy, S., Paterson, D.M., 2004. Salt marsh microbial ecology: microbes, benthic mats and sediment movement. In: Fagherazzi, S., Marani, M., Blum, L.K. (Eds.), *The ecogeomorphology of tidal marshes. Coastal and Estuarine Studies*, American Geophysical Union, pp. 115-135.
- Aziz, S.A.A., Nedwell, D.B., 1986. The nitrogen cycle of an East Coast, U.K. saltmarsh: II. Nitrogen fixation, nitrification and denitrification, tidal exchange. *Estuarine, Coastal and Shelf Science*, 22, 689-704.
- Blackburn, T.H., Sorensen, J., 1988. *Nitrogen cycling in coastal marine environments*. John Wiley and Sons, New-York, pp.1-451.
- Boorman, L.A.. 1999. Salt marshes – Present function and future change. *Mangroves and Salt marsh*, 3, 227-241.
- Cataxana, P., Lloyd, D., 1999. N₂, N₂O and O₂ profiles in a Tagus Estuary salt marsh. *Estuarine, Coastal and Shelf Science*, 48, 751-756.
- Cloern, J.E., 2001. Our evolving conceptual model of the coastal eutrophication problem. *Marine Ecology Progress Series*, 210, 223-253.
- Dauwe, B., Middelburg, J.J., 1998. Amino acids and hexosamines as indicators of organic matter degradation state in North Sea sediments. *Limnology and Oceanography*, 43, 782-798.
- Dauwe, B., Middelburg, J.J., Herman, P.M.J., Heip, C.H.R., 1999. Linking diagenetic alteration of amino acids and bulk organic matter reactivity. *Limnology and Oceanography*, 44, 1809-1814.
- Dionne, J.C., 1986. Érosion récente des marais intertidaux de l'estuaire du Saint-Laurent. *Géographie Physique et Quaternaire*, 50, 307-323.
- Dionne, J.C., 1998. Sedimentary structure made by shore ice in muddy tidal-flat deposits, St. Lawrence Estuary, Québec. *Sedimentary Geology*, 116, 261-274.

- Duarte, C.M., 1995. Submerged aquatic vegetation in relation to different nutrient regimes. *Ophelia*, 41, 87-112.
- Drapeau, G., 1992. Dynamique sédimentaire des littoraux de l'estuaire du Saint-Laurent. *Géographie Physique et Quaternaire*, 46, 233-242.
- Eriksson, P.G., Svensson, J.M., Carrer, G.M., 2003. Temporal change and spatial variation of soil oxygen consumption, nitrification and denitrification rates in a tidal marsh of the Lagoon of Venise, Italy. *Estuarine, Coastal and Shelf Science*, 58, 861-871.
- Gearing, J.N., Pocklington, R., 1990. Organic geochemical studies in the St. Lawrence Estuary. In: El-Sabh, M.I., Silverberg, N. (Eds.), *Oceanography of a large-scale estuarine system, the St. Lawrence*. Springer-Verlag, New York. pp. 170-195.
- Gottschalk, G., 1979. *Bacterial Metabolism*. Springer-Verlag, New-York, pp.101-103.
- Hamersley, M.R., Howes, B.L., 2005. Evaluation of the N_2 flux approach for measuring sediment denitrification. *Estuarine, Coastal and Shelf Science*, 62, 711-723.
- Herbert, R.A., 1999. Nitrogen cycling in coastal marine ecosystems. *FEMS Microbial Reviews*, 23, 563-590.
- Howarth, R.W., 1988. Nutrient limitation of net primary production in marine ecosystems. *Annual Review of Ecology and Systematics*, 19, 89-110.
- Jenkins, M.C., Kemp, W.M., 1984. The coupling of nitrification and denitrification in two estuaries sediment. *Limnology and Oceanography*, 29, 609-619.
- Jickells, T.D., Rae, J.E., 1997. Biogeochemistry of intertidal sediment. In: Jickells, T.D., Rae, J.E. (Eds.), *Biogeochemistry of intertidal sediment*. Cambridge Environmental Chemistry Series. U.K., pp. 2-15.
- Jickells, T., 2005. External input as a contributor to eutrophication problems. *Journal of Sea Research*, 54, 58-69.
- Joye, S.B., Hollibaugh, J.T., 1995. Sulfide inhibition of nitrification influences nitrogen regeneration in sediment. *Science*, 270, 623-625.
- Kaplan, W., Valiela, I., Teal, J.M., 1979. Denitrification in salt marsh ecosystem. *Limnology and Oceanography*, 24, 726-734.
- King, D., Nedwell, D.B., 1985. The influence of nitrate concentration upon the end-product of nitrate dissimilation by bacteria in anaerobic salt marsh sediment. *FEMS Microbiology Ecology*, 31, 23-28.

- Knowles, R., 1981. Denitrification. In: Clark, F.E., Rosswall, T. (Eds.), Terrestrial Nitrogen Cycle. Processes, Ecosystem Strategies and Management Impact, Ecology Bulletin, Stockholm, pp. 315-330.
- Koch, M.S., Malby, E., Oliver, G.A., Bakker, S.A., 1992. Factor controlling denitrification rates of tidal mudflats and fringing salt marshes in South-west England. *Estuarine, Coastal and Shelf Science*, 34, 471-485.
- Lindroth, P., Mopper, K., 1979. High performance liquid chromatographic determination of subpicomole amounts of amino acids by precolumn fluorescence derivatization with *o*-phthaldialdehyde. *Analytical Chemistry*, 51, 1667-1674.
- Louchouarn, P., Lucotte, M., Canuel, R., Gagné, J.-P., Richard, L.-P., 1997. Sources and early diagenesis of lignin and bulk organic matter in the sediments of the Lower St. Lawrence Estuary and the Saguenay Fjord. *Marine Chemistry*, 58, 3-26.
- Lucotte, M., Hillaire-Marcel, C., Louchouarn, P., 1991. First-order organic carbon budget in the St. Lawrence lower Estuary from ^{13}C data. *Estuarine, Coastal and Shelf Science*, 32, 297-312.
- Luther, G.W., Sundby, B., Lewis, B.L., Brendel, P.J., Silverberg, N., 1997. Interactions of manganese with nitrogen cycle: alternative pathways to dinitrogen. *Geochimica et Cosmochimica Acta*, 61, 4043-4045.
- Morissette, A., 2006. Évolution côtière haute résolution de la région de Longue-Rive-Forestville, Côte Nord de l'estuaire maritime du Saint-Laurent. Mémoire, Université du Québec à Rimouski, Québec.
- Nielsen, L.P., 1992. Denitrification in sediment determined from nitrogen isotope pairing. *FEMS Microbiology Ecology*, 86, 357-362.
- Nixon, S.W., 1981. Remineralization and nutrient cycling in coastal marine ecosystems. In: Neilson, B.J., Cronin, L.E. (Eds.), *Estuaries and Nutrients*, Humana Press, Clifton, New Jersey, pp. 111-138.
- Nowicki, B.L., Kelly, J.R., Requintina, E., Keuren, D.V., 1997. Nitrogen losses through sediment denitrification in Boston Harbor and Massachusetts Bay. *Estuaries*, 20, 626-639.
- Pantoja, S., Lee, C., 2003. Amino acid remineralization and organic matter lability in Chilean coastal sediment. *Organic Geochemistry*, 34, 1047-1056.
- Poulin, P., Pelletier, E., 2006. Determination of ammonium using a microplate-based fluorometric technique. *Talanta*, in press.
- Punshon, S., Moore, R.M., 2004. Stable isotope technique for measuring production and consumption rates of nitrous oxide in coastal water. *Marine Chemistry*, 86, 159-168.

Risgaard-Petersen, N., 2003. Coupled nitrification-denitrification in autotrophic and heterotrophic estuarine sediment: On the influence of benthic microalgae. Limnology and Oceanography, 48, 93-105.

Seitzinger, S.P., 1988. Denitrification in fresh and coastal marine ecosystems: ecological and geochemical significance. Limnology and Oceanography, 33, 702-724.

Serodes, J.-B., Dubé, M., 1983. Dynamique sédimentaire d'un estran à Spartines. Le Naturaliste Canadien, 110, 11-26.

Silverberg, N., Bakker, J., Edenborn, H.M., Sundby, B., 1987. Oxygen profiles and organic carbon fluxes in the Laurentian Trough sediment. Netherlands Journal of Sea Research, 21, 95-105.

Silverberg, N., Sundby, B., Mucci, A., Zhong, S., Arakaki, T., Hall, P., Landen, A., Tengberg, A., 2000. Remineralization of organic carbon in eastern Canadian continental margin sediment. Deep-Sea Research Part II, 47, 699-731.

Simek, M., Cooper, J.E., 2002. The influence of soil pH on denitrification: Progress towards the understanding of this interaction over the last 50 years. European Journal of Soil Science, 53, 345-354.

Smith, C.J., DeLaune, R.D., Patrick, W.H., 1985. Fate of riverine nitrate entering an estuary: I. Denitrification and nitrogen burial, Estuaries, 8, 15-21.

Sorensen, J., 1978. Denitrification rates in marine sediment as measured by the acetylene inhibition technique. Applied Environmental Microbiology, 36, 139-143.

Strickland, J.D.H., Parson, T.R., 1972. A practical handbook of seawater analysis. Fisheries Research of Canada, Ottawa, pp.1-310.

Sundbäck, K., Miles, A., Göransson, E., 2000. Nitrogen fluxes, denitrification and role of microphytobenthos in microtidal shallow-water sediment, an annual study. Marine Ecology Progress Series, 200, 59-76.

Thamdrup, B., Würgler Hansen, J., Jørgensen, B.B., 1998. Temperature dependence of aerobic respiration in a coastal sediment. FEMS Microbiology Ecology, 25, 189-200.

Thompson, S.P., 1995. Seasonal pattern of nitrification and denitrification in a natural and a restored salt marsh. Estuaries, 18, 399-408.

- Tuominen, L., Heinanen, A., Kuparinen, J., Nielsen, L.P., 1998. Spatial and temporal variability of denitrification in sediment of the Northern Baltic Proper. *Marine Ecology Progress Series*, 172, 13-24.
- Valiela, I., Teal, J.M., Persson, N.Y., 1976. Production and dynamics of experimentally enriched salt marsh vegetation, below ground biomass. *Limnology and Oceanography*, 21, 245-252.
- Wang, F., Juniper, S.K., Pelegri, S.P., Macko, S.A.. 2003. Denitrification in sediment of the Laurentian Trough. St. Lawrence Estuary, Québec, Canada. *Estuarine, Coastal and Shelf Science*, 57, 515-522.
- Weiss, R.F., 1970. The solubility of nitrogen , oxygen and argon in water and seawater. *Deep-Sea Research*, 17, 721-735.
- Yoon, W.B., Benner, R., 1992. Denitrification and oxygen consumption in sediment of two Texas estuaries. *Marine Ecology Progress Series*, 90, 157-167.

CHAPITRE VIII

Microphytobenthos communities from pristine and impacted salt marshes of the St. Lawrence Estuary (Canada)

Michèle de Sève, Patrick Poulin, Emilien Pelletier and Karine Lemarchand

Submit to Science of the Total Environment

8.1 Abstract

Microphytobenthos (MPB) abundance and diversity were investigated in two northern salt marshes of the Lower St. Lawrence Estuary (eastern Canada) where a pristine salt marsh within a national park was compared with an impacted one (urban and agricultural runoffs). Samples were collected in surface sediment from low and high marsh areas at both studied sites. Based on MPB population composition, bacterial abundance, chlorophyll-*a*, phaeopigments and geochemical analyses (C_{org} , N_{tot} , granulometry, extracellular polymeric substances), the impacted high marsh area appeared to be significantly different from the impacted low marsh, and also from high and low areas of the pristine marsh. A higher diversity of diatom species was observed in the impacted high marsh area with a dominance of epipelic forms, in opposition to the dominant epipsammic forms at the other sites. Dominant epipelic species in sampling sites were *Diploneis interrupta*, *D. smithii*, *Gyrosigma fasciola*, *G. spenceri*, *Navicula cryptocephala*, *N. peregrina*, *N. radiosa* var. *tenella*, *N. salinarum*, *Nitzschia clausii* and *N. tryblionella*. Dominant epipsammic species were *Achnanthes delicatula*, *Navicula cryptocephala* and *Cocconeis disculus*. Statistical analyses showed that MPB density was mainly affected by nutrients availability (variance could be explained at 72% by the combined effect of C_{org} and N_{tot} concentration) while the relative abundance of epipelic and epipsammic species was related to sediment grain size. Estimated surface biomass ranged from 11 to 71 g C m⁻² in the pristine marsh and from 24 to 486 g C m⁻² in the impacted one. This study provides for the first time the MPB composition coupled to geochemical characteristics of surface sediment in two northern marshes and underlines potential effects of anthropogenic alterations of coastal areas on MPB diversity.

8.2 Introduction

Estuaries and coastal wetlands are critical transition zones linking terrestrial and marine habitats. Salt marshes depict highly dynamic environments and are among the most productive ecosystems in the world (Woodward and Wui 2001). They are characterized by high primary production rates and by intense remineralisation processes within surface sediment (Billen and Lancelot, 1988). In addition, they act as natural filters of allochthonous pollutants and actively transform nutrient loads received from the watershed before their introduction in the coastal environment (Mason *et al.*, 2003; Baldwin and Mitchell, 2000). The environmental significance of these particular ecosystems is now widely recognized and protection efforts have been deployed as impacts of human activities on the ecology of the coastal zones became obvious in the last decades (Page *et al.*, 1995; Boorman, 1999; Cloern, 1999).

Sediment-dwelling microalgae and phototrophic bacteria (collectively named microphytobenthos hereafter, MPB) play a central role in the functioning of coastal salt marshes through their contribution to biogeochemical cycles (Liehr *et al.*, 1994; Troccaz 1996, Albertano *et al.*, 2003; Sundbäck *et al.*, 2006) and stabilization of newly deposited sediment (Consalvey, 2002), and to support wetland consumers such as benthic macrofauna, meiofauna, fish and birds (Heip *et al.*, 1995; Guarini *et al.*, 2002). In temperate marsh areas, MPB is dominated by diatoms and phototrophic bacteria. Diatoms are considered as the most important primary producers (Brouwer and Stal, 2001) as they contribute up to one third of the total fixed carbon (Sullivan and Currin, 2000) in these systems. These diatoms can be divided into two distinct groups: the epipsammic forms attached to particles, and the epipelagic free-living forms (Round, 1979). Even if some tidal flats studies reported the dominance of epipsammic diatoms in MPB communities (Sabbe, 1993), epipelagic diatoms are generally the most important component of the autotrophic biomass (Sagan, 2001; Forster *et al.*, 2006) found in these areas. Due to their free-living nature, epipelagic diatoms are affected by water movements and can migrate within the first top cm of the sediment (Saburova and Polikarpov, 2003) allowing the establishment and maintenance of epipelagic forms within sedimentary environments (Consalvey *et al.*, 2004).

The present lack of knowledge concerning density and diversity of microphytobenthos in northern coastal areas limits our understanding of the capacity of resistance and resilience of these systems exposed to drastic modifications of climate or nutrient conditions. In the present context of coastal eutrophication (Cloern, 1999) and global warming (IPCC, 2007), understanding the dynamic of MPB in salt marshes is an essential step to model the effects of direct and indirect anthropogenic activities on nutrient loads toward sub-arctic estuarine systems (Boorman, 1999). Salt marshes located along the south shore of the St. Lawrence Estuary (Eastern Canada) offer ideal sites for studying microphytobenthic communities under severe climatic conditions (Dryade, 1980). Due to their geographical location, these marshes are exposed to freezing about five months a year and their development is mainly affected by sea ice action (Dionne, 1998) and sedimentary dynamics (Sérodes and Dubé, 1983; Drapeau, 1992; Dionne, 2004).

This paper provides first results on the density and diversity of MPB communities inhabiting northern salt marshes during summer time. Our two studied sites are located in the lower St. Lawrence Estuary (Quebec, Canada) and have been subjected to different levels of anthropogenic disturbances in last decades. The structure of diatom communities was examined in relation to pigment concentrations, total bacteria abundance, extracellular polymeric substance concentration, sediment grain size distribution and elementary organic matter composition in an attempt to determine the main environmental factors affecting MPB species distribution in such cold environments and the potential response of MPB community towards anthropogenic perturbations.

8.3 Materials and methods

8.3.1 Study sites

Two marshes from the south shore of the Lower St. Lawrence Estuary (Quebec, Canada) were selected for this study: the Pointe-aux-Épinettes (PE) and the Pointe-au-Père (PP) salt marshes (Fig. 1). Both located in the same geographical area (Rimouski, Qc), these marshes are affected by similar large-scale physical forcing such as tides, winds, and waves reaching up to 4 m during exceptional storms (Drapeau, 1992). The annual mean

tidal range is 3.3 m and the mean spring tidal range is 4.8 m. In addition, Lower St. Lawrence Estuary marshes are exposed to important seasonal variations affecting surface water temperature (typically ranging from 0 to 25°C), salinity (from 10 to 30 ppt), nutrient concentrations ($[NO_3^-]$ from 1 to 25 μM) and biological activity (Poulin, 2008). In both studied sites, low and high marshes areas are included between -1 and 0 m and 1 and 2 m, respectively (related to the mean sea level). One of the main features is the sea ice formation beginning in early December and persisting until April (Saucier *et al.*, 2003). Floating ice can erode intertidal zones by ice-scouring and ice-rafting, but it also contributes to marsh accretion by importing sediment with a large grain-size range.

The PE salt marsh is located in the Bic Provincial Park (Sépaq), a protected area created in October 1984. Enclosed in the Anse à l'Orignal bay and conscripted between two rocky elevations on west and east sides, this marsh is dominated by homogenous emergent macrophyte community (*Spartina alterniflora*, *Spartina patters* and other halophytes in its upper part) surrounded by free-vegetation network creeks. Because PE marsh watershed is part of a forested area without agricultural activity, nor residential zone, this marsh was considered as a pristine site entirely protected from anthropogenic stressors.

The PP salt marsh is part of the Pointe-au-Père National Wildlife area, a protected area under the responsibility of the Canadian Wildlife Services (Environment Canada) since September 2002. Confined in an elongated basin parallel to the main Estuary axis and sheltered from wave actions by a longitudinal rocky structure, this marsh is also dominated with *Spartina alterniflora* community and has geomorphologic characteristics similar to PE marsh. While the lower part is characterized by the presence of unconsolidated fine sediment and buried boulders, the upper marsh is nearly a flat platform which terminates seaward with a micro-cliff of 0.5 m. Unlike PE, the PP coastline is delimitated by roads and residential areas. The PP salt marsh has been subjected for decades to various anthropogenic pressures (urban sewage and agricultural runoffs, landfills and road construction) and is still receiving dissolved nitrogenous inputs from small tributaries (from 0.095 to 4.766 kg N (NH_4^+) d^{-1} and from 0.195 to 55.893 kg N (NO_x) d^{-1} following the season; Poulin, 2008). Freshwater runoffs enter the salt marsh by two main drainage

channels along its southeast border as well as by four municipal effluents. In addition, erosion structures (micro-cliffs, micro-ravines, high marsh collapses) are noticeable along drainage channels and platform edges. A preliminary survey conducted in May and July 2004 indicated that surface sediment of PP salt marsh was not impacted with organic pollutants such as chlorinated compounds (PCBs, DDTs and chlordane), neither with pyrogenic polyaromatic hydrocarbons (PAHs). Only aliphatic hydrocarbons and some light PAHs were detected and their presence attributed to nearby road traffic (Pelletier, unpublished results).

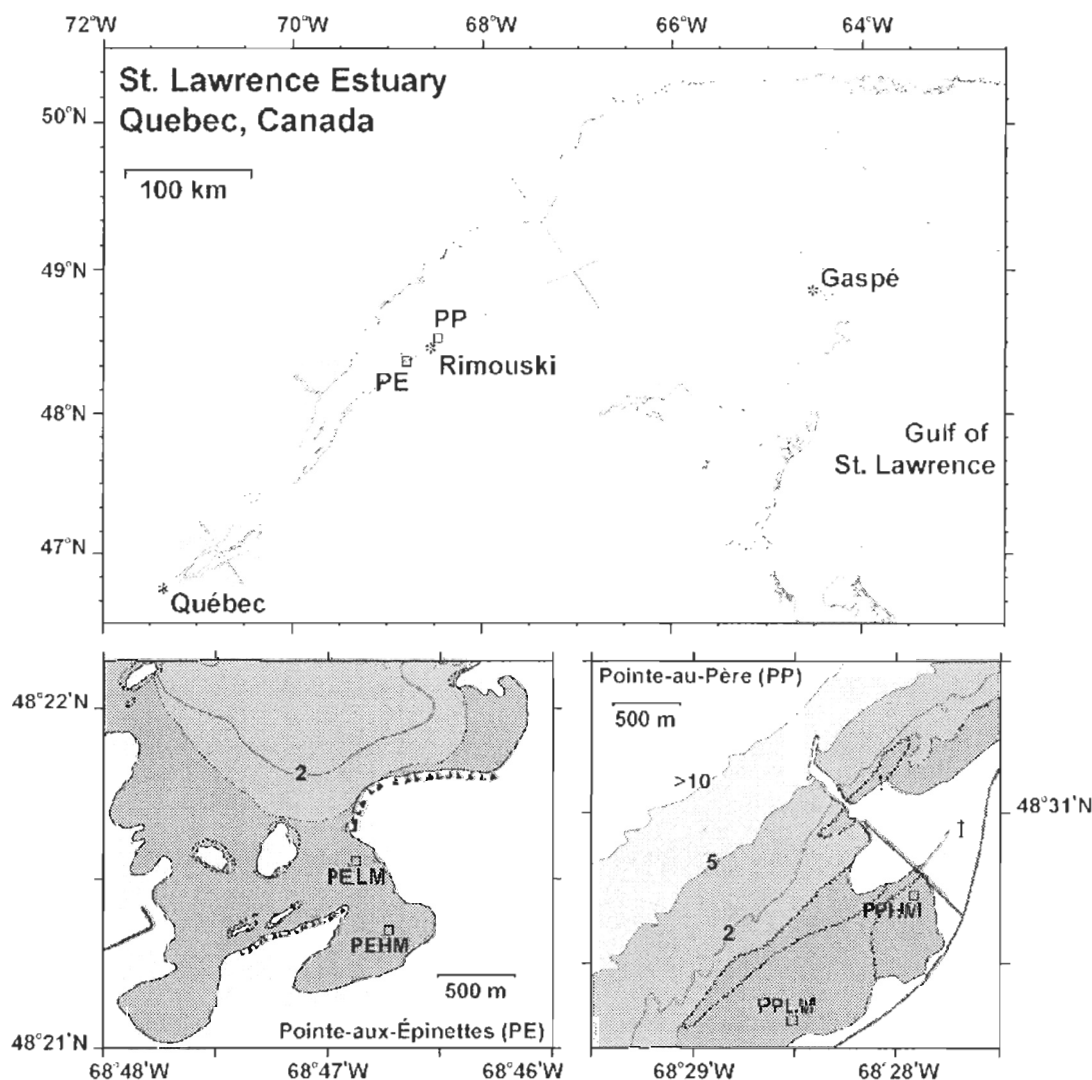


Figure VIII-1 Map of the St. Lawrence Estuary showing the location of the Pointe-aux-Épinettes (PE) and the Pointe-au-Père (PP) salt marshes along with sampling stations.

8.3.2 Sampling and analyses

Sediments were sampled in summer 2005 (7-11 July) from the Pointe-aux-Epinettes low marsh zone (PELM; $48^{\circ} 21.34'N$; $68^{\circ} 46.53'W$) and high marsh zone (PEHM; $48^{\circ} 21.21'N$; $68^{\circ} 46.39'W$), and from the Pointe-au-Père low marsh zone (PPLM; $48^{\circ} 30.18'N$; $68^{\circ} 28.28'W$) and high marsh zone (PPHM; $48^{\circ} 30.44'N$; $68^{\circ} 27.54'W$) as illustrated in Fig. 1. Six cores were randomly collected using truncated 10 cm^3 sterile syringe in a predetermined quadrate of 10 m^2 and the two first top cm were kept for analysis.

Surface sediment samples were processed for diatom analysis following a modification of the Schrader's method (1974). A 0.5 g sub-sample of dried sediment was treated with hydrogen peroxide and hydrochloric acid. The samples were washed with distilled water and centrifuged until no acid remained in the samples. An aliquot of 0.5 ml was placed on a cover slip and air dried. Permanent slides were prepared using Hyrax as mounting media. A Leitz Wetzlar Orthoplan® microscope, equipped with phase contrast and magnification up to $\times 1000$ was used for diatom identification. A minimum of 400 cells were counted in random transects for each sample. Diatom abundance was expressed as number of cells g^{-1} . For statistical analysis, tychoplanktonic, periphytic, epiphytic and epilithic cells were included in the epipsammic group whereas planktonic species were included in the epipelagic group.

Chlorophyll-*a* (Chl-*a*) and phaeopigments (Pheo) were analysed by fluorescence detection (Strickland and Parsons, 1972). Extracellular polymeric substances (EPS) concentrations were determined by a phenol-sulphuric acid dosage technique (Underwood *et al.*, 1995) which measures total carbohydrate concentrations. Total bacterial abundances (TB) were determined by epifluorescence microscopy using a 4',6-diamidino-2-phenylindole (DAPI) staining procedure adapted from Kuwae and Hosokawa (1999). Surface sediment elementary analysis for carbon (C_{org}) and nitrogen (N_{tot}) was performed with a ECS 4010 Costech® instrument equipped with a zero blank auto-sampler, using certified sediment sample ($n = 10$) NIST-1941b as a reference, whereas grain size analyses were done using a Coulter® counter model LS13320C.

8.3.3 Statistical analyses

Spearman's rank correlations were firstly used to test the correlation between MPB population characteristics (*i.e.* epipelic cells abundance, epipsammic cells abundance, total cells abundance) and environmental variables (*i.e.* Chl-*a*, Pheo, EPS, C_{org}, N_{tot}, TB, Clay, Silt Fine Sand, Medium Sand and Coarse Sand). Thereafter, multiple linear regression analyses were used to link these environmental parameters to the variations of MPB population characteristics considering correlation significance at a $p < 0.05$ level. Normality and homoscedasticity were confirmed by the examination of the residuals. Analysis of variance (One Way ANOVA on Ranks) was performed to test the significant difference of MPB density, epipelic and epipsammic species as well as other environmental variable among different sampling sites (PELM, PEHM, PPLM and PPHM). Prior to ANOVA, normality and homoscedasticity were confirmed by the examination of the residuals. To isolate groups that differed from the others, a Holm-Sidak and Tukey post-hoc multiple comparison procedures was performed. Differences between groups were considered significant at the $p < 0.05$ level. Comparisons of means were performed with Sigma Stat® Software Inc.

8.4 Results

8.4.1 Environmental variables

Mean (AV \pm SD) environmental variable values are presented in Table 1a and 1b. According to the ANOVAs, sampling sites show significant differences for several variables [C_{org} ($p < 0.001$); N_{tot} ($p = 0.002$); C/N (0.002); EPS ($p < 0.001$); Chl-*a* ($p = 0.002$); Pheo ($p = 0.017$); TB ($p = 0.002$) and the five sediment types ($p < 0.001$)] while mean Chl-*a*/Pheo ratio presented not significant inter-site differences ($p = 0.611$). The *a posteriori* test showed that C_{org}, Chl-*a*, Pheo, TB as well as C/N ratio remained statistically higher in PPHM compared to PELM and PEHM with no significant difference between PPLM and other sampling sites. N_{tot} concentration was found statistically higher in PPHM and PPLM compare to PELM with no significant difference between PEHM and all other sampling sites whereas EPS concentration remained statistically higher in PPHM compare to other sites. Sediment grain size distribution showed important spatial variability with a

significant higher proportion of clay and silt in PPHM, a significant higher proportion of fine sand in PPLM and a significant higher proportion of medium and coarse sand in PELM.

Tableau VIII-1 Mean values (AV) and standard deviations (SD) of sediment characteristics analyzed at stations PELM (Pointe-aux-Épinettes low marsh), PEHM (Pointe-aux-Épinettes high marsh), PPLM (Pointe-au-Père low marsh) and PPHM (Pointe-au-Père high marsh).

									Clay (%)	Silt (%)	Fine sand (%)	Medium sand (%)	Coarse sand (%)					
	C _{org} (%)		N _{tot} (%)		C/N		EPS (µg g ⁻¹)		<2 µm		(2-63 µm)		(64-257 µm)		(258-494 µm)		(495-2000 µm)	
	AV	SD	AV	SD	AV	SD	AV	SD	AV	SD	AV	SD	AV	SD	AV	SD	AV	SD
PELM	0.32	0.16	0.06	0.01	6.39	2.07	2243.98	728.25	0.29	0.46	2.47	3.04	32.39	9.07	26.07	4.54	37.98	9.70
PEHM	0.67	0.16	0.08	0.03	11.55	4.36	4049.42	826.65	1.45	0.39	20.44	7.71	37.33	7.51	11.19	3.86	32.48	8.14
PPLM	0.98	0.37	0.20	0.07	7.30	6.22	2341.73	479.33	1.57	0.22	11.27	2.09	48.05	10.86	17.34	3.42	21.99	0.96
PPHM	8.06	3.31	0.35	0.24	34.69	16.91	5658.07	1521.37	3.15	0.24	61.10	6.89	20.60	2.16	3.01	2.23	11.51	4.62

Tableau VIII-2 Mean values (AV) and standard deviations (SD) of microphytobenthic variables analyzed at stations PELM (Pointe-aux-Épinettes low marsh), PEHM (Pointe-aux-Épinettes high marsh), PPLM (Pointe-au-Père low marsh) and PPHM (Pointe-au-Père high marsh).

	Chl-a (µg g ⁻¹)		Pheo (µg g ⁻¹)		Chl-a/Pheo		Bacteria (cell g ⁻¹)		MPB density (cell g ⁻¹)		Epipelagic (%)		Epipsammic (%)	
	AV	SD	AV	SD	AV	SD	AV	SD	AV	SD	AV	SD	AV	SD
PELM	62.05	36.18	38.30	23.03	2.86	2.63	1.57E+8	2.81E+7	1.92E+6	1.50E+5	26.77	6.09	63.25	12.93
PEHM	81.00	35.54	77.52	26.93	1.29	0.98	1.77E+8	9.40E+7	1.37E+6	1.02E+5	26.66	4.25	73.61	14.61
PPLM	96.22	27.28	57.17	31.25	2.65	2.24	3.12E+8	1.65E+8	1.58E+6	2.08E+5	12.68	1.62	87.33	18.01
PPHM	570.10	267.49	715.19	319.48	1.17	1.22	2.48E+9	6.72E+8	3.84E+6	6.82E+5	57.86	4.57	41.16	4.01

8.4.2 Microphytobenthos composition

A total of 53 diatom species were identified during this study (Table 2). Most of them are benthic species with only six planktonic species observed: *Aulacoseira subarctica*, *Coscinodiscus marginatus*, *Cyclot Stephanos dubius*, *Ondotalla aurita*, *Thalassiosira eccentrica* and *T. proschkiniae*. Among the 47 benthic taxa observed, 24 belong to the epipelagic group, 12 to the epipsammic group, 4 are tychoplanktonic, 4 are periphytic, 2 are epiphytic and 1 is epilithic. A great similarity in species composition and distribution was observed within and between stations PELM, PEHM and PPLM. The lowest number of species (26 taxa) was observed at PPLM whereas the highest one (31) was observed at PEHM stations. In terms of MPB density, the lowest values (1.22×10^6 cell g $^{-1}$) was observed at PEHM whereas the highest one (2.18×10^6 cell g $^{-1}$) was observed at PELM. The three dominant species were: *Achnanthes delicatula* (abundance $\geq 50\%$), *Navicula cryptocephala* (abundance 10-30%) and *Cocconeis disculus* (abundance 5-10%). MPB diatom density was significantly higher at the PPHM station ($p < 0.001$) with an appreciable difference in the community composition: 44 species were identified and, even if *A. delicatula* remained the most dominant species, it represented less than 20% of total microphytobenthos community. The *a posteriori* test showed that total cells density was statistically higher in PPHM compared to PELM and PEHM with no significant difference between PPLM and other sampling sites.

On the basis of their habitat, diatom species were grouped into epipelagic and epipsammic forms. Comparison between sampling sites showed significant differences in total MPB density ($p < 0.001$), epipelagic ($p < 0.001$) and epipsammic ($p < 0.001$) species with significantly higher total abundance in PPHM and no statistical difference between other sampling sites. The *a posteriori* test showed the dominance of epipelagic forms in PPHM (relative abundance $> 57\%$) compared to PPLM and PEHM whereas epipsammic forms are significantly higher in PPLM compared to all other sites (relative abundance $> 87\%$). Epipelagic species are mainly represented by *Diploneis interrupta*, *D. smithii*, *Gyrosigma fasciola*, *G. spenceri*, *Navicula cryptocephala*, *N. peregrina*, *N. radiosa* var. *tenella*, *N. salinarum*, *Nitzschia clausii* and *N. tryblionella* while the epipsammic species are mainly represented by *Achnanthes delicatula* and *Cocconeis disculus*.

Tableau VIII-3 List of microphytobenthic species and their abundance (%) at stations PELM (Pointe-aux-Épinettes low marsh), PEHM (Pointe-aux-Épinettes high marsh), PPLM (Pointe-au-Père low marsh) and PPHM (Pointe-au-Père high marsh) in July 2005.

	Specific habitat	TAXA	PELM		PEHM		PPLM		PPHM	
			Mean	S.D.	Mean	SD	Mean	S.D.	Mean	SD
1	Epipsammic	<i>Achnanthes affinis</i> Grun.	1.03	0.72	2.71	2.36	0.50	0.49	1.36	1.00
2	Epipsammic	<i>Achnanthes brevipes</i> var. <i>intermedia</i> (Kutz.) Cl.	0.27	0.24	0.43	0.88	0.07	0.16	0.19	0.25
3	Epipsammic	<i>Achnanthes delicatula</i> (Kutz.) Grun.	50.63	2.85	60.85	5.91	65.89	5.84	18.51	5.81
4	Epipsammic	<i>Achnanthes flexella</i> var. <i>alpestris</i> Brun			1.23	1.47	5.31	2.15	1.44	2.06
5	Epipelic	<i>Amphora coffeaeformis</i> (Ag.) Kutz.	1.87	1.00	3.58	2.01	4.47	1.44	4.50	3.08
6	Planktonic	<i>Aulacoseira subarctica</i> (Mull.) Haworth	0.15	0.36						
7	Epipelic	<i>Caloneis</i> sp.							0.35	0.49
8	Epipsammic	<i>Cocconeis disculus</i> (Schum.) Cl.	7.01	3.70	4.27	2.23	10.02	2.40	12.18	3.46
9	Epipsammic	<i>Cocconeis peltoides</i> Hust.			0.26	0.64	2.94	1.74	0.96	0.52
10	Epipsammic	<i>Cocconeis pinnata</i> Greg.	0.47	0.64	1.10	0.85	1.03	0.62	0.88	0.95
11	Epipsammic	<i>Cocconeis placentula</i> var. <i>lineata</i> (Ehrenb.) Van Heurck	0.78	1.91	0.64	0.80	0.48	0.73	2.27	2.09
12	Planktonic	<i>Coscinodiscus marginatus</i> Ehrenb.	0.19	0.15	0.07	0.18	0.05	0.11	0.14	0.24
13	Epipsammic	<i>Ctenophora pulchella</i> (Ralfs & Kütz.) Williams & Round							0.14	0.24
14	Planktonic	<i>Cyclostephanos dubius</i> (Fricke) Round	0.47	0.29	0.35	0.51	0.06	0.14		
15	Tychoplanktonic	<i>Cyclotella meneghiniana</i> Kutz	0.76	0.48	0.92	0.56	0.76	0.71	1.24	0.33
16	Epipelic	<i>Cylindrotheca closterium</i> (Ehrenb.) Reimann & Lewin			0.07	0.16	0.06	0.14		
17	Epipelic	<i>Diploneis interrupta</i> (Kutz.) Cl.							0.69	0.38
18	Epipelic	<i>Diploneis smithii</i> (Bréb.) Cl.							0.22	0.20
19	Epipelic	<i>Fallacia pygmaea</i> (Kutz.) Stickle & Mann	3.02	4.06	1.92	1.50	0.28	0.33	2.26	1.46
20	Epipsammic	<i>Fragilaria brevisistrata</i> (Grun.) Van heurck	0.15	0.24						
21	Tychoplanktonic	<i>Fragilaria capucina</i> (Desm.)			0.19	0.32				
22	Epipsammic	<i>Fragilaria pinnata</i> Ehrenb.	1.62	1.34			0.16	0.25	0.05	0.13
23	Epilithic	<i>Fragilaria vaucheriæ</i> (Kütz.) Petersen			0.06	0.15			0.05	0.13
24	Periphytic	<i>Gomphonema</i> sp.	0.09	0.14	0.06	0.15	0.06	0.14		
25	Epiphytic	<i>Grammatophora angulosa</i> Ehrenb.	0.05	0.12	0.15	0.36			0.05	0.13
26	Epipelic	<i>Gyrosigma acuminatum</i> (Kütz.) Rabenhorst			0.13	0.21			0.24	0.29
27	Epipelic	<i>Gyrosigma lasciola</i> (Ehrenb.) Griffith & Henfrey							0.04	0.09
28	Epipelic	<i>Gyrosigma spenceri</i> (Smith) Cl.							1.01	0.53
29	Epiphytic	<i>Licmophora paradoxo</i> (Lyng.) Ag.			0.13	0.20	0.06	0.14	0.05	0.13
30	Tychoplanktonic	<i>Melosira nummuloides</i> Ag.							0.62	0.89
31	Epipelic	<i>Navicula cryptocephala</i> Kutz.	23.43	3.03	15.80	3.52	5.78	4.16	22.93	6.23
32	Epipelic	<i>Navicula digitoradiata</i> (Greg.) Ralls in Pritchard	0.74	0.63	0.43	0.86	0.11	0.18	1.29	0.95
33	Epipelic	<i>Navicula peregrina</i> (Ehrenb.) Kutz.							0.60	0.49
34	Epipelic	<i>Navicula radiosa</i> var. <i>tenella</i> (Bréb.) Grun.	1.04	0.74	1.16	0.67	0.83	0.59	4.03	1.70
35	Epipelic	<i>Navicula salinarum</i> (Grun.) Cl. & Grun.							0.19	0.46
36	Epipelic	<i>Nitzschia acuminata</i> (Smith) Grun.	0.51	0.72	0.36	0.15	0.17	0.19	1.33	0.97
37	Epipelic	<i>Nitzschia clausii</i> Hantz.							3.28	3.22
38	Epipelic	<i>Nitzschia communis</i> Rabenhorst	1.98	1.42	0.75	0.72			6.41	1.87
39	Epipelic	<i>Nitzschia</i> sp.							1.37	1.02
40	Epipelic	<i>Nitzschia distans</i> Greg.			0.07	0.16			1.17	0.64
41	Epipelic	<i>Nitzschia frustulum</i> (Kütz.) Cl. & Grun.	1.98	1.35					0.06	0.15
42	Epipelic	<i>Nitzschia tubicola</i> (Grun.) Cl. & Grun.	0.13	0.15						
43	Epipelic	<i>Nitzschia tryblionella</i> (Hantz.) Rabenhorst					0.06	0.14	1.79	0.60
44	Planctonic	<i>Odontella aurita</i> (Lyngb.) Ag.	0.14	0.23					0.18	0.14
45	Epipsammic	<i>Opephora Olsenii</i> Moller			0.21	0.36				
46	Epipelic	<i>Pleurosigma aestuaria</i> (Bréb. ex Kütz.) Smith					0.19	0.33	0.79	0.42
47	Periphytic	<i>Remora sinuata</i> (Greg.) Koolek & Stoermer	0.14	0.23	0.07	0.16				
48	Periphytic	<i>Rhoicosphenia curvata</i> (Kütz.) Grun.	0.04	0.10			0.05	0.13	0.96	0.66
49	Epipelic	<i>Surrella ovata</i> Hust.			0.47	0.50			1.00	1.23
50	Periphytic	<i>Tabularia tabulata</i> (Ag.) Snoeijs	0.10	0.24	0.33	0.47			0.10	0.16
51	Tychoplanktonic	<i>Tabellaria flocculosa</i> (Roth) Kütz	0.09	0.22					0.11	0.17
52	Planctonic	<i>Thalassiosira eccentrica</i> (Ehrenb.) Cl.	0.86	0.83			0.15	0.24	1.72	0.85
53	Planctonic	<i>Thalassiosira proschkiniae</i> Makarova	0.26	0.42	1.50	1.41	0.47	0.35	0.27	0.65
		Total number of species	30		31		26		44	

Multiple linear regressions showed that among all sampling sites, the variance of the dependent variable MPB density was mainly affected by a linear combination of surface sediment nutrient concentrations (Table 3). The variance of MPB cell density is explained at 72% by the combination of C_{org} and N_{tot} . As total density, the variance of epipelagic species abundance could be explained at 81% by the combination of C_{org} and N_{tot} whereas the best fit model showed that variance of epipsammic species could be explained only at 33% by coarse sand relative concentration variability.

Tableau VIII-4 Results of multiple linear regression testing the effect of environmental variables on MPB density and abundance of epipelagic and epipsammic forms at stations PELM (Pointe-aux-Épinettes low marsh), PEHM (Pointe-aux-Épinettes high marsh), PPLM (Pointe-au-Père low marsh) and PPHM (Pointe-au-Père high marsh).

Dep Variable	Adj Rsqr	Ind Variable	Coefficient	Std Error	P
Density	0.717	Constant	1820772.300	170145.286	< 0.001
		N_{tot}	-3380497.458	1360553.310	0.021
		C_{org}	373193.078	63288.856	< 0.001
Epipelagic	0.810	Constant	636319.943	110487.317	< 0.001
		N_{tot}	-3495136.424	883503.084	< 0.001
		C_{org}	332633.676	41097.911	< 0.001
Epipsammic	0.326	Constant	1622117.575	103802.830	< 0.001
		Course sand	-12500.474	3588.293	0.002

The determination of the Shannon and Weaver diversity measures (H') revealed a higher diversity at PPHM station (mean $H' = 2.58$) compared to mean values of 1.46 bits cells⁻¹ at stations PELM, PEHM and PPLM. MPB biomass was estimated using calculation model proposed by de Jonge (1988). The conversion from $\mu\text{g Chl-}\alpha\text{ g}^{-1}$ dry sediment to mg Chl- α m⁻² was done by multiplying recorded Chl- α concentrations by 12.7, based on an average bulk density of 1.27 g cm⁻³, whereas the conversion from Chl- α to carbon was obtained using the C/Chl- α ratio of 40. The estimated surface biomass at PE marsh ranged from 267 to 1762 mg Chl- α m⁻² (11 to 71 g C m⁻²) while it ranged from 576 to 12170 mg Chl- α m⁻² at the PP marsh with the highest values observed in PPHM. These values

correspond to carbon concentrations ranging from 132 to 486 g C m⁻² at PPHM and from 24 to 65 g C m⁻² at PPLM.

8.5 Discussion

Our study is first to depict the summer composition of MPB in two northern salt marshes exposed to periodical severe conditions and to different anthropogenic pressures. As summer time is the most productive period in northern salt marshes subjected to important seasonal temperature variations, this study provides a first look to the highest diversity occurring around the year. These first data are crucial to determine microbial community shift in sub-Arctic coastal ecosystems that are increasingly affected by climatic changes. In a long term perspective, this study will enable us to relate diversity changes to variation in functional role of these communities within marsh ecosystems.

MPB abundance and Chl- α concentration reported in this summer study offer some similarities with those reported in the literature in temperate intertidal areas (Admiral *et al.*, 1982; Peletier, 1996; Sabbe, 1993; Tolomio *et al.*, 1999; Sagan, 2001). However, significant differences were observed between the four sampling stations, with higher MPB cell density and Chl- α concentration recorded at the PPHM station compared to all PE sampling sites. Although these differences may be related to spatial heterogeneity, the higher biomass registered at PPHM station could also result from favorable environmental conditions for MPB growth. Among important variables involved in MPB growth, nutrient loads due to anthropogenic activities are generally suggested as the most probable factor leading to an important increase of MPB in coastal areas (Rabalais and Nixon, 2002; Howarth and Marino, 2006). The particular location of the PP salt marsh, partly enclosed within an urbanized area, could contribute to the higher MPB abundance observed at the PPHM station as nutrient deposition may be higher in impacted areas compared to pristine ones. Due to their diversity and abundance in aquatic systems, diatoms have frequently been used as a proxy of aquatic ecosystem perturbations (*e.g.*, Agbeti and Dickman, 1989; Bennion, 1994; Christie and Smol, 1993; Renberg and Hultberg, 1992; Stoermer and Smol, 1999; Stoermer *et al.*, 1996; Underwood, 1994; Underwood *et al.*, 1999). One of the well-documented effects of nutrient inputs on diatom communities is the reduction in number of

species along with an increase in the abundance of the remaining ones (Patrick and Reimer, 1966; De Sèze, 1981; Cooper, 1995; Stoermer and Smol, 1999). Moreover, many diatom species are highly sensitive to water quality alterations and could be considered as reliable ecological indicators through their specific distribution and abundance (e.g., Beaver, 1981; Douglas and Smol, 1993; Lowe, 1974; Patrick, 1977; Patrick and Reimer, 1966; van Dam *et al.*, 1994). Interestingly, we observed important differences between pristine and impacted sites regarding the structure of microphytobenthic diatom communities. A high dominance of epipsammic species within a relatively low diversified community was observed at PPLM, PEHM and PELM stations while a slight dominance of epipellic forms within a much more diverse community was found at PPHM station. The higher diversity observed at PPHM station is attributable to the increase of epipellic species and the presence of some particular species (such as *Diploneis interrupta* and *Gyrosigma acuminatum*) suggesting the presence of eutrophic conditions at this station. The discrepancy observed in Chl- α concentrations between different sites could be partially attributed to the proportion of epipellic versus epipsammic diatoms within the community since epipellic forms are generally larger than the epipsammic ones (Underwood *et al.*, 1995). Although the PP salt marsh can be considered as an anthropogenic impacted area, the high MPB diversity recorded at the PPS station do not reflect the reduction of diatom diversity generally observed in temperate human impacted sites.

Although our results suggest that MPB cells density and more especially the abundance of epipellic forms are mainly affected by the availability of nutrients (see Table 3), we hypothesize that sediment characteristics could have promoted the settlement of epipellic forms cells at the PPHM station. Among marsh sediment characteristics, organic matter lability, grain size distribution and sediment stability are discussed hereafter. In general, the C/N ratio represents a valuable proxy of organic matter lability and varies between 3 to 6 in healthy phytoplankton population (Parsons *et al.*, 1977). In our study, the average C/N ratio ranged from 6.4 to 34.7, but cannot be used as a relevant proxy to determine the lability of the organic matter due to the high relative carbon content (and low nitrogen) of the *Spartina* rhizosphere (*Spartina* C/N ~ 40; Meyers, 1994). For example, *Spartina* roots at PPHM station may account for an important proportion of the observed

high C/N ratio value that does not necessarily stand for the refractory character of interstitial sediment. Nevertheless the *Spartina* rizosphere favors water and oxygen diffusion in marsh sediment allowing the increase of aerobic bacterial mineralization processes and inorganic nutrient availability. Thus, high epipellic cell abundances at PPHM could be better explained by the microbial degradation potential within the *Spartina* rizosphere than by the C/N ratio observed in the sediment. Degradation processes estimated through the Chl-a/phaeopigments ratio support this finding. A ratio of 10 is generally observed in growing populations but values around 3 usually indicate some cell degradation (Sagan, 2001) or important grazing by meiofauna (Cariou-Le Gall and Blanchard, 1995). In the present study, the lowest mean ratio was recorded at PPHM with no significant differences between the sampling sites (Table 1b). Although this result indicates that MPB community fitness was similar among the different sampling sites, it also underlines the importance of microbial degradation processes and grazing pressures on MPB community.

The composition of diatom communities has been previously reported to be influenced by the size of the sediment particles (Zong and Horton, 1998). Previous studies in temperate areas showed that epipsammic taxa were mainly associated with sandy substrates while epipellic taxa were mainly found in muddy to clayey substrates (Sabbe, 1993; Paterson and Hagerthy, 2001; Sagan, 2001; Tolomio *et al.*, 2002; Forster *et al.*, 2006). Our results in St. Lawrence marshes are in agreement with these findings since the abundance of epipsammic forms can be roughly predicted from coarse sand concentrations (Table 3). In addition, the muddy character of the sediments at PPHM station (*i.e.* high clay and silt content; Table 1a) may have contributed to the settlement of many epipellic species in this specific area. According to field observations, we can suggest that specific sediment characteristics have been induced by tidal channels erosion (e.g. drainage work, urban sewage overflow drains) which promoted clay suspension and accumulation at the PPHM. The presence of epipellic diatoms and bacteria in sediment can also play an important role for fine sediment stability and quality. As epipellic diatoms and bacteria have the ability to produce large amounts of extracellular polymeric substances (EPS; mainly consisting of carbohydrates), they contribute to stabilize sediment, reduce evaporation, produce high quantities of organic carbon and favor MPB community settlement (Underwood, 1994;

Deccho and Lopez, 1993). The presence of microphytobenthic biofilms was also correlated with sediment stability parameters (Consalvey, 2002). According to de Deckere *et al.* (2001) the presence of a biofilm could increase the critical erosion threshold of sediment by 300% inducing a much better resistance against erosion. Thus, epipellic diatoms species which move using EPS in unstable shallow estuarine sediments, where burial and erosion events are frequent, have a selective advantage compared with epipsammic ones (Round, 1971; Palmer and Round, 1997). In this study, EPS concentrations were higher at PP and PE high marshes with significantly higher concentrations registered at PPHM station. The dominance of epipellic diatoms at PPHM along with significantly higher bacterial abundance account for the values observed (Table 1b). Similar values were reported by Underwood *et al.* (1995) and correlation of EPS with epipellic diatoms has been previously shown by Paterson *et al.* (1990) and Madsen *et al.* (1993). Even if the EPS concentrations measured during this study remained poorly correlated with epipellic cell abundance (Adj Rsqr = 0.48; P < 0.001), the importance of microphytobenthic biofilms is well illustrated by the results obtained at PPHM.

The benthic biomass inhabiting surface sediment in July 2005 was ranging from 11 to 71 g C m⁻² in PE marsh, and 24 to 65 g C m⁻² at PPLM with a peak at PPHM (132 to 486 g C m⁻²). According to these values, the annual potential marsh productivity can be estimated to range from 10 to 70 g C m⁻² y⁻¹, considering the annual effect of sea-ice which erodes and alters marsh surface sediment. This St. Lawrence salt marsh production may be underestimated since marsh biomass evaluation (using Chl-*a* concentrations) does not take in account bacterial and EPS carbon production which could represent up to 30% of the MPB production (Hall and Fisher, 1985). For comparison purpose, it should be noted that Sagan (2001) observed carbon production ranging from 11 to 63 g C m⁻² y⁻¹ in the Mont Saint-Michel salt marsh. Interestingly, the MPB productivity observed in both studied salt marshes are in the same order of magnitude that the primary production recorded in the adjacent biologically rich St. Lawrence Estuary waters (104 g C.m⁻².y⁻¹ following Therriault and Levasseur, 1985) and underlines the important productivity of sub-arctic salt marshes during summer time.

Providing the first results on the abundance and diversity of the MPB communities inhabiting northern salt marshes during summer time, this study pinpoints the potential effect of anthropogenic disturbance (other than toxic pollutants) on macrotidal system. Evidences have been presented on the role of nutrients, sediment composition and stability on MPB abundance and specific distribution in epipelic and epipsammic forms. Rich organic carbon clayey substrates could account for the high level of production at PPHM station along with effluents enrichment even if no direct links have been established yet. In addition, the higher diversity observed at the PPHM impacted site suggests that a moderate nutrient input may support diversity in such particular case. Relevant correlations were obtained between nutrient concentrations and MPB diatom densities in the sediment while the relative abundance of epipelic and epipsammic forms have been related to the sediment grain size distribution. Thus, even if the higher nutrient input observed at PP marsh could act on MPB density and diversity, alterations of the sedimentary processes by coastal urbanization may have a more specific role on the MPB community structure. Numerous studies of sedimentary dynamics already demonstrated that St. Lawrence Estuary coastal salt marshes became more and more vulnerable to erosion in the last decades (Sérodes and Dubé, 1983; Drapeau, 1992; Dionne, 1998; Morisette, 2006). In progress studies along the St. Lawrence Estuary are focusing on the diversity of dominant MPB and bacteria species throughout seasonal cycle in order to identify a possible structure/function link in this cold environment. These data are crucial to determine what the functional role of these communities is and to adequately model organic matter processes in sub-arctic coastal areas in the light of increasing eutrophication.

8.6 Acknowledgement

This work was supported by the Canada Research Chair in Molecular Ecotoxicology applied to high latitude coastal zones (E.P.) and NSERC Discovery grant (E.P.). This paper is a contribution of the Quebec-Ocean network.

8.7 Literature cited

- Admiral, W., Peletier, H., Zomer, H. Observations and experiments on the population dynamics of epipelagic diatoms from an estuarine mudflat. *Estuar Coast Shelf Sci* 1982; 14: 471-487.
- Agbeti, M., Dickman, M. Use of lake fossil diatom assemblages to determine historical changes in trophic status. *Can J Fish Aquat Sci* 1989; 46: 1013-1021.
- Albertano, P., Guzzon, A., Di Pippo, F., Congestri, R. Potential use of phototrophic biofilms for N and P removal. *Biotechnology of Microalgae, 5th European Workshop on Microalgal Biotechnology*. Bergholz-Rehbrücke (DE), Abstract Book S1, 2003, 7 pp.
- Baldwin, D.S., Mitchell, A.M. The effect of drying and re-flooding on sediment and soil nutrient dynamics of lowland river-floodingplain systems: a synthesis. *Regul Rivers Res Manage* 2000; 16: 457-567.
- Beaver, J. Apparent ecological characteristics of some common freshwater diatoms. Ministry of the Environment, Toronto, Ontario, Canada, 1981, 517 pp.
- Bennion, H. A diatom-phosphorus transfer function for shallow, eutrophic ponds in southeast England. *Hydrobiologia* 1994; 275/276: 391-410.
- Billen, G., Lancelot, C. Modelling benthic nitrogen cycling in temperate coastal ecosystems. In: Blackburn, T.H., Sorensen, J. *Nitrogen cycling in Coastal Marine Environments*. John Wiley and Sons, New-York, 1988, pp. 341-378.
- Boorman, L.A. Salt marshes – present function and future change. *Mangroves Salt Marshes* 1999; 3: 227-241.
- Brouwer, J.F.C., Stal, L.J. Short-term dynamics in microphytobenthos distribution and associated extracellular carbohydrates in surface sediments of an intertidal mudflat. *Mar Ecol Prog Ser* 2001; 218: 33-44.
- Cariou-LeGall, V., Blanchard, G. Monthly HPLC measurements of pigment concentrations from an intertidal muddy sediment of Marennes-Oleron Bay, France. *Mar Ecol Prog Ser* 1995; 121: 171-179.
- Christie, C.E., Smol, J.P. Diatom assemblages as indicators of trophic status in southeastern Ontario lakes. *J Phycol* 1993; 29: 575-586.
- Cloern, J.E. Our evolving conceptual model of the coastal eutrophication problem. *Mar Ecol Prog Ser* 2001; 210: 223-253.
- Consalvey, M. The structure and function of microphytobenthic biofilms. PhD thesis, University of St Andrews, St. Andrews, Scotland, UK, 2002.

- Consalvey, M., Paterson, D.M., Underwood, G.J.C. The ups and downs of life in a benthic biofilm: migration of benthic diatoms. *Diatom Res* 2004; 19: 181-202.
- Cooper, S.R. Chesapeake Bay watershed historical land use: impact on water quality and diatom communities. *Ecol Appl* 1995; 5: 703-723.
- Deccho, A.W., Lopez, G.R. Exopolymer microenvironments of microbial flora: Multiple and interactive effects on trophic relationships. *Limnol Oceanogr* 1993; 38: 1633-1645.
- de Deckere, E.M.G.T., Tolhurst, T.J., De Brouwer, J.F.C. Destabilization of cohesive intertidal sediments by infauna. *Estuar Coast Shelf Sci* 2001; 53: 665-669.
- de Jonge, V.N. Fluctuations in the organic carbon to chlorophyll a ratios for estuarine diatom populations. *Mar Ecol Prog Ser* 1980; 2: 345-353.
- De Sève, M.A., Goldstein, M.E. The structure and composition of epilithic diatom communities of the St. Lawrence and Ottawa Rivers in the Montréal area. *Can J Bot* 1981; 59: 377-387.
- Dionne, J.C. Sedimentary structure made by shore ice in muddy tidal-flat deposits, St. Lawrence Estuary, Québec. *Sediment Geol* 1988; 116: 261-274.
- Dionne, J.C. Âge et taux moyen d'accréation verticale des schorres du Saint-Laurent estuarien, en particulier ceux de Montmagny et de Sainte-Anne-de-Beaupré, Québec. *Géogr Phys Quat* 2004; 58: 83-108.
- Douglas, M.S.V., Smol, J.P. Freshwater diatoms from high arctic ponds (Cape Herschel, Ellesmere Island, N.W.T.). *Nova Hedwigia* 1993; 57: 511-552.
- Drapeau, G. Dynamique sédimentaire des littoraux de l'estuaire du St-Laurent. *Géogr Phys Quat* 1992; 46: 233-242.
- Dryade. Habitats propices aux oiseaux migrateurs. Environnement Canada, Service canadien de la faune, Québec, Canada, 1980, 66 pp.
- Forster, R.M., Créach, V., Sabbe, K., Vyverman, W., Stal, L.J. Biodiversity-ecosystem function relationship in microphytobenthic diatoms of the Westerschelde Estuary. *Mar Ecol Prog Ser* 2006; 311: 191-201.
- Guarini, J.M., Cloern, J.E., Edmunds, J., Gros, P. Microphytobenthic potential productivity estimated in three tidal embayments of the San Francisco Bay; a comparative study. *Estuaries* 2002; 25: 409-417.
- Hall, S.L., Fisher, F.M. Annual productivity and extracellular release of dissolved organic compounds by the epibenthic algal community of a brackish marsh. *J Phycol* 1985; 21: 277-281.

- Heip, C.H.R., Goosen, N.K., Herman, P.M.J., Kromkamp, J., Middelburg, J.J., Soetaert, K. Production and consumption of biological particles in temperate tidal estuaries. *Oceanogr Mar Biol Annu Rev* 1995; 33: 1-149.
- Howarth, R.W., Marino, R. Nitrogen as the limiting nutrient for eutrophication in coastal marine ecosystems: evolving views over three decades. *Limnol Oceanogr* 2006; 51: 364-376.
- Intergovernmental Panel on Climate Change (IPCC), 2007 (<http://www.ipcc.ch/>).
- Kuwae, T., Hosokawa, Y. Determination of abundance and biovolume of bacteria in sediments by dual staining with 4',6-diamidino-2-phenylindole and acridine orange: relationship to dispersion treatment and sediment characteristics. *Appl Environ Microbiol* 1999; 65: 3407-3412.
- Liehr, S.K., Chen, H.J., Lin, S.H. Metal removal by algal biofilms. *Water Sci Technol* 1994; 30: 59-68.
- Lowe, R.L. Environmental requirements and pollution tolerance of freshwater diatoms. U.S. Environmental Protection Agency, Cincinnati, Ohio, USA. 1974, 333 pp.
- Madsen, K.N., Nilsson, P., Südbäck, K. The influence of benthic microalgae on the stability of a subtidal shallow water sediment. *J Exp Mar Biol Ecol* 1993; 170: 159-177.
- Meyers, P.A. Preservation of element and isotopic source identification of sedimentary organic matter. *Chem Geol* 1994; 114: 289-302.
- Mason, C.F., Underwood, G.J.C., Baker, N.R., Davey, P.A., Davidson, I., Hanlon, A., Long, S.P., Oxborough, K., Paterson, D.M., Watson, A. Roles of herbicides in the erosion of salt marshes in eastern England. *Environ Pollut* 2003; 122: 41-49.
- Morisette, A. Évolution côtière haute résolution de la région de Longue-Rive-Forestville, Côte Nord de l'estuaire maritime du Saint-Laurent. MS thesis, Université du Québec à Rimouski, Rimouski, Québec, Canada, 2006.
- Page, H.M., Petty, R.L., Meade, D.E. Influence of Watershed runoff on nutrients dynamics in a Southern California Salt Marsh. *Estuar Coast Shelf Sci* 1995; 41: 163-180.
- Palmer, J.D., Round, F.E. Persistent vertical-migration rhythms in benthic microflora. VI. The tidal and diurnal nature of rhythm in the diatom *Hantzschia virgata*. *Biol Bull* 1997; 132: 44-55.
- Parsons, T.R., Takahashi, M., Hargrave, B. Biological oceanographical processes, 2nd edition, Pergamon Press, Oxford, 1977.
- Paterson, D.M., Crawford, R.M., Little, C. Sub-aerial exposure and changes in stability of intertidal estuarine sediments. *Estuar Coast Shelf Sci* 1990; 30: 541-556.

- Paterson, D.M., Hagerthy, S.E. Microphytobenthos in contrasting coastal ecosystems: biology and dynamics. In: Reise, K. (ed) Ecological comparisons of sedimentary shores. Ecological studies 151, Springer-Verlag, Berlin, 2001, pp. 105-125.
- Patrick, R., Reimer, C.W. The diatoms of the United States exclusive of Alaska and Hawaii. Vol. I. *Fragilariaeae, Eunotiaceae, Achnanthaceae, Naviculaceae*. Academy of Natural Sciences of Philadelphia, Monograph 13, 1966, 688 pp.
- Patrick, R. Ecology of freshwater diatoms and diatom communities. In: *The Biology of Diatoms*, D. Werner (ed). Blackwell Scientific Publications, Botanical Monograph 13, 1977, pp. 284-332.
- Peletier, H. Long-term changes in intertidal estuarine diatom assemblages related to reduced input of organic waste. *Mar Ecol Prog Ser* 1996; 137: 265-271.
- Poulin, P. Cycle biogéochimique de l'azote dans l'estuaire du St-Laurent; rôle des marais côtiers. PhD thesis, Université du Québec à Rimouski. Rimouski, Québec, Canada, 2008.
- Rabalais, N.N., Nixon, S.W. Preface: Nutrient over-enrichment in coastal waters: global patterns of cause and effect. *Estuaries* 2002; 25: 639-900.
- Renberg, I., Hultberg, H. A paleolimnological assessment of acidification and liming effects on diatom assemblages in a Swedish lake. *Can J Fish Aquat Sci* 1992; 49: 65-72.
- Round, F.E. Benthic marine diatoms. *Oceanogr Mar Biol Annu Rev* 1971; 9: 83-139.
- Round, F.E. A diatom assemblage living below the surface of intertidal sand flats. *Mar Biol* 1979; 54: 219-223.
- Sabbe, K. Short-term fluctuations in benthic diatom numbers on an intertidal sandflat in the Westerschelde estuary (Zeeland, The Netherlands). *Hydrobiologia* 1993; 269/270: 275-284.
- Saburova, M.A., Polikarpov, I.G. Diatom activity within soft sediments: behavioural and physiological processes. *Mar Ecol Prog Ser* 2003; 251: 115-126.
- Sagan, G. Typologie et dynamique des communautés de diatomées benthiques dans l'écosystème mégatidal de la baie du Mont Saint-Michel. PhD thesis, Université de Rennes, Rennes, France, 2001.
- Saucier, F.J., Roy, F. and Gilbert, D. Modeling the formation and circulation processes of water masses and the sea ice in the Gulf of St. Lawrence, Canada. *J Geophys Res* 2003; 108: 3269-3289.
- Schrader, H.-J. Proposal for a standardized method of cleaning diatom bearing deep-sea and land-exposed marine sediments. *Nova Hedwigia* 1974; 45: 403-409.

Sérodes, J.-B., Dubé, M. Dynamique sédimentaire d'un estran à spartines. *Naturaliste Can* 1983; 110: 11-26.

Stoermer, E.F., Emmert, G., Juluis, M.L., Schelske, C.L. Paleolimnologic evidence of rapid recent change in Lake Erie's trophic status. *Can J Fish Aquat Sci* 1996; 53: 1451-1458.

Stoermer, E., Smol, J. The diatoms: application for the environmental and earth sciences, Cambridge University Press, New York, 1999, 482 pp.

Strickland, J.D.H., Parsons, T.R. A practical handbook of seawater analysis. 2nd edition, Fisheries Research Board of Canada, 1972, 310 pp.

Sullivan, M.J., Currin, C.A. Community structure and functional dynamics of benthic microalgae in salt marshes. In: Weinstein, M.P., Kruger, D.A. (eds) Concepts and Controversies in Tidal Marsh Ecology. Kluwer Academic Publishers, Dordrecht, 2000, pp. 81-106.

Sundbäck, K., Miles, A., Linares, F. Nitrogen dynamics in non-tidal littoral sediments: role of microphytobenthos and denitrification. *Estuaries Coasts* 2006; 29: 1196-1211.

Theriault, J.-C., Levasseur, M. Control of phytoplankton production in the lower St. Lawrence Estuary : light and freshwater runoff. *Naturaliste Can* 1985; 112: 77-96.

Tolomio, C., Moro, I., Moschin, E., Valandro, A. Résultats préliminaires sur les diatomées benthiques de substrats meubles dans la lagune de Venise, Italie (Mars 1994 – Janvier 1995). *Diatom Res* 1999; 14: 367-379.

Tolomio, C., Moschin, E., Duzzin, B. Distribution des diatomées benthiques de substrats meubles dans le bassin sud de la lagune de Venise, Italie. *Diatom Res* 2002; 17: 401-414.

Troccaz, O. Évolution de la dynamique d'un marais salé: processus fonctionnels internes et relations avec le milieu côtier (Baie du Mont-Saint-Michel). PhD thesis, Université de Rennes, Rennes, France, 1996.

Underwood, G.J.C. Seasonal and spatial variation in epipelagic diatom assemblages in the Severn estuary. *Diatom Res* 1994; 9: 451-472.

Underwood, G.J.C., Paterson, D.M., Parkes, R.J. The measurement of microbial carbohydrates exopolymers from intertidal sediments. *Limnol Oceanogr* 1995; 40: 1243-1253.

Underwood, G.J.C., Kromkamp, J. Primary production by phytoplankton and microphytobenthos in estuaries. *Adv Ecol Res* 1999; 29: 93-153.

van Dam, H., Mertens, A., Sinkeldam, J. A coded checklist and ecological indicator values of freshwater diatoms from the Netherlands. *Netherlands J Aquat Ecol* 1994; 28: 117-133.

Wölfel, J., Adler, S., Hübener, T., Karsten, U. Diatoms inhabiting a wind flat of the Baltic Sea - species diversity and seasonal succession. *Estuar Coast Shelf Sci* 2007; 75: 296-307.

Woodward, R.T., Wui, Y.S. The economic value of wetland services: a meta-analysis. *Ecol Econ* 2001; 37: 257-270.

Zong, Y.. Horton, B.P. Diatom zones across intertidal flats and coastal salt marshes in Britain. *Diatom Res* 1998; 13: 375-394.

CHAPITRE IX

Discussion générale

9.1 Incidence des rejets d'azote de source anthropique sur l'estuaire du Saint-Laurent

Au sein des milieux côtiers densément peuplés, la distribution des nutriments azotés est largement affectée par l'activité anthropique (Justic *et al.*, 1995). À ce chapitre, le Saint-Laurent n'est pas différent des milieux de transition impactés retrouvés de part le monde. Ainsi, Howarth *et al.*, (1996) ont montré que les flux de nitrates en provenance du bassin versant du fleuve Saint-Laurent auraient augmentés de 1.8 à 5.4 fois depuis l'arrivée des colons européens. Une étude pan-Canadienne publiée en 2001 a montré que la pollution issue des milieux urbains et industriels atteignait 12 000 tonnes de phosphore par année et 304 000 tonnes d'azote par année et que les rejets en provenance des stations d'épuration municipales auraient augmentés de 17% entre 1983 et 1996 (Chambers *et al.*, 2001). De plus, les rejets azotés en provenance du milieu agricole sont source d'inquiétude puisque la production agricole a doublé au Canada depuis les 50 dernières années (stimulée par l'utilisation massive de lisier et de fertilisants; Chambers *et al.*, 2001; Gilbert *et al.*, 2007) alors que le dépôts de produits azotés en provenance de l'atmosphère aurait atteint 7 kg N ha⁻¹ a⁻¹ dans la région du Bas Saint-Laurent, une augmentation équivalente à 14 fois les niveaux de la période pré-industrielle (0.5 kg N ha⁻¹ a⁻¹; Ro *et al.*, 1998). Aucune recherche n'indique que la situation ne s'est significativement améliorée au cours des dernières années. D'ailleurs, une récente étude réalisée par de Bruyn *et al.*, (2003) a montré une augmentation des rejets de matière organique et de nutriments de source agricole et urbaine dans les eaux du fleuve.

Afin de mettre en relief l'effet de l'activité anthropique sur la charge de nutriments dissous transitant vers le milieu estuaire, nous citerons ici une étude réalisée par Perakis et Hedin, (2002) qui montre que les eaux non impactées issues des systèmes fluviaux des forêts sud-américaines, avec une concentration moyenne en nitrates équivalente à 0.1 µM, sont davantage enrichies en azote organique dissous (acides aminés, protéines, peptides,

polypeptides...) qu'en composés azotés inorganiques. L'écart entre les concentrations en $\text{NO}_2^- + \text{NO}_3^-$ mesurées à Québec de 2003 à 2007 ($25.50 \pm 13.88 \mu\text{M}$; station 1; salinité = 0.1 ppt) et les concentrations rapportées par Perakis et Hedin constitue un indice éloquent de l'effet de l'activité anthropique du dernier siècle sur l'environnement fluvial du Saint-Laurent. Par ailleurs, lorsque l'on compare les concentrations de nitrates mesurées dans les eaux du fleuve Saint-Laurent à des systèmes tempérés lourdement impactés européen et américain, on constate que la charge de nutriments est moins importante dans les eaux du Saint-Laurent (où la capacité de résilience du milieu est plus élevée; nous reviendrons plus tard sur cette seconde hypothèse). Ainsi, l'estuaire de Humber (UK), 500 μM , Jickells *et al.*, 2000; l'estuaire de Gt. Ouse (UK) 520 μM , Sanders *et al.*, 1997; l'estuaire du Delaware (USA) 128 μM , Fisher *et al.*, 1988; la baie de Chesapeake (USA) 87 μM , Fisher *et al.*, 1988; et le fleuve Mississippi (USA) 240 μM , Nixon *et al.*, 1996), présentent tous des concentrations de nitrates relativement élevées. Tel que mentionné au chapitre III, les apports fluviaux de nutriments azotés n'atteignent pas systématiquement l'estuaire, ces derniers étant affectés par de nombreux processus biogéochimiques et ce, plus particulièrement en saison estivale. De ce fait, les conséquences de ces rejets sur l'estuaire du Saint-Laurent demeurent donc variables et nécessitent d'être étudiées plus en détail. La complexité du patron circulatoire impliquant des échanges advectifs et diffusifs entre les eaux saumâtres issues du golfe, les eaux océaniques en provenance de l'Atlantique (*via* les processus de resurgence verticaux) et les eaux douces d'origine continentale contribue à altérer la signature de la pollution anthropique et en amenuise ses effets potentiels. De ce fait, aucune augmentation significative des concentrations en éléments nutritifs azotés n'a pu être observée tant dans les eaux du golfe (Plourde et Thériault, 2004) que de l'estuaire du Saint-Laurent (cette étude). Considérant, à des fins de comparaison, la seule base de données disponible relatant la variabilité saisonnière des concentrations d'éléments nutritifs dans l'estuaire maritime au cours des années 1970 (radiale de Rimouski; Brindle et d'Amour, 1977), et l'ensemble des données obtenues dans le cadre de cette étude (mai 2003 à février 2006 à la station 8), il est intéressant de noter l'importante variabilité saisonnière ainsi que la relative stabilité décennale des variables mesurées. Alors que les concentrations d'oxygène dissous à la base de la colonne d'eau amorçaient une importante décroissance (passant de ~ 110 μM en 1970 à ~ 65 μM en 1990; Gilbert *et al.*, 2005), on ne constate

aucune variation significative des concentrations de surface en azote organique et inorganique dissous pour cette même période (Fig. IX-1 et IX-2; les données d'azote organique dissous ne sont disponibles que pour les périodes d'échantillonnage mai 2003 et juillet 2004).

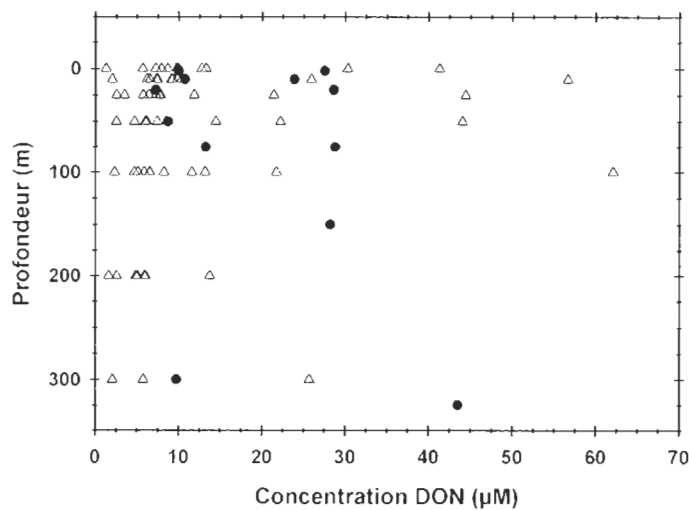


Figure IX-1 Concentration d'azote organique dissous (DON) mesurées à la station 8 (Rimouski). Les triangles représentent les données de 1970 Brindle et d'Amour, (1977) obtenues mensuellement entre août 1973 et octobre 1974. Les cercles noirs représentent les données obtenues lors des campagnes mai 2003 et juillet 2004.

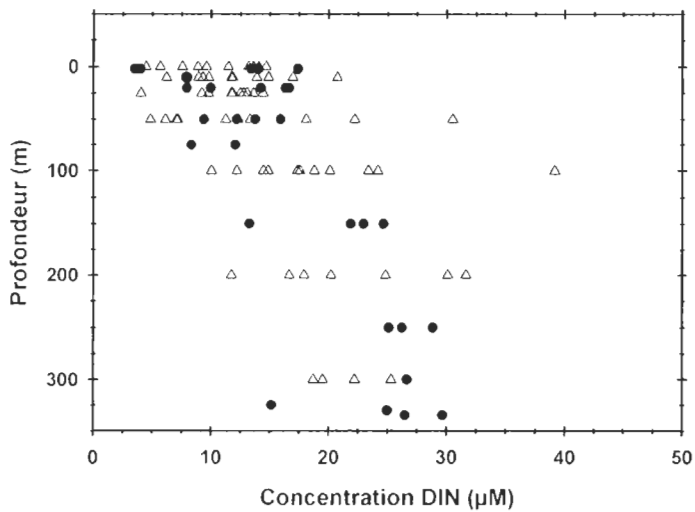


Figure IX-2 Concentration d'azote inorganique dissous (DIN) mesurées à la station 8 (Rimouski). Les triangles représentent les données de 1970 Brindle et d'Amour, (1977) obtenues mensuellement entre août 1973 et octobre 1974. Les cercles noirs représentent les données obtenues lors des campagnes mai 2003 et juillet 2004.

De plus, la variabilité des rapports stoechiométriques semble plus importante à l'échelle saisonnière que décennale suggérant que les processus de dissolution et d'assimilation jouent un rôle primordial dans la dynamique des nutriments azotés dans l'estuaire du Saint-Laurent (Fig. IX-3). Alors que l'incidence des processus de dissolution est difficile à déterminer dans l'estuaire maritime à cause du comportement non conservatif des éléments nutritifs dans ce milieu hautement dynamique (Chap. 3), les récentes études de Louchouarn *et al.*, 1997; St-Onge *et al.*, 2003; Gilbert *et al.*, 2005, Thibodeau *et al.*, 2006 et Gilbert *et al.*, 2007 font, ensemble, la démonstration de l'existence d'un lien causal entre l'accroissement des flux de nutriments de source anthropique, les changements au sein des communautés phytoplanctoniques (thanatocénose d'une série sédimentaire prélevée près de la station 8), l'augmentation des flux de matière organique de source marine vers le compartiment sédimentaire (au cours des 3 dernières décennies) et le développement de conditions hypoxiques à la tête du chenal Laurentien. Bien que ces études suggèrent l'occurrence d'une lente eutrophisation du système (tel que observée par Cloern, (2001) dans de nombreux environnements côtiers) peu d'informations sont disponibles concernant les processus pélagiques impliqués dans le cycle de l'azote (advection, spéciation, assimilation, respiration, minéralisation). Afin de bien cerner le rôle des processus saisonniers impliqués dans la dynamique de l'azote dans l'estuaire du Saint-Laurent, une synthèse des informations recueillies dans cette étude est présentée ci-dessous.

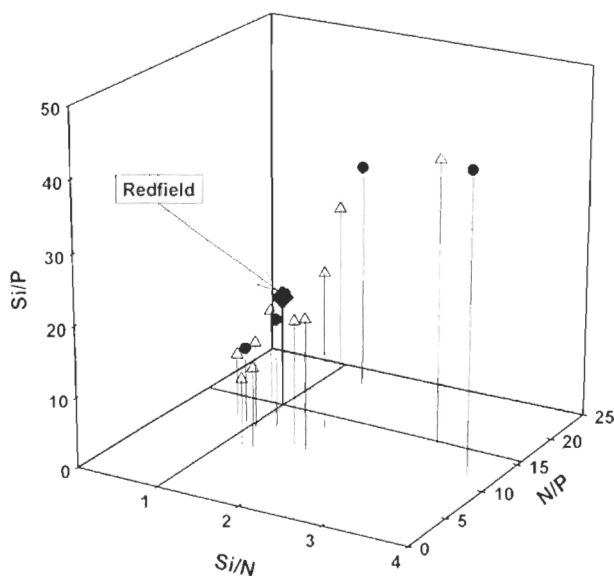


Figure IX-3 Ratios stochiométriques des éléments nutritifs mesurés à la station 8 (Rimouski) dans la masse d'eau de surface (2 m). Les triangles représentent les données de 1970 selon Brindle et d'Amour, (1977) obtenues mensuellement entre août 1973 et octobre 1974. Les cercles noirs représentent les données obtenues lors des campagnes mai 2003 et juillet 2004.

9.2 Variabilité saisonnière des processus pélagiques impliqués dans le cycle de l'azote

Au cours des campagnes d'échantillonnage décembre 2005 et février 2006 (saison hivernale), des températures près du point de congélation ont été observées au niveau de la couche d'eau de surface, induisant la formation d'un couvert de glace qui limite la profondeur de pénétration du rayonnement solaire incident (Annexe 1.4). De faibles concentrations de chlorophylle (*Chl-a*) sont observées dans la colonne d'eau tant de l'estuaire maritime que de l'estuaire supérieur (Tableau III-2), alors que les espèces azotées dissoutes (DIN : NH_4^+ et $\text{NO}_2^- + \text{NO}_3^-$) montrent un comportement conservatif dans ce dernier. À partir des caractéristiques géochimiques de la matière particulaire en suspension (Tableau III-2) et des profils d'éléments nutritifs relevés dans la colonne d'eau (Tableau III-1; similaires à ceux rapportés par Coote et Yeats; 1979), nous pouvons déduire, qu'en cette période, l'activité phytoplanctonique était très faible dans tout le système. De plus, les concentrations de NH_4^+ mesurées dans la colonne d'eau de l'estuaire maritime étant inférieur à la limite de détection (< 0.01 μM ; Tableau III-1 et Fig. III-2), nous pensons que les processus de broutage (*via* l'activité zooplactonique) et de minéralisation (*via* l'activité

bactérienne) ne jouaient qu'un rôle accessoire dans la dynamique de l'azote au cours de cette période. Les abondances de bactérioplancton mesurées en décembre 2005 sont statistiquement similaires sur l'ensemble de la colonne d'eau de l'estuaire maritime et demeurent comparables à celles observées en milieu océanique ($\sim 3.60 \times 10^5$ cells.ml $^{-1}$; Tableau V-1). La présence du couvert de glace affecterait davantage la diversité des communautés bactériennes que l'abondance totale de bactéries. Pour des mesures d'abondance similaire, on observe une augmentation de la proportion de cellules de type LNA (faible concentration d'acide nucléique) en comparaison aux données obtenues en octobre 2005 (Tableau V-1).

Le portrait observé en mai 2003 (au printemps) est radicalement différent (Annexe I.1). Alors que les apports fluviaux de DIN atteignent leur niveau maximum (~ 500 T DIN d $^{-1}$; Tableau III-6), la signature géochimique de la matière particulaire en suspension échantillonnée dans la colonne d'eau de l'estuaire maritime suggère la présence d'une importante activité phytoplanctonique, générant un important pool de matière organique endogène (Tableau III-2). Des concentrations d'ammonium relativement élevées sont observées dans les couches d'eau supérieures de l'estuaire (atteignant 1.73 μM ; Fig. III-2), suggérant que ce pool de matière organique particulaire labile est affecté par de nombreux processus d'altération. Parmi les processus susceptibles d'être impliqués dans la production pélagique de NH $_4^+$, le broutage et l'excrétion zooplanctonique, la dissolution des macromolécules et la minéralisation bactérienne peuvent être mentionnées (Chap. III). Les flux de NH $_4^+$ en provenance de l'estuaire supérieur étant modestes durant cette période (correspondant à < 6% des flux de DIN), nous pensons que la contribution exogène au pool de NH $_4^+$ observée dans l'estuaire maritime demeure négligeable. De plus, les résultats obtenus dans le cadre de cette étude suggèrent qu'une fraction substantielle de la matière organique particulaire labile nouvellement formée est exportée vers les couches d'eau intermédiaire et profonde de l'estuaire maritime (Fig. III-2 et Tableau III-2). Cette dernière observation est validée par les précédents travaux de Levasseur et Thérriault (1987) et Colombo *et al.* (1996) qui ont démontré que de larges particules, principalement constituées de frustules de diatomées et de pelotes fécales de copépodes, sont abondamment formées lors des événements de forte productivité primaire. Comme ces

particules sont éventuellement appelées à sédimenter, elle ne sont que partiellement dégradées par les processus pélagiques de dissolution et d'altération bactérienne (Lucotte *et al.*, 1991), favorisant l'enrichissement en Si de la base de la colonne d'eau (Tableau III-1) tel que relaté par Levasseur et Thérriault, (1987). De façon générale, les profils de $\text{NO}_2^- + \text{NO}_3^-$ répertoriés le long de l'axe principal de l'estuaire maritime sont strictement comparables aux profils retrouvés dans l'étude de Plourde et Thérriault (2004) réalisée dans le golfe. Les concentrations de $\text{NO}_2^- + \text{NO}_3^-$ relativement élevées mesurées à la base de la colonne d'eau suggèrent la présence de processus de nitrification au sein du chenal Laurentien tel que rapporté par Savenkoff *et al.*, (1996) et Plourde et Thérriault, (2004) dans le golfe. Ces dernières observations sont supportées par des analyses isotopiques ($\delta^{13}\text{C}$ et $\delta^{15}\text{N}$) effectuées sur la matière particulaire en suspension présente dans la colonne d'eau de l'estuaire en mai 2003 (Fig. IX-4 et IX-5).

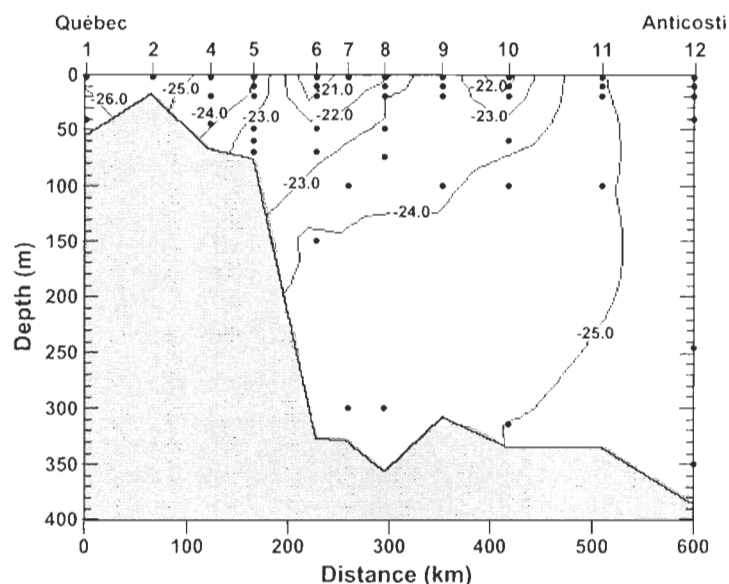


Figure IX-4 Composition isotopique du carbone organique particulaire (exprimée en ‰ par rapport à PDB) dans l'estuaire du Saint-Laurent au cours de la campagne mai 2003.

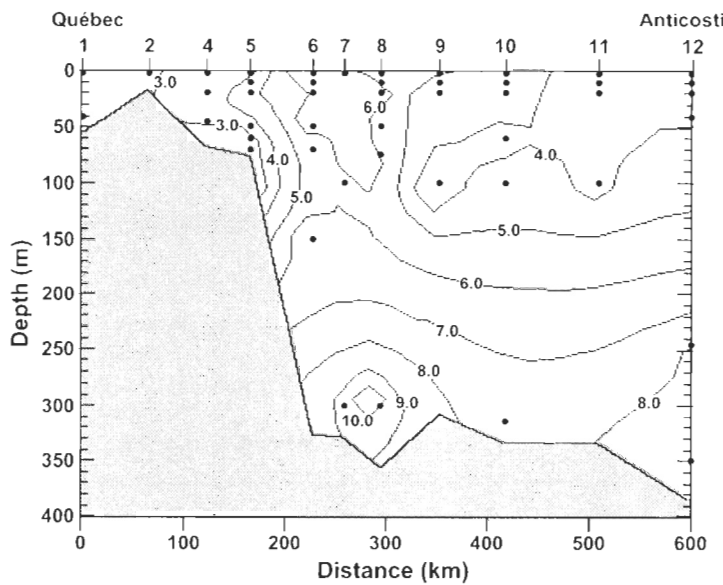


Figure IX-5 Composition isotopique de l'azote particulaire total (exprimée en ‰ par rapport à air) dans l'estuaire du Saint-Laurent au cours de la campagne mai 2003.

La signature isotopique du carbone et de l'azote nous montre l'incidence des processus d'altération différentielle de la matière particulaire autochtone. La composition isotopique du carbone nous indique clairement les zones de production primaire (-20‰; occasionné par l'assimilation d'ions carbonates enrichis comparé au dioxyde de carbone atmosphérique) ainsi que les processus de diagenèse précoce, favorisant l'accumulation préférentielle de matériaux réfractaires généralement appauvris en ^{13}C tel les polysaccharides au détriment de macromolécules labiles (glucose, acétate, carbohydrate, lipide) généralement enrichies en ^{13}C (Pancost and Pagani, 2006). Cependant, ces processus d'altération moléculaires différentiels sont complexes et spécifiques aux communautés fonctionnelles en place et mériteraient donc d'être approfondis (Fig. IX-4). En contre partie, les composés carbonés sont solubilisés plus lentement que les composés azotés (*via* l'hydrolyse enzymatique bactérienne; Smith *et al.*, 1992), la signature isotopique de l'azote nous permet de percevoir beaucoup plus nettement les processus de minéralisation bactériens affectant les particules dans la colonne d'eau de l'estuaire; l'enrichissement

différentiel de la matière particulaire en suspension signalant l'occurrence de processus d'altération bactériens dans la colonne d'eau (Fig. IX-5).

Au cours de la mission de juillet 2004 (été), des concentrations de Chl- α relativement élevées ont été observées tant dans l'estuaire supérieur que maritime (Tableau III-2 et Annexe 1.2). Ces concentrations, similaires à celles observées à la fin de mai 2003 sont caractéristiques d'événements de forte productivité tels que répertoriés et décrits par Sinclair, (1978); Thérriault et Levasseur, (1985) et Levasseur et Thérriault, (1987). Par ailleurs, l'obtention de faibles rapports N/P et de rapports Si/N et Si/P élevés suggèrent que ce bloom phytoplanctonique a atteint un stade de maturation avancé au mois de juillet 2004 (Margalef, 1958). Alors qu'une fraction de la production primaire sénesciente est affectée par des processus de minéralisation au niveau de la thermocline, supportant une production dite régénérée, la fraction complémentaire est exportée vers la base de la colonne d'eau (Chap. 3). Ensemble, les résultats obtenus lors des campagnes d'échantillonnage mai 2003 et juillet 2004 confirment la présence d'un important transfert de matière organique endogène dans l'estuaire maritime. Nos analyses statistiques confirment cette hypothèse en indiquant que ces événements ont significativement modifié les profils verticaux de PON, de Chl- α , de PHAA et des rapports C/N de la matière organique (Tableau III-2; IV-1 et Fig. IV-4).

Bien que l'extension spatio-temporelle de ces événements de transfert de matière autochtone ne peut pas être précisée dans le cadre de cette étude, nous pensons que ces épisodes peuvent être reliés, dans une certaine mesure, au développement de l'hypoxie dans la masse d'eau profonde de l'estuaire du Saint-Laurent puisque la respiration bactérienne est positivement corrélée à la production primaire dans les milieux aquatiques (del Giorgio *et al.*, 1997). Ainsi, nous supposons que ces événements de forte productivité sont susceptibles d'avoir induit certaines modifications au sein du compartiment bactérien pélagique tant au niveau de la composition spécifique des communautés que de l'activité de ces dernières (Lovejoy *et al.* 2000). Bien qu'à notre connaissance, aucune mesure directe d'activité bactérienne n'ait été réalisée à ce jour dans la colonne d'eau de l'estuaire, certaines preuves indirectes ont été obtenues dans le cadre de cette étude. D'abord, les

mesures préliminaires d'abondance bactérienne effectuées en septembre 2004, jumelées aux résultats présentés au chapitre V, montrent la présence localisée de concentrations supérieures dans la masse d'eau de surface ainsi que des abondances généralement uniformes sur toute la colonne d'eau. Ces derniers résultats suggèrent l'occurrence de processus hétérotrophes dans toute la masse d'eau estuarienne indistinctement des horizons riches ou non en oxygène dissous. Ensuite, les profils verticaux d'azote organique dissous (DON) effectués en juillet 2004 sur la radiale de Rimouski fournissent un indice supplémentaire de la présence d'activité bactérienne sur l'ensemble de la colonne d'eau (Fig. IX-1). Puisque la production de DON dans les environnements marins est largement imputable à l'activité bactérienne hétérotrophe (Bronk et Gilbert, 1993) nous pensons que les concentrations élevées de DON mesurées en juillet 2004 pourraient constituer un indicateur de l'activité bactérienne tel que suggéré par Kirchman *et al.* (2004) pour la matière organique dissoute (DOM) dans les environnements dulcicoles. De tels pulses de DON ont été sporadiquement identifiés en août 1974 et juillet 2004 alors que de faibles concentrations ont été mesurées au cours de l'été 1973 ainsi qu'en mai 2003 (Fig. IX-1). La relation entre ces pulses et les conditions océanographiques singulières identifiées en juillet 2004 reste à déterminer.

Alors que ~70% du pool de DON peut être directement utilisé par les communautés microbiennes (Seitzingen *et al.*, 2002), les processus d'assimilation et de production bactérienne pourraient avoir induit un découplage des processus de nitrification/dénitrification au sein de la masse d'eau hypoxique (Pearl *et al.*, 2002) menant à une diminution des concentrations en NO_3^- (*via* la dénitrification et la nitrification incomplète Li *et al.*, 2006). Cette hypothèse est supportée par une série de mesures réalisées dans la colonne d'eau de l'estuaire maritime montrant une diminution concomitante des concentrations de O_2 et de $\text{NO}_2^- + \text{NO}_3^-$ dans la masse d'eau profonde en juillet 2004 (Tableau IV-1; Fig. IV-2 et IV-3) affectée par des conditions hypoxiques. Suite à de nombreux entretiens avec des spécialistes de la géochimie du système laurentien (A. Mucci; D. Gilbert, A. deVernal; B. Sundby), deux hypothèses ont été retenues pour expliquer les basses concentrations de $\text{NO}_2^- + \text{NO}_3^-$ observées à la base de la colonne d'eau; I) une sous-estimation de la concentration en NO_x due à des artefacts liés à la cueillette, à

l'entreposage ou à l'analyse des espèces dissoutes azotées et II) la présence de processus d'assimilation phytoplanctonique et respiration bactérienne. Bien que la première hypothèse ne peut être complètement écartée en raison du caractère ponctuel des observations, un effort substantiel a été déployé pour supporter la seconde (Chap. IV). Nous pensons que tant les processus de dénitrification en milieu pélagique (Li *et al.*, 2006) que l'assimilation des nitrates dans la zone aphotique (Flynn *et al.*, 2002; Clark *et al.*, 2002) pourraient se produire lors des événements estivaux de forte productivité précédemment décrits.

En octobre 2005 (automne), les concentrations de Chl-*a* diminuent significativement tant dans les eaux de surface de l'estuaire supérieur que de l'estuaire maritime. Simultanément, on observe une diminution des concentrations de matière particulaire labile dans la colonne d'eau (Tableau III-1) ainsi qu'une augmentation des concentrations de O₂ et de NO₂⁻ + NO₃⁻ en comparaison aux mesures obtenues en juillet 2004 (Fig. IV-2; IV-3 et Annexe 1.3). Les apports advectifs de matière particulaire endogène vers la base de la colonne d'eau ayant diminués de façon significative, nous supposons que la demande en oxygène par l'activité bactérienne hétérotrophe aurait diminuée de façon concomitante, contribuant à l'établissement d'un nouvel équilibre entre les processus de nitrification et de dénitrification dans la masse d'eau profonde de l'estuaire maritime. Notons que les processus circulatoires de grande échelle impliqués dans l'advection de la masse d'eau profonde vers la tête du chenal Laurentien ont pu contribuer (dans une proportion indéterminée) au renouvellement des stocks de NO₂⁻ + NO₃⁻ au cours de la période automnale. Bien que les apports fluviaux de NH₄⁺ atteignent leur maximum au cours de la période automnale (Tableau III-6) l'activité phytoplanctonique ne semble pas les exploiter puisque les concentrations de Chl-*a* demeurent relativement faibles dans tout le système (Tableau III-2). En comparaison aux mesures d'abondance bactérienne réalisées en décembre 2005, les valeurs moyennes obtenues au cours de la période automnale dans les masses d'eau superficielle et intermédiaire demeurent significativement plus élevées (c'est-à-dire 5.9×10^5 cell ml⁻¹) alors que la masse d'eau de fond ne présente pas de variation significative (c'est-à-dire 3.9×10^5 cell ml⁻¹) d'une saison d'échantillonnage à l'autre (Tableau V-1). De plus, le %HNA (cellules contenant des niveaux élevés d'acides

nucléiques) dans la colonne d'eau de l'estuaire maritime demeure significativement plus élevé en automne qu'en hiver et ce indépendamment de la masse d'eau. Ces résultats suggèrent qu'à la fin de la saison productive, les abondances bactériennes tendent à s'uniformiser au sein de la colonne d'eau, les plus grosses cellules du bactérioplancton (statistiquement dépendantes des concentrations en nutriments) laissant place à de plus petites cellules potentiellement plus compétitives pour les ressources nutritives (Zubkov *et al.*, 2001).

9.3 Variabilité saisonnière des processus impliqués dans le cycle de l'azote au sein des marais côtiers de l'estuaire maritime

Les marais côtiers sont des environnements de transition complexes, dont la dynamique est étroitement liée à de nombreux processus physiques (forçage externe, par exemple: marées, apports sédimentaires) ainsi qu'à de multiples mécanismes biochimiques (régulation interne, par exemple : activité autotrophe et hétérotrophe) interagissant à des échelles spatio-temporelles très variables. La compréhension de ces systèmes, quant à leur rôle fonctionnel, constitue donc un véritable défi pour les océanographes. Afin de bien comprendre l'incidence saisonnière des principaux processus physiques et des mécanismes biochimiques impliqués dans la dynamique de l'azote au sein de ce type d'écosystème, nous avons développé un modèle conceptuel de type holistique. Ce modèle a été appliqué à la dynamique du marais non impacté de Pointe-aux-Épinettes (PAE; possédant une superficie de 15 ha) ainsi qu'au marais impacté de Pointe-au-Père (PAP; 23 ha). Les figures IX-6 à IX-9 présentent les flux saisonniers de nutriments azotés (DIN, $\text{NO}_2^- + \text{NO}_3^-$ et NH_4^+ , respectivement) entre les différents réservoirs limitrophes des marais à l'étude en kg N 90 j^{-1}), en supposant que l'intensité des flux est constante à l'échelle du marais ($\pm 1 \text{ km}^2$) et d'une saison (c'est-à-dire 90 jours).

Les flux advectifs de nutriments azotés en provenance des tributaires ainsi que les flux tidaux sont issus de mesures de terrain présentées au chapitre VI. Parce que nos mesures de production de N_2O sont incomplètes (Annexe 2) les données de Usui *et al.* (2001; moyenne = 1400 nmol N $\text{m}^{-2} \text{ h}^{-1}$) sont utilisées pour évaluer l'incidence relative de ce processus alors que les données du chapitre VII sont utilisées pour définir la contribution

de la dénitrification. Ainsi, les flux associés à la dénitrification incluent la production bactérienne de N₂ et de N₂O. Nous assumerons que les mesures de dénitrification effectuées à 6 °C (moyenne = 17.9 µmol N₂ m⁻² h⁻¹) sont représentatives des conditions printanière et automnale alors que les mesures effectuées à 2 °C (moyenne = 10.4 µmol N₂ m⁻² h⁻¹) et 12 °C (30.3 µmol N₂ m⁻² h⁻¹) sont caractéristiques des saisons hivernale et estivale, respectivement. Les données d'apport atmosphérique (pluie et neige) sont issues de Ro *et al.*, (1998) (données moyennes annuelles répertoriées à Montmorency, Qc., 5.76 kg N ha⁻¹ a⁻¹) alors que les données de fixation sont issues de l'étude de Howarth *et al.*, (1996) (moyenne = 0.56 g N m⁻² a⁻¹). Sur les bases d'une production microphytobenthique moyenne de 35 g C m⁻² a⁻¹ (Chap. VIII) nous pouvons établir la demande en azote du microphytobenthos à 2.40 kg N j⁻¹ pour PAE et à 3.68 kg N j⁻¹ pour PAP et ce, pour chacune des saisons libres de glace, en supposant un rapport C/N moyen de 6. À partir des travaux de Dai et Weigert, (1996) et Dame *et al.*, (1991) (réalisés sur des marais à Spartine situés dans l'état de la Georgie et de la Caroline du Sud (USA), respectivement) l'assimilation de DIN par les phanérogames a été estimée à 14.5 kg N j⁻¹ pour PAE et 22.2 kg N j⁻¹ pour PAP (en supposant une production annuelle moyenne de 1 440 g C m⁻² a⁻¹ [ou 1 080 g C m⁻² pour les 9 mois libres de glace] et un rapport C/N moyen de 40). Les processus d'assimilation du DIN dans les marais côtiers en saison hivernale étant largement inconnus, nous avons extrapolé les flux associés à ce processus à partir des données de productivité primaire moyenne établies pour les algues de glace dans l'Arctique Canadien (41 mg C m⁻² j⁻¹ Gosselin *et al.*, 1998) en supposant une stoechiométrie de 6:1 (C:N) et une épaisseur moyenne de glace de 37 cm. En ce qui concerne les bilans saisonniers présentés aux figures IX-6 et IX-7, les flux de DIN issus des processus de minéralisation de la matière organique (ammonification, nitrification, DNRA) ont été déterminés à posteriori, suivant les déficits ou les excédants de DIN définis à l'aide du modèle. Constituant une approximation sommaire, ces flux sont estimés en vue de produire un bilan équilibré.

En ce qui concerne la seconde série de bilans (NO₂⁻ + NO₃⁻ et NH₄⁺) présentés aux figures IX-8 et IX-9), les flux issus de la réduction dissimilaire des nitrates en ammonium (DNRA) sont tirés du chapitre VII. Pour les fins du présent calcul, nous assumons que la production moyenne d'ammonium observée au cours des expériences réalisées en

microcosme est essentiellement occasionnée par ce processus bactérien. Ainsi, nous assumons que les flux de NH_4^+ mesurés à 6 °C sont représentatifs du DNRA au printemps et à l'automne (33.7 $\mu\text{mol N m}^{-2} \text{ h}^{-1}$) alors qu'aux périodes estivale et hivernale, ces flux (vraisemblablement sur et sous-estimés respectivement; voir discussion ci-dessous) ont été soigneusement ajustés en vue de produire des bilans équilibrés. Enfin, les flux d'espèces azotées engendrées par la nitrification sont tirés de ce même chapitre VII et correspondent à 8.81 $\mu\text{mol N}_2 \text{ m}^{-2} \text{ h}^{-1}$ en période hivernale, à 16.8 $\mu\text{mol N}_2 \text{ m}^{-2} \text{ h}^{-1}$ en période printanière et automnale et à 29.7 $\mu\text{mol N}_2 \text{ m}^{-2} \text{ h}^{-1}$ en période estivale. Les apports sous-terrain, le ruissellement, ainsi que l'effet de la macrofaune ont été négligés dans le cadre du présent bilan. De plus, nous supposons que les processus d'accrétion et d'érosion sont à l'équilibre sur une base saisonnière. La dynamique sédimentaire des marais de PAE et PAP étant actuellement à l'étude, l'approche quantitative adoptée (plaques d'accrétion, piège à sédiment, radiochimie isotopique sur des séries sédimentaires) nous permettra d'aborder cet aspect de façon plus détaillée (Annexe 3). Conscient de la variabilité spatiale et temporelle des processus observés au sein des environnements de type marais côtiers, nous savons que les bilans préliminaires produits dans le cadre de cette étude demeurent fort approximatifs et que par conséquent, ils devront être utilisés avec discernement.

En examinant les flux saisonniers de DIN affectant les marais étudiés (Fig. IX-6 et IX-7), nous pouvons d'abord constater que le marais de PAP est davantage affecté par des apports continentaux que le marais de PAE (moyenne à PAE < 0.01 kg N j^{-1} ; moyenne à PAP = 2.18 kg N j^{-1}). Alors que la contribution des apports continentaux aux flux advectifs totaux d'azote dirigés vers le marais de PAP est relativement importante (entre 9 et 32%), ces déversements ne constituent qu'une infime fraction des flux de N conduit vers le marais de PAE (< 0.01%). Nous pensons que la conséquence première de ces apports azotés dans le marais de PAP est de limiter la rétention de DIN en provenance de la masse d'eau estuarienne (moyenne à PAE = 0.77 kg N j^{-1} ; moyenne à PAP = 0.13 kg N j^{-1}), la demande des communautés autotrophes et hétérotrophes étant satisfaite par les charges azotées en provenance des émissaires et/ou de la minéralisation de la matière organique de source allochtone et autochtone.

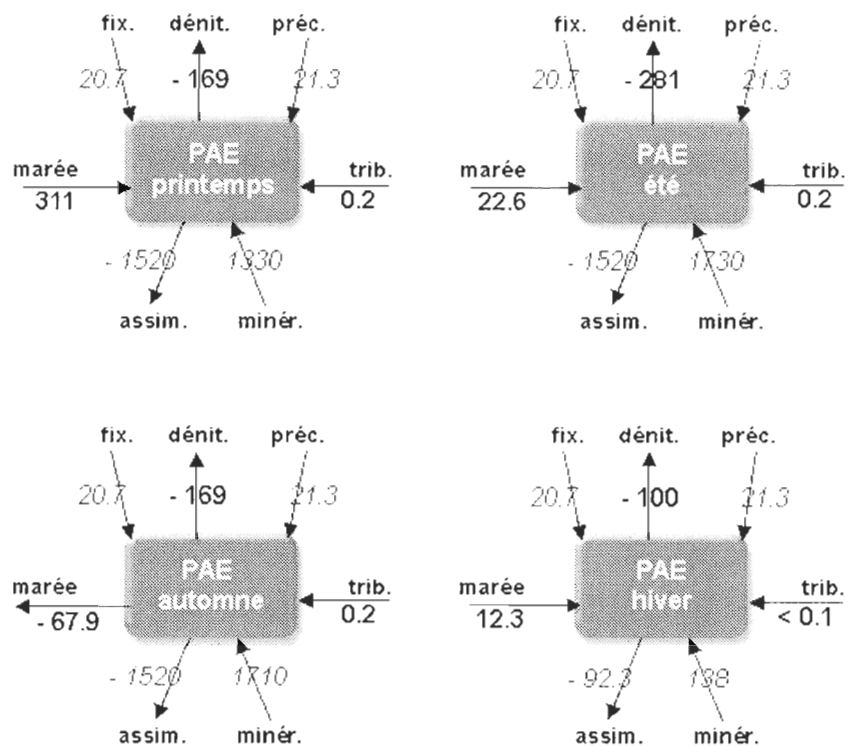


Figure IX-6 Bilan saisonnier d'azote inorganique dissous (DIN) pour le marais de Pointe-aux-Epinette (PAE; présenté en kg N 90j⁻¹). Les flux négatifs indiquent une perte en azote pour le système alors que les flux positifs indiquent un gain. Les flux inscrits in gras sont issus de mesures directes alors que ceux inscrits en italiques sont estimés. fix = fixation; dénit. = dénitrification; préc. = apports atmosphériques solides et liquides; marées = échanges tidaux; trib. = apports continentaux; assim. = assimilation et minér. = minéralisation.

De façon générale, notre modèle semi-quantitatif suggère que ces processus de minéralisation participent de façon importante aux apports totaux de DIN vers le marais. En moyenne, la contribution de la minéralisation est estimée à $89 \pm 7\%$ (AV \pm SD) pour les périodes libres de glace, alors que la contribution relative de la minéralisation en période hivernale semble plus variable d'un marais à l'autre (33% pour PAP et 72% pour PAE). Nous pensons que cette variabilité résulte d'une méconnaissance de l'activité autotrophe et hétérotrophe au sein de la banquise et de la colonne d'eau sous jacente en saison hivernale. Puisque les flux associés à la minéralisation sont déterminés à partir des demandes définies par le modèle, l'incertitude occasionnée par l'insuffisance de données concernant la fixation et l'assimilation limite notre interprétation de la dynamique hivernale des

environnements étudiés. Des mesures réalisées sur des carottes de glace prélevées dans les marais à l'étude (Chap. VI) ont montré la présence de pigments chlorophylliens ($< 7 \mu\text{g l}^{-1}$) et de bactéries (entre 3.07 et 8.32×10^5 cellules ml^{-1}) suggérant l'existence d'une importante communauté microbienne au sein de cet environnement glacé. Bien que le rapport Chl-*a*/Phéopigment nous indique la présence de cellules relativement dégradées (conférant aux communautés autotrophes un rôle marginal dans le cycle de l'azote dans ce milieu hautement turbide) l'incidence du périphyton sur les flux géochimiques demeure largement inconnue en période hivernale.

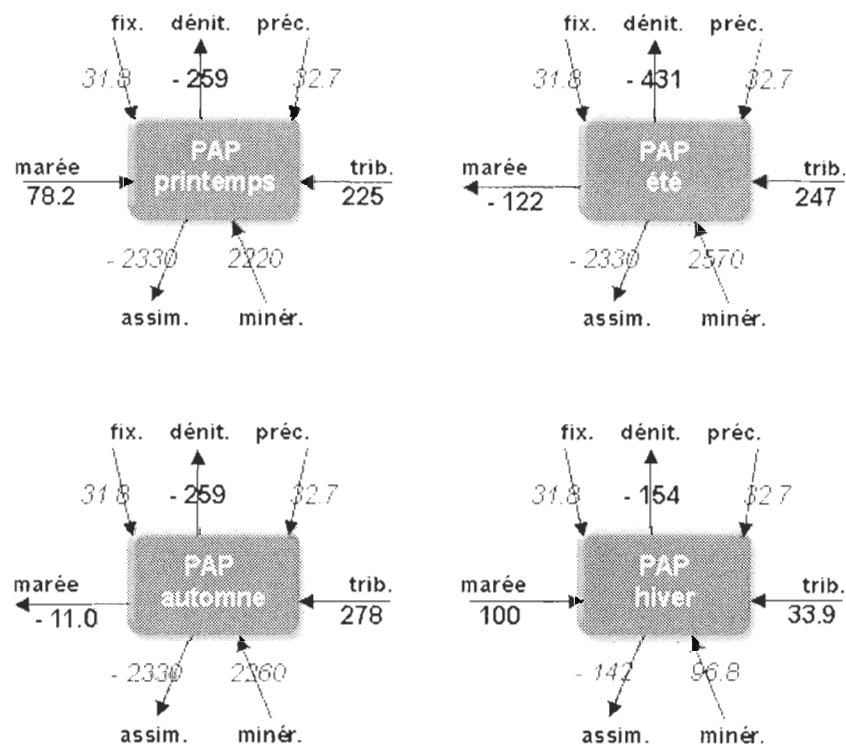


Figure IX-7 Bilan saisonnier d'azote inorganique dissous (DIN) pour le marais de Pointe-au-Père (PAP; présenté en kg N 90j⁻¹). Les flux négatifs indiquent une perte en azote pour le système alors que les flux positifs indiquent un gain. Les flux inscrits in gras sont issus de mesures directes alors que ceux inscrits en italiques sont estimés. fix = fixation; dénit. = dénitrification; préc. = apports atmosphériques solides et liquides; marées = échanges tidaux; trib. = apports continentaux; assim. = assimilation et minér. = minéralisation.

Au cours des saisons libres de glace, les processus de minéralisation (qui atteignent leur intensité maximum en été) semblent étroitement répondre aux demandes des espèces autotrophes halophiles, largement représentées par *Spartina alterniflora*, *Spartina patten* ainsi que par de nombreuses espèces appartenant au microphytobenthos (Chap.VIII). Selon notre modèle, ces processus de dégradation bactérienne pourraient à eux seuls soutenir plus de 88% de la production primaire des marais. Cette hypothèse est supportée par de nombreux travaux qui ont montré que l'ammonification a des effets importants sur les fonctions physiologiques et la croissance des communautés autotrophes des zones côtières (par exemple Nixon *et al.*, 1996). Par ailleurs, comme la disponibilité de l'ammonium est reconnue pour inhiber l'activité de la nitrogénase (enzyme nécessaire à la fixation de l'azote atmosphérique) au sein des marais à Spartine (Yoch et Whiting, 1986), la prédominance des processus d'ammonification dans les milieux étudiés nous mène à reconsiderer à la baisse l'intensité de la fixation telle que décrite dans le modèle.

Bien que les bilans d'azote établis pour les deux marais à l'étude montrent de nombreuses similitudes, certains aspects, liés à l'incidence de l'activité anthropique, engendrent des variations appréciables des différents flux présentés. Alors que, l'assimilation est plus importante que la minéralisation dans le marais de PAE au printemps (condition hypothétiquement induite par l'éclosion printanière de la flore), la situation opposée est observée au cours des autres saisons investiguées. En première approximation, nous pensons que les caractéristiques intrinsèques de ce milieu non-impacté (caractérisé par la présence d'un réseau hydrographique élaboré de type anastamosé et par d'importantes étendues de colonies bactériennes spécialisées) semble favoriser une intense minéralisation du matériel organique de source allochtone et autochtone. Le bilan saisonnier établi pour le marais de PAP demeure différent; à l'exception de la saison estivale, où les processus de minéralisation bactériens atteignent leur intensité maximale favorisant la dispersion de DIN vers le bassin estuaire, l'expression des processus d'assimilation semble plus importante que la minéralisation tant au printemps qu'à l'automne, qu'en hiver. Deux hypothèses sont avancées expliquer cette variabilité; 1) considérant que les abondances et la composition spécifique du microphytobenthos sont reliées au niveau et à la nature des perturbations observées, il est plausible que les assemblages phytobenthiques puissent induire certains

changements au niveau du bilan d'azote du marais de PAP, 2) le marais de PAP étant affecté par l'érosion, il est possible que le temps de transition du matériel organique ne soit pas suffisamment long pour permettre une diagenèse complète.

La première hypothèse est supportée par une étude présentée au chapitre VIII qui montre la présence d'une plus grande abondance de cellules phytobenthiques dans le marais de PAP, dominée par des formes épipélique (notamment *Achnanthes delicatula*, *Navicula cryptocephala* et *Cocconeis disculus*) ayant des demandes en nutriments plus importantes que les formes épipsammiques, dominantes dans le marais de PAE. Ainsi, il est intéressant de constater que les rejets de nutriments azotés observés dans le marais de PAP ont pu stimuler l'activité phytobenthique tant en terme de productivité que de diversité. Tel qu'énoncé dans les récents travaux de Emmett (2007), de faibles amendements de nutriments azotés peuvent momentanément favoriser la productivité nette d'un milieu donné. Bien que plausible, la seconde hypothèse, essentiellement basée sur des observations ponctuelles, mérite d'être approfondie en procédant notamment à des mesures de temps de résidence des eaux de ruissellement sur la plate-forme herbacée.

En tenant compte de la spéciation des espèces de l'azote impliquées dans les flux de DIN précédemment décrite, on apprécie davantage l'incidence respective des processus impliqués. De plus, ces bilans additionnels présentés aux figures IX-8 et IX-9, nous permettent de poser un regard semi-quantitatif sur des processus bactériens associés à la minéralisation et à la transformation des espèces azotées tels l'ammonification, la nitrification et le DNRA.

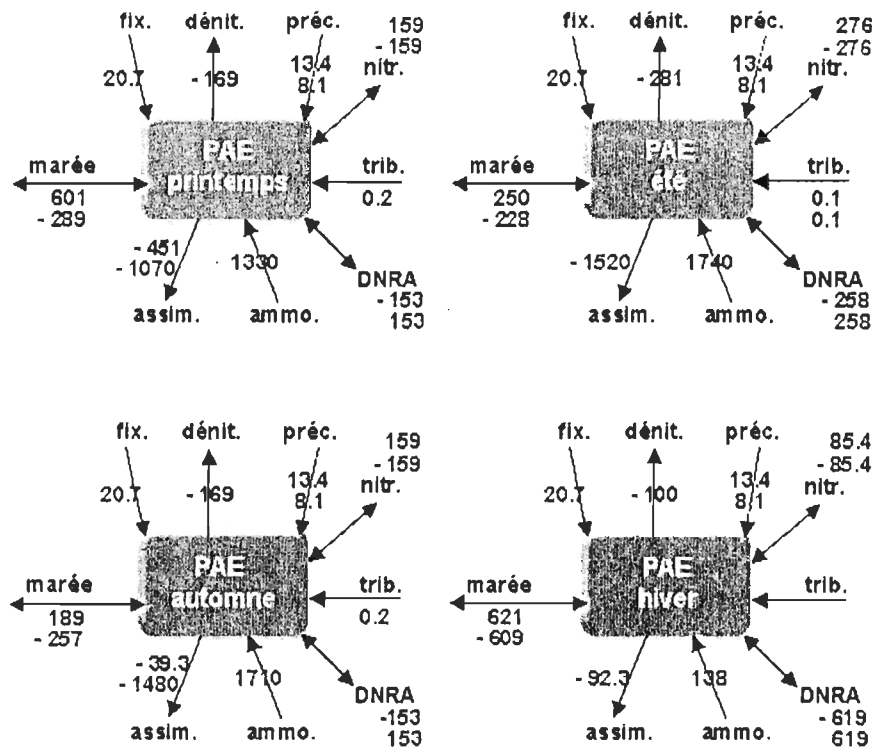


Figure IX-8 Bilan saisonnier de $\text{NO}_2^- + \text{NO}_3^-$ (bleu) et NH_4^+ (rouge) pour le marais de Pointe-aux-Épinette (PAE; présenté en kg N 90⁻¹). Les flux négatifs indiquent une perte en azote pour le système alors que les flux positifs indiquent un gain. fix = fixation; dénit. = dénitrification; préc. = apports atmosphériques solides et liquides; marées = échanges tidaux; trib. = apports continentaux; assim. = assimilation, ammo. = ammonification; DNRA = réduction dissimilatrice des nitrates en ammonium et nitr. = nitrification.

Ainsi, tel que décrit au chapitre VI, les marais étudiés se comportent généralement comme des puits de $\text{NO}_2^- + \text{NO}_3^-$ (de 7.84 à 32.1 mg N j⁻¹ m⁻²) et des sources de NH_4^+ (de 8.69 à 30.4 mg N j⁻¹ m⁻²) pour la masse d'eau estuarienne et ce, indépendamment de la saison ou des niveaux de stress anthropiques impliqués. En utilisant une simulation numérique nous avons fait la démonstration que des masses significatives de $\text{NO}_2^- + \text{NO}_3^-$ sont séquestrées dans la frange herbacée lors des incursions tidales alors que de façon simultanée, un important pool de NH_4^+ est formé dans les eaux de surface et interstitielles des marais (Chap. VI).

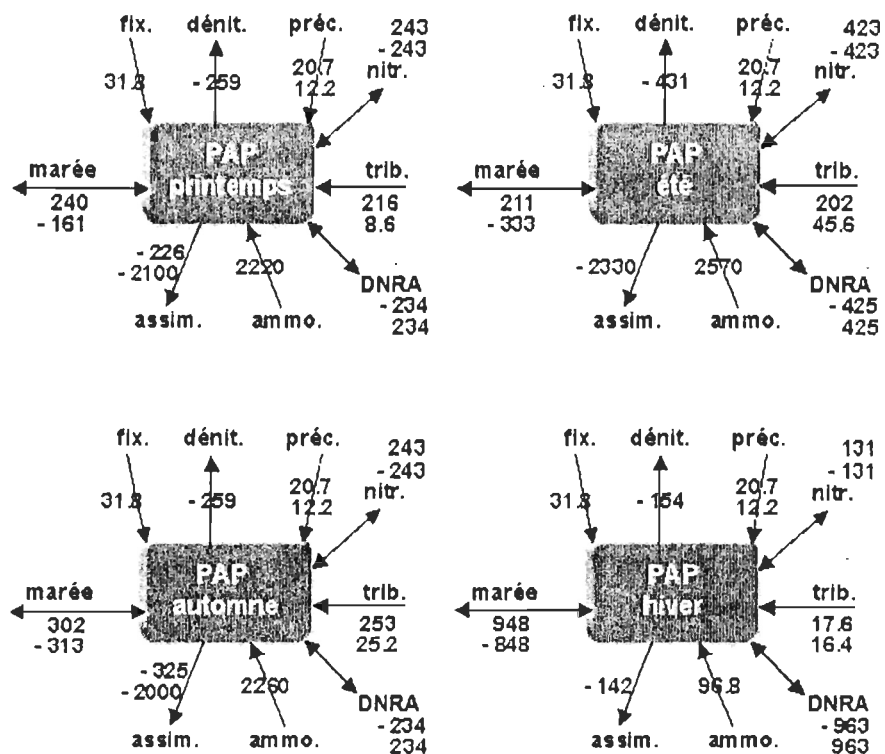


Figure IX-9 Bilan saisonnier de $\text{NO}_2^- + \text{NO}_3^-$ (bleu) et NH_4^+ (rouge) pour le marais de Pointe-au-Père (PAP; présenté en kg N 90⁻¹). Les flux négatifs indiquent une perte en azote pour le système alors que les flux positifs indiquent un gain. fix = fixation; dénit. = dénitrification; préc. = apports atmosphériques solides et liquides; marées = échanges tidaux; trib. = apports continentaux; assim. = assimilation, ammo. = ammonification; DNRA = réduction dissimilatrice des nitrates en ammonium et nitr. = nitritation.

Puisque NH_4^+ s'accumule plus rapidement qu'il n'est consommé, un important flux de NH_4^+ vers la masse d'eau estuarienne est observé. Les apports continentaux de $\text{NO}_2^- + \text{NO}_3^-$ n'excèdent pas la demande biochimique des marais (tel que défini par les bilans), nous réitérons que les déversements observés dans le marais de PAP ont davantage induit des problèmes d'érosion que tout autre type de perturbations écosystémiques. En effet, de nombreuses structures issues de processus érosifs sont visibles dans le marais de PAP comme la présence de micro-ravins, de micro-falaises en marge des chenaux tidaux alimentés par les tributaires ainsi que de plans de glissement engendrés par la solufluxion et la gélifluxion. En général, les déversements de $\text{NO}_2^- + \text{NO}_3^-$ et de NH_4^+ dans les marais côtiers sont potentiellement plus problématiques pour la masse d'eau estuarienne que pour

les marais eux-mêmes puisqu'en somme, la disponibilité de ces espèces favorisera la dispersion de NH_4^+ vers les eaux côtières.

L'intensité des processus biochimiques impliqués dans la dynamique des espèces inorganiques dissoutes de l'azote dans les marais côtiers a été déterminée en laboratoire, à l'aide d'une technique d'enrichissement isotopique appliquée sur des microcosmes (Chap. VII). Nous avons ainsi déterminé que la nitrification constitue la principale source de nitrate pour la dénitrification, satisfaisant plus de 80% de la demande. De plus, cette étude a montré que moins de 31% des nitrates consommés par l'activité chimiotrophe sont retirés des marais par la dénitrification, alors que la fraction complémentaire est transformée en ammonium *via* la DNRA. Ce dernier résultat n'est cependant pas supporté par les bilans établis; les $\text{NO}_2^- + \text{NO}_3^-$ consommés par la dénitrification (production de N_2 et N_2O) atteignant 52 et 50% de la consommation estivale totale (assimilation et DNRA) dans les marais de PAE et PAP, respectivement. Comparativement aux expériences menées en microcosme (où des artefacts liés au confinement sont systématiquement observés), nous pensons que les bilans saisonniers d'azote réalisés dans le cadre de cette synthèse sont davantage représentatifs de la dynamique des marais côtiers (notamment concernant certaines réactions sensibles aux conditions redox) parce qu'ils tiennent compte du contexte environnemental. Ainsi, l'importance relative de la DNRA par rapport à la dénitrification telle qu'estimée dans le chapitre VII mérite d'être révisée. Puisque la DNRA est un phénomène moins sensible à l'effet inhibiteur de l'oxygène que la dénitrification, la disponibilité de la matière organique demeure le principal facteur agissant sur l'équilibre entre les deux transformations (Fazzolari *et al.*, 1998) Ainsi, il est fort intéressant de constater qu'en période estivale, alors que les processus de dégradation hétérotrophe atteignent leur maximum (stimulés par les températures élevées), la dénitrification demeure plus importante que la DNRA. Alors que le printemps et l'automne peuvent être distingués comme des périodes transitoires, la situation inverse est observée en hiver. Au cours de la période hivernale, nous pensons que l'action érosive de la banquise combinée aux épanchements d'eaux froides et riches en oxygène et en nitrates favorisent la DNRA comparativement à la dénitrification. De plus, les contraintes de compression appliquées à la plate-forme herbacée, induites par le poids de la banquise au cours des cycles de marées,

pourrait contribuer à soutenir la DNRA en mobilisant des sulfures (H_2S , FeS_2 , $CuFeS_2$) vers les horizons sédimentaires superficiels.

Des études ont démontré que certaines bactéries impliquées dans l'oxydation des sulfures en sulfates utiliseraient les nitrates comme agent oxydant (comme accepteur d'électrons) donnant lieu à une production significative d'ammonium (Brunet et Garcia-Gil, 1996). D'autres auteurs ont montré que la disponibilité du carbone organique pourrait avoir une incidence importante sur la prédominance respective de ces processus (Kelso *et al.*, 1997; Silver *et al.*, 2001; Tiedje, 1988). Alors que la dénitrification serait favorisée dans des environnements relativement pauvres en matière organique (condition rencontrée en période estivale), la disponibilité du carbone (induit par l'action abrasive de la glace en période hivernale) favoriserait les organismes qui utilisent les accepteurs d'électrons de façon plus efficace; la DNRA transfert huit électrons pour chaque mole de nitrates réduits alors que la dénitrification en permet le transfert de cinq. Nous pensons que des efforts substantiels doivent être déployés pour définir l'intensité des processus de production d'ammonium tel la DNRA et l'ammonification puisque, selon nos modèles, ils constituent des processus clés dans la dynamique de l'azote au sein des marais côtiers du Saint-Laurent maritime.

9.4 Incidence des marais côtiers dans la dynamique estuarienne du DIN

Constituant un milieu important pour les processus de minéralisation de la matière organique et de recyclage des nutriments inorganiques dissous, les marais côtiers peuvent être considérés à bien des égards comme de véritables stations d'épuration tertiaires. La nature poreuse de l'assise sédimentaire constituant les marais favorise l'établissement de macro/microflores benthiques spécialisées qui participent activement à la rétention et à la séquestration des espèces azotées impliquées dans la problématique de l'eutrophisation des zones côtières. Afin de déterminer les rôles des marais côtiers sur le cycle dans l'estuaire maritime du Saint-Laurent, nous avons tenté de définir un bilan provisoire d'azote au sein de cet environnement de transition. (Fig. IX-10). Bien que fort approximatif, ce bilan annuel demeure très utile pour définir le potentiel de résilience de ce milieu au prise avec des apports significatifs de nutriments tant de source urbaine, agricole qu'industrielle. De

façon plus spécifique, notre étude à montrée des fluctuations considérables des apports fluviaux de DIN avec une moyenne annuelle de ($AV \pm SD$) $85\ 200 \pm 67\ 600\ T\ N\ a^{-1}$ (Chap. III). Sachant que les processus d'advection vertical sont responsables d'apports totalisant plus de $240\ 000\ T\ N\ a^{-1}$ vers la masse d'eau superficielle de l'estuaire maritime (Savenkoff *et al.*, 2001), nos données suggèrent que les apports fluviaux contribuent de façon significative à la charge de DIN retrouvée à la surface de l'estuaire ($\sim 26\%$). Des $325\ 000\ T\ N\ a^{-1}$ transitant par la masse d'eau superficielle de l'estuaire maritime, $25\ 300 \pm 15\ 500\ T\ N\ a^{-1}$ seraient transférées vers le golfe du Saint-Laurent (Sinclair *et al.*, 1976: ou $\sim 8\%$ des apports totaux) alors qu'environ $300\ 000\ T\ N\ a^{-1}$ seraient disponibles pour l'activité autotrophe estuarienne. En accord avec les travaux de Thériault et Levasseur (1985), l'assimilation du DIN par la production primaire pélagique serait responsable du retrait d'environ $162\ 000\ T\ N\ a^{-1}$ de la couche superficielle (basé sur une production annuelle moyenne de $104\ g\ C\ m^{-2}\ a^{-1}$, une stoechiométrie de 6:1 (C:N) et une superficie de $9\ 350\ km^2$), soit $\sim 54\%$ de la charge de DIN disponible dans la couche d'eau de surface de l'estuaire maritime. La fraction de DIN résiduelle (soit $138\ 000\ T\ N\ a^{-1}$) serait vraisemblablement consommée dans les zones littorales (incluant les marais) par les microphytes (diatomées, dinoflagellés, cocolithophoridés), macrophytes (fucus, laminaires) et phanérogames (zostère, rupia et spartine) ainsi que par des processus biochimiques sédimentaires (incluant la dénitrification, la nitrification incomplète, l'anammox, la réduction des NO_3^- par Mn^{2+}).

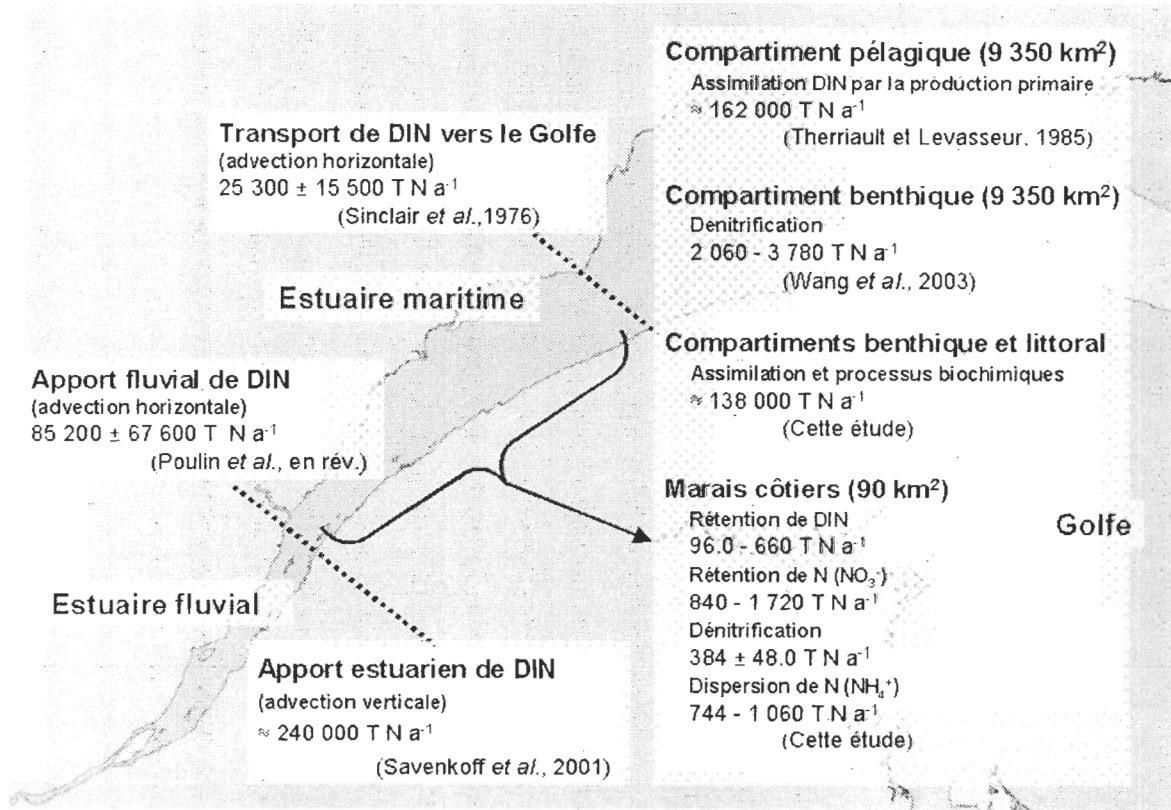


Figure IX-10 Bilan annuel d'azote inorganique dissous (DIN) dans l'estuaire du Saint-Laurent (présenté en T N a^{-1}) (moyenne \pm écart type).

Les marais côtiers de l'estuaire maritime seraient responsables du rabattement d'environ $96.0 \text{ T N(DIN) a}^{-1}$ (selon la moyenne de nos bilans saisonniers et considérant une superficie de 90 km^2 ; Dionne, 1986) ou de $\sim 660 \text{ T N(DIN) a}^{-1}$ (selon la moyenne des incubations saisonnières réalisées en microcosme et considérant une superficie de 90 km^2). Ce potentiel de rabattement correspond à $\sim 0.44\%$ des apports fluviaux (c'est-à-dire entre 0.11 et 0.77%), à $\sim 0.12\%$ des apports totaux (c'est-à-dire entre 0.03 et 0.20%) ou encore à 0.28% de la capacité de rétention des zones littorales (c'est-à-dire entre 0.07 et 0.48%). Dans leur ensemble, ces résultats nous montrent que les marais côtiers ont une incidence très limitée sur la dynamique de l'azote dans l'estuaire maritime, en comparaison à la production primaire pélagique. Bien que l'efficacité de ces milieux, à titre de processeurs de nutriments inorganiques azotés est incontestable, leur superficie limitée restreint la portée des processus impliqués. De façon plus spécifique, le rabattement des $\text{NO}_2^- + \text{NO}_3^-$ atteindraient 840 T N a^{-1} (selon la moyenne de nos bilans saisonniers) ou $1\ 720 \text{ T N a}^{-1}$ (selon nos expériences en microcosme), soit entre 1 et 2% des apports fluviaux moyens de

$\text{NO}_2^- + \text{NO}_3^-$ (c'est-à-dire $73\ 500\ \text{T N a}^{-1}$). Par ailleurs, la dispersion de NH_4^+ atteindrait entre $744\ \text{T N a}^{-1}$ (selon la moyenne de nos bilans saisonniers) et $1\ 060\ \text{T N a}^{-1}$ (selon nos expériences en microcosme). Puisque la DNRA est au centre de la dynamique des espèces inorganiques dissoutes azotées au sein des marais côtiers de l'estuaire maritime du Saint-Laurent, le véritable potentiel épurateur de ces derniers réside au niveau de la dénitrification. Cette capacité dénitritifiante a été évaluée à $384 \pm 168\ \text{T N a}^{-1}$ soit $\sim 0.5\%$ des apports de $\text{NO}_2^- + \text{NO}_3^-$ en provenance du fleuve. Bien que l'impact de la dénitrification dans les marais côtiers puissent paraître insignifiant au vue des masses considérables de $\text{NO}_2^- + \text{NO}_3^-$ transitant par l'estuaire, les populations bactériennes occupant les milieux de type marais côtiers demeurent en moyenne 6 fois plus efficaces que celle présentes des les sédiments estuariens (Chap. VII).

9.5 Potentiel de résilience de l'estuaire

Quoique nous ne disposions que des données de dénitrification benthique de Wang *et al.* (2003) pour estimer des bilans annuels et que nous connaissons la grande variabilité saisonnière des flux de matière organique vers le compartiment benthique (Lavigne *et al.*, 1997), nous avons tout de même tenté l'exercice afin d'obtenir en première approxiamtion de la capacité dénitritifiante des sédiments de l'estuaire. Ainsi, Wang *et al.* (2003) ont montré que l'activité dénitritifiante dans les sédiments de l'estuaire varient entre 1.80 et 3.30 $\mu\text{mol N m}^{-2}\ \text{h}^{-1}$ soit des valeurs oscillant entre environ $2\ 060\ \text{T N a}^{-1}$ et $3\ 780\ \text{T N a}^{-1}$, en considérant que la superficie de l'estuaire est d'environ $9\ 350\ \text{km}^2$. En faisant la somme de la capacité dénitritifiante moyenne du compartiment benthique et des marais côtiers, nous pouvons évaluer la capacité totale annuelle de l'estuaire maritime à $3\ 300\ \text{T N}$. Ce potentiel dénitritifiant correspond à $\sim 4\%$ des apports de DIN en provenance du fleuve. Même si une sous-estimation majeure de la dénitrification nous amenait à doubler ou tripler cette valeur dans une étude future, la contribution de la dénitrification demeurerait relativement modeste. Ainsi, une bien faible proportion des nitrates importés dans l'estuaire via l'advection de la masse d'eau profonde et l'écoulement des eaux continentales ou issus de la minéralisation de la matière organique tant de source allochtone et autochtone sera retournée vers l'atmosphère sous forme d'azote moléculaire. Malgré que l'on puisse ajouter à ce potentiel épurateur l'incidence des processus de dénitrification pélagique

ponctuellement observés au cours de l'été 2004 (dont l'intensité reste à déterminer), l'estuaire maritime du Saint-Laurent demeure vulnérable aux problèmes relatifs à l'eutrophisation.

Récemment, il a été suggéré que l'anammox pourrait constituer un processus alternatif d'épuration très efficace au sein des milieux anaérobies (Dong et Sun, 2007). Bien que les marais constituent des sources d'ammonium pour le système estuarien, il demeure que ce processus bactérien pourrait affecter le bilan d'azote élaboré si on venait à quantifier le rendement de ce processus dans les marais et dans les sédiments de l'estuaire. Par ailleurs, même si de façon optimiste on parvenait à démontrer que les communautés bactériennes impliquées dans l'anammox sont aussi efficace que les communautés dénitritifiantes au sein du milieu estuarien (tel que proposé par Engstrom *et al.*, 2005 dans divers milieux côtiers), il en demeure que moins de 10% des apports de DIN en provenance du fleuve pourrait être retranché. Par conséquent, nous pouvons affirmer qu'à cours terme, le potentiel de résilience de l'estuaire maritime demeure relativement faible. Puisque les apports de nitrates vers le bassin estuarien sont en hausse depuis les années 90 (dû à l'utilisation croissante d'engrais inorganique; Gilbert *et al.*, 2007), l'émergence de problèmes associés à la prolifération d'algues toxiques (par exemple: *Alexandrium tamarense*) demeure un risque bien réel. De façon rétroactive, l'ensemble des processus associés à l'eutrophisation du système (abondamment discutés dans cette étude) pourrait mener à une production accrue de N₂O au sein des sédiments estuariens peu profonds (Usui *et al.*, 2001) et ainsi, augmenter la contribution de l'écosystème estuarien à la problématique des émissions de gaz à effet de serre (Smith, 1990). De plus, l'écosystème Laurentien serait exposé à une multitude de contaminants et de polluants de source anthropique (par exemple: Ray *et al.*, 1991; Hobbs *et al.*, 2002). Ces substances sont susceptibles de perturber les communautés microbiennes endogènes qui jouent un rôle essentiel dans le maintien de l'équilibre des écosystèmes tant en terme de production, de recyclage des nutriments, qu'en terme de biorémédiation des polluants (Siron *et al.*, 1993; Lebaron *et al.*, 2001; Crump *et al.*, 2003).

De multiples facteurs environnementaux régissent l'activité et la survie des microorganismes en milieu aquatique. Outre les stress biotiques et abiotiques naturels (c'est-à-dire le rayonnement, la température, la compétition pour les nutriments), on note l'apparition de nouveaux facteurs liés à l'utilisation grandissante des zones côtières, tels que la présence croissante de substances immunotoxiques et génotoxiques. L'ensemble de ces paramètres est susceptible d'affecter le fonctionnement des communautés bactériennes marines et d'entraîner, à plus long terme, un dysfonctionnement plus général des écosystèmes marins côtiers. Nous devons ajouter à ces effets directs de l'activité anthropique, les effets indirects dont les changements climatiques (IPCC). Certaines études ont montré que ces changements contribuent actuellement au rehaussement du niveau moyen des mers et à l'érosion des milieux littoraux (Morisette, 2006). Ces milieux constituant l'ultime interface entre les environnements terrestres et marins demeurent affectés par divers processus d'érosion, dont le sapement par les vagues et les courants de marées, l'affouillement et l'arrachement par les glaces littorales, le gel-dégel, la dessiccation et les activités biologiques tel le broutage par les faunes aillées. Ainsi, bien que l'estuaire du Saint-Laurent puisse être considéré comme un important bassin de dilution pour les apports continentaux, son potentiel de résilience actuel et futur paraît bien mince.

9.6 Conclusion et perspective

Notre étude a montré que les modifications écosystémiques induites tant par les changements saisonniers que par l'activité anthropique sont susceptibles de produire des effets significatifs sur la dynamique de l'azote au sein de l'estuaire du Saint-Laurent. Aux vues des objectifs initiaux, à savoir : 1) identifier et quantifier les principaux processus et les mécanismes saisonniers impliqués dans le cycle de l'azote à l'échelle de l'estuaire ainsi que dans les écosystèmes de type marais salants bordant son littoral, 2) définir le rôle des marais côtiers (en tant que puits/source d'azote) sur la dynamique de l'azote en milieu estuarien, 3) définir le potentiel de résilience du système estuarien face à l'activité anthropique, nous pouvons tirer les conclusions suivantes.

Concernant le premier objectif, notre étude a montré qu'au cours des périodes automnale et hivernale, tant l'activité phytoplanctonique que bactérienne sont appelées à

jouer un rôle secondaire dans la dynamique de l'azote au sein de l'estuaire; les processus de mélange physique ordonnant la distribution spatiale des espèces azotées d'origine essentiellement allochtone. Au cours des périodes printanière et estivale, cette tendance est inversée. Les processus d'assimilation, de broutage et d'excrétion semblent jouer un rôle prépondérant sur la dynamique des espèces azotées dans la masse d'eau superficielle de l'estuaire. Plus en profondeur, les processus couplés de dissolution des macro-molécules et de minéralisation bactérienne affectent de façon importante la composition géochimique du matériel particulaire appelé à sédimentier ainsi que les conditions physico-chimiques de la colonne d'eau. Parmi les processus observés au cours des périodes de forte productivité, on note la présence d'une importante translocation du pool de matière particulaire de source endogène accompagnée d'une augmentation des abondances bactériennes dans la colonne d'eau de l'estuaire. Lors de ces événements, on observe d'importantes variations des concentrations de DIN, de DON et d'oxygène dissous vraisemblablement imputables à l'activité bactérienne hétérotrophe pélagique.

Reconnaissant le rôle essentiel du compartiment microbien sur le cycle de l'azote, il est impératif de mieux documenter cet aspect en identifiant les constituantes majeures des communautés bactériennes impliquées dans le recyclage de la matière organique de source autochtone et allochtone. Des efforts substantiels devront être déployés afin de mieux comprendre les effets des changements environnementaux (notamment l'augmentation des apports de nutriments) sur la composition des communautés bactériennes estuariennes ainsi que les relations entre la diversité bactérienne et la productivité de l'écosystème. L'application de techniques moléculaires telles que l'électrophorèse sur gel en gradient dénaturant (DGGE), le séquençage et clonage du rARN 16S et l'hybridation *in situ* (Abed *et al.*, 2002; Taton *et al.*, 2003) pourraient constituer une approche intéressante pour étudier le compartiment bactérien de l'estuaire du Saint-Laurent. De plus, les nouveaux outils moléculaires, tels que les micro-réseaux, pourraient fournir des informations pertinentes en ce qui concerne la diversité phylogénétique et fonctionnelle des communautés bactériennes (Greer *et al.*, 2001). Enfin, l'utilisation de la géochimie isotopique pourrait nous fournir un large éventail d'informations concernant la variabilité des processus de fixation.

d'assimilation et de respiration au sein du milieu estuaire (Pancost et Pagani, 2006 ; Altabet, 2006).

De façon fort intéressante, la dynamique de l'azote dans les marais côtiers de l'estuaire maritime semble faiblement affectée par les variations saisonnières. Dans l'atteinte du second objectif, notre étude a montré que tant les processus de production de DIN (minéralisation) de transformation (DNRA et nitrification) que de consommation (assimilation et dénitrification) seraient peu affectés par la température. Cette première série de résultats suggère que les communautés microbiennes évoluant au sein des marais côtiers de l'estuaire maritime sont bien adaptées aux écarts de température engendrés par la succession des saisons. Bien que les basses températures, la présence du couvert de glace et les faibles apports de matière organique contraignent tant la production primaire que les processus de minéralisation, nos bilans saisonniers montrent que les communautés bactériennes responsables de la DNRA pourraient être stimulées par l'action mécanique de la banquise sur le substrat organo-minéral des marais. De plus notre étude a montré que les marais côtiers de l'estuaire maritime du Saint-Laurent se comportent généralement comme des puits d'azote inorganique dissous. Indépendamment du contexte saisonnier ou des niveaux de stress anthropiques observés, les marais étudiés agissent comme des puits de $\text{NO}_2^- + \text{NO}_3^-$ et des sources de NH_4^+ pour la masse d'eau estuarienne. Notre étude a montré que des masses significatives de $\text{NO}_2^- + \text{NO}_3^-$ sont séquestrées dans la frange herbacée lors des incursions tidales alors que de façon simultanée, un important pool de NH_4^+ est formé dans les eaux de surface et interstitielles des marais. Puisque ce NH_4^+ s'accumule plus rapidement qu'il n'est consommé, un important flux de NH_4^+ vers la masse d'eau estuarienne est observé. Parmi les principaux processus biochimiques impliqués dans cette dynamique singulière, nous pouvons mentionner le rôle prépondérant de l'assimilation par les flores autotrophes ainsi que l'ammonification, la nitrification, la dénitrification et la DNRA accomplis par l'activité bactérienne hétérotrophe.

Afin de compléter notre revue des processus bactériens et de valider les bilans saisonniers produits dans les marais étudiés, il serait fort intéressant d'investiguer de façon plus directe certains de ces processus dont l'ammonification, l'anammox et la DNRA. De

plus, il serait souhaitable d'explorer les processus rétroactifs existant entre les cycles rédox du C, S, Mn, Fe et de l'azote afin d'approfondir notre connaissance des voies métaboliques impliquées dans le recyclage des espèces azotés (voir Hulth *et al.*, 2005). L'absence de données détaillées concernant les processus d'assimilation d'azote par les micro/macro flores (spécialement en période hivernale) a pu conduire à la surestimation ou à la sous-estimation des flux de DN impliqués dans ces transformations. Ainsi, il serait opportun de mieux définir la variabilité spatiale et saisonnière de la productivité des communautés autotrophes présentent tant au niveau du sédiment, de la banquise que des marelles. Constituant de véritables micro-environnements aux caractéristiques physico-chimiques singulières, ces milieux devraient être l'objet d'études plus poussées car ils abritent de multiples colonies microbiennes (formant par endroit de véritables tapis) dont l'activité est rétroactivement impliquée tant dans la formation que dans le maintien des marais, que dans les processus biochimiques de recyclage des espèces carbonées, phosphatées, soufrées et azotées. Les consortiums spécifiques constituant ces tapis microbiens présente une grande valeur scientifique car ils sont des analogues modernes des premiers écosystèmes côtiers et pourraient donc fournir des indices sur l'origine et l'évolution de la vie (Vincent *et al.*, 2004). Contenant des molécules spécifiques telles des enzymes, des pigments, des protéines et peptides leur permettant entre autre, de résister à des variations extrêmes de température, les organismes trouvés dans les tapis microbiens suscitent un grand intérêt chez de nombreux chercheurs car leur étude pourrait mener au développement de nouvelles applications tant sur le plan scientifique qu'industriel (par exemple Rodgers *et al.*, 2008).

En ce qui à trait au troisième objectif, notre étude a montré qu'une infime proportion des nitrates importés dans l'estuaire *via* l'advection de la masse d'eau profonde et l'écoulement des eaux continentales ou issus de la minéralisation de la matière organique tant de source allochtone et autochtone sera retournée vers l'atmosphère sous forme d'azote moléculaire. Bien que le bilan annuel préliminaire à partir duquel ces conclusions ont été tirées est incertain en raison de multiples approximations, nous pensons que l'estuaire maritime du Saint-Laurent demeure vulnérable aux problèmes relatifs à l'eutrophisation et que, par conséquent, son potentiel de résilience demeure bien faible. Parmi les incertitudes susceptibles d'affecter notre compréhension du système, nous devons d'abord mentionner

le manque d'information concernant la variabilité spatiale et temporelle des processus biochimiques impliqués dans le cycle de l'azote, tel que précédemment mentionné. Ensuite, il nous paraît clair que de nombreux aspects concertant la dynamique du pool de DON présent dans l'estuaire mérite d'être grandement approfondis.

Sachant que les substances constituant le DON ont un taux de renouvellement ~ 14 fois plus rapide en milieu côtier qu'en milieu océanique (Bernam et Bronk. 2003), il paraît évident que les substances constituant ce pool sont appelées à jouer un rôle important au niveau du compartiment microbien des milieux côtiers tant en terme de nutriments qu'en terme de vecteur de population microbienne exogène (Bronk, 2002). Il est donc essentiel de définir avec plus de rigueur les constituants moléculaires du réservoir de DON estuaire (urée, protéine, acide aminé, nucléotide, substance humique) afin d'identifier les sources potentiels de ces produits azotés. Certaines données préliminaires ont montré la présence d'importantes concentrations de DON tant dans la masse d'eau estuarienne que dans les marais côtiers (atteignant plus de 80 µM dans le marais de PAE). La caractérisation de ce pool nous fournirait un premier outil pour définir l'implication de ces substances dans le cycle de l'azote. Enfin, il serait intéressant d'étudier les processus saisonniers responsables de la production/consommation de ces substances dont notamment l'incidence des processus photochimiques, de l'activité de certaines bactéries cultivables ainsi que des mécanismes de coagulation et de polymérisation induits par les larges variations de salinité et de pH rencontrées en milieu estuaire.

Au cours du dernier siècle, la demande d'eau a constamment augmenté au Canada, et ce notamment à cause de l'accroissement de la population et de la consommation d'eau dans les municipalités. De plus, le développement d'industries énergivores, l'expansion de l'agriculture industrielle/irriguée et la hausse du niveau de vie imposent des pressions croissantes sur le système laurentien. Il existe à l'heure actuelle de nombreuses solutions qui peuvent aider à réduire les pertes d'éléments nutritifs vers les milieux côtiers. Par ailleurs, il est primordial de mener des activités de recherche et de surveillance afin de s'assurer que l'exploitation des ressources aquatiques n'excède pas la capacité de support du milieu. Il est essentiel de ne pas annuler les progrès réalisés grâce au traitement des eaux

usées et à d'autres mesures de contrôle en relâchant les normes ou en se laissant dépasser par la croissance démographique et le lobby de l'entreprise privée. À cet égard, la levée du moratoire sur l'élevage porcin ou l'imposition d'un décret dans la construction du port méthanier de Lévis fourni des exemples éloquents. La compréhension et la gestion des changements écosystémiques induits par l'activité anthropique sont des défis de taille pour la communauté scientifique et les décideurs publics. Actuellement, les discussions relatives aux réalités géopolitiques et aux intérêts économiques minent le débat concernant cette problématique. Les questions entourant le bien-être des générations futures et la conservation du patrimoine environnemental sont trop souvent considérées comme accessoires, voire contraignantes. Il est urgent de trouver des solutions concrètes aux problèmes que nous générerons ici et ailleurs. Nous devons nous engager collectivement à entreprendre de l'action afin de remédier à la lente détérioration de notre environnement.

9.7 References

- Abed, R.M.M., Schonhuber, W., Amann, R.. et Garcia-Pichel, F. (2002) Picobenthic cyanobacterial populations revealed by 16S rRNA-targeted *in situ* hybridization. Environ. Microbiol. 4, 375-382.
- Altabet, M.A. (2006) Isotopic tracers of the marine nitrogen cycle:present and past. Env. Chem. 2, 251–293.
- Berman, T. et Bronk, D.A. (2003) Dissolved organic nitrogen: a dynamic participant in aquatic ecosystems. Aquat. Microb. Ecol. 31, 279-305.
- Brindle, J.-R. et d'Amour, M. (1977) Distribution saisonnière des éléments nutritifs sur la radiale de Rimouski. Cahier d'information. Université du Québec à Rimouski. n°1.
- Bronk, D.A. et Gilbert, P.M. (1993) Contrasting patterns of dissolved organic nitrogen release by two size fractions of estuarine plankton during a period of rapid NH_4^+ consumption and NO_2^- production. Mar. Ecol. Prog. Ser. 96, 291-299.
- Bronk, D.A. (2002) Dynamic of organic nitrogen. Dans: Hansell, D.A. et Carlson, C.A. (Eds.) Biogeochemistry of marine dissolved organic matter. Academic press, San Diego, p.153-247.
- Brunet, R.C. et Garcia-Gil, L.J. (1996) Sulfide-induced dissimilatory nitrate reduction to ammonia in an anaerobic freshwater sediment. FEMS Mircobiol. Ecol. 21, 131-138.

- Chambers, P.A., Guy, M., Roberts, E.S., Charlton, M.N., Kent, R., Gagnon, C., Grove, G. et Foster, N. (2001) Nutrients and their impact on the Canadian environment. Agriculture and Agri-Food Canada, Environment Canada, Fisheries and Oceans Canada, Health Canada and Natural Resources Canada. Ottawa.
- Clark, D.R., Flynn, K.J. et Owens, N.J.P. (2002) The large capacity for dark nitrate-assimilation in diatoms may overcome nitrate limitation of growth. *New. Phyto.* 155, 101-108.
- Cloern, J.E. (2001) Our evolving conceptual model of the coastal eutrophication problem. *Mar. Ecol. Prog. Ser.* 210, 223-253.
- Colombo, J.C., Silverberg, N. et Gearing, J.N. (1996) Biogeochemistry of organic matter in the Laurentian Trough. I. Composition and vertical fluxes of rapidly settling particles, *Mar. Chem.* 51, 277-293.
- Coote, A.R. et Yeats, P.A. (1979) Distribution of nutrients in the Gulf of St. Lawrence. *J. Fish. Res. Board Can.* 36, 122-131.
- Crump, B.C., Kling, G.W., Bahr, M. et Hobbie, J.E. (2003) Bacterioplankton community shifts in an arctic lake correlate with seasonal changes in organic matter source. *Appl. Environ. Microbiol.* 69, 2253-2268.
- Dai, T. et Wiegert, R.G. (1996) Estimation of the primary productivity of *Spartina alterniflora* using a canopy model. *Ecography.* 19, 410-423.
- Dame, R.F., Spurrier, J., Williams, T., Kjerfve, B., Zing-mark, R., Wolaver, T., Chrzanowski, T., McKellar, H. et Vernberg, J. (1991) Annual material processing by a salt marsh-estuarine basin in South Carolina. *Mar. Ecol. Progr. Ser.* 72, 153-166.
- de Bruyn, A.M.H., Marcogliese, D.J. et Rasmussen, J.B. (2003) The role of sewage in a large river food web. *Can. J. Fish. Aquat. Sci.* 60, 1332-1344.
- del Giorgio, P.A., Cole, J.J. et Cimberis, A. (1997) Respiration rates in bacteria exceed phytoplankton production in unproductive aquatic system. *Nature.* 385, 148-151.
- Dionne, J.C. (1986) Érosion récente des marais intertidaux de l'estuaire du Saint-Laurent, *Géo. Ph. Quat.* 3, 307-323.
- Dong, Z., et Sun, T. (2007) A potential new process for improving nitrogen removal in constructed wetlands—Promoting coexistence of partial-nitrification and ANAMMOX. *Ecol. Eng.* 31, 69-78
- Emmett, B.A. (2007) Nitrogen saturation of terrestrial ecosystems: some recent findings and their implications for our conceptual framework. *Wat. Air Soil Pollut.* 7, 99-109.

- Engstrom, P., Dalsgaard, T., Hulth, S. et Aller, R. (2005) Anaerobic ammonium oxidation by nitrite (anammox): Implications for N₂ production in coastal marine sediments. *Geochim. Cosmochim. Acta.* 69, 2057-2065.
- Fazzolari, E., Nicolardot, B. et Germon, J.C. (1998) Simultaneous effects of increasing levels of glucose and oxygen partial pressures on denitrification and dissimilatory nitrate reduction to ammonium in repacked soil cores. *Eur. J. Soil Biol.* 34, 47-52.
- Fisher, T.R., Harding Jr., L.W., Stanley, D.W. et Ward, L.G., (1988) Phytoplankton, nutrients and turbidity in the Chesapeake, Delaware and Hudson Estuaries. *Est. Coast. Shelf Sci.* 27, 61-93.
- Flynn, K.J., Clark, D.R. et and Owens, N.J.P. (2002) Modelling suggests that optimization of dark nitrogen-assimilation need not be a critical selective feature in phytoplankton. *New. Phytol.* 155, 109-119.
- Gilbert, D., Sundby, B., Gobeil, C., Mucci, A. et Tremblay, G.H. (2005) A seventy-two-year record of diminishing deep-water oxygen in the St. Lawrence Estuary: The northwest Atlantic connection. *Limnol. Oceanogr.* 50, 1654-1666.
- Gilbert, D., Chabot, D., Archambault, P., Rondeau, B. et Hebert, S. (2007) Appauvrissement en oxygène dans les eaux profondes du Saint-Laurent marin : causes possibles et impacts écologiques. *Nat. Can.* 131, 67-75.
- Gosselin, M., Levasseur, M., Wheeler, P.A., Horner, R.A. et Booth, B.C. (1998) New measurements of phytoplankton and ice algal production in the Arctic Ocean. *Deep-Sea Res. II*, 44, 1623-1644.
- Greer, C.W., Whyte, L.G., Lawrence, J.R., Masson, L., et Brousseau, R. (2001) Current and future impact of genomics-based technologies on environmental science. *Environ. Sci. Technol.* 35, 360A-366A.
- Hobbs K.E., Lebeuf, M. et Hammill, M.O. (2002) PCBs and OCPs in male harbour, grey, harp and hooded seals from the Estuary and Gulf of St. Lawrence, Canada. *Sci. Total Environ.* 296, 1-18.
- Howarth, R.W., Billen, G., Swaney, D., Townsend, A., Jarworski, N., Lajtha, K., Downing, J.A., Elmgren, R., Caraco, N., Jordan, T., Berendse, F., Freney, J., Kueyarov, V., Murdoch, P. et Zhao-liang, Z. (1996) Riverine inputs of nitrogen to the North Atlantic Ocean: Fluxes and human influences. *Biogeochemistry.* 35, 75-139.
- Hulth, S., Aller, R.C., Canfield, D.E., Dalsgaard, T., Engstrom, P., Gilbert, F., Sundback, K. et Thamdrup, B. (2005) Nitrogen removal in marine environments: recent findings and future research challenges. *Mar. Chem.* 94, 125-145.
- Intergovernmental Panel on Climate Change (IPCC) (2007) (<http://www.ipcc.ch/>).

- Jickells, T., Andrews, J., Samways, G., Sanders, R., Malcolm, S., Sivyer, D., Parker, R., Nedwell, D., Trimmer, M. et Ridgway, J. (2000) Nutrient fluxes through the Humber Estuary - past, present and future. *Ambio.* 29, 130-150.
- Justic, D., Rabalais, N.N. et Turner, R.E. (1995) Stoichiometric nutrient balance and origin of coastal eutrophication. *Mar. Pollut. Bull.* 30, 41-46.
- Kelso, B.H.L., Smith, R.V., Laughlin, R.J. et Lennox, S.D. (1997) Dissimilatory nitrate reduction in anaerobic sediments leading to river nitrite accumulation. *Appl. Environ. Microbiol.* 63, 4679-4685.
- Kirchman, D.L., Dittel, A.I., Findlay, S.E.G. et Fischer, D. (2004) Change in bacterial activity and community structure in response to dissolved organic matter in the Hudson River, New-York. *Aquat. Microb. Ecol.* 35, 243-257.
- Lavigne, C., Juniper, S. K. et Silverberg, N. (1997) Spatio-temporal variability in benthic microbial activity and particle flux in the Laurentian Trough. *Deep-Sea Res.* 44, 1793-1813.
- Lebaron, P., Servais, P., Agogue, H., Courties, C. et Joux, F. (2001) Does the high nucleic acid content of individual bacterial cells allow us to discriminate between active cells and inactive cells in aquatic systems? *Appl. Environ. Microbiol.* 67, 1775-1782.
- Levasseur, M. and Therriault, J.-C. 1987. Phytoplankton biomass and nutrient dynamics in a tidally induced upwelling: the role of the $\text{NO}_3^- : \text{SiO}_4$ ratio. *Mar. Ecol. Prog. Ser.* 39: 87-97.
- Li, Y-H., Menviel, L. Peng, T-H. 2006. Nitrate deficits by nitrification and denitrification processes in the Indian Ocean. *Deep-Sea Res. I.* 53: 94-110.
- Louchouarn, P., Lucotte, M., Canuel, R., Gagné, J.-P. and Richard, L.-P. 1997. Sources and early diagenesis of lignin and bulk organic matter in the sediments of the Lower St. Lawrence Estuary and the Saguenay Fjord. *Mar. Chem.* 58: 3-26.
- Lovejoy, C., Legendre, L., Therriault, J.-C., Tremblay, J.-E., Klein, B., Ingram, G.R. (2000) Growth and distribution of marine bacteria in relation to nanoplankton community structure. *Deep Sea Res. II.* 47, 461-487.
- Lucotte, M., Hillaire-Marcel, C. et Louchouarn, P. (1991) First-order organic carbon budget in the St-Lawrence Lower Estuary from ^{13}C Data. *Est. Coast. Shelf Sci.* 32, 297-312.
- Margalef, R.. (1958) Temporal sucession and spatial heterogeneity in phytoplankton. Dans: Buzzati-Traverso, A.A. (Ed.). *Perpective in marine biology*. University of California Press, Berkeley and Los Angeles, pp.323-349.

Morisette, A. (2006) Évolution côtière haute résolution de la région de Longue-Rive-Forestville, Côte Nord de l'estuaire maritime du Saint-Laurent. MS thesis , Université du Québec à Rimouski, Rimouski, Qc. Canada.

Nixon, S.W., Ammerman, J.W., Atkinson, L.P., Berounsky, V.M., Billen, G., Boicourt, W.C., Boynton, W.R., Church, T.M., Ditoro, D.M., Elmgren, R., Garber, J.H., Giblin, A.E., Jahnke, R.A., Owens, N.J.P., Pilson, M.E.Q. et Seitzinger, S.P. (1996) The fate of nitrogen and phosphorus at the land sea margin of the North Atlantic Ocean. *Biogeochemistry*. 35, 141– 180.

Pancost, R.D. et Pagani, M.P. (2006) Controls on the carbon isotopic compositions of lipids in marine environments. *Env. Chem.* 2, 209-249.

Pearl, H.W., Dyble, J., Twomey, L., Pinckney, J.L., Nelson, J. et Kerkhof, L. (2002) Characterisation man-made and natural modification of microbial diversity and activity in coastal ecosystems. *Antonie Van Leeuwenhoek*. 81, 487-507.

Perakis, S.S. et Hedin, L.O. (2002) Nitrogen loss from unpolluted South American forests mainly via dissolved organic compounds. *Nature*. 415, 416– 419.

Plourde, J. and Therriault, J.-C. 2004. Climate variability and vertical advection of nitrate in the Gulf of St. Laurence, Canada. *Mar. Ecol. Prog. Ser.* 279, 33-43.

Ray, B.P., Dunn, J.F., Payne, L., Fancey, R. Helbig et P. Béland (1991) Aromatic DNA-carcinogen adducts in beluga whales from the Canadian Arctic and Gulf of St Lawrence. *Mar. Pollut. Bull.* 22, 392-396.

Ro, C., Vet, R., Ord, D. et Holloway, A. (1998) Canadian air and precipitation monitoring network (CAPMoN) Annual summary reports (1983-1996). Air quality research branch. atmospheric environment service. Environment Canada. Downsview. Ontario.

Rodgers, M., de Paor, D. et Clifford, E. (2008) Dairy washwater treatment using a horizontal flow biofilm system. *J. Environ. Manage.* 86, 114–120.

Sanders, R., Klein, C. et Jickells, T. (1997). Biogeochemical nutrient cycling in the upper Great Ouse Estuary, Norfolk, UK. *Est. Coast. Shelf Sci.* 44, 543-555.

Savenkoff, C., Vézina, A.F., Packard, T.T., Silverberg, N., Therriault, J.-C., Chen, W., Bérubé, C., Mucci, A., Klein, B., Mesplé, F., Tremblay, J.-E., Legendre, L., Wesson, J. et

Ingram, R.G. 1996. Distributions of oxygen, carbon, and respiratory activity in the deep layer of the Gulf of St. Lawrence and their implications for the carbon cycle. *Can. J. Fish. Aquat. Sci.* 53, 2451–2465.

Seitzinger, S.P., Sanders, R.W. et Styles, R. (2002) Bioavailability of DON from natural and anthropogenic sources to estuarine plankton. *Limnol. Oceanogr.* 47, 353-366.

- Sinclair, M., El-Sabh, M. et Brindle, J.-R., (1976) Seaward nutrient transport in the Lower St. Lawrence Estuary. *J. Fish. Res. Board Can.* 33, 1271-1277.
- Sinclair, M. (1978) Summer phytoplankton variability in the Lower St. Lawrence Estuary. *J. Fish. Res. Board Can.* 35, 1171-1185.
- Silver, W.L., Herman, D.J. et Firestone, M.K. (2001) Dissimilatory nitrate reduction to ammonium in upland tropical forest soils. *Ecology*. 82, 2410-2416.
- Siron, R., Pelletier, E., Delille, D. et Brochu, C. (1993) Réponse de la flore bactérienne de l'estuaire du Saint-Laurent à un déversement éventuel de pétrole. *Water Pollut. Res. J. Can.* 28, 385-414.
- Smith, K.A. (1990) Greenhouse gaz fluxes between land surfaces and the atmosphere. *Prog. Phys. Geo.* 14, 349-372.
- Smith, D.C., Meinhard, S., Alldredge, A.L. et Azam, F. (1992) Intense hydrolytic enzyme activity on marine aggregates and implications for rapid particle dissolution. *Nature*. 359, 139-142.
- St-Onge, G., Stoner, J.S. et Hillaire-Marcel, C. (2003) Holocene paleomagnetic records from the St. Lawrence Estuary, eastern Canada: centennial to millennial-scale geomagnetic modulation of cosmogenic isotopes. *Earth Planet. Sci. Lett.* 209, 113-130.
- Taton, A., Grubisic, S., Brambilla, E., De Wit, R. et Wilmotte, A. (2003) Cyanobacterial diversity in natural and artificial microbial mats of Lake Fryxell (McMurdo dry valleys, Antarctica): A morphological and molecular approach. *Appl. Environ. Microbiol.* 69, 5157-5169.
- Theriault, J.C. et Levasseur, M., (1985) Control of phytoplankton production in the lower St. Lawrence Estuary : light and freshwater runoff. *Nat. Can.* 112, 77-96.
- Thibodeau, B., de Vernal, A. et Mucci, A. (2006) Recent eutrophication and consequent hypoxia in the bottom waters of the Lower St. Lawrence Estuary: micropaleontological and geochemical evidence. *Mar. Geol.* 231, 37-50.
- Tiedje, J.M. (1988) Denitrification hysteresis during wetting and drying cycles in soil. *Soil Sci. Soc. Am. J.* 52, 1626-1629.
- Usui, T., Koike, I. et Ogura, N. (2001) N_2O production, nitrification and denitrification in an estuarine sediment. *Est. Coast. And Shelf Sci.* 52, 769-781.
- Vincent, W.F., Mueller, D.R., Van Hove, P. et Howard-Williams, C. (2004) Glacial periods on early Earth and implications for the evolution of life. Dans: Seckbach, J. (ed.) *Origins: Genesis, Evolution and Diversity of Life*. Kluwer Academic Publishers, Dordrecht. pp. 481-501.

Wang, F., Juniper, S.K., Pelegri, S.P. et Macko, S.A. (2003) Denitrification in sediment of the Laurentian Trough, St. Lawrence Estuary, Québec, Canada. *Est. Coast. and Shelf Sci.* 57, 515-522.

Yoch, D.C. et Whiting, G.J. (1986) Evidence for NH_4^+ switch-off regulation of nitrogenase activity by bacteria in salt marsh sediments and roots of the grass *Spartina alterniflora*. *Appl. Environ. Microbiol.* 51, 143-149.

Zubkov, M.V., Fuchs, B.M., Burkill, P.H. et Amann, R. (2001) Comparison of cellular and biomass specific activities of dominant bacterioplankton groups in stratified waters of the Celtic Sea. *Appl. Environ. Microbiol.* 67, 5210-5218.

ANNEXE 1

Inventaire des conditions physico-chimiques observées lors des campagnes d'échantillonnage dans l'estuaire du Saint-Laurent.

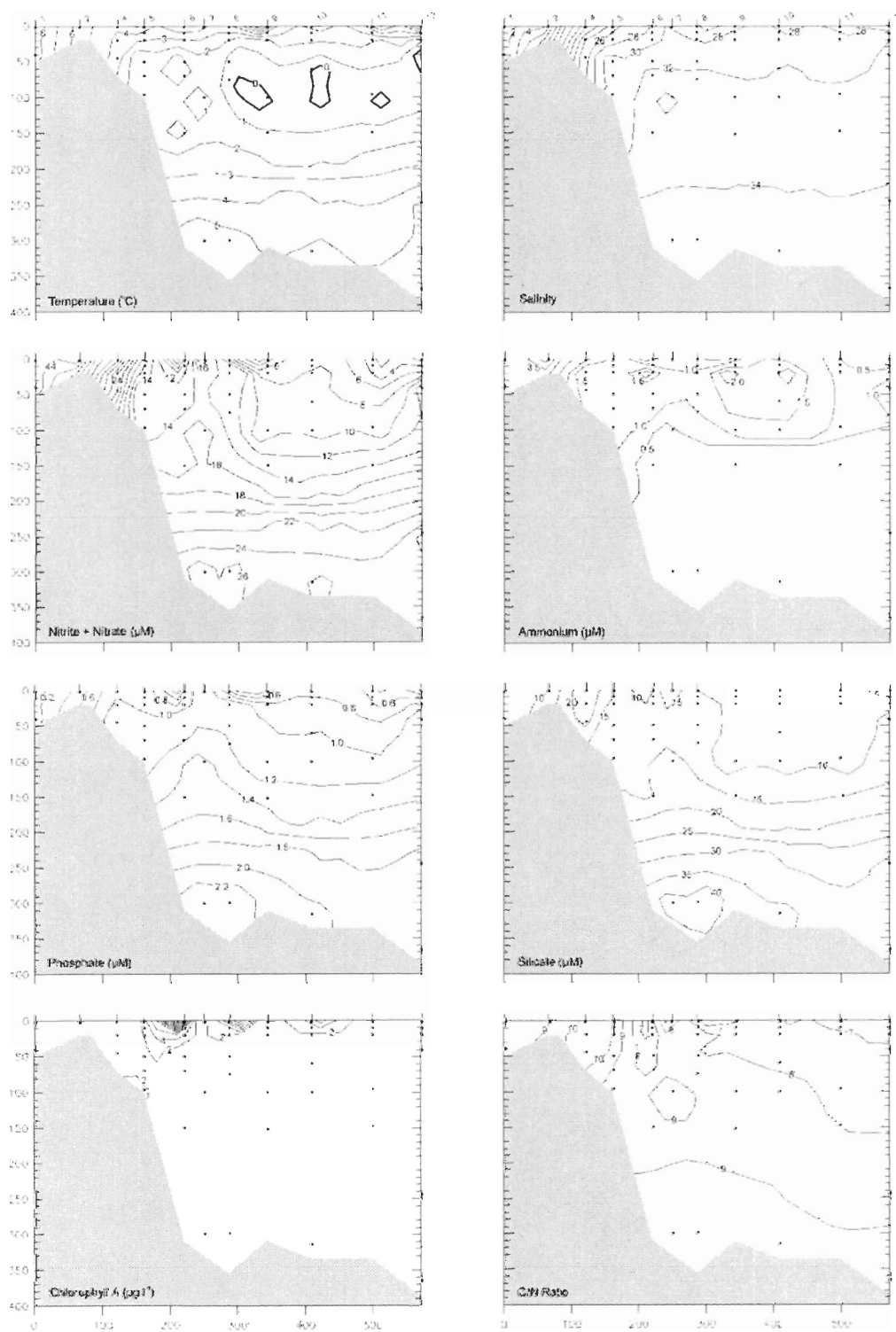


Figure A-1 Mai 2003

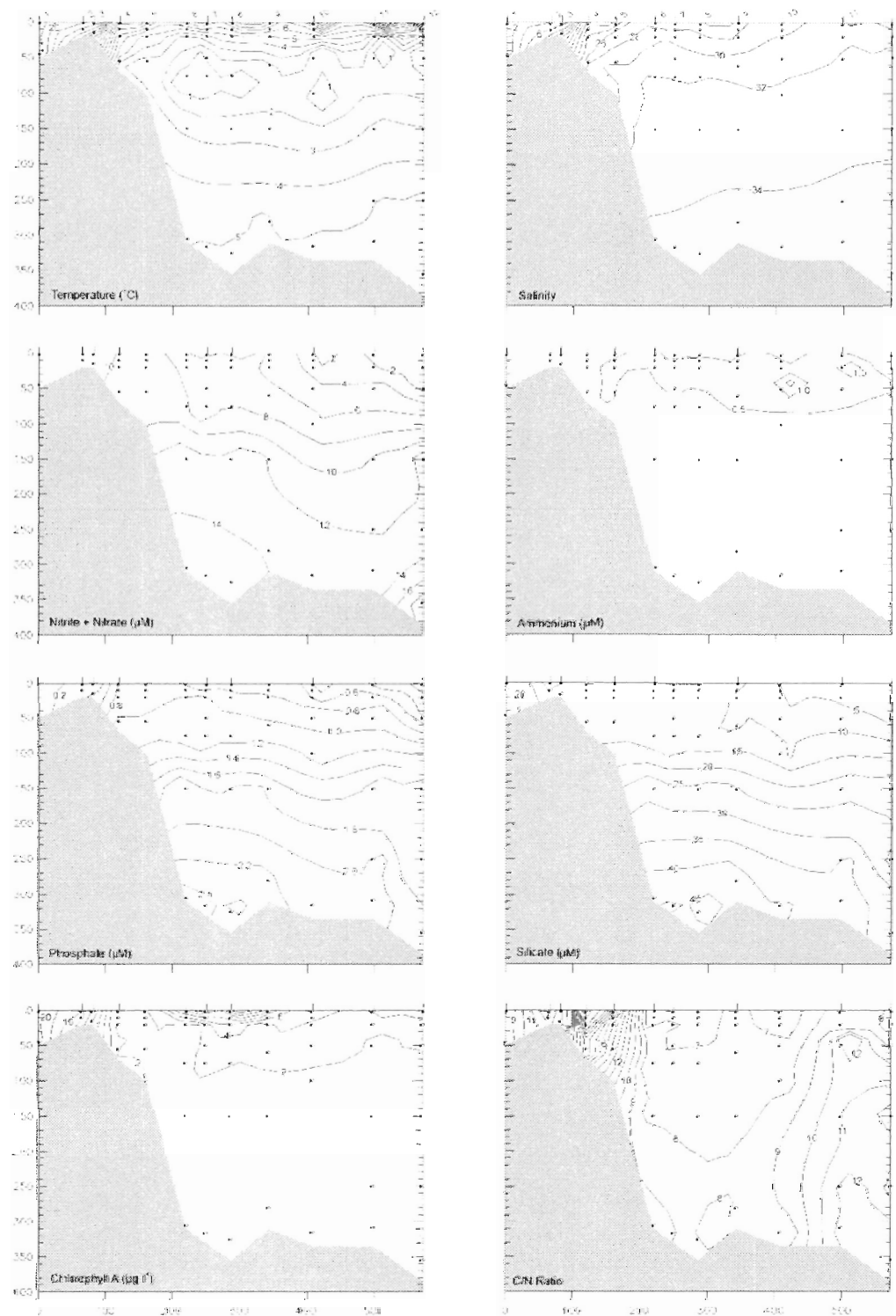


Figure A-2 Juillet 2004

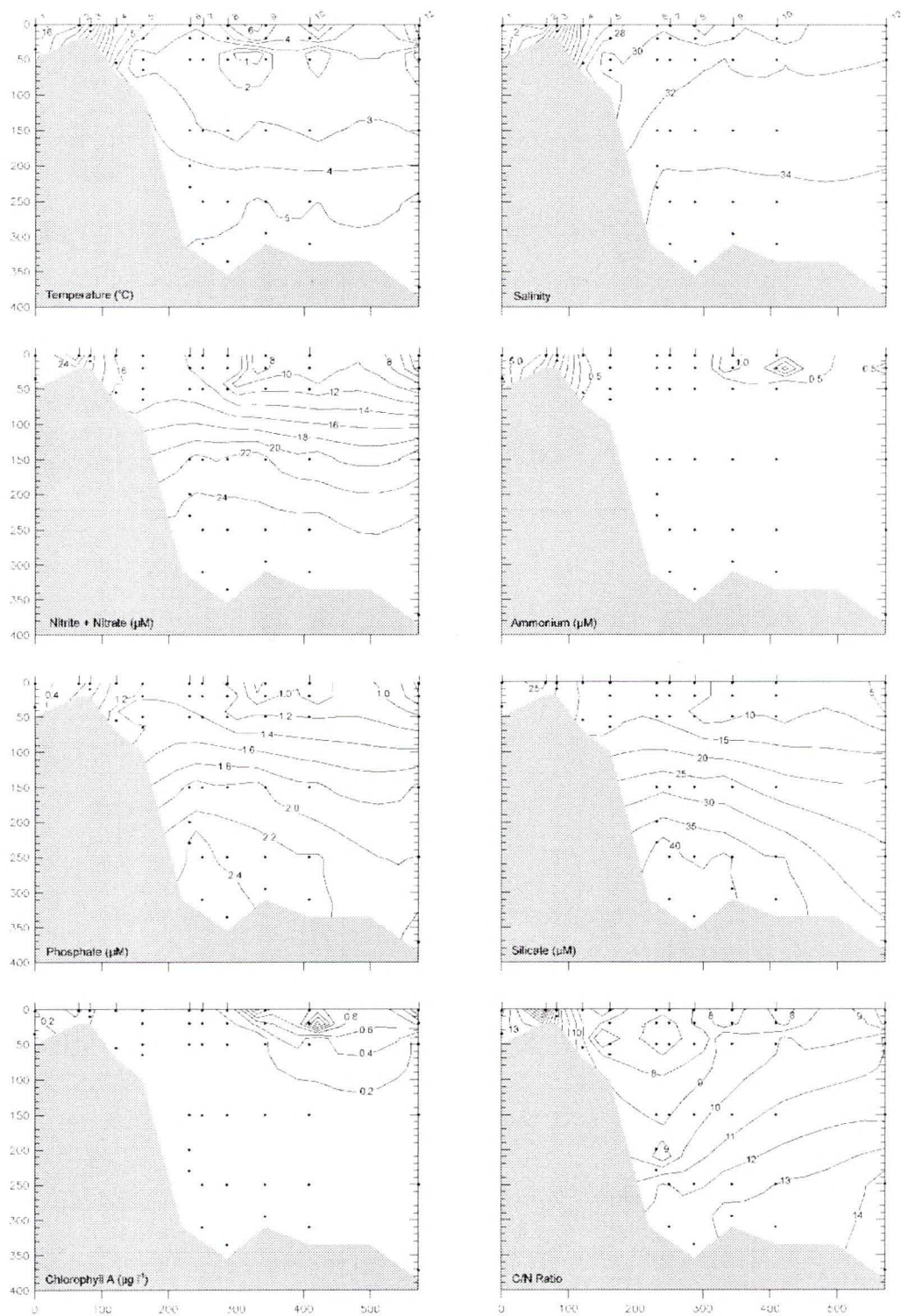


Figure A-3 Octobre 2005

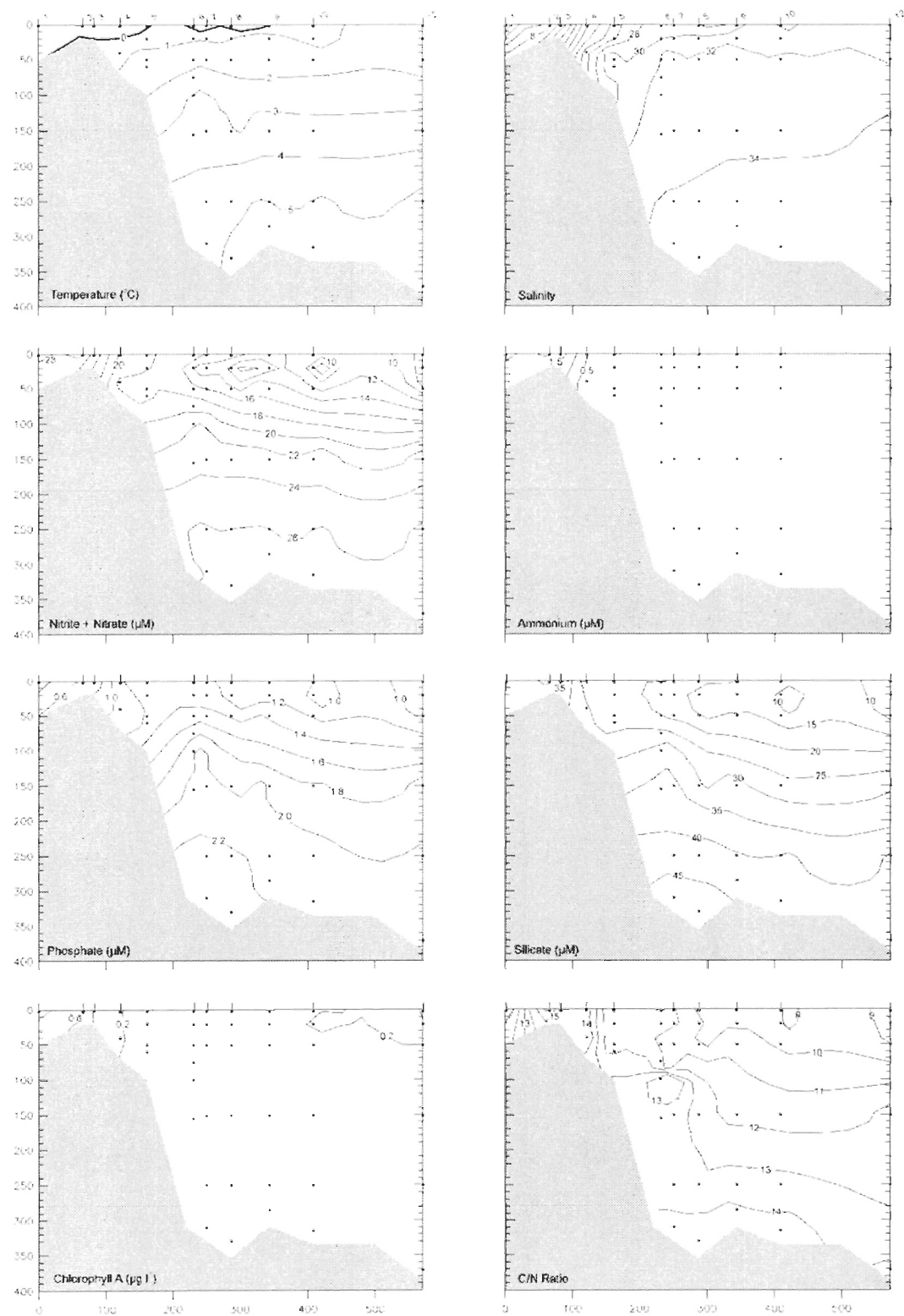


Figure A-4 Décembre 2005

